

Technische Universität München
TUM School of Engineering and Design

Upgrading Fuel Properties of Residual Biomass by Hydrothermal Carbonisation

Lynn Johanna Hansen

Vollständiger Abdruck der von der TUM School of Engineering and Design
der Technischen Universität München zur Erlangung
des akademischen Grades einer
Doktorin der Ingenieurwissenschaften
genehmigten Dissertation.

Vorsitzender: Prof. Rafael Macián-Juan, Ph.D.
Prüfer der Dissertation: 1. Prof. Dr.-Ing. Hartmut Spliethoff
2. Prof. Dr.-Ing. Martin Kaltschmitt

Die Dissertation wurde am 18.08.2022 bei der Technischen Universität
München eingereicht und durch die TUM School of Engineering and Design
am 22.11.2022 angenommen.

Danksagung

Diese Arbeit entstand während meiner Tätigkeit als wissenschaftliche Mitarbeiterin am Lehrstuhl für Energiesysteme der Technischen Universität München. Die Finanzierung meiner Arbeit erfolgte zum größten Teil über das EU geförderte Verbundprojekt "Bioefficiency".

An dieser Stelle danke ich Prof. Dr.-Ing. H. Spliethoff für die Betreuung der Arbeit. Mein Dank gilt ebenfalls Prof. Dr.-Ing. M. Kaltschmitt für die Übernahme des Korreferates und die rasche Begutachtung der Arbeit.

Die Zeit am Lehrstuhl möchte ich nicht missen und das liegt nicht zuletzt an den vielen tollen Menschen, mit denen ich dort zusammenarbeiten durfte. Es folgt eine unvollständige Liste: Sebastian Fendt, der mich als Betreuer immer gut beraten und aufgebaut hat und viel Verständnis für das Interesse seiner Schützlinge an den schönen Seiten der Promotion hat. Andrea Hartung und Margarethe Schwindl, die mit dem BrennstoffanalySELabor für mich immer einen Wohlfühlort am Lehrstuhl geschaffen haben. Das Sekretariat, welches auf dem gesamten Weg der Promotion immer zuverlässig unterstützt hat. Das gesamte Bioefficiency Konsortium und im Besonderen das TUM-Team Richard, Christian und Thorben, mit denen ich den ein oder anderen tollen Ausflug in Europa unternehmen durfte. Mein Bürokollege Wolf, mit dem man jederzeit neue Arbeitsmodelle, Stichwort 5h Tag, ausprobieren konnte. Die Laufgruppe, dank der man im Winter zumindest zweimal die Woche etwas Sonne abbekommen hat. Dabei ist besonders Felix hervorzuheben, dessen nicht enden wollende Motivation zu Laufen ich auch gerne hätte. Auch meinen Studenten Roland, Max, Andreas, Elena, Moritz, Clara, Emilie und Youssef möchte ich danken: Bei der Betreuung der Arbeiten hatte ich stets viel Spaß und viele der Ergebnisse wären ohne ihre Unterstützung nicht zustande gekommen.

Zuletzt möchte ich Michi danken, der mich zu jeder Zeit moralisch unterstützt hat und der im Gegensatz zu mir nie an meiner Doktorwürdigkeit gezweifelt hat!

This project has received funding from the European Union's Horizon 2020 research and innovation programme under grant agreement No 727616.

Abstract

With an increasing demand for biofuels, residual biomass streams offer a large untapped potential for renewable energy. However, poor fuel quality prevents their widespread application in power generation. Hydrothermal carbonisation (HTC) is an innovative technology for the upgrading of fuel properties. During HTC biomass is treated in hot compressed water to yield a solid, lignite-like fuel. In the presented work, a holistic evaluation of the technology for the provision of high quality fuels from residual biomass is conducted.

An assessment of nineteen substrates showed that HTC is most suitable for feedstock with high lignocellulosic content that exceed 50 % moisture content. Substrates used as feed or functional material should not be converted by HTC. Lignocellulosic biomass composition was found to influence mass yield and energy densification. High lignin content led to poor energetic compaction after HTC but achieved higher mass yields.

The impact of HTC on properties relevant for combustion was investigated experimentally. Feedstock type, treatment temperature, time and solid concentration were examined as influencing factors. Treatment temperature and solid concentration have the highest impact on fuel properties. For lignocellulosic feedstock HTC increases lower heating values by 10–15% at 180 °C and 45-55% at 270 °C. Mass yield decreases for increasing treatment temperature. The inorganic composition of fuels is strongly altered after HTC: On average over 75 % of K and Cl are removed during HTC. Inorganics with lower solubility like Ca, Mg, P, Si and Al are removed to a lesser extent and thus accumulate in the hydrochar ash. Higher overall removal rates are observed for higher treatment temperature and lower solid concentration. The transformations in inorganic composition lead to improved ash melting temperatures for alkali-rich fuels. The risk for corrosion, deposition and aerosol emission assessed by fuel indices is significantly lower for HTC fuels. In contrast, the expected NO_x emission risk

is higher for HTC fuels. Applying the same criteria, the fuel quality of high ash substrates like digested sludge are not improved significantly. Yet, HTC improves dewatering, storage and feedstock logistics of said feedstock. Kinetic analysis of selected samples reveals a strong decrease in reactivity with increasing treatment severity.

The amount of process water generated by HTC was calculated. Typically, around 2.3 m³ of process water arise per ton of HTC fuel. Experimental examinations showed that process water is heavily contaminated with organic material that could contribute around 10 % of the thermal energy demand of the process, if valorised by anaerobic digestion. However, convincing treatment concepts still need to be developed.

The thermal efficiency of a HTC plant determined by process modelling is in the range of 50-70 %. Lower treatment temperature and higher solid concentration during processing increases efficiency. Major losses are attributed to chemical energy losses in the process water. A techno-economic assessment reveals fuel production cost of around 9 € GJ⁻¹ rendering HTC fuels economically uncompetitive in the current market situation. Treating substrates with a considerable gate-fee or increasing CO₂ taxes could improve the economics of HTC.

Key words: Biomass pre-treatment, hydrothermal carbonisation, residual biomass, combustion, inorganic elements, fuels indices

Kurzfassung

Angesichts einer steigenden Nachfrage erneuerbaren Brennstoffen, bieten biogene Reststoffe ein großes ungenutztes Potenzial. Die oft schlechte Brennstoffqualität verhindert jedoch eine breite Anwendung dieser Brennstoffe in der Energieerzeugung. Eine innovative Technologie zur Verbesserung von Brennstoffeigenschaften ist die hydrothermale Karbonisierung (HTC). In diesem Verfahren wird Biomasse bei Temperaturen von 150-300 °C unter Druck in flüssigem Wasser zu einem braunkohleähnlichen Brennstoff umgewandelt. In der vorliegenden Arbeit wird eine ganzheitliche Bewertung der Technologie zur Bereitstellung von Brennstoffen aus Reststoffen vorgenommen.

Eine Bewertung von neunzehn Einsatzstoffen zeigt, dass HTC am geeignetsten für Substrate mit hohem Lignozellulosegehalt ist, die mehr als 50 % Wassergehalt aufweisen. Einsatzstoffe, die stofflich oder als Futtermittel verwendet werden können, sollten nicht verwendet werden. Die Zusammensetzung der lignozellulosehaltigen Biomasse beeinflusst die Massenausbeute und energetische Verdichtung stark. Die Karbonisierung von Substraten mit hohem Ligningehalt führt zu einer schlechten energetischen Verdichtung, erzielt aber höhere Massenausbeuten.

Der Einfluss der HTC auf die Brennstoffqualität wurde experimentell untersucht. Als Einflussfaktoren wurden Substrattyp, Behandlungstemperatur, -zeit und Feststoffkonzentration untersucht. Temperatur und Feststoffkonzentration haben den größten Einfluss auf die Brennstoffeigenschaften. Bei lignozellulosem Ausgangsmaterial erhöht HTC den unteren Heizwert um 10-15 % bei 180 °C und 45-55 % bei 270 °C. Die Massenausbeute nimmt bei steigender Behandlungstemperatur ab. Auch die anorganische Zusammensetzung der Brennstoffe wird durch die HTC stark verändert: Durchschnittlich werden über 75 % der anfänglichen Menge von K und Cl ausgewaschen. Anorganische Stoffe mit geringerer Löslichkeit wie Ca, Mg, P, Si und Al werden in geringerem Maße entfernt und reichern sich daher in der Asche der HTC Biomassen an. Eine stärkere Auswaschung von anorganischem Material wird bei einer höheren

Temperatur und geringeren Feststoffkonzentration beobachtet. Die Veränderungen der anorganischen Zusammensetzung führen zu verbesserten Ascheschmelztemperaturen für Brennstoffe mit hohem Alkaliengehalt. Die Bewertung der Brennstoffqualität mithilfe von Brennstoffindices ergab ein deutlich geringeres Risiko für Korrosion, Depositionen und Feinstaubbildung für HTC-Brennstoffe. Im Gegensatz dazu ist das erwartete Risiko für NO_x-Emissionen bei HTC-Brennstoffen höher. Bei Anwendung der gleichen Kriterien kann die Brennstoffqualität von aschereichen Substraten wie Faulschlamm nicht verbessert werden. Dennoch verbessert HTC die Entwässerbarkeit, Lagerung und Logistik solcher Einsatzstoffe. Eine kinetische Analyse ausgewählter Proben zeigt eine starke Abnahme der Reaktivität mit zunehmender HTC Behandlungsintensität.

Die Menge des bei der HTC anfallenden Prozesswassers wurde berechnet. Unter typischen Bedingungen fallen etwa 2,4 m³ Prozesswasser pro Tonne Brennstoff an. Experimentelle Untersuchungen zeigen, dass das Prozesswasser stark mit organischem Material belastet ist. Mithilfe einer anaeroben Vergärung dieser Stoffe könnte jedoch etwa 10 % des thermischen Energiebedarfs des Prozesses gedeckt werden. Schlüssige Verwertungsprozesse für HTC Prozesswasser müssen zukünftig noch entwickelt werden.

Der thermische Wirkungsgrad einer HTC Anlage wurde durch eine Prozessmodellierung ermittelt und liegt im Bereich von 50-70 %. Eine niedrigere Behandlungstemperatur und eine höhere Feststoffkonzentration im Reaktor erhöhen die Effizienz des Prozesses. Die größten Verluste sind auf den Verlust chemischer Energie im Prozesswasser zurückzuführen. Eine wirtschaftliche Berechnung ergab Produktionskosten von 9 € GJ⁻¹ für HTC-Brennstoffe. Somit ist die Technologie in der derzeitigen Marktsituation wirtschaftlich nicht konkurrenzfähig. Die Behandlung von Substraten mit einer Entsorgungsgebühr oder die Erhöhung von Steuern auf CO₂ Emissionen könnten die Wirtschaftlichkeit der HTC verbessern.

Table of Contents

Table of Contents	V
List of Figures	VII
List of Tables	X
Abbreviations	XII
Nomenclature	XIII
Subscripts	XIII
1 Introduction	1
1.1 Previous Work at the Chair of Energy Systems	5
1.2 Structure of the Thesis	5
2 Biomass as Bioenergy Carrier	7
2.1 Availability of Biomass Energy Carriers	8
2.2 Biomass Fuel Composition and Properties	12
2.2.1 Organic Composition of Biomass	12
2.2.2 Inorganic Matter in Biomass	14
2.3 Technologies for Biomass Valorisation	17
2.3.1 Overview	18
2.3.2 Thermo-Chemical Biomass Pre-treatment	19
2.3.3 Technologies for the Conversion of Wet Feedstock	23
3 Hydrothermal Carbonisation	27
3.1 Fundamentals of Hydrothermal Processes	27
3.2 Main Reaction Pathways during HTC	29
3.3 Main Influencing Process Parameters	32
3.4 HTC Product Properties	34
3.4.1 Solid Product	35
3.4.2 Liquid and Gaseous By-products	37
4 State of the Art in Research and Technology of Hydrothermal Carbonisation	40
4.1 Fate of Inorganics during HTC	40
4.2 Quality Assessment for Solid Fuels	44
4.3 HTC Process Variations and Techno-economic Evaluation	48
5 Research Demand, Aims and Methodology	55

6	Materials and Methods	57
6.1	Holistic Assessment of HTC for Solid Fuel Production	57
6.2	Fuel Characterisation	58
6.3	Experimental HTC Investigations.....	63
6.4	Characterisation of Process Water.....	67
6.5	Process Modelling and Techno-economic Analysis.....	67
6.5.1	Conceptual Process Design.....	68
6.5.2	Techno-economic Assessment.....	71
7	Considerations for the Selection of Feedstock	76
7.1	Feedstock Characteristics and Current Utilisation	77
7.2	Quality of Carbonisation	86
7.3	Feedstock Moisture Content.....	89
7.4	Alternative Conversion for Wet Feedstock	92
8	Impact of Hydrothermal Carbonisation on Characteristics Relevant for Combustion	96
8.1	Heating Value, Mass- and Energy yield	96
8.2	Fate of Inorganic Elements during HTC.....	100
8.3	Fuel Quality Assessment.....	118
8.4	Reactivity of HTC Chars	129
9	Characterisation and Utilisation Options for HTC By-products	133
9.1	Amount of Process Water Generated.....	133
9.2	Characterisation of HTC Process Water	134
9.3	Valorisation and Treatment Options for Process Water.....	141
10	Techno-economic Evaluation of HTC	144
10.1	Results of Process Simulation	144
10.2	Economic Evaluation.....	151
11	Summary and Recommendations	157
11.1	Summary of Findings	157
11.2	Recommendations for Future Work.....	162
12	References	163
	Appendix	196

List of Figures

Figure 1.1: Contribution of gaseous, liquid and solid bioenergy carriers to bioenergy supply from 2005-2017 in Europe. Data from [7].	2
Figure 2.1: Gross inland energy consumption of biomass in 2017 and projected technical, energetic and sustainable potential in 2030 for EU-28 countries in Mtoe. Data from [21, 22].	10
Figure 2.2: Contributions of different feedstock types and categories to EU-28 theoretical potential of biomass residues. Data from [20].	11
Figure 2.3: Schematic of the structure of lignocellulose. Adapted from [31, 32].	13
Figure 2.4: Ash forming elements in various biomass feedstock investigated in this study. Wood and lignite are shown as reference materials.	15
Figure 2.5: Forms of ash-forming matter. Adapted from [39].	17
Figure 2.6: Conversion pathways of biomass energy resources to biomass energy carriers. Adapted from [40].	19
Figure 3.1: Phase diagram (p,T) of water and related hydrothermal processes. Adapted from [87].	28
Figure 3.2: Simplified representation of the chemical processes during hydrothermal carbonisation. Adapted from [91].	30
Figure 3.3: Examples for the hydrothermal conversion of grass cuttings and rice husk for different process parameters (T, τ) in a van-Krevelen diagram. Theoretical elimination scenario of carbohydrates and typical ranges of H/C and O/C ratios of fossil solid fuels. Adapted from [61]. Data for rice husk from [17].	32
Figure 3.4: Qualitative HTC mass balance. Adapted from [61].	35
Figure 4.1: Energy flows during HTC of sewage sludge and subsequent drying to 90 % dry matter. Q_R = heat of reaction, DM = dry matter. Adapted from [159]. Data from TerraNova pilot plant [157, 160].	49
Figure 6.1: Overview on the approach used for the assessment of HTC for solid fuel production.	57
Figure 6.2 Schematic of the lab-scale test rig for the experimental investigation of biomass HTC, $V = 600$ mL, $T_{max} = 350$ °C, $p_{max} = 200$ bar. Adapted from [17].	63
Figure 6.3: Schematic flowsheet of the modelled HTC plant.	68
Figure 7.1: Overview on substrates for HTC and respective biomass classes investigated in this study. In-depth examination was carried out on substrates with solid outline.	76
Figure 7.2: Approximate prices and gate-fee for the investigated feedstocks. Wood pellet price is included as a reference. Data collected from [218–230].	82
Figure 7.3: Inorganic element concentration in biomass substrates.	85
Figure 7.4: Mass- and energy yield of different substrates after HTC at 210 °C for 2 h. The rating of energy yields is indicated on the right hand side.	87
Figure 7.5: Specific increase in LHV and specific increase in carbon content of different substrates after HTC at 210 °C for 2 h.	88

Figure 7.6: Typical feedstock moisture content upon collection and provision and threshold moisture content above which HTC conversion is favored towards direct combustion.....91

Figure 7.7: Comparison of substrate usage in a biogas plant and in an HTC plant, in each case in combination with a biomass CHP; the net energy was calculated. *Data for food waste from [69].....92

Figure 7.8: Proposed decision tree for the selection of suitable feedstock for HTC and results of its application of the considered substrates.94

Figure 8.1: HTC Mass yield of different substrates as a function of temperature (left) and residence time (right).....96

Figure 8.2: LHV of different substrates after HTC as a function of temperature (left) and residence time (right).....97

Figure 8.3: HTC energy yield of different substrates as a function of temperature (left) and residence time (right).....98

Figure 8.4: Relative ash content of different substrates after HTC as a function of treatment temperature (left) and residence time (right).101

Figure 8.5: Mass balance of ash-, volatile and fixed-C content (left) and changes in fuel composition (right) before and after HTC at 180 °C and 270 °C for 2 h. The absolute amount of ash is decreasing, while the relative ash content is dependent on feedstock ash composition.102

Figure 8.6: Relative ash content (left) and ash removal (right) of different feedstock after HTC at 210 °C for 2 h as a function of substrate alkali content.104

Figure 8.7: Relative element concentration of main ash forming elements in different biomass substrates after HTC treatment at 210 °C for 2 h.....105

Figure 8.8: HTC removal efficiency of main ash elements K, Cl, Mg, Ca, Al, Si, P and S in treated AD digestate as a function of treatment temperature and residence time.109

Figure 8.9: Removal efficiency (left) and relative content of inorganic components (right) for liquid-to-solid-ratio 5, 10 and 20 in orange peels HTC treated at 210°C for 2 h.112

Figure 8.10: Mass yield, HHV and ash content of substrates HTC treated at 210 °C for 2 h with Argon (Ar) and carbon dioxide (CO₂) as pressurising agent.....114

Figure 8.11: Characteristic ash fusion temperatures of untreated and HTC treated EFB, AD digestate, spruce bark and fallen leaves.117

Figure 8.12: Molar 2 S/Cl ratio (a) and fuel Cl content (b) of raw substrates and hydrochars treated at different temperatures for 2 h. Corrosion risk is indicated with coloring (low=green, medium=orange, high= red). The values of wood pellets serve as a reference.120

Figure 8.13: Specific fuel-N content per unit energy (a) and fuel-N with indicated ranges of NO_x emission risk (b) of biomass samples HTC treated at different temperatures at a residence time of 2 h and wood pellets as reference. Emission risk propensity is indicated with coloring (low=green, medium=orange, high= red)...122

Figure 8.14: Sum of the concentration of K, Na, Zn and Pb in mg per kg fuel as indicator for fine particle emission tendency for raw and HTC treated feedstock, wood pellets shown as reference. Emission risk propensity is indicated with coloring (low=green, medium=orange, high= red).....	125
Figure 8.15: Molar (Si+K+P) to (Ca+Mg) ratio of raw biomass including wood pellets as reference and HTC fuels treated at different temperatures at a residence time of 2 h. Below a value of 1 a minor slagging risk is expected.....	126
Figure 8.16: Fouling index calculated for raw biomass and HTC fuels treated at different temperatures at a residence time of 2 h. The risk of slagging is indicated with coloring (low=green, medium=orange, high= red).....	128
Figure 8.17: (a) Relative intrinsic reaction rate in 5 % O ₂ atmosphere conversion of the pyrolysed hydrochar samples versus carbonisation temperatures at residence times of 0.5 h, 2 h and 4 h at 425 °C compared to the pyrolysed raw biomass under the same conditions. (b) Relative C-fix content versus relative intrinsic reactivities for reaction temperatures from 180-270 °C and residence times from 0.5 h-4.....	129
Figure 8.18: Intrinsic reactivity measured for substrate and HTC chars as a function of fixed-C (a) and fuel alkali content (b). HTC samples were treated at 270 C for 2 h.....	131
Figure 9.1: EC of process water from various substrates treated at 210 °C for 2 h as a function of the alkali content in the starting material.....	137
Figure 9.2: BOD ₅ /COD ratio (a) and C/N ratio (b) of process water obtained after HTC of different biomass types at temperatures of 150-270 °C for 4 h.....	139
Figure 9.3: Overview on possible treatment and valorisation options for HTC process water.....	141
Figure 10.1: (a) Specific auxiliary thermal energy demand per kg hydrochar produced at different reaction temperatures; (b) Net thermal process efficiency of HTC plant at different reaction temperatures.....	146
Figure 10.2: (a) Specific thermal energy demand per kg hydrochar as a function of feedstock moisture; (b) Net thermal process efficiency of HTC plant as a function of feedstock moisture.....	148
Figure 10.3: Simplified mass balance of the modelled HTC plant operating at 210 °C, 2 h.....	151
Figure 10.4: Proportionate costs of different cost categories in the cost of production of fuels originating from a HTC plant processing (a) green cut in Germany, (b) EFB in Malaysia.....	154

List of Tables

Table 2.1: Biomass classification by origin. Adapted from [18].	7
Table 2.2: Overview on the three thermo-chemical pre-treatment methods explored.	21
Table 2.3: Technologies for the energetic valorisation of wet biomass feedstock.	25
Table 3.1: Physical properties of water in different temperature and pressure regimes [89, 90].	29
Table 3.2: Impact of the hydrothermal conversion of biomass the properties of the solid product.	36
Table 3.3: Characteristics and composition of process water from hydrothermal carbonisation after filtration. Data from [61, 69, 105, 110–113].	38
Table 4.1: Overview of studies investigating the fate of inorganics during HTC.	43
Table 4.2: Quality-relevant properties of biogenic solid fuels with their respective effects. Adapted from [133].	44
Table 4.3: Risk classification for biomass combustion related challenges using fuel indices.	48
Table 4.4: Basic process characteristics for selected processes from commercial technology providers of hydrothermal carbonisation.	50
Table 4.5: Summary of results from techno-economic analyses of academic studies and HTC technology providers.	52
Table 6.1: Overview on used equipment and international norms used for fuel characterisation.	61
Table 6.2: Applied temperature and pressure during experimental HTC investigations and water vapour pressure according to Antoine equation at the respective temperature.	64
Table 6.3: Assumptions and units used in ASPEN Plus HTC process model.	69
Table 6.4: Assumptions for the calculation of the total annual capital charge for the considered HTC plant.	72
Table 6.5: Assumptions for the calculation of the cash cost of production.	73
Table 6.6: Key data on site capacity, labour- and utility prices for both locations considered in the case study.	74
Table 7.1: Proximate, ultimate, heating value analysis of investigated fuels by sector of origin. All reported on dry basis, except for moisture content.	84
Table 7.2: Fuel quality assessment for examined substrates using fuel indices for risk evaluation of biomass combustion related challenges.	86
Table 7.3: Summary and rating of selection criteria applied to the investigated feedstock. (green=suited for HTC, grey=neutral, red=not suited for HTC)	95

Table 8.1: Ash melting temperatures of substrate and hydrochar ash treated for a residence time of 2 h.....	116
Table 9.1: Amount of process water generated by HTC according to own calculations and literature values.....	134
Table 9.2: Water analysis data of effluent obtained from hydrothermal carbonisation of various feedstock at different temperatures for a reaction time of 4 h.....	135
Table 10.1: Electric and thermal power requirements at different HTC process conditions for a plant processing 40 kt a ⁻¹ (2.7 t h ⁻¹) EFB at 70 % moisture.....	145
Table 10.2: HTC process specifications for energy demand calculations, process energy demand and efficiency of own and data from literature.....	149
Table 10.3: Key data on both considered plant sites and total cost for on-site equipment.....	152
Table 10.4: Annual capital and cash costs of production for HTC fuels in Germany from a local plant and a Malaysian plant including delivery.....	153

-

Abbreviations

AD	Anaerobic digestion
AFI	Ash fusion index
BOD	Biological oxygen demand
CC	Contingency capital
CEC	Cation exchange capacity
COD	Chemical oxygen demand
DM	Dry matter
e.-%	Energy percentage
EC	Electrical conductivity
EC	Engineering cost
EFB	Empty fruit bunches
EU	European Union
FCOP	Fixed cost of production
FM	Fresh matter
GHG	Greenhouse gases
HHV	Higher heating value
HMF	Hydroxymethylfurfural
HTC	Hydrothermal carbonisation
HTG	Hydrothermal gasification
HTL	Hydrothermal liquefaction
ISBL	Inside battery limits
ISO	International organisation for standardisation
L/S ratio	Liquid-to-solid ratio
LHV	Lower heating value
COD	Chemical oxygen demand
BOD	Biological oxygen demand
OSBL	Outside battery limits
PM	Particulate matter
SCG	Super-critical gasification
SCG	Spent coffee grounds

TGA	Thermo-gravimetric analysis
TN	Total nitrogen
TOC	Total organic carbon
VCOP	Variable cost of production
WO	Wet oxidation
wt.-%	Weight percentage
WWTP	Waste water treatment plant

Nomenclature

a	year
F_u	Fouling index
HHV	Higher heating value
LHV	Lower heating value
n	Number of moles
r	Molar ratio of CO ₂ and H ₂ O
$R_{B/A}$	Base-to-acid ratio
t	tons
toe	tonnes oil equivalent
Y	Yield
ϵ_R	relative dielectric constant of water
η	Efficiency

Subscripts

ar	As received
B/A	Base-to-acid
daf	Dry ash free basis
db	Dry basis
e	energy
m	mass
th	thermal

1 Introduction

Moving towards a more sustainable society has become one of the most important challenges of the 21st century. With a growing world population and increasing greenhouse gas (GHG) emissions, mitigating climate change is vital for the survival of our society [1–3]. A major part of the worldwide greenhouse gas emissions originates from the energy production using fossil fuels. In 2018, coal-fired power plants were the single largest contributor to the growth in GHG emissions, accounting for roughly 30 % of the global CO₂ emissions [4].

Biomass as an abundant, renewable energy carrier offers the possibility to reduce net GHG emissions by substituting fossil fuels. In the European Union (EU), bioenergy continues to be the main source of renewable energy with a share of almost 60 % [5]. As Figure 1.1 shows, within the bioenergy sector, solid biomass fuels constitute the most important energy carrier.

Compared to other renewable energy resources, like wind or photovoltaic, biomass offers several advantages: First of all, the electricity production from biofuels is a known, dispatchable technology. Biomass can be combusted in traditional steam-boilers or gasified for further use in combined cycles. For these systems long-term experience for operation exists and by using present infrastructure a fast implementation with a low incremental learning curve and fairly low capital expense can be realised. Biomass can be regarded as a baseload power source and can help to compensate grid fluctuations caused by other volatile renewables. Further, the combination of biomass combustion that produces no net CO₂ emissions with carbon capture and storage offers the potential of negative emissions [6]. Being a widely available energy source, biomass could also facilitate climate change mitigation in regions that may have limited solar, wind, or geothermal alternatives. Biomass is a local resource that is unlikely to be transported long distances for economic reasons. Consequently, using

biomass rather than imported fossil fuels for energy production could benefit energy security.

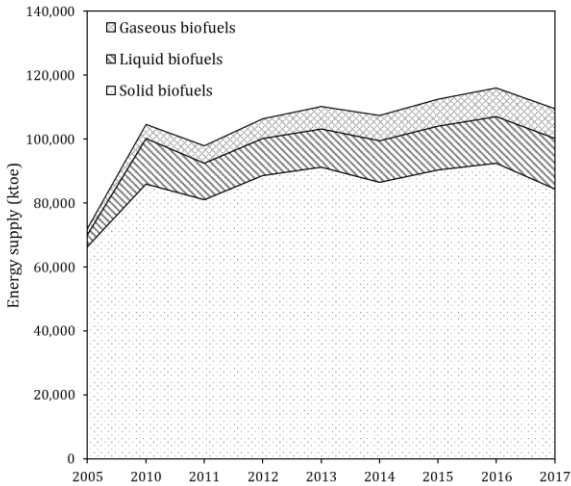


Figure 1.1: Contribution of gaseous, liquid and solid bioenergy carriers to bioenergy supply from 2005-2017 in Europe. Data from [7].

Challenges in the use of solid biomass fuel include the need for sufficient and sustainable feedstock supply, increased difficulty in fuel handling, transportation and potential health impact by emissions from biomass-fired power plants. In recent years, also the carbon neutrality of biomass combustion has been questioned and the sustainability of bioenergy practices in the EU is currently being reassessed [8]. Especially the utilisation of wood, which accounts for over 60 % of biomass feedstock used for bioenergy in the EU [9], is seen as problematic. Burning biomass for energy purposes releases large amounts of carbon into the atmosphere all at once. But the uptake of the same amount of CO₂ by forests producing wood might take decades or even centuries depending on the tree type [10]. Moreover, biofuel provision should have minimal impact on the food chain, water supply, land use and environment. Consequently, to boost sustainability of bioenergy and to enable further growth in the market of solid biofuels, novel feedstock need to be exploited.

Biomass residues seem to be a suitable candidate for this: Agriculture, forestry, municipalities and industry are the main sectors that produce biomass residues. Among them, agricultural residues offer the biggest untapped biomass potential. Currently, this sector contributes less than 3 % to the total bioenergy production, but has the potential of contributing up to 17 % of the total energy supply worldwide [11].

Agricultural residues typically originate from plants that regrow within a year, balancing the emissions from their combustion much faster. In contrast to energy crop production, no further land use is required, thus avoiding potential conflict between food and energy production. Additionally, residue utilisation avoids GHG emissions from the decomposition of biomass residues that are left and sometimes burned on-site after harvesting. Commonly, biogenic residues are also disposed in landfills where GHG emissions from their biological degradation arise.

Unfortunately, biomass residues often exhibit poor fuel quality posing challenges in their energetic utilisation. Most residual biomass feedstock have low bulk density, high moisture content, low calorific value and a highly hydrophilic nature. With these properties, multiple problems arise [12, 13]: Firstly, hydrophilic biomass is subjected to biological deterioration, limiting the practical time for storage which is a challenge for seasonally available agricultural residues. Further, the fibrous nature of a lot of biomass materials brings milling and handling difficulties that negatively influence their economic utilisation. Compared to fossil fuels, biomass often contains higher amounts of alkali metals and chlorine. Common problems in biomass combustion are often ash-related, such as deposit formation, corrosion, ash-melting and particle formation, as well as problems regarding NO_x , SO_x and HCl emissions.

A promising approach to overcome these problems is a thermo-chemical pre-treatment. Several competing technologies exist that aim to improve the physio-chemical properties of biomass fuels. Hydrothermal carbonisation (HTC), torrefaction and steam-explosion are the most prominent technologies for the valorisation of challenging feedstock. The desire to

access difficult feedstock for fuel production by pre-treatment leads to the motivation of this work:

This work focuses on the pre-treatment of residual biomass streams by HTC. A holistic approach to assess the possibilities and limitations of this technology for the production of solid fuels is taken.

During HTC, biomass is treated at elevated temperatures of 180-300 °C in hot compressed water. The process yields a solid product, called hydrochar or HTC fuel, that has an increased energy density, higher hydrophobicity and is more brittle than the original material [14–16]. First, selection criteria for the identification of suitable HTC substrates are developed by comparing the conversion efficiency of HTC to other technologies of energetic valorisation. HTC leads to significant changes in the both the organic and inorganic composition of the resulting fuel. Therefore, the core of this study investigates the impact of HTC on the fuel quality regarding combustion-related challenges. An emphasis is set on the changes in inorganic composition of the resulting hydrochars.

Further, the resulting process water from HTC, representing the main side product of the process, is characterised and evaluated. Some utilisation options for this process water are discussed.

Finally, the commercial viability of the process is assessed in a case study by techno-economic analysis.

1.1 Previous Work at the Chair of Energy Systems

In previous work Ulbrich considered the optimisation of HTC process parameters for the application of HTC fuels in gasification processes [17]. In an in-depth experimental parameter study the hydrothermal carbonisation of brewer's spent grains, rice husk and corn cobs was investigated. The transformations of the organic biomass matrix during HTC at different temperatures and residence times were examined in detail. Significant changes in the organic fuel composition were attributed to the degradation of principal biomass components hemi-cellulose, cellulose and lignin. The gasification reactivity was found to be significantly reduced for HTC chars. The decline in reactivity was attributed to the transformation of the biomass matrix to an aromatic graphite-like structure with increased amount of fixed carbon. Ulbrich also performed an initial assessment of the fate of inorganic matter during HTC. He found increased ash melting temperatures and decreased alkali and chlorine contents in all fuels. The findings of this previous study are considered for this work. The investigated temperature and treatment times are reduced to include only conditions where significant changes in the biomass structure are expected. Residence time is limited to time-scales of up to 4 h, within which Ulbrich determined the main HTC reactions to be completed. Transcending previous work at the chair, a much broader range of substrates, considering number and origin of feedstock is considered. In contrast to the focus on the transformation of the organic biomass components and an application of the resulting HTC fuels in gasification reactions covered in Ulbrich's thesis, the spotlight of the current work is set on ash-related challenges in biomass combustion and the fate of inorganic elements during HTC.

1.2 Structure of the Thesis

The thesis is structured as follows: Chapter 2 explores the opportunities of the use of biomass for energy purposes. The availability, composition and possible energetic valorisation pathways of biofuels are summarised. In Chapter 3 the fundamentals of hydrothermal processes including governing conversion mechanisms and characteristics of solid, liquid and gaseous

products from the process are presented. Subsequently in Chapter 4, the state-of-the-art of HTC for the provision of high-quality fuels is summarised. Current research considering the fate of inorganic elements during HTC, fuel quality assessment and economic performance of the process are presented. Chapter 5 discusses the research demand identified in the previous chapter. The methodology used in this work and targeted contributions beyond the state-of-the-art are presented. In chapter 6 the analytic techniques, test-rig and modelling tools used in this work are described in detail. The following chapters discuss the findings of the holistic assessment of HTC for the provision of fuels from residual biomass: Chapter 7 discusses criteria for the selection of suitable feedstock for HTC. In chapter 8 the impact of HTC on fuel properties relevant for combustion is explored. Chapter 9 provides insights to the amount of process water generated during HTC, its characterisation and possible utilisation and treatment options. The technical and economic performance of HTC is discussed in chapter 10. Finally, chapter 11 summarises the findings and provides some recommendations for future work in the research field.

2 Biomass as Bioenergy Carrier

The term biomass is defined as organic matter derived from plants and animals. It can be used as a source of energy and is generally considered a renewable energy source, since it contains stored energy from the sun that has been transformed to solid matter by photosynthesis. Biomass is used in a broad spectrum of applications ranging from traditional use for cooking and heating, to modern combined heat and power generation. Biomass can be collected from various sectors. Table 2.1 shows a classification of different biomass sources by sector.

Table 2.1: Biomass classification by origin. Adapted from [18].

Main sector	Sub sector	Examples
Agriculture	Dedicated cultivation	Crops for biofuels (corn, sugarcane, rapeseed, oil palm, cassava etc.), energy grasses, short rotation forests, others
	By-products and residues	Herbaceous by-products: straw from cereals, rice, corn, bagasse, empty fruit bunches, prunings from stover, empty corn cobs, etc.
		Woody biomass: pruning from vineyards, olive and oil palm plantations
	Farm manure	Other forms: Processing residues such as kernels, sunflower shells, rice husks, foliage
Forestry	Main product	Digestate, solid manure (horse, chicken, cattle), liquid manure (pig, cattle)
	By-products and residues	Stems, wood fuel from forests or trees outside forests, woody biomass from landscape cleaning
Industry	Waste management	Harvesting residues (branches, tops, stumps), residues of wood industry (bark, sawdust, black liquor, recycled wood)
		Food residues from dairy, sugar, beer, wine, fruit juice industry, olive oil filter cake, waste from slaughterhouses
Municipal	Waste management	Food waste from stores, restaurants and households, green cut from landscaping, autumn foliage
	Water management	Sewage sludge, screenings

As Table 2.1 shows, the main biomass source sectors are agriculture, forestry, industry and waste from municipalities. The majority of feedstock

under consideration for an energetic utilisation originate from plants. Therefore, the following sections focus on the structural properties of plant-based, lignocellulosic biomass.

Any conversion of the biomass feedstock is strongly dependent on its chemical and physical properties that determine the outcome of these processes. This applies especially for processes which form pollutants. Compared to fossil fuels, biomass exhibits a large variety in its fuel characteristics. Consequently, for an environmentally friendly energetic conversion of biogenic solid fuels, the respective special features or properties of the fuel must be adequately taken into account. Mainly the elemental composition as well as basic fuel properties such as moisture and ash content are of high importance.

Therefore, availability, composition and characteristics of biogenic solid fuels are described in more detail in the following sections. In addition, different options for the energetic valorisation of biofuels are introduced. In this context, fuel upgrading by HTC is compared to other thermo- and biochemical pre-treatment technologies.

2.1 Availability of Biomass Energy Carriers

Due to the transition of the European energy system towards higher shares of renewable resources and energy carriers, there is an increasing demand for biomass to be used for energy purposes. That is in addition to the existing use for production of e.g. construction materials, pulp and paper, and even for more novel uses such as chemicals. Therefore, an important question is how much biomass resources will be available for bioenergy in the future.

Large quantities of carbon are fixed in the form of terrestrial and aquatic biomass each year. However, only a small proportion of this biomass is available for an energetic utilisation. First of all, not all growing biomass is accessible for harvesting and collection by current technical means and economic framework conditions. Secondly, as mentioned in the

introduction, several factors, like growth cycles, logistics, land or fertiliser use determine the sustainability of a certain feedstock.

Consequently, there is a distinction between technical potential, potential for energy and sustainable potential as subsequently defined:

Technical potential is the available biomass for all uses under current framework conditions with the current technological possibilities including existing harvesting techniques, infrastructure, and accessibility as well as processing techniques.

Economic potential is the proportion of the technical potential that can be exploited economically.

Potential for energy use is a proportion of the technical potential after satisfying other existing and projected competing uses of the same biomass feedstock.

Sustainable potential constricts energy potential based on sustainability criteria (i.e. carbon flux, land use, fertiliser use).

The technical potential can be assessed most easily and serves as a first indicator of the availability and geographic distribution of a specific feedstock. Several studies have calculated the domestically available biomass sources in Europe from 2020 onwards [19–23]. Generally, the results of different studies are difficult to compare, since the applied definitions of biomass potential, methodologies used, constraints for biomass potentials and the geographic scopes vary significantly. Therefore, the figures presented remain indicative:

Studies predict the technical biomass potential to range between 169 and 737 Mtoe. A meta-analysis by Faaji [19] concludes that a middle range potential for energy of 406 Mtoe could be achieved. This is in accordance with two other assessments that predict 411 Mtoe and 483 Mtoe of technical biomass potential by 2030 [20, 21].

This would be equivalent to about 25% of the gross available energy in the EU-28 [24] and provide room to almost triple current amount of bioenergy

in the European energy mix, which amounted to 144 Mtoe in 2017 [22]. Figure 2.1 shows the technical biomass potential, the potential for energy use and the sustainable biomass potential predicted for 2030 in the EU-28 countries. The bioenergy use in 2017 is shown for comparison.

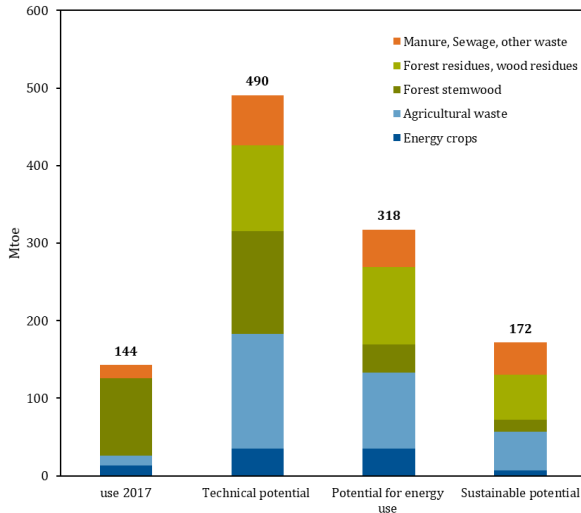


Figure 2.1: Gross inland energy consumption of biomass in 2017 and projected technical, energetic and sustainable potential in 2030 for EU-28 countries in Mtoe. Data from [21, 22]

Comparing the technical potential and the sustainable potential of biomass it becomes clear, that a sustainable growth in the bioenergy sector is limited. It can be observed that a large, currently unused potential is comprised of residues from agriculture and forestry. In contrast, additional resources from forest stem wood are limited. The predicted growth in theoretical biomass potential towards 2030 is attributed to improved forest management and the cultivation of energy crops on abandoned or unused land. Yet, the biomass potential for energy and the sustainable potential are much lower:

It should be noted that, already today, there is a mismatch between the available sustainable resources of wood in the EU and their current use. Currently, approximately 40 % of wood pellets used for bioenergy are being

imported from overseas diminishing the environmental advantage of their use [25, 26]. For a sustainable bioenergy provision, it is essential to rely on local resources, decrease the use of woody biomass and replace it with agricultural and other residues. Figure 2.2 shows the technical potential of biomass residues by origin in the EU-28, as determined by Elbersen et al. [20].

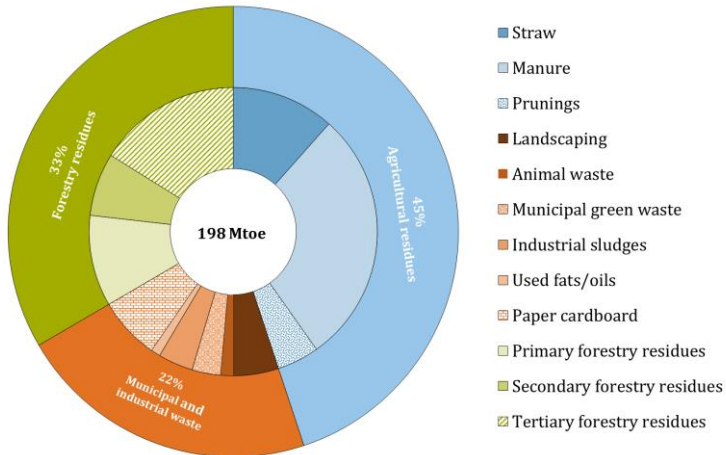


Figure 2.2: Contributions of different feedstock types and categories to EU-28 theoretical potential of biomass residues. Data from [20].

Agricultural residues are the most abundant resource within the technical residual biomass potential in Europe. Animal manure and cereal straw make up for the largest part of the theoretical potential. Forestry is the second largest source of residual biomass [20, 23]. Here, primary forestry residues are left over materials from logging operations - thinning or final felling (branches, tree tops, stumps, bark, sawdust, etc.). Secondary forestry residues are by-products and co-products of industrial wood-processing operation (black liquor, sawmill and other industrial residues.). Tertiary forestry residues are comprised of waste wood products after use in households or building sites [20]. Municipal and industrial waste account for 22 % of the technical residue potential with cardboard residues, landscaping material and biogenic municipal waste contributing the largest proportions.

Consequently, tapping into the potential of residual biomass feedstock is key for the future of a sustainable bio-economy. However, most of these biomass feedstock suffer from low bulk density, high moisture content, low calorific value and their highly hydrophilic nature. These properties pose multiple challenges on the energetic valorisation of such feedstock. Hence, pre-treatment steps are applied in order to upgrade the fuel quality and to facilitate an energetic use of these feedstock with the highest possible efficiencies.

2.2 Biomass Fuel Composition and Properties

The chemical structure of plant derived biomass consists of a variety of components that are of organic and inorganic nature. The main structural components are cellulose, hemicellulose and lignin. Considering the abundance of single elements one can classify major- (> 1.0 wt.-%), minor (0.1-1.0 wt.-%) and trace elements (< 0.1 wt.-%) according to their elemental concentrations on dry basis of feedstock [27]. Major elements in decreasing abundance are carbon (C), oxygen (O) and hydrogen (H). Minor elements include nitrogen (N), potassium (K), calcium (Ca), silicon (Si), magnesium (Mg), sulphur (S), phosphorous (P), chlorine (Cl) and sodium (Na). Trace elements typically include iron (Fe), aluminium (Al), manganese (Mn) and some heavy metals [27, 28]. This order can change due to the large variability of biomass that depends not only on type or part of the plant, but also on the growing location and harvesting season.

The composition of solid fuels can also be differentiated into organic and inorganic matter. Organic matter is combustible and yields the energy content of the fuel, whereas many challenges in thermal biomass utilisation are related to its inorganic content.

2.2.1 Organic Composition of Biomass

The organic matter of biomass typically consists of C, O and H bound in complex macromolecules. The basic organic components of biomass include the three main structural biopolymers cellulose, hemi-cellulose and lignin plus some extractives, lipids and proteins [28, 29]. The structure formed by

these components is called lignocellulose, which is a composite material responsible for the structural integrity of plant cells providing mechanical strength. Figure 2.3 illustrates the association of cellulose, hemi-cellulose and lignin in lignocellulosic structures.

Plant walls consist of cellulose micro fibrils, i.e. bundles of cellulose coated with hemi-cellulose and lignin deposits in between the fibrils. The strongly entangled components are chemically bound by non-covalent forces and covalent cross-linkages [29, 30].

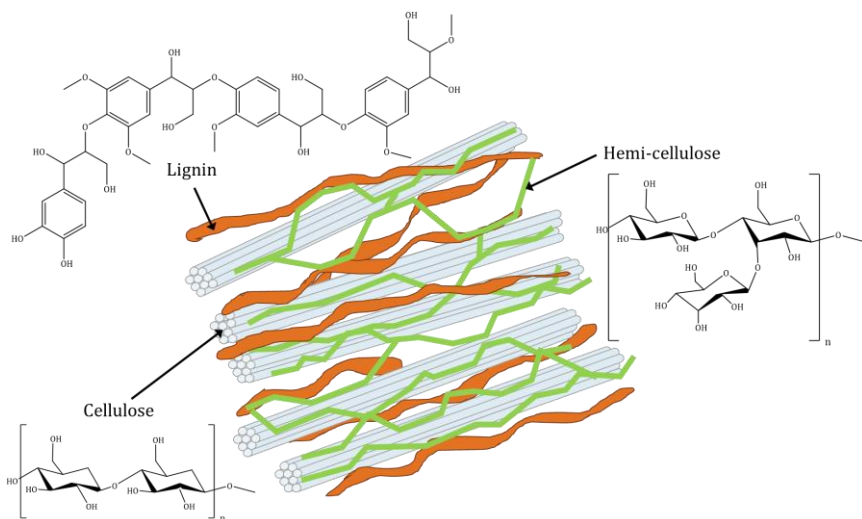


Figure 2.3: Schematic of the structure of lignocellulose. Adapted from [31, 32].

With a proportion of 40-80 wt.-% cellulose is the basic component of lignocellulose. It is a polymer which consists of D-glucose monomers that are linked by a β -1,4-glykosidic bond [29, 30]. Hydrogen bonds are formed between individual and neighbouring polymer chains, forming the above described cellulose micro fibrils that are of high crystallinity and possess high mechanical strength.

On the other hand, hemi-cellulose that accounts for 10-15 wt.-% of lignocellulose and is a disorganized, amorphous macromolecule. Hemi-cellulose consists of sugar molecules that form a heterogeneous and highly

branched polymer chain which are associated with poor interaction through hydrogen bonding and are ultimately responsible for the amorphous structure and low crystallinity of hemi-cellulose [29, 30].

The content of lignin, the third main component of lignocellulose is highly variable. Its structure is very different from that of cellulose and hemicellulose: It is a high molecular weight compound, consisting of aromatic alcohols that are strongly cross-linked via ether or carbon bonds in a three-dimensional network. Lignin is considered to be the main binder for fibrous components in plants. The lignin content is higher in biomass that is composed of tightly bound fibres such as woody biomass and is decreasing in the order softwood > hardwood > herbaceous and agricultural biomass [28, 29, 33].

Extractives are defined as compounds that are not an integral part of the biomass structure. They consist of various organic and inorganic components that are extracted by different solvents such as water or alcohols from biomass. According to Vassilev et al. [34] they include commonly various saccharides and other carbohydrates, proteins, hydrocarbons, oils, aromatics, lipids, fats, starches, phenols, waxes and inorganic materials.

2.2.2 Inorganic Matter in Biomass

Inorganic matter also plays a substantial role for the utilisation of biomass. After combustion of biomass, the solid residue is called biomass ash. It originates mainly from inorganic fuel constituents. Technical inefficiencies in biomass combustion are often ash-related, leading to deposit formation, corrosion and fine particle emissions. Therefore, understanding characteristics of inorganic matter in biomass is essential to overcome these challenges. Compared to the organic phase, it exhibits an even higher variability and constitutes between 0.1-46 wt.-% of biomass material [27].

The origin of inorganics in biomass can either be authigenic (formed in biomass mainly by plant growth), detrital (formed outside biomass but fixed

on/in it) or technogenic (inorganic materials introduced to biomass during harvesting, processing, etc.).

The concentration of individual elements depends on biomass type, growth environment, but also on physiological and morphological differences in plant structures. During growth plants acquire inorganics from the soil and air. Each plant part has a unique inorganic composition, depending on its functionality [35]. For instance, considering spruce, in branches K and Na levels are significantly increased compared to spruce stem wood and bark where Ca and Mg account for the major mineral phases [36]. Figure 2.4 shows the large variety of inorganic ash forming matter in biomass fuels investigated in this study with lignite and wood as a reference material.

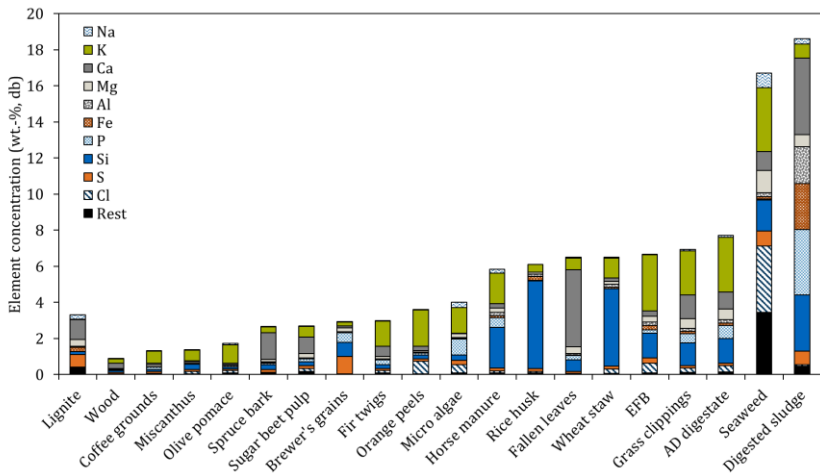


Figure 2.4: Ash forming elements in various biomass feedstock investigated in this study. Wood and lignite are shown as reference materials.

The most common inorganic elements in biomass are P, S, K, Mg, Ca and Cl that typically occur in concentrations ranging from 0.2-4.0 wt.-%. Inorganic elements like Fe, Mn, Zn, Cu, B, Mo, Cl and Ni with concentrations below 0.2 wt.-% are less abundant in biomass [35].

The most common approach to study technological and ecological challenges in biomass processing is to evaluate the concentration of

individual elements in biomass. However, such problems are more likely connected to the different phases and minerals in which these elements are present in biomass. Figure 2.5 shows a more advanced characterisation of inorganic - or ash-forming matter and its classification according to the way they are bound in the fuel.

These fractions can be obtained by a sequential leaching procedure, that was originally developed for coal by Benson et al. [37] and later adapted for biomass [38]. The method involves leaching of samples in increasingly aggressive solvents (water, 1 M ammonium acetate (NH_4Ac) and 1 M hydrochloric acid (HCl)), thus identifying in which modes the respective elements occur in the fuels.

1. Leachable salts that include inorganic matter dissolved in plant fluid, e.g. cation K^+ , Na^+ , Ca^{2+} , and anion Cl^- SO_4^- HPO_4^{2-} . These substances mostly remain water soluble after biomass drying (water fraction).
2. Organically bound matter: Inorganic elements associated with the organic matter of biomass. Mostly metal cations (K^+ , Na^+ , Ca^+ , Mg^{2+}) that are ion exchangeable with NH_4^+ are bound to anionic organic forms in the fuels; typically containing S, P and sometimes Cl (NH_4Ac fraction).
3. Minerals that are included in the fuel structure. In plants minerals originate from precipitation of Si as SiO_2 and Ca as Ca-oxalate during the growth process. Silica is insoluble while Ca-oxalate is dissolved in acid (HCl fraction).
4. External minerals are typically inorganics of technogenic origin from biomass harvesting and processing.

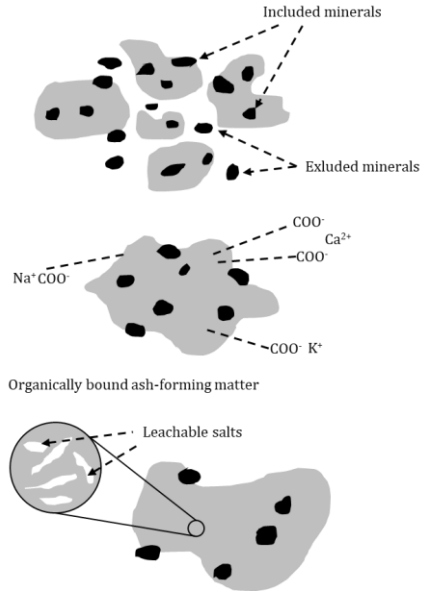


Figure 2.5: Forms of ash-forming matter. Adapted from [39].

Especially the two first classes of ash-forming matter in biomass are easily volatilised during combustion, making them available for reactions that contribute to the majority of ash-related challenges in biomass combustion [39]. Concerning the impact of pre-treatment on ash-forming matter, HTC that constitutes a conversion of biomass in water, should be easily capable of removing leachable salts from the biomass matrix. If structural changes induced by HTC also lead to the removal of inorganic species of the other classes is not known.

2.3 Technologies for Biomass Valorisation

Several pathways exist to access the energy contained in biomass fuels. The easiest way is a direct conversion of the biomass fuel by e.g. combustion or gasification. However, depending on the fuel characteristics this might not be the best option for all biomass resources. For example, high moisture feedstock requires an energy intensive drying step prior to combustion which limits the net energy output of a direct thermal conversion. Other

feedstock contain high proportions of sugars and are more efficiently converted via a biochemical pathway to yield higher added value products like ethanol. This chapter aims to provide an overview on the different energetic biomass utilisation options with a focus on thermo-chemical biomass conversion for the provision of solid fuels.

2.3.1 Overview

Bioenergy carriers are defined as fuels produced from biomass. As described in Section 2.1, they include biomass from forests, dedicated cultivation, residues and waste streams. They can be processed via different conversion routes. As depicted in Figure 2.6, biomass can be used to provide solid, liquid and gaseous fuels for power generation, transportation and heating in different conversion routes.

Besides direct utilisation by incineration, thermo-chemical conversions include processes that transform biomass into charcoal, pyrolysis oil, product gas and thermo-chemically treated solid biomass. Physicochemical conversion is mostly applied in the treatment of oilseeds for the provision of vegetable oil or biodiesel. Finally, bio-chemical conversion routes include anaerobic digestion of biomass to produce biogas from organic matter and the fermentation of sugar-rich feedstock into bioethanol [28, 40].

Worldwide 86 e.-% of biomass undergoes direct conversion by incineration, mostly for the provision of heat, and without any further processing [4, 11]. Also in developed regions like the EU, where modern biomass utilisation prevails, currently 63 e.-% of bioenergy stems from the utilisation of primary solid biofuels like wood chips or pellets [5]. Biofuels and biogas both account for roughly 9.5 % of bioenergy provided. The remaining share of 20 % originates from municipal and industrial waste.

The supply of primary solid fuels with sufficient quality for a direct conversion is limited. On the other hand, thermo-chemical pre-treatment technologies such as carbonisation or pyrolysis offer the possibility to upgrade fuel properties of biomass residues making them accessible for an energetic utilisation.

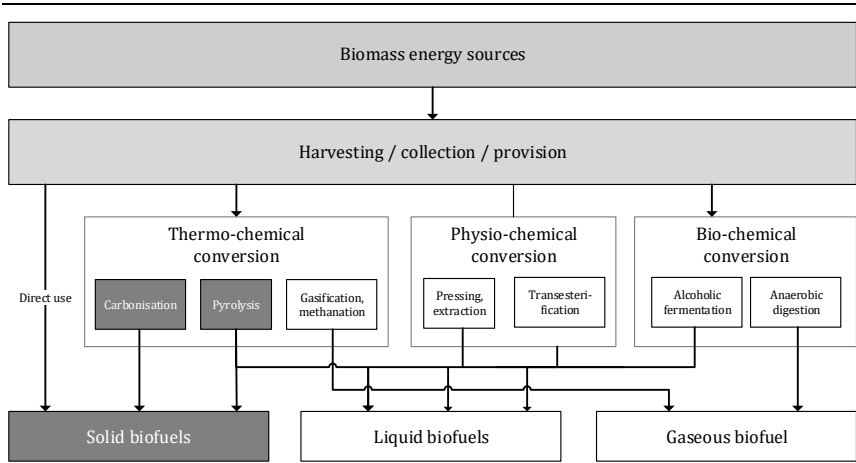


Figure 2.6: Conversion pathways of biomass energy resources to biomass energy carriers. Adapted from [40]

Bio-chemical conversion focuses on the conversion of sugars and often requires a dedicated cultivation of a feedstock. In contrast to that thermo-chemical conversion impose little feedstock requirements and can be applied to a broad spectrum of different substrates.

Hence, the focus of this work is on the thermo-chemical upgrading of biomass residues to solid fuels by hydrothermal carbonisation. Residue utilisation neither causes any additional land use, nor does it compete with food production. Additionally, methane-emitting landfilling can be avoided by tapping into the energetic potential of biogenic waste streams. In the following, thermo-chemical conversion technologies for the production of solid fuels from residues and competing technologies to HTC in the conversion of wet biomass streams will be considered in more detail. This includes feedstock requirements and fuel properties after upgrading.

2.3.2 Thermo-Chemical Biomass Pre-treatment

Biomass pre-treatment offers the possibility to modify undesirable properties of lignocellulosic biomass to improve their conversion efficiency and handling properties. Thermo-chemical pre-treatment are used to provide solid biofuels with characteristics more similar to those of fossil

coal. Compared to the starting materials (“white pellets”), these so-called black pellets have higher volumetric energy density, are less subject to biological degradation, are safer to transport and have water resistant properties. Three different technologies have emerged for the production of black pellets: Torrefaction, steam explosion and HTC. Table 2.2 presents an overview comparing the three different pre-treatment technologies.

Torrefaction

In torrefaction, biomass is heated in absence of oxygen at temperatures around 200-320 °C. During this mild pyrolysis, water content, cellulose sugars and other volatile organic compounds are removed from the biomass matrix [41]. More specifically, biomass undergoes dehydration and decarboxylation reactions that remove oxygen from the material. As a consequence, the carbon content of torrefied biomass is increased, leading to a higher energy density of the material. In addition, torrefied biomass is more brittle and hydrophobic. Compared to the starting material, the ash content of torrefied material is increased due to the volatilisation of organic material during torrefaction [42]. Thus, to extract problematic ash components from the feedstock, a washing step has to be conducted prior or after the torrefaction treatment. Typically mass yield after torrefaction is around 70 %. However, this value strongly depends on process condition and feedstock. Values ranging from 43 to 91 % have been reported [43].

Apart from the solid biochar, the torrefaction process produces combustible off-gas, which can be used to cover most of the thermal energy needed. However, for an energy efficient torrefaction process, the feedstock moisture content should not exceed 10 wt.-% when entering the main torrefaction zone [44]. Most feedstock do not meet this requirement and often an energy intensive drying step is needed prior to torrefaction.

Table 2.2: Overview on the three thermo-chemical pre-treatment methods explored.

Method	Torrefaction	Steam explosion	HTC	Ref.
Short description	thermal treatment in oxygen-deficient atmosphere	steaming of biomass at high pressures, followed by explosive decompression	thermal treatment in water at elevated temperatures and pressures	
Process conditions	T = 200-320 °C p = atmospheric $\tau \approx$ minutes	T = 160-280 °C p = up to 20 bar $\tau \approx$ seconds to minutes	T = 180-300 °C p = 20-100 bar $\tau \approx$ minutes to hours	[44, 45]
Typical mass yield	70 %	90 %	65 %	[44, 45]
Product properties				
Carbon Content	increased	slightly increased	strongly increased	[45]
HHV	increased	slightly increased	strongly increased	[45]
Grinding energy	lowered	lowered	lowered	[45-48]
Outdoor storage	possible	possible	possible	[42, 49]
Hydrophobic	yes	yes	yes	[42, 45, 49]
Bulk density	decreased	decreased	decreased	[46-48]
Pelletization	aggravated	facilitated	facilitated	[45, 50, 51]
Impact on ash properties	increased ash content no compositional changes	no compositional changes, slightly decreased ash melting temperature	decrease of alkali and chlorine content, higher ash melting temperature	[45, 52]
Feedstock moisture	< 10 wt.-%	8-10 wt.-%	> 40-85 wt.-%	[44]

Steam Explosion

A pre-treatment by steam explosion involves steaming of biomass for 5-25 min at elevated pressure (1-20 bar) and temperature (160-280 °C) followed by a release of the hot and softened biomass to a lower pressure [53–55]. The expanding steam breaks the structure of the biomass, which is origin of the wording “steam explosion”. The extent to which the biomass structure is disintegrated depends on temperature and residence time. During steam explosion, hemi-cellulose as well as acetic acid is released from the biomass which results in partial hydrolysis the biomass structure. Further, lignin partly depolymerizes and the released sugars combine to so-called pseudo-lignin, which spreads over the biomass surface and forms a strong moisture repelling coating [56]. Prior to steam explosion the feed is usually dried to a moisture content of 8-10 wt.-% to reduce the consumption of steam during the steaming phase. The obtained mass yield after steam explosion of wood and bark is around 90 %. Overall, steam exploded biomass is durable, water resistant, easy to grind, and has a higher energy density compared to the raw material [45, 48, 57].

The method is established as a pre-treatment method in second generation bioethanol production [53, 58, 59]. In the production of solid fuels steam explosion is mostly applied to upgrade woody biomass. Recently, also residual biomass feedstock such as bark, forestry residues and have been used [45]. Steam-explosion of straw and other agricultural residues is mostly applied in bio-refinery processes.

Hydrothermal Carbonisation

In HTC biomass is suspended in water and heated to temperatures around 180-300 °C. Pressure is applied to keep water in the liquid phase. During the treatment, the material undergoes a similar transformation as during natural coalification, only much faster. Similar to torrefaction, these transformation yields a solid that has a higher carbon content, energy density, is more brittle and more hydrophobic. In comparison to other thermal treatment methods, HTC allows direct conversion of wet biomass without any pre-drying of the feedstock. After hydrothermal conversion, the

solid product can be mechanically dewatered to about 35 wt.-% moisture [60, 61], saving a considerable amount of energy compared to drying prior to a direct conversion. A rough calculation taking into account mass loss, energy densification and thermal energy need for HTC shows, that HTC is energetically favourable to drying if the feedstock moisture exceeds 60 wt.-% [15]. Another advantage arises from a pre-treatment in water: Species active in corrosion, slagging and fouling such as chlorine and alkali metals are often present as water-soluble compounds that can be removed with the process water. Yet, the treatment in water also causes the biggest challenges the technology faces. Per ton of hydrochar produced approximately 2 m³ [62–64] of waste water is generated that is highly contaminated with organic matter and needs to be treated at a cost.

To sum up, all of the tree pre-treatment technologies yield fuels that, in comparison with the raw material, have increased carbon content and HHV, require less grinding energy, are more hydrophobic and therefore storable. Pelletisation is facilitated for steam-exploded and HTC treated biomass, while torrefied pellets are less stable. Torrefaction and steam explosion both have little effect on ash composition and are most effective in the treatment of dry feedstock. HTC on the other hand is effective in the conversion of wet feedstock and fundamentally changes the ash properties of the fuel.

2.3.3 Technologies for the Conversion of Wet Feedstock

Besides HTC, also biochemical conversion technologies are well suited for the conversion of wet feedstock. The most prominent technology is anaerobic digestion (AD). During AD, organic matter is decomposed to biogas by various anaerobic microorganisms in the absence of oxygen. Biogas consists mainly of methane, carbon dioxide and small amounts of other gases [65]. The produced biogas is used in small CHP units or is fed to the natural gas grid after upgrading. Two process variations exist: The widespread wet anaerobic digestion, that is easily scalable and treats a slurry of biomass in water and dry fermentation, which is a simpler and robust, small-scale technology, where biomass is piled up and biologically

converted in gas-tight fermenter boxes [65]. Today, AD is used as a waste management technology in the treatment of waste water, municipal solid waste and manures. Often also substrates from dedicated cultivation like maize, whole plant silage, sugar beet, grass silage are used in biogas plants.

In principle, all biogenic material is suitable for AD. However, the obtained biogas yield, and thus carbon efficiency, of the process is heavily dependent on the feedstock composition. Generally, the higher the proportion of easily degradable organic substances such as fats, proteins and carbohydrates in the substrate, the more methane can potentially be produced by AD [66]. Fibrous substrates with high concentrations of poorly degradable carbon compounds such as lignocellulosic biomass is unsuitable for AD because they are highly resistant towards a fast biological degradation by bacteria [67, 68]. For example, AD of food waste achieves carbon efficiencies of around 60 %, while for straw (27 %) or fallen leaves (12 %) it is considerably lower [69].

Compared to HTC, the conversion temperature in AD is much lower. AD is a mature technology that is widely applied, especially in Germany. On the other hand, the required time for the conversion is longer. Thus the throughput is lower and land requirement higher in AD. Table 2.3 provides an overview on key characteristics, advantages and disadvantages of wet AD, dry fermentation and HTC. Consequently, AD is usually the preferred treatment technology for moist biomass that contains high amounts of sugar, fats and proteins. For example, biogenic municipal waste or residues from food industry are often treated by AD or dry fermentation.

On the other hand, in cases where a high throughput is needed and limited space is available, like in metropolitan areas, HTC could be considered as a suitable alternative treatment technology to AD. While being a technology still in the research and development phase, HTC offers a high input flexibility and can be used to treat a wide range of different feedstock, including lignocellulosic biomass.

Table 2.3: Technologies for the energetic valorisation of wet biomass feedstock.

	Anaerobic digestion	Dry fermentation	HTC	Ref.
Substrate requirements	Liquid substrate, biodegradability	Biodegradability	None	[68, 70]
Feedstock moisture	> 80 wt.-%	60-85 wt.-%	> 40-85 wt.-%	[44]
Temperature	35-37 °C (mesophilic) 55-70 °C (thermophilic)	34-38 °C	180-250 °C	[71, 72]
Treatment time	15-30 d	4-5 d	1-8 h	[72]
Carbon efficiency	57 % (food waste) 27 % (straw)	-	50 % (food waste) 80 % (straw)	[69]
Products	Biogas, heat, Power	Biogas, heat, power, compost	Biochar	
Space requirement	0.31 m ² t ⁻¹ a ⁻¹		0.16 m ² t ⁻¹ a ⁻¹	[73, 74]
Advantages	Mature technology, low capital investment, reduces water pollution	Mature technology, fuel flexibility, reduced water usage	No substrate requirements, high throughput, low space requirements	
Disadvantages	High space requirement, low throughput	Difficult inoculation of new substrates, low throughput, high space requirement,	New technology, wastewater treatment	

While AD can be seen as a competing technology to HTC in the treatment of wet feedstock both technologies could also complement each other: As described above, the biological treatment of lignocellulosic biomass is strongly limited due to the recalcitrant structure of these substrates. Typically, biomass hydrolysis becomes the rate-limiting step during traditional AD [75]. Thermo-chemical and physical pre-treatment are considered as a way to enhance the digestibility of lignocellulosic biomass [76, 77]. Among others, milling, steam explosion and hot water

washing have been applied with the goal to facilitate biological conversion of lignocellulosic biomass by a disruption of the complex biomass structure that increases porosity and reduces overall crystallinity of the material.

HTC is also a potential candidate to be integrated with AD increasing the energy recovered from a feedstock. One possible strategy is to subject biomass to a low temperature HTC treatment to hydrolyse the substrates [78]. Afterwards the entire HTC slurry including hydrochar and process water is fed to the AD plant. Another possibility is to separate process water and hydrochar and to only subject HTC process water to AD [79]. The separated hydrochar can be used as solid fuel or in other applications. HTC alters the biomass structure and also leads to the solubilisation of considerable amounts of organic material in the process water. This organic fraction is readily digestible and can bypass the hydrolysis stage of AD. The applicability of HTC process waters in AD has been proven by a range of studies for different feedstock, including lignocellulosic materials [79–84].

3 Hydrothermal Carbonisation

This chapter discusses hydrothermal carbonisation (HTC) as a pre-treatment technology for biomass fuels in more detail. First the fundamentals of HTC and related processes are discussed, followed by a brief summary of governing conversion paths as well as the characteristics of solid, liquid and gaseous products from the process.

3.1 Fundamentals of Hydrothermal Processes

The term hydrothermal is used to describe processes that involve hot water under pressure. It originates from the scientific fields of geochemistry and mineralogy, but is also used to describe technical processes using such conditions. In biomass conversion three hydrothermal processes are applied [85, 86]:

- **Hydrothermal Carbonisation (HTC).** Hydrothermal carbonisation is generally conducted at conditions below the critical point of water, i.e. temperatures below 647 K and pressures above the respective vapour pressure of water. Biomass is subjected to heating and partial pyrolytic decomposition. The presence of water favours hydrolytic reactions. The main goal of the process is to provide a solid product.
- **Hydrothermal Liquefaction (HTL).** Hydrothermal liquefaction is typically conducted under subcritical conditions in proximity of the critical point. Compared to HTC, the applied pressures are higher in HTL. Biomass is subjected to heating and partial pyrolytic decomposition. The presence of water favours hydrolytic reactions. The main goal of the process is to provide a liquid product.
- **Hydrothermal Gasification (HTG).** During hydrothermal gasification biomass is subjected to supercritical conditions where it is heated, pyrolytically decomposed and gasified. The aim is a complete conversion of biomass to product gas.

Figure 3.1 shows the typical conditions of the three processes in the p, T phase diagram of water.

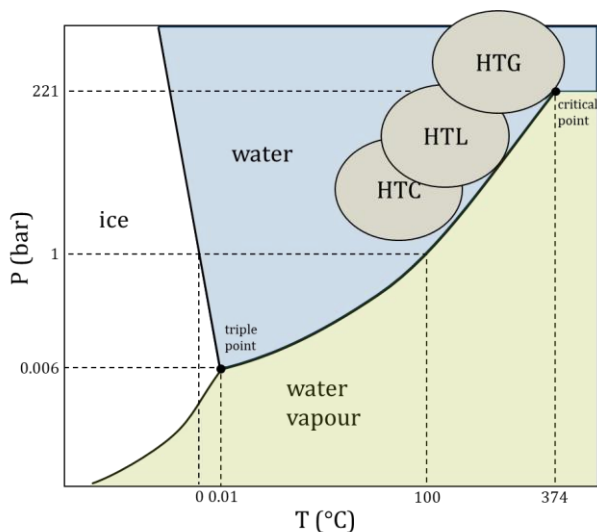


Figure 3.1: Phase diagram (p,T) of water and related hydrothermal processes. Adapted from [87].

Water properties under hydrothermal conditions

Under hydrothermal conditions, the properties of water are changed significantly. Water density under HTC- and HTL condition is lower than under ambient conditions, approaching similar densities as liquid hydrocarbons [88]. In the proximity of the critical point and under supercritical the density of water is decreasing even further. The specific enthalpy is increasing with increasing severity of hydrothermal process conditions. The specific heat capacity of water reaches a maximum under near-critical conditions. Dynamic viscosity also decreases from HTC to HTG conditions. Finally, the relative dielectric constant of water ϵ_R , which is a measure of the solvent polarity. This constant drops sharply at HTC conditions, where the polarity of water lies in the range of glycerol. Increasing process severity leads to a further decrease in ϵ_R . Specifically, at HTL conditions ϵ_R corresponds approximately to acetone and at HTG conditions, ϵ_R approaches values of weakly polar (e.g. diethyl ether) up to

non-polar solvents (e.g. n-hexane) [88]. Moreover, at HTC and HTL conditions the ion product of water is several times higher than at ambient conditions. That means that under these conditions the concentration of protons and hydroxide ions is greatly increased, which in particular accelerates hydrolysis reactions without the need of acidic or alkaline catalytic additives [85]. Table 3.1 summarizes the properties of water under hydrothermal conditions corresponding to HTC, HTL and HTG.

Table 3.1: Physical properties of water in different temperature and pressure regimes [89, 90].

	Ambient Conditions	HTC	HTL	HTG
Temperature (°C)	25	200	330	400
Pressure (bar)	1	20	200	300
Density (kg m⁻³)	997	865	667	357
Spec. Enthalpy (kJ kg⁻¹)	105	852	1506	2153
Heat capacity (J kg⁻¹ K⁻¹)	4181	4493	6268	25868
Dynamic Viscosity (Pa s)	8.9·10 ⁻⁴	13.4·10 ⁻⁵	7.8·10 ⁻⁵	4.4·10 ⁻⁵
Ion product (mol² kg⁻²)	1.0·10 ⁻¹⁴	7·10 ⁻¹⁴	1.8·10 ⁻¹²	1.7·10 ⁻¹⁵

3.2 Main Reaction Pathways during HTC

The most important hydrothermal process for the production of solid fuels is HTC. The main reaction pathways during HTC are based on the conversion of plant-derived biomass and its major constituents. Although the application of HTC is not limited to these type of feedstock, the majority of available biomass residues originate from plants or mixtures that contain a large proportion of plant material. Therefore, the studies discussed in the following chapter focus on the conversion of the three main components of lignocellulosic biomass, namely hemi-cellulose, cellulose and lignin. The discussed reaction mechanisms can also be applied to non-lignocellulosic feedstock such as sludges or algal biomass.

During HTC, organic biomass constituents undergo a complex series of many different reactions [91]. Figure 3.2 shows a simplified scheme of the chemical processes during HTC. Hydrochar formation proceeds through two main reaction pathways A and B. Pathway A comprises solid-solid reactions and intramolecular condensation reactions that lead to the

formation of so-called primary char. Following pathway B, hydrochar formation proceeds through biomass degradation and polymerisation of solved intermediates to so-called secondary char. More stable biomass constituents like lignin preferably react according to pathway A, whereas carbohydrates react to hydrochar preferably according to carbonisation route B.

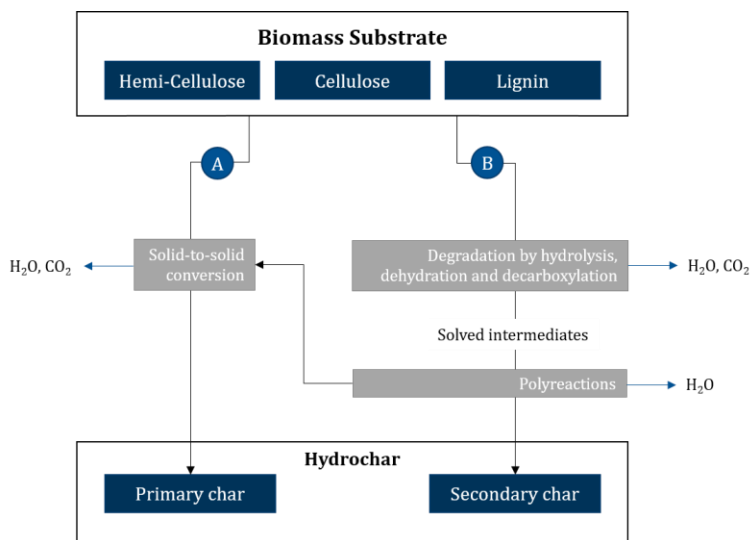


Figure 3.2: Simplified representation of the chemical processes during hydrothermal carbonisation. Adapted from [91].

Although the exact reaction network of HTC is not yet fully understood and is subject of current research, general reaction mechanisms have been identified: It has been shown that main HTC reaction mechanisms comprise hydrolysis, dehydration, decarboxylation, polymerisation and, to some extent, aromatisation [30, 92]. These fundamental reaction steps are explained in more detail in the following:

Biomass degradation primarily occurs through hydrolysis reactions, which destroy a large part of its physical structure. Hydrolysis predominantly splits ether- and ester-bonds in the plant matrix. Thereby plant biopolymers are extracted and degraded. Aside from carbohydrates, lignin is also partially hydrolysed [30, 92].

Dehydration takes place by the elimination of hydroxyl groups from the biomass matrix and by acid-catalysed reactions that lead to the formation of furfural and hydroxymethylfurfural (HMF) from monosaccharides [30, 87, 92]. The latter reactions are auto-catalysed due to the formation of acidic by-products. Decarboxylation (CO_2 elimination) and decarbonylation (CO elimination) are also typical reactions during HTC that dissolve, decompose and convert biomass constituents further [92].

Some of the fragments formed during biomass degradation are highly reactive and undergo subsequent polymerization and condensation. Depending on the degree of polymerization, the substances either occur dissolved or form fine solid particles. As the poly-reactions progress, more and more solids are formed or react with the remaining solid leading to solid biochar formation [30, 87].

All in all, the above-mentioned reactions lead to the formation of a material that exhibits a higher carbon content than the starting material. The reduction of oxygen results approximately 70 % from dehydration and approximately 30 % from decarboxylation [93]. The degree and reaction processes of the coalification occurring during HTC can be determined using a so-called van-Krevelen diagram as depicted in Figure 3.3. Based on the elemental analysis of a solid fuel, its H/C molar ratio is plotted versus its O/C molar ratio. As the conversion progresses, the H/C to O/C ratio moves from the top right (input material) to the bottom left. Figure 3.3 also shows data from the hydrothermal conversion of rice husk and grass cuttings which corresponds to the orange line, which shows the theoretical carbonisation pathway of a carbohydrate. To illustrate further, the reaction lines of dehydration and decarboxylation (according to [94]) and the theoretical range of the natural coalification, starting from cellulose via peat, lignite, hard coal to anthracite, are also depicted in Figure 3.3.

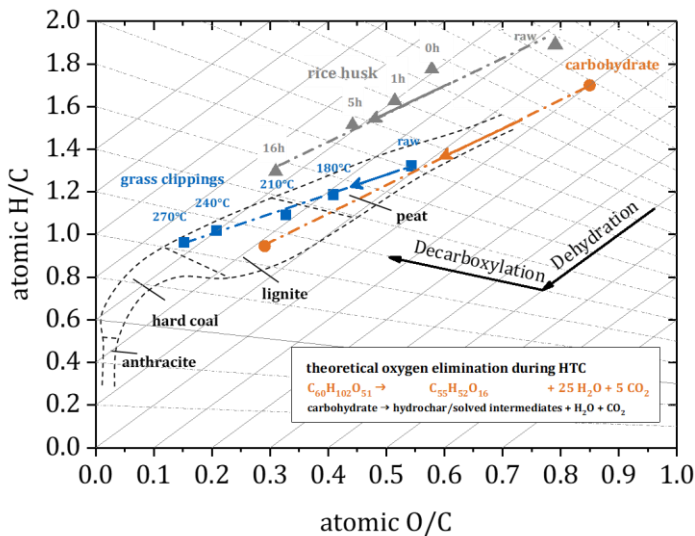


Figure 3.3: Examples for the hydrothermal conversion of grass cuttings and rice husk for different process parameters (T, τ) in a van-Krevelen diagram. Theoretical elimination scenario of carbohydrates and typical ranges of H/C and O/C ratios of fossil solid fuels. Adapted from [61]. Data for rice husk from [17].

3.3 Main Influencing Process Parameters

This section describes the main parameters influencing HTC. Reactor design, mixing behaviour and heating rate are of minor importance for reaction engineering in HTC and are therefore not discussed herein.

Temperature: Temperature is one of the main influencing process parameters in HTC. A higher reaction temperature is known to increase the reaction rate of degradation and polymerisation reactions [95]. Further, reaction temperature governs the onset of the degradation of key components such as cellulose, hemicellulose and lignin. Characteristic temperature regimes of HTC are 150 °C where the decomposition of carbonyl groups starts and 180 °C, 200-230 °C and 220-260 °C where hemicellulose, cellulose and lignin degradation occur [30, 70, 96]. According to van't Hoff's law, the reaction rate doubles upon a temperature increase of

10 K. Consequently in HTC, the degree of carbonisation, i.e. the carbon content increases with increasing reaction temperature [71, 93]. Most HTC processes work with maximum temperatures of 250 °C. This allows the conversion of biomass to hydrochar with a maximum carbon content of about 70 wt.-% (db) and a higher heating value above 30 MJ kg⁻¹(db).

Residence time: Typical residence times for HTC in scientific studies lie in the range of 30 min up to 72 h. The influence of residence time on the reaction intensity can be described by equation (3.1) developed by Ruyter [93].

$$f = 50 \cdot \tau^{0.2} \cdot e^{-\frac{3500}{T}} \quad (3.1)$$

The calculation of the reaction intensity f is based on Arrhenius law and is calculated using reaction temperature T in Kelvin and residence τ in seconds. This approach shows that the reaction temperature (T) has a much greater influence on the conversion than the reaction time (τ). Shorter residence times facilitate higher reactor throughput, although they can also impose kinetic limitations [97]. As described in Section 4.2, the carbonisation proceeds via first stage reactions such as hydrolysis, dehydration and decarboxylation and second stage reactions that include polymerisation and aromatisation of the hydrolysed and dehydrated fragments that were created in the first stage. While the first stage reactions occur fast, the second stage reactions are slower. Hence, the advantage of longer residence times is that they promote polymerisation and aromatisation of the fragments in the liquid phase and thereby enhance the obtained mass yield [98].

Liquid-to-solid ratio: The liquid-to-solid ratio (L/S ratio) plays a decisive role, ensuring that a liquid aqueous phase is present during HTC. A high L/S ratio, leads to a high proportion of dissolved organic and thus to a lower mass yield of hydrochar [96]. For an efficient conversion, L/S ratio should be as low as possible, while still ensuring that the biomass is fully submerged in water and forms a mixable slurry. The common range of L/S ratio on mass basis during HTC is 1-10.

pH value: An acidic pH value below 3 catalytically accelerates carbonisation [95]. However, for the optimisation of a technical HTC process it is questionable if a strong reduction of pH is reasonable. The addition of acid is an additional cost factor and potentially leads to corrosion of equipment. Moreover, an economic acid dosing is not trivial since during HTC also buffering compounds like CO₂ and NH₃ are formed.

Particle size: Compared to HTL and HTG, HTC is characterised by a relatively slow chemical conversion. Hence, mass transfer limitations only play a role for short HTC times in the range of seconds to a few minutes [99, 100]. Particle size becomes more important in process engineering of HTC: For example during a continuous HTC operation, particle size is often reduced to below 2 cm for a reliable conveying and reactor feeding process, while batch processes are favoured for larger particle sizes.

Pressure: Pressure does not influence the product characteristics in HTC. Although the reaction pressure influences the reaction network according to Le Chatelier's principle, the effect has been proven to have a low impact on hydrothermal carbonisation and natural coalification [70, 101–104]. Still, the pressure must be high enough to ensure the presence of a liquid water phase during the process. Most of the time a pressure slightly above the water vapour pressure at the given temperature is chosen for HTC. A process variant of HTC is the so-called vapothermal carbonisation (VTC). VTC takes place in saturated vapour conditions, where the pressure of the reactor is set on the vapour pressure of water at the respective reaction temperature.

3.4 HTC Product Properties

Hydrothermal carbonisation yields solid, liquid and gaseous products. A qualitative mass balance on dry basis is shown in Figure 3.4. The exact quantity and composition of the individual products is strongly dependent on feedstock and process parameters.

In HTC, the main product is the solid hydrochar which contains about 50-65 wt.-% of the input material. The majority of mass losses are attributed to

water elimination by dehydration reactions during HTC (cf. loss H_2O in Figure 3.4) [30, 92].

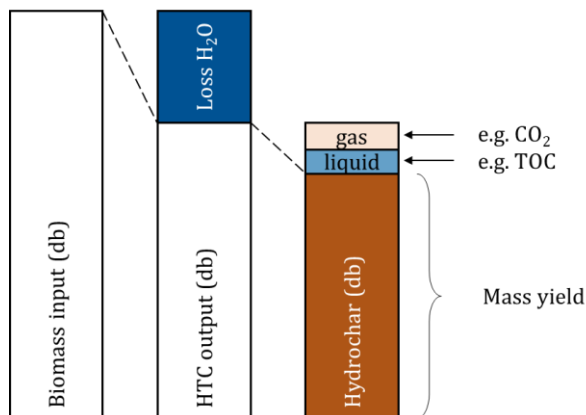


Figure 3.4: Qualitative HTC mass balance. Adapted from [61].

Liquid products are mostly comprised organic compounds that are extracted from the biomass matrix or formed during HTC [30]. The gaseous products consist mainly of CO_2 from decarboxylation reactions [105]. A qualitative energy balance is discussed in section 4.3. In the following sections the composition and physio-chemical characteristics of the solid, liquid and gaseous HTC products are described in more detail.

3.4.1 Solid Product

The main product of HTC is the solid hydrochar. As introduced in Section 4.2 two types of hydrochar are formed during carbonisation: primary hydrochar by dehydration and decarboxylation of biomass structures and secondary hydrochar that is formed by the polymerisation of solved intermediates. While the structure of primary hydrochar is similar to the structure of the respective substrate, secondary hydrochar comprises small coke particles that form larger coke structures at higher temperatures. Unsurprisingly, these structural and compositional changes lead to fundamentally altered properties of the material.

Compared to the substrate hydrochar has an increased carbon content and energy density. Depending on the process conditions, the higher heating value of the fuel can be increased by up to 60 %, mostly on the account of a higher carbon content of the hydrochar. Higher reaction severity, i.e. higher temperature and residence time, leads to a higher degree of coalification and lower volatile content. On the other hand, higher reaction temperatures decrease mass yield due to dissolution of organic material in the water phase.

Another essential property of hydrochar is its dewatering behaviour. After HTC, a slurry of hydrochar in water is obtained. To recover the solid product it has to be separated from the liquid phase which is usually done by mechanical dewatering followed by a thermal drying step. HTC causes a decrease in oxygen containing functional groups. This reduces the amount of inherent moisture which is defined as the water moisture that is not readily removable by mechanical methods, chemically bound to the particle, and which is a part of the particle [60, 106]. Consequently, after mechanical dewatering considerably lower water contents can be observed when comparing hydrochar to the raw material. Depending on feedstock, applied pressure and temperature, the water content of HTC fuels can be reduced to 30-50 wt.-% by mechanical dewatering [60, 61]. For comparison, the moisture content of untreated biomass after mechanical dewatering typically lies in the range from 60-70 wt.-% [61, 107]. Thus, process heat demand for the drying step declines substantially.

Table 3.2: Impact of the hydrothermal conversion of biomass the properties of the solid product.

Impact	Explanation
Reduction of the mass yield with higher HTC temperature	Conversion of organic matter to H ₂ O, CO ₂ and solved organic intermediates
Relative increase in carbon content	The elimination of O and H from organic biomass matrix prevails over the elimination of C, thus despite CO ₂ elimination, the C-content increases.
Increase in calorific value	Shift of the elemental composition (decrease in O, H) towards components like C, that improve combustion enthalpy
Improved stability	Conversion of volatiles, increase in and formation of fixed carbon.

Furthermore, hydrothermally carbonised biomass possesses higher chemical and biological stability than untreated biomass [15]. They are therefore less susceptible for microbial degradation and impose less requirements on storage and handling [15, 108].

3.4.2 Liquid and Gaseous By-products

Aside from hydrochar, also liquid and gaseous by-products are produced from the hydrothermal conversion of biomass by HTC. Currently, the further utilisation and treatment of process water from HTC poses one of the main challenges in the commercial use of the technology. In the following section, previous research on the characterisation of process water constituents as well as the composition of gaseous product emerging from HTC will be summarised.

Process water containing liquid by-products of HTC is obtained after HTC of biogenic material. It is estimated that per ton of hydrochar approximately 2 m³ of effluent is produced [62–64]. The exact amount of process water arising primarily depends on the moisture content of the substrate treated, the extent of conversion of the substrate by HTC, the use of additional water in mixing and heating (i.e. by steam-heating). A higher water content and a stronger dehydration of the substrate leads to larger amounts of process water generated. Furthermore, if external water sources are needed for the mashing of the biomass-water mixture, the amount of process water increases. On the other hand, the amount of process water can be reduced if relatively low-moisture biomass is used and/or mixed with recycled process water.

The quantitative composition and characteristic properties are determined by feedstock type and applied process conditions. Depending on the feedstock, biomass constituents differ in their solubility, extraction and conversion behaviour, which results in different molecular transitions to the process water [61].

Qualitatively, process water contains mainly organic compounds and inorganic trace substances, which are summarised in Table 3.3. Organic

substances include organic acids, dry residues and aromatic aldehydes. Typical values for the total organic carbon (TOC) concentration in process water, are estimated at values between 4-32 g l⁻¹, of which 30-50% of is present in the form of organic acids [109]. The chemical oxygen demand (COD) lies in the range of 4.9-73.8 g l⁻¹. COD is a measure of the quantity of all oxidisable species in waste water and can therefore be used to quantify the amount of pollutants. Biological oxygen demand (BOD_x) indicates the amount of oxygen that microorganisms consume in a water sample at 20°C during a specific period *x* in days. Often BOD₅ is used to characterise the amount of organic matter that can be decomposed by the organisms and is therefore bio-degradable. BOD₅ of HTC process water possesses is highly variable and in the range of 1.7-42 g l⁻¹.

Table 3.3: Characteristics and composition of process water from hydrothermal carbonisation after filtration. Data from [61, 69, 105, 110-113].

Parameter	Unit	Range
pH-values	pH	-
Electrical conductivity	EC	mS cm ⁻¹
Total organic carbon	TOC	g l ⁻¹
Chemical oxygen demand	COD	g l ⁻¹
Biological oxygen demand	BSB ₅	g l ⁻¹
Filterable substances		g l ⁻¹
Acetic acid		g l ⁻¹
Propionic acid		g l ⁻¹
Glycolic acid		g l ⁻¹
Levulinic acid		g l ⁻¹
Formic acid		g l ⁻¹
Phenol		g l ⁻¹
Furfural		g l ⁻¹
HMF		g l ⁻¹
Glucose		g l ⁻¹

The formed aromatics can have environmentally harmful properties and contribute significantly to the toxicity of the process water. The conversion of biomass constituents, cellulose, hemicellulose and lignin lead to the

formation of aromatic aldehydes like furfural or 5-hydroxyl-methylfurfurale (5-HMF) and phenols [109, 114–116].

With increasing temperature and residence time, i.e. conversion, the concentration of furfurals and HMF decreases, while the concentration of acids and phenols increases. Hence, HMF and furfurals are believed to be intermediates in biomass decomposition that further decompose to acids and phenols [109, 114–116]. pH value of process water from the conversion of lignocellulosic biomass are in the range of 3.7-5.6 due to the formation of organic acids. pH can also be higher than 7 for biomasses with a pronounced buffer capacity, like sewage sludge or residues from anaerobic digestion [85]. Electrical conductivity is feedstock dependent and lies in the range of industrial waste water from 5-26 mS cm⁻¹.

Gases are a minor by-product from HTC. Their proportion in the product distribution from solid, liquid and gaseous products increases with increasing reaction severity. Only at high treatment temperatures above 275 °C their share in the product distribution exceeds 10 wt.-% [117, 118]. CO₂ is the dominant gaseous species, typically accounting for 70-95 % emerging gases from HTC. The second most abundant species is CO. The remaining trace-gases comprise hydrogen and some low molecular hydrocarbons.

4 State of the Art in Research and Technology of Hydrothermal Carbonisation

During the last years an increasing amount of scientific studies have investigated HTC as a conversion technology for residual biomass feedstock. The considered applications for the resulting solid products cover energetic as well as material use. Consequently, most studies focus on the reaction mechanism and influence of HTC on structure, morphology and chemical functionality of the hydrochars. As presented in the previous chapter the transformations of the organic phase during HTC and associated fuel properties are well known today. The transformation of the inorganic matter in biomass during HTC has been studied to a much lesser extent. The presented work studies HTC as a technology for the provision of solid fuels from residual biomass streams. This covers considerations for the selection of suitable feedstock for HTC, fuel quality assessment as well as an economic classification of the technology. A focus is placed on the impact of HTC on fuel properties relevant for biomass combustion. Challenges in biomass combustion are often ash-related, thus the fate of inorganic elements during HTC and ash properties of HTC fuels are studied in detail. The quality of HTC fuels is assessed with the help of fuel indices. The following chapter therefore summarises recent work on the fate of inorganic elements during HTC and the application of fuel indices for prediction of challenges in biomass combustion. In addition, an overview on commercial HTC projects and techno-economic studies of the technology is provided.

4.1 Fate of Inorganics during HTC

HTC not only alters the organic structure of biomass, but also largely affects the ash composition by leaching of inorganics to the process water. The extent to which inorganics can be removed from the feedstock by HTC is determined by the nature of the inorganic matter: Ash forming elements in biomass exist in different forms e.g. as soluble ions, organically associated, as included minerals or as excluded minerals [39, 119]. Washing and HTC

have been proven to be effective in reducing the amount of soluble inorganics like alkalis and Cl [46, 52, 97, 120–127].

Compared to water washing, several factors promote the removal of inorganic species from the feedstock during HTC: HTC breaks down structural biomass components like hemi-cellulose and cellulose that contain a large proportion of inorganic biomass species, facilitating their dissolution [13]. Additionally, water under hydrothermal conditions has a lower density, viscosity and decreased polarity compared to water at ambient pressure and temperature [128]. Thus, the dissolution of inorganics with different solubility is possible.

Only few studies have investigated the effect of HTC on the fate of inorganics. Table 4.1 provides an overview on the investigated feedstock, process conditions and findings of these studies. Reza et al. [46] have investigated the influence of HTC temperature on the ash composition of corn stover, miscanthus, switch grass, and rice hulls. They found that calcium, magnesium, sulphur, phosphorous and potassium can be reduced by up to 90 % during HTC, which they linked to the decomposition of hemi-cellulose. Silicon is removed to a low extent at higher temperatures. Smith et al. [52] have investigated the influence of feedstock on the combustion behaviour of hydrochar. They observed a significant reduction of alkali metals. Smith et al. [97] have also investigated the influence of residence time on the inorganic composition of miscanthus and concluded that the extraction of some inorganics like sulphur and phosphorous is decreasing with increasing residence time. They confirmed that also for miscanthus more than 75% of alkali metals are removed from the feedstock after HTC treatment. Ekpo et al. [120] compared the distribution of inorganic contents in the liquid and solid phases after thermal hydrolysis, HTC, HTL and HTG. Investigated feedstock included manure, micro algae and digestate from AD. They observed that phosphorous levels in the solid residues increase with reaction severity (i.e. higher temperature). For most samples Ca, Mg and Si were concentrated in the residue like P, while K, Na and Cl were found mainly in process aqueous phase. Benavente et al. [129] also studied the

combustion properties of HTC fuels from wastes of olive mills, orange juice production and artichoke food production. They reported decreasing K, Cl, Mg and Si concentrations and increasing P concentrations in the hydrochar ash.

Bach et al. [44] investigated the effect of CO₂ addition on hydrothermal carbonisation of forest residues. They found that in CO₂ enriched conversion atmosphere, 60-69 % of ash-forming matter was removed compared to only 14-26 % using nitrogen as pressurizing agent. They attributed this observation to the higher acidity in the process water due to the formation of carbonic acid and the conversion of Na and K salts to water-soluble carbonate salts upon CO₂ addition. However, they did not conduct an in depth analysis of the influence the CO₂ addition had on the ash composition after HTC.

The impact of pH on combustion properties and ash composition was also investigated in a recent study by Smith et al. [130]. They conducted HTC of swine manure at pH level ranging from 1-13 which they adjusted using different acids (acetic-, formic- and sulfuric acid) and sodium hydroxide as base. They found that lowering the pH prior to HTC reduces ash content of the HTC fuels obtained, due to mobilisation of Ca, Mg and P at low pH. Alkaline pH on the other hand had little effect on ash composition. Mäkela et al. [131] have studied HTC of paper sludge at varying pH conditions. They reported increased K, Mg, Si, Cl and Al concentration in ash of HTC treated paper sludge, while the concentration of Ca and Na was decreasing. Since paper sludge possesses inherently different composition of inorganics and only very low concentrations of Cl, K and Mg, these results should be considered with caution and are not transferable to other biomass feedstock types.

To date no comprehensive study covering the influence of feedstock, temperature, residence time, L/S ratio and additives exists. Yet, for a fuel quality assessment after HTC, the knowledge concerning the fate of inorganics is vital for the mitigation of ash-related problems in i.e. combustion of HTC fuels.

Table 4.1: Overview of studies investigating the fate of inorganics during HTC.

Ref.	Feedstock	T (°C)	t (h)	L/S ratio	pH	Impact of HTC on element ash concentration								
						Na	K	Mg	Ca	Al	P	Si	Cl	S
[46]	Corn stover, miscanthus, switchgrass, rice hulls	200-260	0.08	5	nd	↓	↓	↓	○	↑	↑	↑	↓	↓
[52]	Willow, miscanthus, oak wood, greenhouse waste, AD press cake, municipal waste, sewage sludge, micro algae, micro algae	200, 250	1	10	nd	↓	↓	↑	○	nd	↑	↑	nd	○
[97]	Miscanthus	200, 250	0, 1, 4, 8, 24	10	nd	↓	↓	↓	○	↑	↑	↑	↓	○
[129]	Olive mill waste Artichaut waste Orange peels	200-250	2-24	nd	nd	nd	↓	↓	nd	nd	↑	↓	↓	○
[120]	Microalgae, manure, digestate	170, 250	1	9	nd	↓	↓	↓	↑	↑	↑	↑	↓	nd
[132]	Seaweed	200, 250	1	9	nd	↓	↓	↑	↑	nd	↑	↑	↓	nd
[130]	Swine manure	120-270	1	9	1-13	↓	↓	↓	↓	○	↓	↑	nd	nd
[131]	Paper sludge	180-260	0.5	1-9	2-12	↓	↑	↑	↓	↑	nd	↑	↑	nd

↓ = decreasing ash concentration, ↑ = increasing ash concentration, ○ = unclear trend, nd = no data

Therefore, in the presented study, the impact of temperature, residence time, feedstock type, L/S ratio and addition of CO₂ on the fate of inorganic elements is investigated.

4.2 Quality Assessment for Solid Fuels

For high energy efficiency and availability of combustion processes that use biomass feedstock, it is necessary to attain information about the behaviour of these fuels and to assess their fuel quality. Commonly, standard fuel analysis is used to acquire a first implication of the quality of a new fuel. Table 4.2 summarises the basic conclusions that can be drawn from a standard fuel analysis for technical applications.

Table 4.2: Quality-relevant properties of biogenic solid fuels with their respective effects. Adapted from [133].

Property	Important implications
Major element concentration	
Carbon (C)	Higher and lower heating value, air requirement, particle emissions
Oxygen (O)	Higher and lower heating value, air requirement
Hydrogen (H)	Higher and lower heating value, air requirement
Minor element concentration	
Nitrogen (N)	Ash recycling, NO _x - and N ₂ O-emissions
Potassium (K)	Ash softening behaviour, ash utilisation, high temperature corrosion, particulate emissions
Magnesium (Mg)	Ash softening behaviour, retention of pollutants in ash, ash recycling, particulate emissions
Sodium (Na)	Ash softening behaviour, retention of pollutants in ash, ash recycling, particulate emissions
Calcium (Ca)	Ash softening behaviour, retention of pollutants in ash, ash recycling, particulate emissions
Phosphorous (P)	Retention of pollutants in ash, ash recycling, particulate emissions
Sulphur (S)	SO _x emissions, high temperature corrosion, particulate emissions
Silicon (Si)	Ash softening, ash recycling, particle emissions
Chlorine (Cl)	Emissions of HCl and organohalogens, high temperature chlorine corrosion, particulate emissions
Trace element concentration	
Heavy metals	Ash recycling, heavy metal emissions, particulate emissions

Basic fuel properties such as moisture content, heating value and ash content provide information about e.g. the energy content of the fuel, shelf-life and extent of particle emissions to be expected. The organic composition considering major components like C, O and H of the biomass fuel mostly contains information about its energy density, heating value and determine the operation conditions in terms of fuel input, combustion air requirement, etc. The concentration of minor organic elements like N and S provides an indication of the levels of NO_x and SO_x emissions. Inorganic fuel constituents are associated with ash-related combustion issues such as slagging, fouling, corrosion and fine particulate emissions. The inorganic composition of biomass ash also determines its possible valorisation pathway: For example ash with a high concentration of nutrients might be used as fertiliser, while contaminated biomass ash, e.g. by heavy-metals, has to be disposed in landfills.

By calculating fuel indices derived from fuel analysis, more detailed information on the likelihood of a specific issue can be obtained. Of course the accuracy of predictions solely relying on fuel indices is limited, still compared to fuel testing in pilot- and full-scale facilities, the fuel characterisation by fuel indices provides a quick and straightforward first evaluation of fuel quality. Challenges in biomass combustion are often ash-related, such as e.g. corrosion, ash-melting, particle formation and deposit formation, as well as the formation of NO_x and SO_x emissions that are hazardous to the environment and health. In principle, fuel indices establish a connection between the fuel chemistry and the chemistry of undesirable reactions in power boilers. For example, high temperature corrosion in power boilers is a consequence of alkali chloride condensation and successive reaction of the superheater metal with chlorine [13, 134]. Thus, suppressing alkali chloride formation prevents high temperature corrosion as well. One possibility to achieve this is the binding of alkali with sulfur as alkali sulfate in the furnace [135], a second option is to remove chlorine from the feedstock. Although the exact underlying reaction mechanisms of high-temperature corrosion are not yet fully understood, the prediction of

the corrosion rate with the molar S/Cl ratio has proved to be a useful indicator [136].

Correspondingly, particulate matter (PM) emissions are estimated by evaluating the concentration of inorganics that are prone to form fine particles during combustion. PM emissions from inorganic fuel components originate from the release of volatile inorganics such as alkali metals, heavy metals, S and Cl that are released to the gas phase during combustion and subsequently nucleate and condense to fine particles [137–139]. In biomass fuels, K being an abundant inorganic species constitutes the most relevant element for PM formation. Indices estimating the formation of NO_x rely on the assessment of the concentration of nitrogen in the fuel, since NO_x formation is known to originate mainly from the oxidation of fuel nitrogen [140–142]. Indices predicting ash-melting and slagging behaviour evaluate the fuel ash composition with respect to components that are known to lower resp. elevate ash-melting temperatures.

Traditionally, fuel indices have been developed for solid fossil fuels such as lignite or coal. Yet, due to the inherently different composition and structure of biomass compared to coal, a direct application of these indices for the assessment of biofuels is questionable [143–145]. A few studies exist that evaluate new indices for the prediction of undesired furnace reactions specifically for biomass fuels: Sommersacher et al. [143] have performed lab- and real-scale combustion test of a large variety of biomass fuels. They evaluated fuel indices derived from chemical fuel analysis regarding their applicability for biomass combustion by comparison of the index' prediction to their measurements using statistical analysis. This way they identified that, for instance, the molar S/Cl ratio is a suitable indicator for corrosion risk. The fuel N content is an indicator for NO_x emissions, and the sum of the concentrations of K, Na, Zn, and Pb can predict aerosol emissions. Näzelius et al. [144] have shown that for the estimation of slagging in fixed-bed combustion of phosphorous-poor biomass fuels, none of the traditional fuel indices performs well. Instead they proposed the use of a ternary diagram with $\text{K}_2\text{O}(+\text{Na}_2\text{O})$, $\text{CaO}(+\text{MgO})$, and SiO_2 as crucial components to predict

slagging behavior. Zeng et al. [146] also demonstrated the usefulness of ternary diagrams for the prediction of slagging behaviour in a (CaO+MgO+MnO), (K₂O+P₂O₅+SO₃+Cl₂O) and (SiO₂+Al₂O₃+Fe₂O₃+Na₂O+TiO₂) diagram for the combustion of wood, miscanthus, wheat straw and blends thereof. They also confirmed the applicability of the molar (Si+P+K)/(Ca+Mg) as fuel index for the slagging propensity as introduced by Sommersacher et al [143]. In a recent study, Feldmann et al. [147] investigated 23 different fuel indices for slagging testing 33 different biomass fuels. They found a better applicability of the indices to Ca-rich wood derived fuels and emphasised that P- and Si-rich fuels required closer investigation. Nevertheless, also in this study the index using molar (Si+P+K)/(Ca+Mg) ratio was found to yield a good correlation with slagging propensity. In the second part of their study Feldmann et al. [148] further confirmed the applicability of fuel-N as indicator for NO_x emissions and sum of (Na, K, Zn and Pb) for particulate matter (PM) emissions. They pointed out that also K content alone is sufficient to predict PM emission severity. Molar (Si+P+K)/(Mg+Ca), sum of (Na, K, Zn and Pb) and molar 2 S/Cl ratio have also been confirmed as suitable indices for slagging, PM emissions and corrosion in a study investigating the fixed-bed combustion of straw by Obernberger et. al. [149]. Another implication for corrosion risk during biomass combustion is the chlorine content of the fuel [150–152]. Fouling risk during biomass combustion can be assessed using the Fouling index F_u as well as the same index as for PM emission risk, since the two phenomena are closely related and [143, 152, 153]. The fouling index F_u is based on the base-to-acid ratio $R_{B/A}$ which is calculated according to equation (4.1), but gives higher relevance to the alkali elements that are pre-dominantly responsible for fouling in biomass combustion. By multiplying the $R_{B/A}$ with the concentration of alkali oxides in the ash F_u is obtained.

$$R_{B/A} = \frac{Fe_2O_3 + CaO + MgO + K_2O + Na_2O}{SiO_2 + TiO_2 + Al_2O_3} \quad (4.1)$$

Table 4.3 provides an overview on the fuel indices selected for the prediction of challenges in biomass combustion used in this study.

Table 4.3: Risk classification for biomass combustion related challenges using fuel indices.

Combustion related challenge	Fuel index	Risk classification	Ref.
Corrosion risk	Molar S/Cl ratio	Low for $2 S/Cl > 4$	[136, 143, 149]
	Fuel-Cl content	Low < 0.2 wt.-% Medium 0.2-0.3 wt.-% High > 0.3 wt.-%	[150, 151]
NO _x emissions	Fuel-N content	Low < 0.4 wt.-% Medium 0.4-1 wt.-% High > 1 wt.-%	[143, 146, 148, 149]
Aerosol- / PM emissions	Sum of K, Na, Zn and Pb	Low < 1,000 mg kg ⁻¹ Medium 1,000-10,000 mg kg ⁻¹ High > 10,000 mg kg ⁻¹	[143, 148]
Fouling	$F_u = R_{B/A} \cdot (Na_2O + K_2O)$	Low < 0.6 Medium 0.6-40 High > 40	[150, 152-154]
Slagging	Molar $(Si+K+P)/(Mg+Ca)$	> 1 ash sintering below 1100°, linear relationship with ash sintering temperature	[146, 147, 155]

The objective of this work is to provide an overview of the impact of HTC on the fuel quality regarding combustion related issues. Both changes in organic and inorganic composition and their implications on fuel quality are discussed, with an emphasis on the fate of inorganic elements during HTC. Only fuel indices that have proven suitable for the assessment of biomass-derived fuels are applied.

4.3 HTC Process Variations and Techno-economic Evaluation

A number of different HTC process variations exist that have been primarily been developed in Europe. There is an estimated amount of 200 companies worldwide that are involved in research and development as well as application of the HTC technology [156].

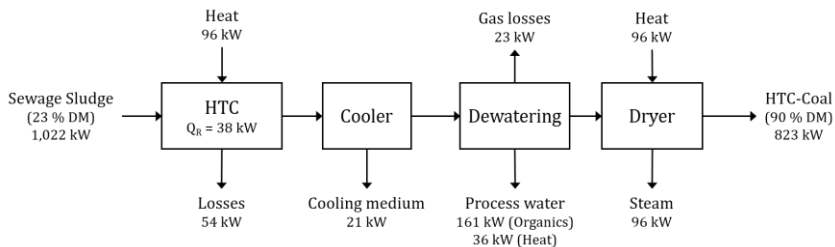
Prominent companies developing HTC processes include Ingelia (Spain), C-Green (Sweden), HTCycle (Germany), SunCoal (Germany), Revatec (Germany), TerraNova Energy (Germany) and Antaco (UK). Most of these

companies own demonstration-scale HTC plants that are operated in campaign mode. The process designs are often modular, allowing for scalability according to customer needs and future plant expansion.

A few commercial plants exist: In 2016, TerraNova energy commissioned a full-scale HTC plant in Jining (China) that processes 14,000 t of sewage sludge per year [157]. More recently, in 2019, C-Green built a pilot-scale HTC plant for Stora Enso's pulp and board mill in Heinola, Finland. The plant is used for conversion of around 16,000 t of biomass sludges per year to biochar that will be incinerated in the mill's power boiler [158]. Ingelia currently plans several commercial HTC facilities: In Belgium a plant for 20,000 t of organic waste per year is under construction and four additional plants are under permitting, expected to start construction in 2021.

Table 4.4 includes an overview of a selection of developed HTC processes. On larger scale, reaction temperatures for HTC are typically on a moderate level of around 200°C. Investigated residence times applied by companies in their pilot scale plants range from 1 to 16 h. All processes use heat recovery systems to ensure an energy efficient operation. Figure 4.1 summarizes the energy flows in a typical HTC process as evaluated by Vogel [159].

Figure 4.1: Energy flows during HTC of sewage sludge and subsequent drying to 90 % dry matter. Q_R = heat of reaction, DM = dry matter. Adapted from [159]. Data from TerraNova pilot plant [157, 160].



Heating up the biomass slurry to reaction temperature and drying are the most energy intensive process steps. The largest energetic losses is attributed to the dissolution of organic material in the process water. External heat needed accounts for roughly 10 % of the energy content of the

Table 4.4: Basic process characteristics for selected processes from commercial technology providers of hydrothermal carbonisation.

	HTCycle	SunCoal	TerraNova	Ingelia	Antaco	C-green	Revatec
Ref.	[161]	[28, 162]	[163]	[164]	[28, 165]	[166]	[167]
Temperature (°C)	220	200	200	180-220	200	200	187-200
Residence time (h)	2-4	6-10	2-4	4-16	4-10	1	4-8
Operation mode	multi batch	continuous	continuous	continuous	continuous	continuous	multi batch
Heat recovery system	steam recovery	steam recovery	heat-exchange between product and feed stream, thermal oil cycle	steam recovery, thermal oil cycle	heat-exchange between product and feed stream	steam recovery	thermal oil cycle
Thermal Efficiency (%)	59 (sewage sludge) 80 (brewers spent grains)	84 green cut	75 sewage sludge	n/a	85	n/a	79-81
Largest plant (t a ⁻¹)	8,400	1,440	14,000	20,000	n/a	16,000	450

feed stream [62, 159, 168]. To date, no consensus on the heat of reaction from HTC is reached [92].

The reaction is expected to be slightly exothermic, but the small amount of heat released during the conversion of real substrates and their inhomogeneity prevent a reliable assessment. Ultimately, the significance of the heat of reaction for the overall energy balance of the process is relatively small. The overall plant efficiency is strongly dependent on the maximum possible energy yields, i.e. chemical efficiency achievable for the conversion of a specific feedstock. Thus, the reported thermal plant efficiencies fall within the range of 50-75 % for HTC of sewage sludge (HTCycle, TerraNova energy) which has a low chemical efficiency and around 80 % for lignocellulosic material (Suncoal, Antaco) with higher energy yields.

Most processes operate in continuous systems; some rely on multi batch reactors, where the concerted operation of several batch units provides a steady biomass intake and output.

Techno-economic Evaluation of HTC

Currently, little data on mass- and energy balances of integrated HTC processes is available. Commercial HTC plants are scarce and operational data is rarely shared to the scientific community. The techno-economic performance of HTC however, needs to be known to evaluate if the technology is suitable for the production of fuel from residual biomass.

Table 4.5 provides an overview over the results on existing techno-economic analyses from academic studies and HTC technology providers. Only a few holistic studies exist that consider the whole process chain of fuel production by HTC. Stemann et al. [62, 169] considered two plant sizes converting empty fruit bunches (EFB) with a capacity of 40 kt a⁻¹ and 97 kt a⁻¹ in south-east Asia. In the design, heat is recovered by recycling steam from cooling and depressurisation of the HTC slurry. External heat is provided by combustion of surplus EFB fibers and shells. The design includes process water recycling to decrease the amount of process water. Thermal energy demand is calculated to be 1.74 kWh kg⁻¹ of product and

electrical energy demand 0.42 kWh kg⁻¹ of product. The slurry pumps and pelletiser are identified as main power consumers. No information is provided on thermal energy consumers. HTC fuel costs are calculated as 7.7-9.7 € GJ⁻¹. The main cost factors for the fuel price are raw biomass costs and shipping costs to Europe.

Table 4.5: Summary of results from techno-economic analyses of academic studies and HTC technology providers.

Ref.	Feedstock	Input (kg h ⁻¹)	Energy consumption		Production cost	
			thermal (kWh kg ⁻¹)	electric (kWh kg ⁻¹)	(€ GJ ⁻¹)	(€ t ⁻¹)
Stemann [62]	EFB	5,700	1.74	0.42	7.7-9.7	215-270
Lucian [64]	Grape marc	2,500	1.17	0.02	8.3	220
Akbari [170]	Yard waste	6,600	nd	nd	11-14	270-350
Saba [63]	Miscathus/Coal	65,000	nd	nd	3.8	90-100
Ingelia [171]	Biomass	1,000	1.38	nd	nd	150-200
Terra Nova [163]	Digested sludge	1,100	0.93	0.22	10	170

In another publication Lucian et al. [64] assess a HTC plant converting grape marc and off-specification compost in Italy. The process scheme is similar to Stemann et al. [62], with steam recovery from flash depressurisation of HTC slurry and process water recycling to reduce waste water. External heat is provided by a gas boiler. Mass- and energy balance of the HTC plant are calculated for a broad range of HTC conditions varying temperature from 180-250 °C and residence time from 1-8 h. Concerning thermal energy consumption, heating up the biomass slurry to reaction temperature is identified as the most energy intensive step. The biggest electrical consumers are slurry pumps and pelletiser. For the production of 1 kg hydrochar (7 kWh kg⁻¹) from grape marc at 220 °C and 1 h, 1.17 kWh kg⁻¹ of thermal energy and 0.42 kWh kg⁻¹ of electrical energy are needed. The overall plant efficiency is found to be strongly dependent on feedstock moisture and solid concentration in the reactor. A production cost for HTC fuels between 6.1 and 7.8 € GJ⁻¹ is calculated in the economic analysis.

While the studies by Stemann and Lucian obtain comparable results concerning energy consumption and fuel cost, deviant values are obtained in more straightforward evaluations: Saba et al. [63] evaluated the co-conversion of a 1:1 blend of miscanthus and coal and determined much lower production costs of 3.8 € GJ⁻¹ for HTC fuels. The low price is most probably related to an optimistic value of total capital investment (TCI) of only 10 Mio € for a plant processing 65,000 kg h⁻¹. For comparison, Stemann et al. estimated 9 Mio € TCI for a plant processing 5,700 kg h⁻¹. In another study by Akbari et al. [170] the production price for HTC fuels from yard waste in the U.S. are estimated to be higher. They calculated a production price of 11-14 € GJ⁻¹ with a considerable gate fee of 23 € t⁻¹ for yard waste. They identified capital investment and labor cost as the main cost drivers. Commercial HTC technology providers such as Terra Nova and Ingelia quantify HTC fuel production prices as 170 € t⁻¹ (10 € GJ⁻¹) and 150-200 € t⁻¹ respectively.

Two other recent studies deal with the technical description of a HTC plant but do not provide sufficient data for a production cost comparison: Stobernack et al. [169] conducted a life-cycle assessment of a HTC plant processing green waste. They followed a gate-to-grave approach, considering also the impact of waste water treatment and ash disposal. A global warming potential (GWP) of 0.45-0.7 kg CO₂ eq. kWh⁻¹ was revealed for electricity generation from HTC fuels, which outperforms the GWP of lignite (1.05-1.40 kg CO₂ eq. kWh⁻¹). Compared to the electricity generation from natural gas (0.4 kg CO₂ eq. kWh⁻¹) the advantage of HTC is limited. They found that a large proportion of the GWP for HTC stems from the required process heat, that Stobernack et al. supplied using natural gas. Substituting natural gas with carbon neutral fuels could lower the GWP for electricity generation from HTC fuels to around 0.2-0.5 kg CO₂ eq. kWh⁻¹.

Benvan et al. [156] have investigated a small HTC plant processing 580 t a⁻¹ digested sewage sludge and organic waste in Chirnside, UK. They concluded that the locally produced HTC fuels could meet 35.6 % of the energy demand

of the municipality with 2,200 inhabitants. A capital investment of 1-2 Mio € and 120.000 € annual operating cost were estimated.

In previous work at the Chair of Energy Systems Ulbrich [17] calculated the thermal efficiency of HTC using brewer's spent grains to be in the range of 50.5-53.1 % at 180 °C and 44.1-45.8 % at 280 °C. Heating of biomass to reaction temperature was found to be the major energy consuming process step. Since no heat integration was considered, the thermal efficiencies calculated by Ulbrich are lower than reported in other studies that are in the range of 60-80 % [62, 64, 163].

In brief, several HTC processes ready for rollout are available. The thermal efficiency of the process is around 70 % with major losses being attributed to chemical energy lost in the process water. Currently, the technology is applied in waste management to facilitate dewatering of high moisture waste streams. In these cases, the main driver for the application of HTC is the energy savings for drying that can be realised for waste streams that are disposed of by incineration. Commercial HTC plants with the aim of producing high quality fuels from biomass do not yet exist. Only a few techno-economic evaluations of HTC have been conducted, that estimate HTC fuel production cost in the range of 8-14 € GJ⁻¹. All in all, data on the economic viability of HTC is scarce. Consequently, a techno-economic study investigating two site locations and input materials is carried out in this work, investigating current bottlenecks, essential process performance indicators and needed policy changes for a successful implementation of HTC for solid fuel production.

5 Research Demand, Aims and Methodology

A growing worldwide bioenergy market needs increasing amounts of biogenic feedstock for energy production. The sustainable provision of fuels from dedicated crop cultivation and wood is, however, limited. Residual biomass from agriculture, forestry, as well as biogenic municipal and industrial waste represent a largely untapped source for bioenergy. These biomass streams however often exhibit poor fuel quality that hinders their introduction to the biofuel market. Thermo-chemical biomass pre-treatment offers the possibility to enhance fuel properties, making challenging fuels available for an energetic utilisation. Commonly, pre-treatment changes the physio-chemical properties of a fuel, increasing the energy content and facilitating storage, pellet production and fuel provision logistics.

In contrast to other thermo-chemical pre-treatment technologies, hydrothermal carbonisation is a pre-treatment technology that is suitable for the direct conversion of wet feedstock. Efficient conversion of moist biomass can otherwise only be achieved by a biological treatment, i.e. in biogas production.

To date, no comprehensive study on the provision of high quality fuels from residual biomass by HTC exists. Therefore, the following contributions beyond the state of the art are made by this work:

- A systematic **identification of suitable feedstock** for HTC is performed. The conversion by HTC is compared to other competing technologies for energetic biomass valorisation, emphasizing the strengths and weaknesses of the technology. Moreover, current utilisation options and availability of feedstock are taken into account for the selection of feedstock for further investigations.
- A **quantification of fuel quality improvement after hydrothermal carbonisation** considering biomass combustion related issues is carried out. Fuel indices that have proven suitable for an application to biofuels are used for this purpose. Besides

compositional changes in the combustible organic fraction of the fuels and fuel reactivity, a strong focus is set on the **fate of inorganic elements during HTC**. Handling ash-related issues in biomass combustion is key for the introduction of residual biomass to the bioenergy market, and therefore the presented work provides insights to the extent to which HTC can help to overcome these challenges.

- Effluent from HTC is characterised. The advantage of an efficient conversion of wet feedstock also poses the biggest challenge for the technology: process water strongly contaminated with organic matter is generated by HTC, which needs further treatment at a cost. Yet, data on process water characterisation is scarce. The work presented therefore includes **process water characterisation and discusses subsequent utilisation options** for effluent from HTC.
- Besides technical challenges, biomass upgrading also needs to be economically viable to be implemented to the market. Therefore, a **techno-economic evaluation**, analysing two scenarios, is carried out to identify essential process performance indicators, current economic bottlenecks and needed policy changes for a successful market introduction of HTC fuels.

6 Materials and Methods

This chapter first describes the overall methodology applied in the holistic assessment of HTC as a technology for solid fuel production. Next, fuel characterisation techniques used to analyse potential biomass fuels prior to and after HTC treatment are introduced. Further the experimental set-up that was used to perform HTC experiments as well as the thermogravimetric analysis test rig are described in more detail. Additionally, the HTC process model and assumptions for the technical and economic evaluation of HTC as a technology for fuel production is presented.

6.1 Holistic Assessment of HTC for Solid Fuel Production

Figure 6.1 provides a schematic overview of the applied methodology in the assessment of HTC as a technology for solid fuel production from biomass.

Assessment of HTC for Solid Fuel Provision				
	Selection of Feedstock	HTC Fuel Quality Assessment	Process Water Characterisation	Techno-economic Evaluation
Examined Influencing Factors	<ul style="list-style-type: none"> Feedstock type Current utilisation HTC conversion efficiency Competing valorisation options 	<ul style="list-style-type: none"> Feedstock type Temperature Residence time L/S ratio CO₂ additive 	<ul style="list-style-type: none"> Feedstock type Temperature 	<ul style="list-style-type: none"> Temperature Residence time Feedstock moisture Plant location
Parameter Range	T: 210 °C τ: 2 h L/S ratio: 10 No. of substrate: 19	T: 150-270 °C τ: 0.5-5 h L/S ratio: 5-20 No. of substrates: 8 (19)	T: 180-270 °C τ: 4 h L/S ratio: 10 No. of substrates: 5	T: 180-270 °C τ: 0.5-2 h L/S ratio: 1-20 No. of substrates: 2
Evaluation Criteria	<ul style="list-style-type: none"> Mass- and energy yield Conversion efficiencies Competition with alternative use 	<ul style="list-style-type: none"> Mass- and energy yield LHV Ash content Fate of inorganics Ash melting Fuel indices 	<ul style="list-style-type: none"> Organic water pollutants Nutrient concentration Basic characterisation Treatment options 	<ul style="list-style-type: none"> Mass- and energy balance Thermal and electrical energy demand Fuel production cost

Figure 6.1: Overview on the approach used for the assesemnt of HTC for solid fuel production.

Initially, criteria for the selection of suitable substrates for HTC are considered. For this purpose 19 different substrates covering different biomass classes from all possible sourcing sectors (agriculture, forestry,

etc.) are screened. HTC experiments are carried out at 210 °C for 2 h which corresponds to HTC conditions of intermediate severity as they are typically applied in pilot- and large scale plants.

Second, the impact of HTC on fuel quality is examined. For this purpose, a parameter study covering temperatures from 150-270 °C, treatment duration from 0.5-4 h with 8 different feedstock is conducted. The temperature range is selected to cover all temperatures where major changes in the biomass structure are expected (see Section 3.2). As previous work by Ulbrich showed, the influence of residence time on hydrochar properties is less pronounced and major reactions are completed after a treatment time of 6 h [17]. Therefore, the covered range of treatment duration is considerably smaller and covers 0.5, 2 and 4 h of treatment time. In addition to that, the influence of feedstock type as well as some variations in L/S ratio and CO₂ addition on the inorganic fuel composition are studied.

Next, the amount and characteristics of process water, the main by-product from HTC, are investigated. The impact of feedstock type and treatment temperature are discussed. Current possibilities for the treatment of process water from HTC are presented.

Finally the economic performance of HTC for the production of solid fuels is investigated. A process model developed with the simulation software Aspen Plus is used to assess the impact of temperature, residence time and feedstock moisture on the energy balance of a HTC plant. The economic evaluation of the technology covers two different feedstock and plant locations.

6.2 Fuel Characterisation

Fuel analysis was carried out at the laboratory of the Chair of Energy Systems according to the relevant industrial norms for biomass fuel characterisation. A detailed fuel analysis is crucial to understand the transformations biomass substrates undergo in a pre-treatment by HTC. Untreated biomass as well as hydrochar resulting from HTC treatment are analysed thoroughly: Proximate analysis to obtain moisture, ash- and

volatile content was performed using gravimetric measurements. Moisture content is determined using a Denver IR60 moisture analyser according to DIN51718. Ash content is determined following a complete combustion at 550 °C in a muffle furnace according to EN14775:2009. Volatile matter is analysed by mass loss after heating the samples to 900 °C for 7 min in a muffle furnace according to ISO562:1998. The amount of fixed carbon is calculated by closing the mass balance. The relative error of measurement for proximate analysis is in the range of 2 %.

Ultimate analysis to obtain the proportions of C, H, N, S, O and Cl in the fuels is performed using the elemental analyser Vario Macro Cube from elemental following ISO/CD 12902:2006-1. In this device, 50 mg of fuel sample undergo complete catalytic combustion in oxygen/helium atmosphere at 1150 °C before the emerging product gases CO₂, SO₂, H₂O and N₂ are separated in adsorption columns. After a sequential, temperature-induced desorption, the quantity of product gas is detected by a thermal conductivity sensor. The obtained value for hydrogen content is corrected by the amount of H₂O originating from the evaporation of fuel moisture. The oxygen content is calculated by closing the mass balance. Cl content is measured in a similar set-up (elementar MACRO cube) by complete combustion of the sample and electro-chemical measurement of HCl in the exhaust gases. Both devices produce results with measurement errors below 2 %.

The calorific value or higher heating value (HHV) is experimentally identified using the IKA bomb calorimeter C200 as specified in EN ISO 18125:2017. 1 g of sample is compressed in tablet form, placed in the pressure vessel and pressurised with 30 bar of pure oxygen. The combustion is triggered by an ignition wire, while the whole set-up is placed in a water bath. The temperature increase in the water bath after the combustion of sample is measured and can be correlated to the higher heating value of the fuel. The lower heating value (LHV) is derived by subtracting the latent heat of condensation of water vapour.

The ash composition analysis is determined following ISO 16996:2015 by X-ray fluorescence (XRF) measurements using the instrument EDX-800 from Shimadzu. The device analyses pellets containing 100 mg of fuel ash sample and 20 mg of a binder wax. Biomass ashes are produced by complete combustion at 550 °C according to EN14775:2009 in a muffle furnace. During the measurement, x-rays are irradiated onto the sample, leading to a removal of inner shell electrons. The hole left behind by this electron is filled by an electron from an outer shells that drops into its place. This transition leads to the emission of a characteristic fluorescent radiation whose energy and intensity can be correlated to a specific element and its concentration within the sample. Results are usually provided on metal oxide basis but can be approximated to elemental concentration in the fuel sample using the mass fraction of metal in the oxides and the fuel ash content.

Ash melting behaviour under oxidising conditions is characterised by an optical method where a cylindrical ash sample is heated to up to 1550 °C. The sample deformation is detected and characteristic ash melting temperatures are determined according to ISO 21404:2020. For biomass ash, the characteristic temperatures are shrinkage starting temperature (SST), deformation temperature (DT), hemisphere temperature (HT) and flow temperature (FT). The measurements are conducted in an ash melting microscope EM201 from the company Hesse instruments.

Table 6.1 summarises the used equipment and applied norms for standard fuel analysis.

The number of repetitions for each measured quantity is defined in the respective norm. In most cases, each measurement is repeated two times. A higher number of repetition is only conducted if the deviation between the first two measurements exceeds a certain threshold value.

Table 6.1: Overview on used equipment and international norms used for fuel characterisation.

Analysis	Instrument	Applied Norm
Moisture content	Denver IR60 moisture analyser	ISO 18134:2015
Volatile content	Muffle furnance	ISO 18123:2015
Ash content	Muffle furnance	ISO 18122:2015
Elemental analysis	elementar Vario Macro Cube	ISO 29541:2010
Chlorine content	elementar MACRO cube	ISO 16994:2015
Higher heating value	IKA bomb calorimeter C200	ISO 18125:2017
Ash composition	Shimadzu EDX-800	ISO 16996:2015
Ash melting	EM 201 Hesse instruments	ISO 21404:2020

For the interpretation of data different reference states for a measured entity are used:

As received (ar): measured value refers to the whole mass of fuel sample including organic and inorganic constituents as well as fuel moisture.

Dry-basis (db): measured value refers to the mass of organic and inorganic fuel constituents.

Dry-ash-free-basis (daf): measured value refers to the mass of organic fuel constituents.

Fuel Quality Assessment

On the basis of standard fuel analysis, fuel indices that provide predictions on the likelihood of undesired events in biomass combustion, such as slagging, fouling, high temperature corrosion as well as particulate and nitrous oxide (NO_x) emissions are evaluated. Fuel indices provide a quick pre-evaluation of the improvements of fuel quality by HTC with respect to biomass combustion related challenges. Although the accuracy of prediction solely based on fuel indices is limited, they allow for a preliminary assessment of a large number of fuel samples without time consuming and expensive pilot-scale testing. The applied fuel indices to assess the risk of operational challenges in biomass combustion have been introduced

thoroughly in Section 4.2. Table 4.3 of this section summarises the used indicator indices and respective threshold values applied in this study.

Thermo-gravimetric Fuel Characterisation

In addition to standard fuel analysis, some samples were characterised using thermo-gravimetric analysis to assess the impact of HTC process conditions on intrinsic char reactivity. Kinetic analysis is carried using a thermo-gravimetric analyser (TGA). In this characterisation method, a solid sample is exposed to a certain gaseous atmosphere and the mass changes upon the reaction of solid and gas are measured. This allows a determination of fuel reactivity. The experimental procedure followed to obtain the intrinsic reactivity r_{int} is described extensively in previous work by Steibel and Ulbrich [17]: In brief, in a first step an appropriate temperature for measurements in the regime of kinetic control are determined by non-isothermal experiments. Next, the reaction rate is measured in isothermal TGA experiments. Afterwards, the specific reactivity is averaged in the conversion range between 5 and 20 %.

In this work, chars are obtained from sample pyrolysis at 1100 °C for 7 min in a preheated muffle furnace in inert atmosphere to ensure uniform pyrolysis and high heating rates, following the procedure of ISO 562:1998. Experiments were conducted in an atmospheric pressure TGA (Linseis). Surface area was characterised by CO₂ adsorption with the gas sorption analyser Autosorb 1C from Quantachrom. In the isothermal experiment 20 mg of char sample are placed on a ceramic sample plate and mounted to the measurement device. The sample is heated to 425 °C with a heating rate of 10 K min⁻¹ in inert atmosphere (N₂). After a 1 h stabilization of the reaction temperature the gas flow is changed to reaction atmosphere. Chars are converted in a flow of 50 mL min⁻¹ synthetic air diluted with 150 ml min⁻¹ to obtain an oxygen concentration of 5 %. The samples are kept at reaction temperature and atmosphere for 24 h to ensure complete conversion.

6.3 Experimental HTC Investigations

A systematic investigation of different process conditions on the characteristics of HTC treated biomass fuels requires a flexible and well-defined experimental set-up. The test rig should allow for the production of a sufficient amount of sample for complete fuel analysis (approximately 20 g) while at the same time limiting material and work required. These criteria are satisfied by a lab-scale batch reactor. The used set-up allows the investigation of a wide range of process conditions, while offering strict control over the experimental setting.

HTC lab-scale test rig

The lab-scale test rig at the Chair of Energy Systems is a stirred, pressurised vessel operated in batch-mode. The test rig was designed by M. Ulbrich [17] who provides an in-depth description of the test rig: The Parr 4563 Mini-Batch stirred vessel has a volume of 1000 mL which supports a conversion of around 600 mL of biomass slurry. The maximum temperature and pressure allowed are 350 °C and 200 bar respectively. A schematic of the set-up is shown in Figure 6.2.

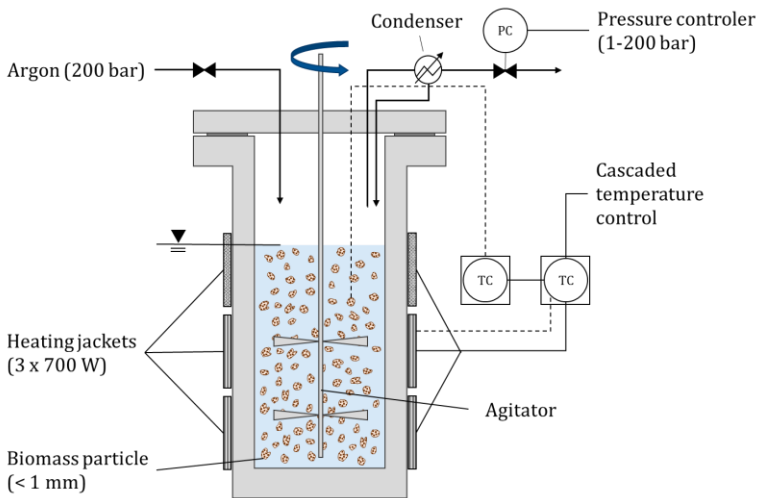


Figure 6.2 Schematic of the lab-scale test rig for the experimental investigation of biomass HTC, $V = 600\text{ mL}$, $T_{\text{max}} = 350\text{ °C}$, $p_{\text{max}} = 200\text{ bar}$. Adapted from [17].

Since reaction temperature is one of the major influencing process parameters, a special emphasis on accurate temperature control was set in the design of the test rig. The reactor is heated by three electrical heating jackets with a power of 700 W each and a maximum temperature of 400 °C. The temperature control strategy was developed by Ulbrich and is described in detail in previous work [17]. All in all, the temperature can be controlled with an accuracy of ± 2 K during ramp up and ± 0.5 K in steady-state operation.

The vessel is pressurised using Argon (purity 5.0) from a pressure cylinder. Pressure is controlled using a mechanical Swagelok KPB pressure controller with a control range of 1-200 bar. Table 6.2 shows pressures applied at the respective experimental temperatures.

Table 6.2: Applied temperature and pressure during experimental HTC investigations and water vapour pressure according to Antoine equation at the respective temperature.

Treatment Temperature (°C)	Water vapour pressure (bar)	Set experimental pressure (bar)
150	4.7	20
180	10.0	20
210	19.0	40
240	33.7	40
270	55.6	80

Pressure is adjusted to the respective temperature targeted in each experiment to ensure that water remains in the liquid state. Further a certain safety margin is added to the required pressure. As discussed in Section 3.3 reaction pressure plays a subordinate role in HTC and has the primary function to ensure that water in liquid state is present. A condenser upstream of the pressure controller is used to condensate evaporated process water from the reactor and feed it back to the reaction vessel. The reactor is equipped with an agitator with two propellers to provide homogeneous mixing throughout the experimental operation.

Experimental procedure

The raw biomass samples are dried at ambient conditions and homogenised to a particle size < 1 mm using a Retsch ZM1000 rotary mill prior to HTC. After thorough mixing of the homogenised biomass, substrates are divided into aliquots of 30 g dry material. For hydrothermal conversion 30 g of substrate and 300 mL of deionized water are poured into the reactor. Afterwards the vessel is pressurised using Argon and brought to reaction temperature with an average heating rate of 7 K min^{-1} . After reaction at designated temperature and residence time, the reactor is air-quenched to room temperature. The resulting hydrochar slurry is separated using vacuum filtration and the isolated solid product is dried at ambient conditions for at least 48 h. Fuel analysis is carried out according to the procedures described in Section 6.2.

Repeatability of HTC experiments

The repeatability of HTC experiments was checked by repeating the treatment of EFB, brewers spent grains and spruce bark at temperatures of $180 \text{ }^\circ\text{C}$, $230 \text{ }^\circ\text{C}$ and $280 \text{ }^\circ\text{C}$ at least two times under repeatability conditions. This means that the experiments were run following the same procedure, using the same material, by the same operator and the analysis was performed using the same measurement equipment within a short period of time. The results were evaluated using ISO 5725-1:1997 where repeatability is defined as the precision under repeatability conditions. The same standard also describes the repeatability limit r , which is defined as “*the value less than or equal to which the absolute difference between two test results obtained under repeatability conditions may be expected to be with a probability of 95 %*” [172].

For two runs r is calculated using the standard deviation S_r calculated from experiments at repeatability conditions according to equation (6.1).

$$r = 2.8 \cdot S_r \quad (6.1)$$

The discrepancy between different experiments was found to be within an acceptable range. The repeatability limit r for the HTC treated samples was within the same range as for the raw materials. This means variations

between runs most probably stem from biomass inhomogeneity. In addition, the discrepancy between different experiments was found to be within an acceptable range (relative standard deviation generally < 5%). For data on the repeatability experiments see Appendix A. Therefore, one run was performed for each variation of process conditions.

HTC key performance indicators

To quantify the impact of different process conditions (temperature, residence time, L/S ratio, etc.) on energy efficiency and fuel characteristics, several performance indicators are used within this work that will be defined in the following section.

Mass yield in % is defined as the ratio between the mass of hydrochar obtained after the treatment on dry basis $m_{HTC,db}$ in g and the input mass of substrate on dry basis $m_{raw,db}$ in g. It is calculated according to equation (6.2).

$$Mass\ yield_{db} = \frac{m_{HTC,db}}{m_{raw,db}} \cdot 100 \quad (6.2)$$

Energy yield which is a measure of the proportion of chemical energy preserved in the solid product after conversion, is defined as the ratio of lower heating value of hydrochar on dry-basis $LHV_{HTC,db}$ in MJ kg⁻¹ and the lower heating value of the substrate on dry-basis $LHV_{raw,db}$ multiplied by the mass yield. Thus, energy yield is calculated according to equation (6.3).

$$Energy\ yield_{db} = Mass\ yield_{db} \cdot \frac{LHV_{HTC,db}}{LHV_{raw,db}} \quad (6.3)$$

To facilitate the comparison of results obtained from different feedstock, relative values are calculated: This means that the individual property after HTC is given in relation to the property of the starting material. For example, the relative ash content after HTC is obtained by dividing the ash content $a_{HTC,db}$ of the HTC fuel with the substrate ash content $a_{raw,db}$ according to equation (6.4).

$$Relative\ ash\ content\ (db) = \frac{a_{HTC,db}}{a_{raw,db}} \quad (6.4)$$

Other relative fuel properties are calculated correspondingly. To investigate how effective HTC is in removing certain impurities from a biomass

substrate the removal efficiency is calculated. For example, the ash removal efficiency is calculated by subtracting the relative ash content multiplied with the mass yield from 100 according to equation (6.5).

$$\text{Ash removal efficiency (db)} = 100 - \left(Y_m \cdot \frac{a_{HTC,db}}{a_{raw,db}} \right) \quad (6.5)$$

Removal efficiency for other fuel constituents is calculated accordingly.

6.4 Characterisation of Process Water

Electrical conductivity and pH value were determined at room temperature following filtration with conductivity meter GMH 3431 and pH meter GMH 3511 from Greisinger. Electrolyte concentrations were determined using ICP-OES spectrometer Arcos FHX22 from spectro. 10 mL of liquid sample was filtered with a 0.45 μm syringe filter and diluted to 50 mL prior to analysis. Subsequently effluent samples were frozen and stored. Additional water characterisation was carried out by an external lab: TOC was determined according to EN 1484, DEV H3, BOD₅ according to DIN EN 1899-1. COD, total phosphorous (P_{tot}), total nitrogen (TN), nitrate ($\text{NO}_3\text{-N}$), nitrite ($\text{NO}_2\text{-N}$) and ammonium ($\text{NH}_4\text{-N}$) concentrations were characterised using Lange cuvette tests.

6.5 Process Modelling and Techno-economic Analysis

To assess the current economic viability of fuel production by HTC, a techno-economic analysis of the process is carried out. In a first step, a process design is developed in Aspen Plus to determine energy and equipment requirements for a commercial HTC plant. In a next step, a techno-economic analysis estimates the current total costs of production for HTC fuels. The techno economic analysis includes a case study that compares fuel production costs at a local site processing green cut in Germany and a production site processing EFB in Asia. The two scenarios are chosen to compare sites with low and high labour costs. The capacities of the plants were adjusted to logistically feasible sizes in the respective region.

6.5.1 Conceptual Process Design

A HTC plant was designed in Aspen Plus to determine the electrical and thermal energy demand and thus, the energy efficiency of the process. In the following the proposed process scheme as well as boundary conditions and assumptions for the process model are provided.

Figure 6.3 shows the schematic process model of the developed HTC plant.

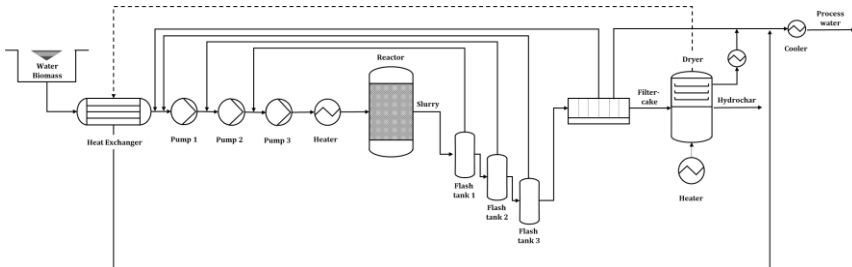


Figure 6.3: Schematic flowsheet of the modelled HTC plant.

In a first step, biomass is mixed to the desired L/S ratio and heated to reaction temperature. After the reaction, the biomass-water slurry is cooled down, depressurised and the liquid and solid fraction are separated in a filter press. Thermal drying of the hydrochar is the last process step. A pelletisation step was not considered in this work. Heat integration is based on a previous study by Briesemeister et al. [173]: First, part of the exhaust steam from thermal drying is used to preheat the biomass feed stream prior to the first pressurisation stage in a heat exchanger. Secondly, to decrease the pressure of HTC slurry to ambient conditions after reaction, three flash tanks are used. These flash tanks produce steam that is recycled upstream of the reactor to the respective pressurisation stage and pre-heats the biomass feed stream. The choice of three pressurisation stages was found to be a good compromise between saved expenses in operating costs due to energy savings and complexity of the whole operation (see [174]). Comparable configurations are found in the literature [62, 64, 168]. Finally, hot water from the slurry separation unit is recycled to the feed stream further decreases needed energy for heating and reducing the amount of

waste water produced by the plant. The impact of process water recycling on mass- and energy yield of HTC are, however, neglected.

The HTC plant is modelled with the software Aspen Plus. The assumptions regarding the plant components and unit operations are summarized in Table 6.3.

Table 6.3: Assumptions and units used in ASPEN Plus HTC process model.

Plant component	Assumptions
Biomass, Hydrochar	non-conventional components using DCOALIGT density and HCOALGEN enthalphy model
H ₂ O, CO ₂	Conventional component described by Soave-Redlich-Kwong state equation
Heater	Heat loss corresponding to 5 % of the fuel input pressure drop of 0.1 bar
Slurry pumps	Mechanical efficiency of 45 %, hydraulic efficiency 99 %
Reactor	Black box with defined in and outputs, no external heating or cooling needed, pressure inside the reactor is above vapor pressure of water at the corresponding reaction temperature with a safety margin of at least 5 bar
Filter press	Dewatering to 50 % dry matter in the filter cake
Dryer	Heat losses correspond to 3 % of the energy of the steam supply, drying to a final moisture content of 8 wt.-%
Other	No energy consumption for cooling considered, pelletising step and waste water treatment not considered, dependence of mass yield on process water recycling and L/S ratio not taken into account

As biomass is a complex material, a complete description of the process by chemical reaction modelling is not feasible. Therefore, conventional and non-conventional material flows are used to describe the HTC conversion in the process model. The needed component attributes for this descriptions are provided by experimental data as reported in Appendix D. To represent the transformation of biomass to hydrochar during the HTC process in the reactor, a RYield reactor is used. This unit can be controlled by specifying the component yields and compositions of the inputs and outputs (biomass

and slurry) as determined by laboratory experiments, at a given temperature and pressure and estimates the corresponding enthalpies of the mass flows.

As mentioned in Chapter 4.3, data for the reaction enthalpy (ΔH) of HTC is scarce. An exact determination of the process enthalpy is difficult due to the large variety in composition of different biomass types.

Most data suggests that the HTC reaction is slightly exothermic with ΔH being in the range of -1.0 to -7.3 MJ kg⁻¹ [92, 175, 176]. Therefore, it is assumed in the presented model that once brought to reaction temperature, the reactor does neither need to be heated nor cooled. The pressure inside the reactor is chosen to be at least 5 bar above the vapour pressure of water at the respective temperature to provide a safety margin. Dewatering in the filter press is conservatively assumed to yield a filter cake with 50 % dry matter. Thermal dryer losses are assumed to be 5 % of the steam energy input and the hydrochar is dried to a final moisture content of 8 %. The energy consumption for cooling, waste water treatment, pelletising and shredding of biomass are not accounted for.

Based on these assumptions, a calculation of the thermal and electrical power consumption of the process was performed. The impact of process temperature and reaction time as well as feedstock moisture content was investigated. Process temperature is varied from 180-270 °C, residence time from 0.5-4 h and feedstock moisture content ranging from 55-95 wt.-%. In the base design, the HTC plant is designed to process 40.000 t a⁻¹ of EFB with a moisture content of 70 wt.-% at 210 °C for 2 h which corresponds to a HTC treatment of intermediate severity.

The process performance was assessed with help of the thermal efficiency η_{th} , which is calculated according to equation (6.6).

$$\eta_{th} = \frac{E_{Hydrochar,HHV}}{E_{Biomass,HHV} + E_{th}} = \frac{\dot{m}_{hydrochar} \cdot HHV_{hydrochar}}{\dot{m}_{biomass} \cdot HHV_{biomass} + P_{th}} \quad (6.6)$$

HHV is used for better comparability with other studies. Consequently, it is a measure of the proportion of the energy output of the process in form of chemical energy contained in the produced hydrochar and the energy entering the process in form of chemical energy from the biomass feed stream plus auxiliary energy demand.

6.5.2 Techno-economic Assessment

The objective of the techno-economic analysis is to estimate the economic competitiveness of HTC for the production of high quality fuels from residual biomass. Standard procedures in cost engineering following Towler and Sinnott [177] are used to determine the cost of production for HTC fuels. This way a selling price for HTC fuels can be assessed, which covers the expenses for their production over a given period of time. The estimated selling price indicates, if HTC for the production of biofuels is competitive at the current market conditions and if not which changes, in e.g. CO₂ pricing, are necessary to make HTC fuels profitable. The analysis is carried out with the assumption that the investment is amortized after 10 years and no profits is included in the calculation. Therefore, the calculated selling price is to be considered as the so-called *breaking point* price, which marks the price above which the production of HTC fuels would be economically viable. The cost estimation is based on correlations and estimations from literature since only limited data on cost is available and the design of the plant is not completed in detail. This is an approach often used in academic studies and typically produces results with $\pm 30\%$ accuracy. In the following the assumptions for the economic assessment are provided, which correspond to a conservative, i.e. more-cost intensive cost estimate for HTC fuels.

The total cost of production is composed of two parts: the total annual capital charge, which corresponds to the total fixed capital investments that are converted to an annual equivalent using the annuity factor, and the cash cost of production, which cover operating costs of the plant such as labour, maintenance or energy costs.

The total annual capital charge is calculated by multiplying an annuity factor with the total fixed capital charge. For the calculation of the annuity factor it is assumed that the HTC plant is amortized after $n = 10$ years and the interest rate is 1 %. The total capital charge is calculated by the addition of four building blocks: the investments for the principal plant components (inside battery limits = ISBL) like reactor, heat exchangers and other equipment that is calculated by cost correlations following Erlach et al. [178]. A scaling factor, calculated according to Eq. (6.7) was used to account for the impact of plant size on capital cost [177].

$$C_2 = C_1 \cdot (S_2/S_1)^{0.7} \tag{6.7}$$

With C_2 being the target value for the equipment cost, C_1 being the known cost for the equipment and S_1 and S_2 being the old and new production capacity respectively. The exponent of 0.6-0.7 is commonly used in the chemical industry [177]. Second, the investments needed for other infrastructure like electricity installations, water and power connections, buildings (outside battery limits = OSBL) that are assumed to account for 40 % of the ISBL. Engineering costs (EC) of 25 % of combined ISBL and OSBL as well as some financial buffer that accounts for 20 % of ISBL and OSBL combined. The assumptions for the calculation of the total annual capital charge are summarized in Table 6.4.

Table 6.4: Assumptions for the calculation of the total annual capital charge for the considered HTC plant.

Contributor	Short definition	Assumptions
i	Interest rate	1 %
n	Number of periods	10 years
ISBL	Investments for principal plant components (i.e. reactor, flash tanks, filter press)	Calculated by cost correlations following [64, 177]
OSBL	Other infrastructure investments (electricity network, connection to water grid, etc.)	40 % of ISBL
EC	Cost for engineering	25 % of (ISBL+OSBL)
CC	Contingency capital	20 % of (ISBL + OSBL)

The cash cost of production is divided into fixed and variable cost of production. Variable cost of production (VCOP) include costs for energy, waste water treatment and procurement costs for the raw biomass. VCOP is therefore directly dependent on the plant size and the associated changes in mass- and energy flows that are determined by the process model introduced in the previous section. The fixed cost of production (FCOP) occur independent on capacity or output of the considered plant. In the presented work FCOP originating from personnel cost, maintenance, overhead and cost for property use and insurance. Assumptions for these costs are provided in Table 6.5.

Table 6.5: Assumptions for the calculation of the cash cost of production.

Cost factor	Assumptions
Personnel cost	Work force: 1 supervisor, 2 workers per shift Shift factor: 3.6 for 7000 h a ⁻¹ Worker salary: 40.000 € a ⁻¹ Supervisor salary: 125 % worker salary
Overhead cost	35 % of personnel cost
Maintenance cost	4 % of ISBL
Insurance cost	1 % of (ISBL+OSBL)

Additionally, a certain amount of working capital is needed in the start-up and operation of the plant. According to Towler and Sinnott [177], working capital is estimated to be the equivalent of sum of fixed and variable production costs for 7 weeks plus two weeks' worth of needed raw materials and 1 % of ISBL+OSBL.

To assess the impact of the geographic location of a HTC plant a case study investigating two different sites is conducted. Table 6.6 summarises key data and assumptions for both plant sites. One site is located in Germany and converts 40,000 t of green cut per year. The plant capacity was chosen using a study by Wiegel et al. [179] that estimated the technical potential of green waste from landscaping in the metropolitan region of Berlin to amount to roughly 41,000 t of biomass per year. For green cut an acceptance price or gate-fee ranging from 20-35 € t⁻¹ is common, as indicated by a local composting company [180]. A similar gate fee was reported by Abelha et al.

[181]. The analysed HTC plant is operated continuously in shifts by two operators. To maintain a continuous operation the work force needed is higher than three people which is accounted for with a shift factor.

Table 6.6: Key data on site capacity, labour- and utility prices for both locations considered in the case study.

	Germany	Malaysia	Ref.
Biomass type	Green cut	EFB	
Plant capacity (t a ⁻¹)	40,000	80,000	[62, 179, 187]
Biomass price (€ t ⁻¹)	-25	3	[180, 188]
Freshwater price (€ m ⁻³)	1.72	0.55	[185, 189]
Feedstock moisture (%)	65	60	[179, 188]
Worker salary (€ a ⁻¹)	40,000	7,600	[177, 185]
Worker per shift	2	3	
Gas price (ct kWh ⁻¹)	2.53	2.0	[190, 191]
Electricity price (ct kWh ⁻¹)	16.54	6.0	[191, 192]
Wastewater treatment (€ m ⁻³)	8.0	8.0	[61, 62, 64]
Shipping cost (€ t ⁻¹) (17,000 km sea, 50 km land)	-	36	[186]

The other site is located in Malaysia and converts 80,000 t of EFB per year. Malaysia is one of the main producers of palm oil that yields EFB as a side product that is currently either landfilled, composted or incinerated on site. Per year approximately 33 Mio t of EFB are produced at 450 palm oil mills [182–184]. On average, this yields 74 kt EFB per year at each site. The larger plant requires 3 operators per shift, however labour costs in Malaysia are considerably lower [185]. The differences in capital investments cost are taken into consideration using location factors [177], which are 1.11 for Germany and 1.12 for Malaysia, so no strong differences on capital investments are expected between the two sites. Shipping costs to transport the produced HTC fuels to Germany by ship and truck are based on a study by Visser et al. [186] and amount to 36 € t⁻¹ of product.

Both plants are designed to run with a capacity factor of 80 % which amounts to 7000 operating hours per year. Waste water treatment costs are estimated to be 8 € m⁻³ based on the average of literature values [61, 62, 64].

At both sites the total cost of production per ton of HTC fuels for the provision to the European market is calculated. With this, a break-even point for a minimum selling price above which the plant would be profitable can be estimated. A variation of process and plant parameters is not performed within the scope of this study, but in joint work with A. Möbius [174]. Finally, the obtained results are compared to current solid fuel prices for fossil fuels and other biofuels.

7 Considerations for the Selection of Feedstock

Within this work 19 different potential substrates for HTC were tested. Figure 7.1 provides an overview on the classification and origin of the biomass types used. Feedstock from all possible biomass source sectors including agriculture, forestry, industry and municipalities are considered.

Agriculture			Forestry	Industry		Municipal	
Energy crops	By-products residues	Farm manure	By-products residues	National	International	Waste management	Water management
Miscanthus	Wheat straw	AD Digestate	Spruce bark	Sugar beet pulp	Olive pomace	Fallen leaves	Digested sludge
	Rice husk	Horse manure	Fir needles	Brewer's spent grains	Orange peels	Grass clippings	Seaweed
	Empty fruit bunches			Spent coffee grounds			Micro algae
	Corn cobs						

Figure 7.1: Overview on substrates for HTC and respective biomass classes investigated in this study. In-depth examination was carried out on substrates with solid outline.

All feedstock, except miscanthus, represent residual biomass streams. Preliminary testing is conducted for all depicted substrates, an in-depth experimental investigation covering a wide range of process parameters is carried out for substrates with solid outline.

To determine which substrates are suitable feedstock for the production of high quality fuels by HTC, several aspects are considered and discussed in more detail in the following chapter:

Fuel characteristics and current feedstock utilisation: A positive environmental impact of HTC can only be expected if the technology allows for the conversion of biomass streams that are otherwise landfilled or incinerated without energetic utilisation (i.e. on-field incineration). Further, material use of biomass has a higher priority than the production of fuels. In addition, only feedstock with poor fuel quality should be upgraded.

Quality of Carbonisation: Energy densification, mass- and energy yield can vary significantly between different substrates. When producing a fuel for energy production, it is of utmost importance that the input energy is preserved to a large extent in the final product, in our case HTC hydrochar. To assess this aspect the energy yield following HTC at reaction conditions of intermediate severity is experimentally determined.

Feedstock moisture content: HTC allows a direct conversion of wet feedstock without drying allowing energy savings for the former. Consequently, the technology should be applied for the treatment of wet biomass streams to benefit from this advantage. A comparison of HTC prior to combustion and direct-combustion is provided.

Competing utilisation pathways: Other technologies exist that allow the conversion of wet feedstock. To decide whether a thermo-chemical or biochemical utilisation is more favourable for a given substrate, net energy output of HTC and anaerobic digestion are analysed.

7.1 Feedstock Characteristics and Current Utilisation

This section first describes a literature review on current utilisation of the 19 investigated feedstock. Afterwards a discussion of own experimental analysis of the fuel properties follows.

An important aspect of feedstock selection for energy purposes is their current utilisation. The utilisation of a renewable resource in food or feed production as well as material use, always has a higher priority than an energetic valorisation. In the following, the current utilisation of the biomass substrates investigated in this work are briefly summarised:

Digestate from anaerobic digestion (AD digestate) is a wet solid residue from biogas production. Digestates are mostly applied as fertiliser and for soil amendment due to their high nutrient and organic content. Their transportation is only economically viable within a small range due to their high moisture content. In Germany annually around 3 Mio t of solid AD digestates are produced [193]. With increasingly strict legislative restrictions concerning the amount and timelines for spreading of

digestates on fields, new disposal and utilisation methods are necessary [194].

Corn cobs are the central core of maize and are an agricultural residue from corn production. They are used as fibre additive in animal feed, bedding material, bio abrasive, absorbent and drying agent. Due to their abundance, their application as biofuels has received increasing attention as feedstock for bioethanol, co-firing and gasification. Assuming 1 t of maize yields 180 kg of cobs [195], globally around 150-200 Mio t of corncobs arise each year [196, 197].

Digested sewage sludge is the remaining slurry from waste water treatment plants. In Germany around 1.7 Mio t of dry sewage sludge result from waste water treatment plants [198]. A large proportion of digested sludge is used in landscaping, agriculture and is co-combusted in coal-fired power plants. Due to a legal change these disposal methods will be banned in Germany starting from 2029. Consequently, municipalities are desperately seeking alternative disposal techniques for digested sludge which lead to a surge in disposal fees. Mono-incineration in fluidised bed boilers is discussed and partly already implemented to solve the issue [199]. However due to the high moisture content (72-75 wt.-%), the combustion efficiencies are low and the energetic potential of this waste stream is not sufficiently utilised.

Empty fruit bunches (EFB) are a residue from palm oil production. Palm oil plantations produce roughly 1.5 t of EFB (db) per hectare of land [200]. With palm oil being the most consumed vegetable oil worldwide, approximately 30 Mio t of EFB are produced annually [201]. Currently, EFB is mostly used for mulching, landfilled and to some extent incinerated for fertiliser production [202]. Due to their moisture content of approximately 65 %, high K and Cl concentration they are poorly suited as fuel for direct combustion. In addition, EFB contain residual oils that cause water pollution upon excessive mulching.

Fallen leaves or leaf litter is considered organic municipal waste and is collected in municipalities during fall. Urban biomass could substantially

contribute to sustainable energy production. A study conducted in Oklahoma finds that per hectare of planted urban land 8-13 t a⁻¹ of biomass could be collected [203]. In Berlin, an estimated amount of 17 t of fallen leaves and 27 t of green cut could be valorised every year [204]. Today fallen leaves are either composted or incinerated in waste combustion plants [203].

Grass cuttings are also categorised as municipal waste. They originate from landscaping activities and are either left on site for decay, composted, landfilled or incinerated at waste combustion facilities [205]. Grass cuttings from grasslands that are used as animal feed and are not considered in this study. Anaerobic digestion of grass cuttings is possible, however since 2012 grass cuttings are no longer considered as a renewable resource but as waste in Germany. Their conversion in biogas plants receiving subsidies has since become increasingly difficult.

Fir needles are a representative for forestry residue and are either incinerated or left on the harvesting site with high associated GHG emissions. Removing forestry residues from harvesting sites leads to commercial and environmental benefits by optimised forest health while at the same time providing feedstock for energetic valorisation.

Horse manure consists of faeces, urine and bedding material. It contains a large amount of nutrients and organic material and is therefore used as fertiliser and for soil improvement. In some cases, horse manure is treated by AD which suffers from low efficiency due to the high solid content and the presence of bedding materials. On average, a horse produces around 10 t of wet manure yearly, including bedding material [206]. In Germany, this amounts to 4-7 Mio t dry mass per year. Thus, the disposal of horse manure has become increasingly difficult, new treatment alternatives are needed.

Miscanthus is a perennial plant that is mostly cultivated as an energy crop. In addition miscanthus can be used as raw material in the construction and pulp and paper industry. Since the cultivation of energy crops is associated with significant GHG emissions due to land and fertiliser use, the

environmental benefit from its energetic utilisation is lower compared to the use of residual materials [207].

Olive pomace or olive filter cake is a processing residue from olive oil production. Per year roughly 20 Mio t of olives are produced worldwide of which 90 % are processed to oil, yielding around 5-7 Mio t of olive pomace as residue [18, 208, 209]. This residue is used as fertiliser, in biogas plants or combusted. The use as fertiliser is considered questionable, since olive pomace contains considerable amount of polyphenols that are non-biodegradable and toxic to microorganisms [210]. Consequently, the biogas yield in AD is low. In addition, due to the high moisture content of 45-74 wt.-% direct-combustion might be inefficient.

Orange peels are a wet residue from juice production. With over 80 % of produced oranges worldwide being used for juicing, around 5 Mio t of orange peel waste accrue per year [211, 212]. Landfilling and composting are the main disposal alternatives used today, including the negative environmental impacts from associated GHG emissions [213]. AD of citrus peel waste is sometimes applied, however orange peels contain d-limonene that inhibits biological degradation of this waste stream.

Rice husk are an abundant by-product from rice milling. With an estimated amount between 730-2,000 Mio t annual production, it offers a tremendous potential [18, 214]. Rice husk is being used as fuel for rice processing plants and their ash can be used in concrete applications due to its high Si content.

Algal biomass often results from algal blooms that occur more often in recent years [215]. The consequences for maritime ecology, tourism and fishing industry are severe. The last prominent algal bloom was in Mexico where a carpet of sargassum with approximately 20 Mio t formed in 2018 that was washed up on the Mexican shores. In a large-scale action the seaweed was collected and dumped in landfills at high costs. Using seaweed for energy applications might help to reduce cost and environmental harm from algal blooms.

Spent coffee grounds (SCG) are the final residue from the preparation of coffee. Globally 7-9 Mio t of coffee are produced annually, generating a massive amount of SCG (0.65 t per t coffee) as a by-product [216]. SCG are mostly considered as waste and therefore the majority is landfilled [217].

Spent grains (or brewer's spent grains) are a high moisture residue from beer production. They possess high protein and fibre content and are therefore used as animal feed as well as ingredient for bread or cereals. Using spent grains for energy purposes is therefore only interesting for breweries, if the savings in energy costs outweighs the revenue from selling of this aliment or if breweries do not find an outlet for their spent grains on the regional markets.

Spruce bark is a side product from pulp and paper production. Although a proportion of bark can be sold as mulching material, especially large pulp and paper mills are seeking for alternative valorisation pathways due to the large amount of bark they are producing.

Sugar beet pulp is a side product from sugar refineries that is sold as cattle and horse feed. Globally, between 60-120 Mio t of this residue are produced [18]. Similarly to spent grains, an energetic utilisation of sugar beet pulp only becomes interesting, if energy cost reductions exceed revenue from feed sales.

Wheat straw is an agricultural residue with one of the largest energetic potentials globally. Between 620-1,200 Mio t accrue annually [18]. A proportion of straw arising from harvest is used as bedding material or for mulching, however due to its abundance and lack of effective utilisation the majority is incinerated on-fields with serious environmental pollution associated. Combustion of straw is often problematic due to high K and Cl contents, transportation is expensive due to the low bulk density of the material.

Feedstock prices or disposal costs also reflect the need for new utilisation pathways. Figure 7.2 shows an overview on feedstock prices.

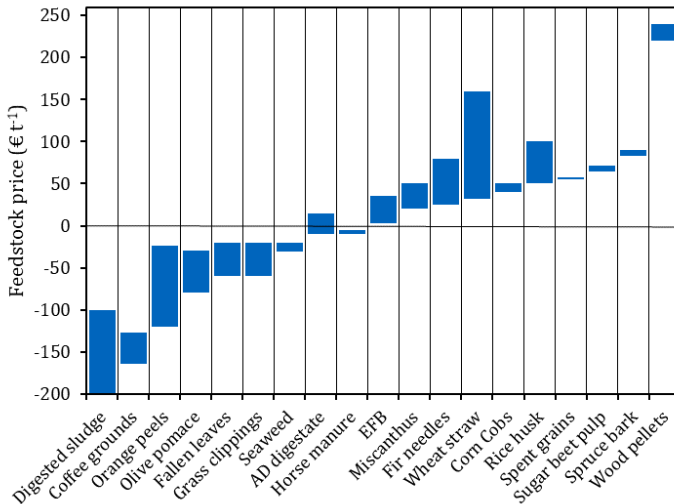


Figure 7.2: Approximate prices and gate-fee for the investigated feedstocks. Wood pellet price is included as a reference. Data collected from [218–230].

Feedstock with economically viable utilisations pathways as animal feed possess higher prices, such as brewers spent grain’s or sugar beet pulp. Lower or negative feedstock prices (so-called gate-fees) indicate the need for alternative utilisation. Generally, European prices on wet basis are reported. Negative feedstock prices are based on the costs for landfilling (gate-fee) issued in the country of origin, e.g. Spain, France, Greece and Italy for olive pomace. Seaweed price is based on Latin-American gate-fees.

Besides current utilisation and availability of biomass feedstock, the fuel quality of a given substrate is another important factor for choosing adequate energetic valorisation. A pre-treatment for fuel production is only necessary, if the substrate exhibits low fuel quality. In experimental work, the 19 feedstock are characterised using standard fuel analysis (see section 6.2) to assess the fuel quality of the raw biomass. The following section briefly discusses the results of the standard fuel analysis of the input materials.

As expected, fuel properties of the selected biomass feedstock diverge widely. Table 7.1 shows the proximate and ultimate analysis of the investigated feedstock. Fuel analysis reveals a strong variability in the fuel characteristics of the substrates. All substrates exhibit high volatile content. Carbon is the most abundant element with a range between 41.5-54.2 wt.-%. Second most abundant element is oxygen with concentrations between 17-42.3 wt.-%. Hydrogen accounts for 3-7 wt.-% of the substrate mass. Nitrogen concentration typically is in the range of 0.4-2.2 wt.-%. Exceptionally high N-contents (> 1 wt.-%) pointing towards high NO_x emission risk are observed for algal biomass, empty fruit bunches (EFB), sugar beet pulp, AD digestate, coffee grounds, grass cuttings, digested sludge and spent grains. Sulphur (S) content is below 1 wt.-% for all investigated feedstock. S content of lignocellulosic biomass is usually below 0.2 wt.-%, higher S contents are observed for seaweed and sewage sludge. The reported moisture contents reflect the obtained values after drying, moisture contents upon collection will be discussed in the next section.

Ash content varies strongly from 1.8-31.7 wt.-%. High ash feedstock with ash content exceeding 10 wt.-% include AD digestate, grass cuttings, rice husk, seaweed, sewage sludge and wheat straw. On the other hand, substrates like brewer's grains, corn cobs, fir needles, miscanthus, olive pomace, orange peels, spent coffee ground, spruce bark, sugar beet pulp exhibit ash contents below 5 wt.-%. High ash content also correlates with a lower heating value of the raw materials, since ash forming matter represents a non-combustible fuel constituent. For example, the LHV of seaweed with an ash content of 21.8 wt.-% is only 14.37 MJ kg⁻¹. In contrast, spent coffee grounds with an ash content of 1.8 wt.-% possess the highest LHV of 21.33 MJ kg⁻¹.

Table 7.1: Proximate, ultimate, heating value analysis of investigated fuels by sector of origin. All reported on dry basis, except for moisture content.

Biomass type	Moisture (wt.-% _{ar})	Ash (wt.-%)	Volatiles (wt.-%)	Fixed-C (wt.-%)	C (wt.-%)	H (wt.-%)	N (wt.-%)	S (wt.-%)	O (wt.-%)	Cl (wt.-%)	LHV (MJ kg ⁻¹)
AD digestate	8.5	11.5	67.4	21.1	50.2	4.9	1.8	0.14	31.5	1.71	17.58
Corn cobs	8.3	2.2	79.9	17.9	49.2	6.2	0.3	0.40	41.8	0.18	17.50
Empty fruit bunches	7.7	9.0	81.0	10.0	50.6	5.9	1.1	0.34	33.1	0.57	19.11
Horse manure	11.1	9.8	67.0	23.2	49.0	4.8	1.4	0.14	34.9	0.12	18.01
Miscanthus	5.2	1.8	81.1	17.1	51.8	4.8	0.3	0.10	41.3	0.15	18.42
Sugar beet pulp	10.23	3.80	82.42	13.79	48.1	4.5	1.2	0.2	42.3	0.14	16.73
Rice husk	10.4	11.9	70.6	17.5	48.8	3.4	0.5	0.14	35.3	0.10	17.23
Wheat straw	7.3	11.7	70.5	17.8	45.1	4.4	0.7	0.17	38.1	0.26	16.40
Fir needles	5.7	4.0	81.2	14.7	52.8	5.3	1.3	0.11	36.4	0.14	19.99
Spruce bark	8.7	3.8	85.0	11.2	52.7	5.7	0.4	0.17	37.3	0.02	19.11
Olive pomace	3.4	2.1	78.0	19.9	54.7	5.7	0.5	0.10	37.0	0.13	20.64
Orange peels	6.8	3.9	74.6	21.5	48.5	5.8	1.0	0.13	40.8	0.69	16.55
Spent grains	8.8	3.7	83.4	12.9	52.7	6.9	3.1	0.11	33.5	0.04	19.18
Spent coffee grounds	3.0	1.8	82.7	15.6	54.2	6.4	1.9	0.14	35.6	0.02	21.33
Fallen leaves	9.0	9.6	70.5	19.9	50.1	4.6	0.8	0.11	34.7	0.09	18.06
Grass cuttings	9.5	10.5	72.7	16.9	48.0	4.9	2.2	0.18	34.2	0.26	17.07
Micro algae	6.0	5.5	78.8	15.7	51.5	6.7	8.0	0.24	28.0	1.60	19.97
Digested sludge	11.5	31.7	60.9	7.3	38.6	4.8	6.8	0.84	17.2	0.09	15.34
Seaweed	13.2	21.8	67.9	10.3	41.5	3.0	0.8	0.95	21.0	3.68	14.37

Figure 7.3 shows the inorganic element concentration in the investigated biomass substrates, as well as wood and lignite as reference. The concentration of individual elements depends on biomass type, growth environment, processing of the feedstock, but also on physiological and morphological differences in plant structures. Consequently, the amount of inorganic matter and its composition varies heavily between the different substrates.

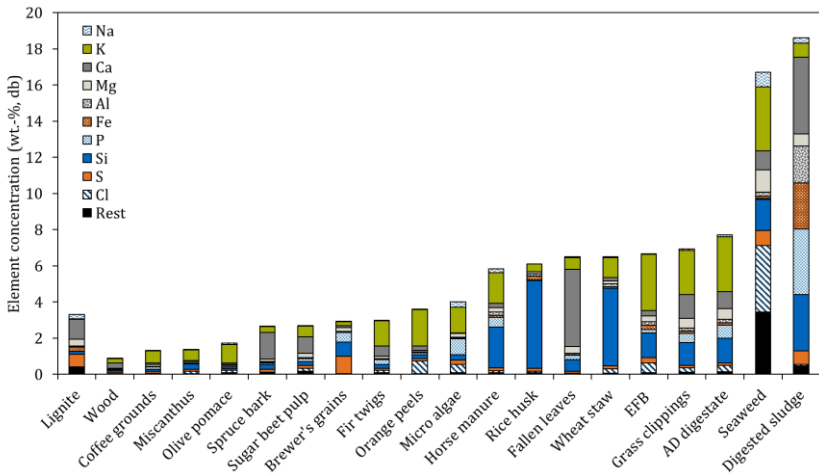


Figure 7.3: Inorganic element concentration in biomass substrates.

Nevertheless, the following general observations can be made: In biomass major ash forming elements (accounting for > 10 wt.-% of ash) are K and Si. Ca, P, Mg, Cl and S occur in concentrations between 1-10 wt.-%. The concentrations of sodium Na, Al and Fe usually stay below 5 wt.-%. Only in digested sludge Al and Fe concentrations are higher due to the precipitating agent used in waste water treatment plants. Some feedstock are specifically rich in Si like rice husk, others in Ca (e.g. spruce bark) or K (e.g. orange peels). The fuel quality of the raw material can be assessed with the fuel indices introduced in section 4.2. Feedstock containing high contents of potassium and chlorine represent challenging fuels for biomass combustion. Additionally, high ash content, high fuel-N contents are not

desired in a biofuel. Table 7.2 provides an overview on the initial fuel quality of the examined substrates prior to HTC with respect to the expected challenges in biomass combustion.

Table 7.2: Fuel quality assessment for examined substrates using fuel indices for risk evaluation of biomass combustion related challenges.

Biomass type	Corrosion risk	NO _x emission risk	PM emission risk	Slagging risk	Fouling risk
AD digestate	high	high	high	high	high
Corn cobs	low	low	high	high	high
Dig. sludge	high	high	high	high	medium
EFB	high	high	high	high	high
Fallen leaves	high	medium	medium	low	high
Fir needles	high	high	high	high	high
Grass cuttings	high	high	high	high	high
Horse manure	low	high	medium	low	high
Micro algae	high	high	high	high	high
Miscanthus	high	low	medium	high	high
Olive pomace	high	medium	high	high	high
Orange peels	high	high	high	high	high
Rice husk	low	medium	medium	high	low
Seaweed	high	medium	high	high	high
Coffee grounds	low	high	medium	high	high
Spent grains	high	high	medium	high	medium
Spruce bark	low	medium	medium	low	high
Sugar beet pulp	high	high	medium	high	high
Wheat straw	high	medium	high	high	medium

It can be observed that all examined substrates exhibit poor fuel quality. Thus, a pre-treatment prior to combustion is needed. For some substrates, the expected challenges in combustion might be overcome with the use of additives or flue gas treatment.

7.2 Quality of Carbonisation

As described above the investigated raw materials originate from various source sectors and whose fuel properties vary over a broad spectrum. In principle, all biogenic material can be hydrothermally carbonised. However, substrate specific properties lead to different outcomes in terms of mass yield and energy densification which determine the overall efficiency of the

process. Energy yield, being the combined measure of mass yield and energy densification, determines the performance of HTC with competing energetic valorisation options.

Figure 7.4 shows the mass- and energy yield obtained after HTC of the different substrates at 210 °C for 2 h, representing process conditions of intermediate severity.

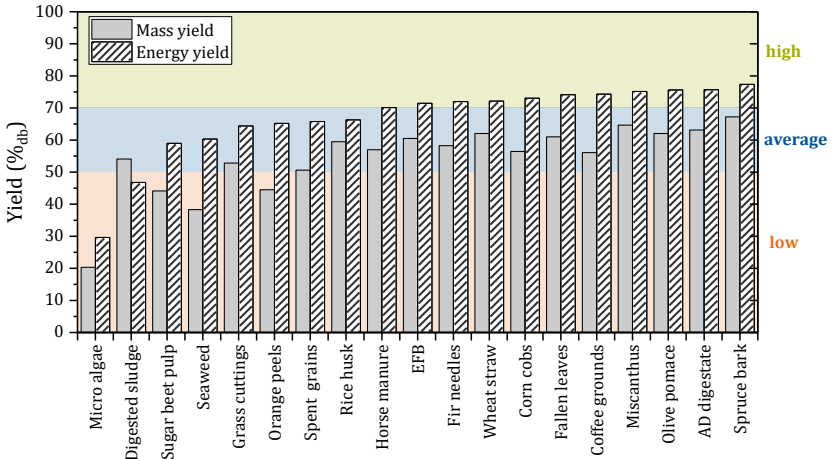


Figure 7.4: Mass- and energy yield of different substrates after HTC at 210 °C for 2 . The rating of energy yields is indicated the the right hand side.

At these conditions the obtained mass yields range widely from 20-67 %. The lowest mass yields are observed for micro algae, seaweed, sugar beet pulp and orange peels. These substrates have a biochemical composition that comprises mainly carbohydrates, lipid and proteins that are liquefied to a large extend under hydrothermal conditions. This lowers the obtained mass yield. On the other hand, higher mass yield is observed for lignocellulosic feedstock. A higher lignin content correlates with higher mass yield after HTC. A mass yield above 60 % was observed for all raw materials whose lignin content exceeds 20 wt.-%. The biochemical composition of all feedstock is summarised in Appendix B.

Mass yield gives a first indication about the suitability of HTC for a certain feedstock. Yet, to determine which proportion of chemical energy from the starting material is preserved in the produced hydrochar, the energy yield needs to be considered.

As seen in Figure 7.4 energy yield does not fluctuate as strongly as mass yield. For most investigated feedstock it ranges roughly between 60-80 % at the given process condition. Energy yields below 60 % are only observed for micro algae and digested sludge. Therefore, it seems that low mass yields are compensated to some extent by a stronger energy densification. How strongly a substrate is carbonised by HTC is illustrated in Figure 7.5. It shows the specific increase in LHV as a function of the specific increase in carbon content. The data is presented on dry-ash free basis for better comparability.

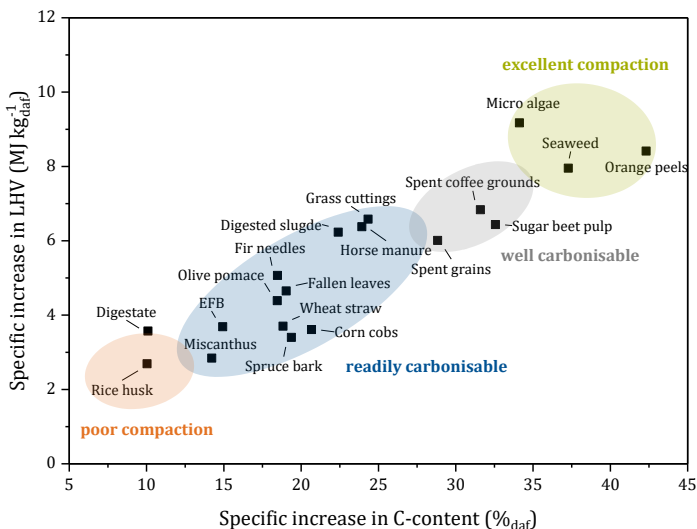


Figure 7.5: Specific increase in LHV and specific increase in carbon content of different substrates after HTC at 210 °C for 2 h.

Significant differences in the quality of carbonisation exist between different feedstock types: The highest increase in energy density is observed for micro algae, seaweed and orange peels. Coffee grounds, sugar beet pulp

and brewer's spent grains also prove to be well carbonisable. All these feedstocks contain relatively high amounts of proteins, fats, lipids and carbohydrates (see Appendix B). The majority of investigated feedstocks undergo intermediate energy densification after HTC. Low energetic compaction is observed for digestate and rice husk, which both have a high proportion of lignocellulosic biomass ("hard biomass") and little protein, fat and lipid content.

However, energy densification of the organic dry matter (daf) is not the only factor influencing energy yield: For example, while sewage sludge in this study showed average increase in carbon content and heating value on daf basis, the observed energy yield after HTC is lower than its mass yield. This can be explained with the high ash content of this feedstock, containing mostly insoluble species. During HTC of sewage sludge, combustible organic matter is partly solubilised, while inorganics mostly remain in the solid. Thus, although carbon content is increased by HTC, the increased ash content diminishes the improvements a higher carbon content would have on LHV.

In summary due to the different biomass compositions, significant substrate-specific influences on HTC mass- and energy yield are observed. The main influencing factors are the proportion of inorganic constituents, the composition of the substrates with regard to the proportions of lignocellulosic biomass ("hard biomass") and the proportions of carbohydrates, fats and proteins in the substrates. In particular, energy yield determines the overall HTC process efficiency and, thus, has a profound impact on the performance of the technology compared to competing energetic valorisation options. This aspect is discussed in the following two sections.

7.3 Feedstock Moisture Content

An important fuel characteristic that determines the energetically most favourable utilisation pathway is its moisture content. Figure 7.6 shows typical feedstock moisture contents of the investigated HTC substrates upon

their collection. The feedstock include some low moisture biomass like, rice husk, wheat straw, miscanthus and corn cobs. All other investigated substrates typically exceed 50 wt.-% moisture, when being collected. Variability in moisture content is low for feedstock that originates from well-defined industrial or agricultural processes like AD digestate, sugar beet pulp or brewer's grains. On the other hand, larger variations are observed for biomass streams which are collected or stored outdoors and are therefore exposed to weather conditions that influence their moisture content.

Since HTC is a process that takes place in water, the implementation of this pre-treatment step prior to combustion makes most sense for high moisture feedstock. The efficiency of a combustion process without flue gas condensation decreases with increasing water content of the fuel. Consequently, a threshold value exists beyond which the efficiency of HTC plus the subsequent utilisation in a combustion process exceeds the efficiency of a direct combustion. Besides moisture content, the energy yield after HTC, comprising the maximum achievable conversion efficiency is a major influencing factor in this assessment.

Figure 7.6 shows the results of a theoretical comparison of biomass combustion with and without HTC pre-treatment. Boiler efficiency was calculated by the indirect method following procedures described in the literature [231, 232]. By comparing the boiler efficiency in direct combustion to the efficiency of HTC at 210 °C for 2 h, drying and subsequent combustion, a threshold moisture content was determined above which HTC prior to combustion represents the energetically more viable utilisation route.

As Figure 7.6 shows, the threshold moisture content for all biomass substrates ranges from 47-80 wt.-%. For wood the threshold moisture was calculated to be at 54 wt.-% which corresponds to value of 55 wt.-% reported by Erlach [178] in a similar consideration for wood.

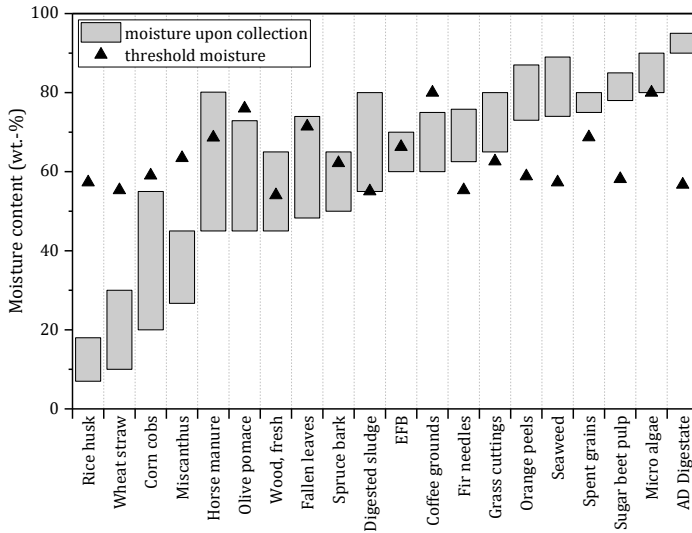


Figure 7.6: Typical feedstock moisture content upon collection and provision and threshold moisture content above which HTC conversion is favored towards direct combustion.

It can be seen that for most feedstock exceeding 50 wt.-% moisture, HTC prior to combustion is favoured towards direct combustion. A higher threshold moisture is observed for low ash substrates that exhibit high heating values like olive pomace ($LHV_{db}=20.64 \text{ MJ kg}^{-1}$) and spent coffee grounds ($LHV_{db}=21.33 \text{ MJ kg}^{-1}$). A high threshold moisture is also observed for feedstock with low mass yield after HTC like micro algae ($Y_{m,db}=20 \text{ wt.-%}$). For most substrates the threshold moisture content lies within the range of 50-70 wt.-% with a median value of 60 wt.-%.

Consequently, considering energetic efficiency, low moisture biomass like rice husk, wheat straw, corn cobs and miscanthus are not well-suited for a conversion by HTC. Further, for raw materials already possessing relatively high calorific value like olive pomace or spent coffee grounds, HTC might not be the best utilisation option. Finally, for high moisture biomass streams, where a HTC treatment results in low mass yield (i.e. micro algae), other hydrothermal conversion processes like liquefaction should be considered.

7.4 Alternative Conversion for Wet Feedstock

Apart from HTC other technologies exist that allow for an efficient conversion of wet feedstock. In the following a comparison of the performance of HTC and the most prominent alternative conversion process for wet feedstock, anaerobic digestion (AD), is made. To decide which utilisation technique should be chosen for a specific substrate a simple consideration can be made: For one ton of raw material input the amount of energy contained in the product from both processes, hydrochar from HTC and biogas from AD, is calculated. In each case the produced energy carrier is afterwards utilised in a CHP unit. For each substrate the useful energy available from both processes is shown in Figure 7.7. The data used for the calculation is provided in Appendix B.

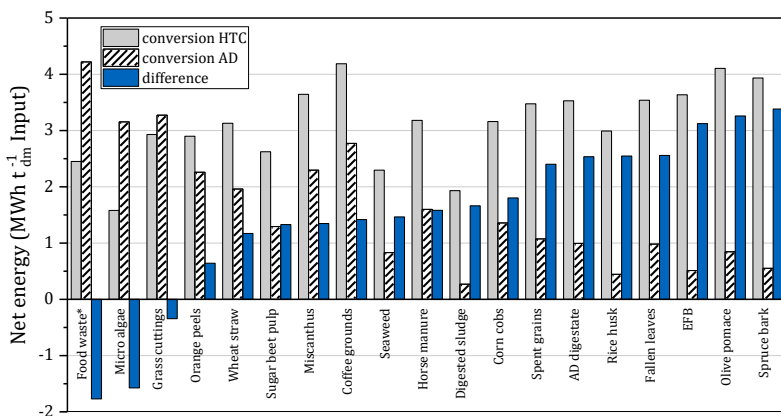


Figure 7.7: Comparison of substrate usage in a biogas plant and in an HTC plant, in each case in combination with a biomass CHP; the net energy was calculated. *Data for food waste from [69].

Accordingly, AD of micro algae and grass cuttings can provide higher usable energy than HTC. AD performs better for feedstock with large proportions of bioavailable carbon, like food waste and grass cuttings. On the other hand, HTC is favoured for the conversion of poorly fermentable substrates like

fallen leaves, digested sludge and straw due to its high carbon efficiency in the conversion of lignocellulosic material compared to AD.

Chapter summary: In conclusion, when considering a biomass stream for HTC, several factors should be taken into account: only feedstock where adequate disposal or valorisation pathways are missing should be considered for HTC. Being a rather expensive upgrading technology, low or negative fuel prices (gate-fees) are needed for an economic production of HTC fuels. More on this topic will be discussed in Chapter 10.

Biochemical composition dictates the quality of carbonisation of the substrate, i.e. the enhancement in heating value and the proportion of energy recovered in the solid product (energy yield). Energy yield determines the overall efficiency of HTC that can be achieved and therefore also its performance with respect to competing technologies.

Further, hydrothermal conversion makes most sense for feedstock with a water content above 50 %, otherwise direct combustion or upgrading via other thermo-chemical processes should be considered. The higher the heating value of the starting material, the higher threshold moisture content above which HTC exceeds the performance of direct combustion. Energy yield is also decisive in the performance of HTC compared to direct combustion: Lower energy yields also increases the obtained threshold moisture content: However, in this case both HTC and direct combustion are inefficient valorisation technologies. For substrates with high water content and low energy yield other valorisation pathways such as HTL, HTG or AD should be considered.

Finally, substrates containing high amounts of sugar are more efficiently converted by AD which is a proven technology. On the other hand, substrates with high lignocellulosic content are converted with much higher carbon and energy efficiency by HTC.

Applying these considerations, a decision tree for the selection of suitable feedstock for HTC is proposed which is presented in Figure 8.1.

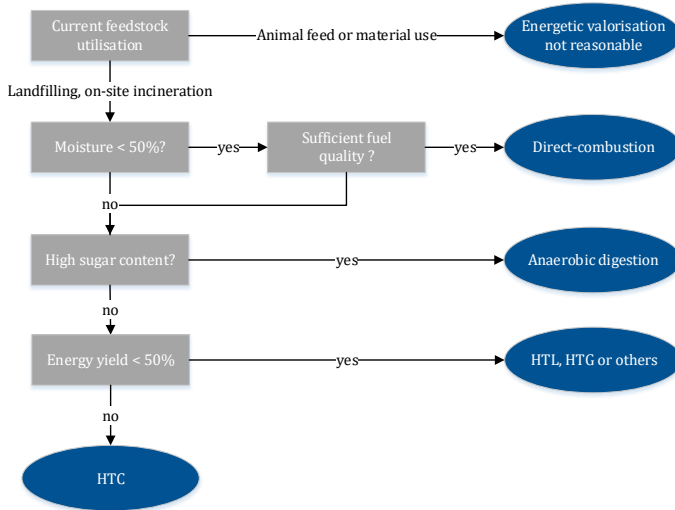


Figure 7.8: Proposed decision tree for the selection of suitable feedstock for HTC.

Table 7.3 summarises the findings made for the investigated feedstock with respect to these criteria. Fuels with alternative use and higher performance in direct-combustion or AD are deemed unsuited for the conversion by HTC. Accordingly, corn cobs, grass cuttings, micro algae, miscanthus, olive pomace, rice husk, spent coffee grounds, sugar beet pulp and wheat straw do not represent suitable substrates for HTC. In some cases HTC might still represent a viable utilisation path, for example for challenging feedstock with high alkali and chlorine content such as olive pomace and wheat straw, or for feedstock, where regulatory aspects interfere, e.g. for grass cuttings.

As a result, AD digestate, digested sewage sludge, EFB, fallen leaves, fir needles, horse manure, orange peels, seaweed and spruce bark are identified as well suitable substrates for HTC.

Table 7.3: Summary and rating of selection criteria applied to the investigated feedstock. (green=suited for HTC, grey=neutral, red=not suited for HTC)

Biomass type	Current use	Performance: HTC vs. comb.	Performance: HTC vs. AD	Fuel price	Energy yield	Overall HTC rating
AD digestate	fertilizer	HTC	HTC	low	high	suited
Corn cobs	material use	combustion	HTC	high	average	not suited
Digested sludge	landfilling, incineration	HTC	HTC	low	low	suited
EFB	mulching, landfilling	HTC	HTC	intermediate	high	suited
Fallen leaves	waste incineration	HTC	HTC	low	high	suited
Fir needles	mulching, incineration	HTC	HTC	intermediate	high	suited
Grass cuttings	composting, landfilling	HTC	AD	low	average	not suited
Horse manure	landfilling	HTC	HTC	low	average	suited
Micro algae	landfilling	HTC	AD	low	low	not suited
Miscanthus	energy crop	combustion	HTC	high	high	not suited
Olive pomace	landfilling, incineration	combustion	HTC	low	high	not suited
Orange peels	landfilling	HTC	HTC	low	average	suited
Rice husk	incineration, material use	combustion	HTC	high	average	not suited
Seaweed	landfilling	HTC	HTC	low	average	suited
Coffee grounds	landfilling	combustion	HTC	low	high	not suited
Spent grains	animal feed	HTC	HTC	high	average	not suited
Spruce bark	material use	HTC	HTC	high	high	suited
Sugar beet pulp	animal feed	HTC	HTC	high	average	not suited
Wheat straw	material use	combustion	HTC	high	high	not suited

8 Impact of Hydrothermal Carbonisation on Characteristics Relevant for Combustion

This chapter considers the impact of HTC on fuel characteristics relevant for combustion. First, the impact of HTC process conditions on heating value as well as mass and energy yield is discussed for 8 different substrates. In the second section the fate of inorganics during HTC is discussed in detail: the influence of feedstock type comparing 19 different substrates, temperature, residence time, L/S ratio as well as the impact of CO₂ additive are examined. Subsequently, the quality of HTC fuels is assessed with the help of biomass fuel indices. Finally, changes in reactivity of HTC fuels are discussed.

8.1 Heating Value, Mass- and Energy yield

The influence of process temperature and residence time on mass yield of different substrates after HTC is shown in Figure 8.1.

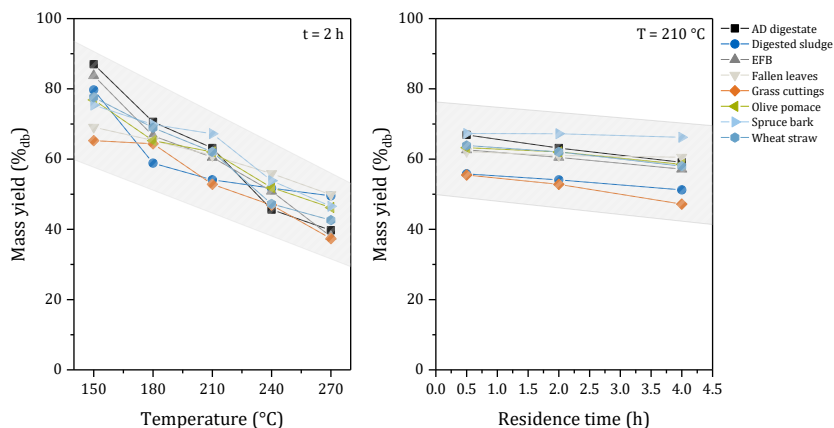


Figure 8.1: HTC Mass yield of different substrates as a function of temperature (left) and residence time (right).

Mass yield decreases with increasing treatment temperature and time in the parameter range considered. For example mass yield of olive pomace decreases from 77 % at 150 °C to 46 % at the highest treatment

temperature of 270 °C. At the same time, increasing the residence time from 0.5 h to 4 h decreases mass yield from 63 % to 58 % at 210 °C treatment temperature. Similar observations are made for the other feedstock. Differences observed between different substrates seem to be more pronounced at lower temperatures: At 150 °C, mass yield varies by up to 21 %, while at 270°C the biggest observed difference in mass yield is 13 % points. Overall, the influence of temperature on mass yield is much stronger than the influence of residence time.

Figure 8.2 depicts the development of LHV with HTC temperature and residence time for different substrates.

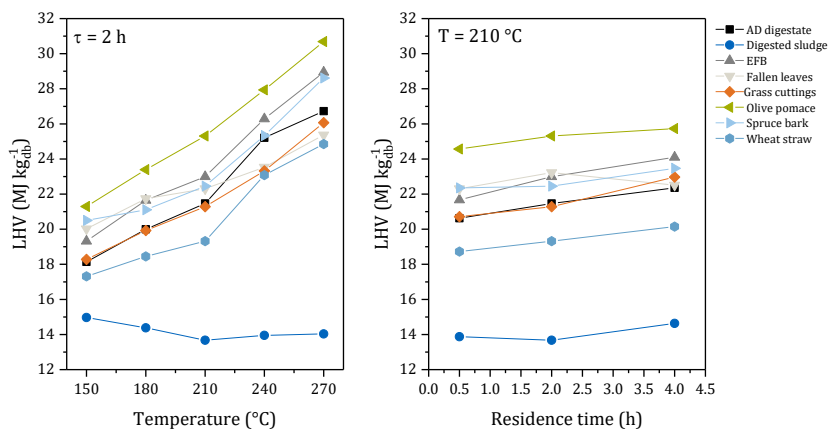


Figure 8.2: LHV of different substrates after HTC as a function of temperature (left) and residence time (right).

LHV increases with increasing treatment temperature and residence time for all substrates except digested sludge. Once more, the effect of temperature is more pronounced than the effect to residence time. At 150 °C only small changes in LHV are observed, on average LHV is increased by 3-11 % points compared to the raw material (see Table 7.1). LHV increases significantly for temperatures above 180 °C. At 270 °C, LHV value is increased by 40-52 % points compared to the raw material. The highest LHV of 31.17 MJ kg⁻¹ is reported for olive pomace treated at 270 °C. Increasing residence time also increases LHV but to a much smaller extent: For

example, increasing residence time from 0.5 h to 4 h on average increased LHV by 3-13 % points. The observed LHVs of digested sludge constitutes an exception to these findings: Upon increasing HTC temperature, LHV is found to decrease slightly. Increasing residence time does not show significant influence on LHV.

Figure 8.3 shows energy yields obtained for the substrates after HTC at different temperatures and residence times.

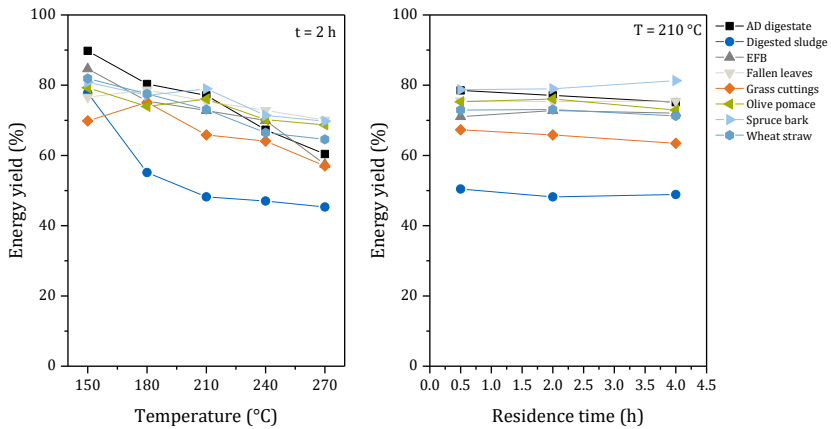


Figure 8.3: HTC energy yield of different substrates as a function of temperature (left) and residence time (right).

The observed energy yields decrease with increasing treatment temperature. The lowest energy yield is obtained for digested sludge with only 45–55% of energy from the input material being recovered in the solid product after HTC. The other feedstock exhibit fairly similar energy yields of around 70-90% at the lowest treatment temperature of 150 °C, which decrease to around 60-75% at the highest treatment temperature of 270 °C. Energy yield is higher than mass yield at corresponding temperatures, due to the increase in LHV at higher temperatures. No clear trend is observed for the dependence of energy yield on residence time. For some feedstock like spruce bark a slight increase in energy yield is observed, while for other substrates, e.g. olive pomace or grass cuttings, a slight decrease is noted.

The investigated parameter range covers a wide range of HTC conditions with different prevailing reaction mechanisms: At 150 °C structural changes of biomass are hardly expected, changes in mass yield, LHV and energy yield are most probably related to the removal of extractives and inorganic species by water leaching. Significant structural changes are induced at temperatures above 180 °C, where hydrolysis of hemicellulose (180 °C), cellulose (220 °C), and lignin (180–220 °C) take place [70, 96, 233]. These biomass degradation reactions lead to a reduction of mass yield with increased treatment temperature and residence times. Soluble organic biomass fractions are formed and dissolved in the process liquid. A higher sensitivity of mass yield to temperature changes can be seen at temperatures above 210 °C, where cellulose degradation occurs. Deviations between different substrates are the consequence of different biochemical composition of these input materials.

The increase in LHV with increasing reaction severity is also a consequence of profound structural changes: During HTC a complex series of reactions occur, which ultimately lead to the removal of oxygen and hydrogen from the fuel matrix. The governing reactions are dehydration and decarboxylation [15, 70, 92]. In consequence, carbon content of the treated biomass increases, leading to a higher energy content i.e. LHV of the resulting fuel. Oxygen content is decreased. As mentioned, the exception to these findings is the processing of digested sludge, which results in a lower LHV. Ash forming matter is retained in the fuel, while carbon-containing fuel constituents are partly solubilised during HTC. This leads to a higher proportion of incombustible material in the resulting HTC fuels which lowers LHVs. Ash content is increased from 31.7 wt.-% to 57.6 wt.-% when comparing the substrate with digested sludge HTC treated at 270 °C. On dry-ash-free basis, also the LHV of digested sludge is increased 1.4-fold.

The decrease in energy yield, being a combined measure of mass yield and energy densification (i.e. evolution of LHV), is also a consequence of increasing biomass liquefaction at higher treatment temperatures. However, the simultaneous energy densification partly compensates mass

loss, leading to a less dramatic decline in energy yield at higher treatment temperatures.

Similar observations have been reported in the literature [15, 99, 234]. For example, a study by Lynam et al. [234] investigated HTC of various lignocellulosic substrates: They found that mass yield decreases from 85-95 % at 200 °C to around 30-65 % at 260 °C, while the energy content of the fuels increased up to 1.45-fold. Similarly to the findings in the present work, they determined lignocellulosic composition as well as ash content as the governing factors for obtained mass- and energy yields.

8.2 Fate of Inorganic Elements during HTC

Besides fundamentally altering the organic structure, HTC also has a strong influence on the inorganic composition of a fuel. The following section addresses the impact of HTC on ash content, ash composition, ash melting properties as well as the expected improvements these changes have on ash-related challenges in biomass-firing. Fuel indices that have proven suitable for an application to biomass will be used for this purpose.

Impact of HTC on Ash Content

Figure 8.4 shows the relative ash content of different feedstock after a hydrothermal treatment as a function of treatment temperature and residence time. A value above 1 indicates that ash content after HTC is increased compared to the starting material.

Feedstock type seems to have the biggest impact on the change of ash content after HTC. An increased ash content is observed for grass cuttings, digested sludge and wheat straw. HTC does not strongly affect ash content in spruce bark and fallen leaves. For EFB and olive pomace ash content after HTC is decreased. At low temperatures also ash content in pre-treated AD digestate is decreased but increases for higher treatment temperatures.

HTC treatment temperature influences ash content: Especially for feedstock where HTC increases ash content, a further, strong rise in ash content is observed for higher treatment temperatures. For example, relative ash

content of grass cuttings increases from 1.3 at 150 °C to 2.1 at the highest treatment temperature of 270 °C. In treated fallen leaves or AD digestate, ash content is found to increase at temperatures above 210 °C. On the other hand, the ash content of olive pomace, spruce bark and EFB does not further change significantly with increasing treatment temperature.

Residence time does not strongly influence ash content in the investigated parameter range. A slight increase in ash content with increasing residence time is observed for all substrates except olive pomace. Comparable observations are made for the other investigated parameters of residence time and temperature (see Appendix C).

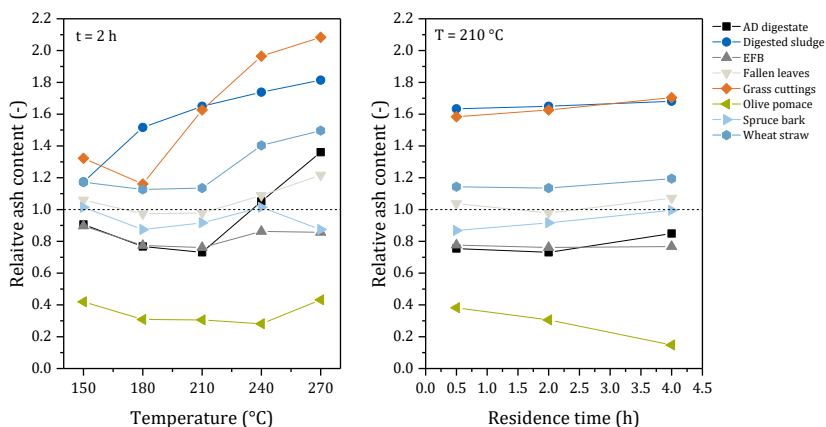


Figure 8.4: Relative ash content of different substrates after HTC as a function of treatment temperature (left) and residence time (right).

HTC changes the inorganic composition and ash content of a fuel mostly by the dissolution of certain inorganic species in the process water. Consequently, the water solubility of the different ash constituents has a strong influence on the final ash content after HTC. For example, alkali metals are known to be highly soluble, hence substrates with alkali rich ash (i.e. EFB, olive pomace) exhibit lower ash content after HTC. In contrast, for substrates with a high proportion of insoluble ash constituents and low alkali content (i.e. wheat straw, digested sludge), HTC leads to an increase in ash content.

Not only inorganic mass is reduced during HTC: As described in the previous section, HTC breaks down biomass constituents which leads to a reduction of organic matter in the solid product as well. Consequently, ash content decreases if the reduction in inorganic matter is stronger than the reduction of organic matter by biomass degradation reaction during HTC. This is illustrated in Figure 8.5, which shows a component mass balance as well as the evolution of fuel composition of the untreated substrate and hydrochar treated at 180 °C and 270 °C for 2 h respectively. One alkali-rich (EFB) and one low-alkali (wheat straw) feedstock were selected for this illustration.

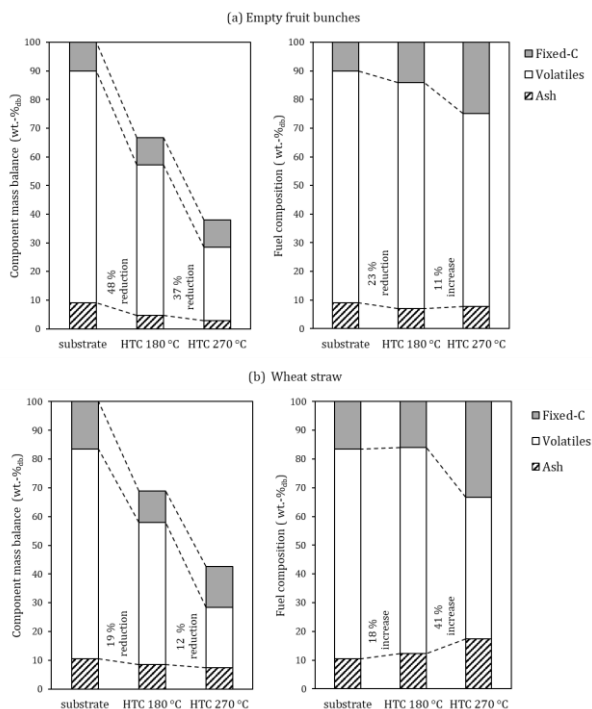


Figure 8.5: Mass balance of ash-, volatile and fixed-C content (left) and changes in fuel composition (right) before and after HTC at 180 °C and 270 °C for 2 h. The absolute amount of ash is decreasing, while the relative ash content is dependent on feedstock ash composition.

Considering the component mass balance on the left hand side of Figure 8.5, it is seen that in both cases the absolute amount of ash is decreased by HTC. A substantial decrease of 48 % is seen after HTC treatment of EFB at 180 °C,

which decreases further by 37 % when increasing treatment temperature to 270 °C. The absolute amount of ash in wheat straw also decreases by 19 % after a treatment at 180 °C, further decreasing by 12 % for a more severe treatment at 270 °C. Simultaneously, HTC also reduces the mass of organic biomass constituents, i.e. fixed-carbon (fixed-C) and volatiles. At 180 °C, volatiles and fixed-C combined are reduced by 41 % in EFB and 65 % in wheat straw. Considering the fuel composition on the right hand side of Figure 8.5, it can be seen that in the final solid product for both substrates volatile content decreases, while fixed-C increases. Ash content after HTC decreases in alkali-rich feedstock EFB, while it increases in low-alkali feedstock wheat straw. Thus, during HTC of EFB the reduction of inorganic matter is higher than the reduction of organic matter, while for wheat straw the opposite is the case. This leads to a lower ash content in EFB and a higher ash content in wheat straw after HTC. With this observation, also the increasing trend of ash contents with treatment temperature can be explained. Increasing reaction severity drastically increases biomass degradation and diminishes yield of organic matter after HTC. Meanwhile, removal of inorganic constituents does not increase to the same extent leading to an overall increase in ash content with increasing treatment temperature.

The correlation between relative ash content and ash removal efficiency with alkali content in the ash of the starting material is shown in Figure 8.6 for all investigated feedstock. The lowest relative ash contents are found in the substrates with the highest ash alkali content like corn cobs, olive pomace, spent coffee grounds, EFB and orange peels. For these feedstock also the removal efficiency of ash is highest. High relative ash contents and low removal rates of ash from the feedstock are observed for feedstock that are rich in Si and P like digested sludge, horse manure, rice husk and grass clippings.

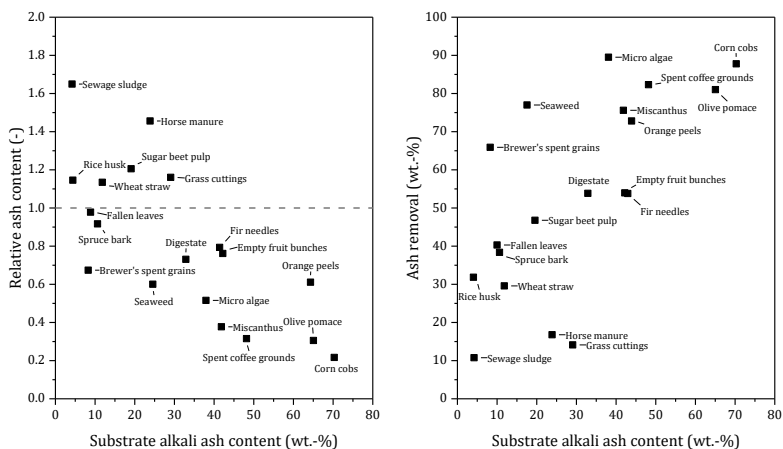


Figure 8.6: Relative ash content (left) and ash removal (right) of different feedstock after HTC at 210 °C for 2 h as a function of substrate alkali content.

As the dispersion of the measurement values indicates, the alkali content is not the only influencing factor for ash removal efficiency. Biomass ash consists of a variety of different inorganic components with varying solubility. Besides alkali metals, chlorine also represents a highly water soluble ash compound. For example, the high ash removal efficiency in seaweed and micro algae is a consequence of their particular high chlorine content. Yet, with potassium being the most abundant inorganic element in biomass ash its concentration in the raw material provides a good first indication for the development of ash content after HTC.

In summary, HTC removes inorganic matter from biomass by their dissolution in the process water. Depending on the individual inorganic composition of the substrate, ash content after HTC increases or decreases. Substrates with a large proportion of water soluble inorganics like potassium or chlorine are more likely to exhibit lower ash content after HTC. A more severe HTC treatment is prone to increase ash content mostly on account of the increased loss of organic material by biomass degradation.

Impact of HTC on Ash Composition

As introduced in the previous section, the nature and proportions of different ash forming elements determine the ash properties of HTC treated biomass. In the following the influence of feedstock, process conditions, L/S ratio as well as additives on the individual concentrations of major ash forming elements (K, Mg, Ca, Al, P, Si, Cl and S) is discussed.

Feedstock Dependence

Figure 8.7 shows the relative element ash content of main ash forming elements K, Mg, Ca, Al, P, Si, Cl and S in 17 different substrates after a hydrothermal treatment at 210 °C for 2 h. A relative element ash content below 1 means that the concentration of the corresponding element in the hydrochar is lower than in the starting material, if it is above 1 this indicates lower removal efficiency and the respective element increases in concentration in the product ash. The ash composition of the raw materials is shown in Figure 7.3.

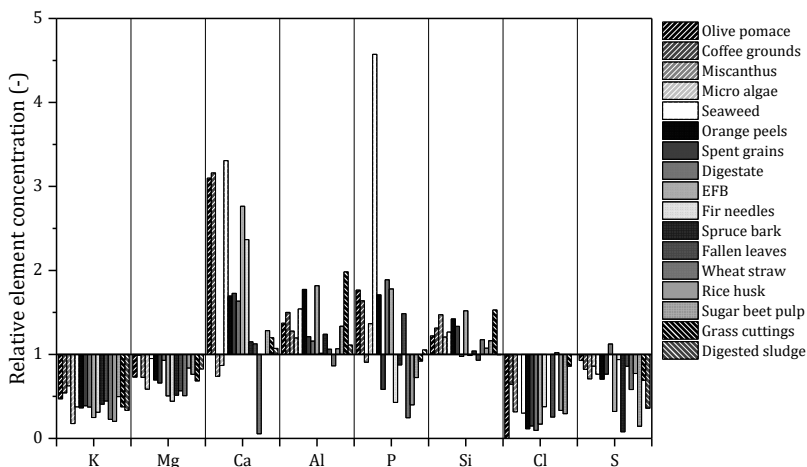


Figure 8.7: Relative element concentration of main ash forming elements in different biomass substrates after HTC treatment at 210 °C for 2 h.

Significant differences in the relative concentrations depending on both element and feedstock type can be seen. A strong reduction in K is observed

for all feedstock, the concentration in the product ash is reduced to a relative content of 0.37 on average after HTC. The strongest reduction is seen in micro algae ($X_{K,ash} = 0.18$) and the lowest reduction in miscanthus ($X_{K,ash} = 0.63$). Likewise, with an average relative concentration of 0.35, Cl is removed to a large extent in all treated substrates, but with a more widespread distribution. Mg is also reduced in concentration in all feedstock, but to a lesser extent: Relative Mg content is 0.70 on average. The concentration of Ca, Al and Si is, with some exceptions, mostly increased in the hydrochar ash, indicating limited removal during HTC. Only in miscanthus, wheat straw and micro algae, a reduction of Ca concentration is found in ash of HTC fuels. P removal at the given conditions seems to be feedstock specific. For most feedstock P concentration in the ash increases, with the exception of wheat straw, rice husk, fir needles and spent grains, for which P content in the hydrochar ash decreases. Finally, S fuel content is decreased in all feedstock except AD digestate. Stronger variation in removal efficiency and thus stronger feedstock dependency is observed compared to e.g. K or Cl removal.

Ash forming matter in biomass can be classified to three groups: (1) Water soluble ions, (2) organically associated metals and (3) amorphous, crystalline or precipitated compounds. The chemical form in which each element is present in biomass strongly influences the ability of HTC to remove it from the biomass matrix. Being a process that takes place in water, HTC should easily remove water soluble salts. HTC also leads to a profound transformation of the organic matter in biomass, thus potentially also affecting organically bound metals. Most of the observed removal and concentration trends of different ash forming matter can be explained by their chemical nature in biomass: For example, over 90 % of K in plants is present in the form of ionic salts like potassium chlorides or -nitrates, explaining the strong reduction in K after HTC [235]. Cl, which is also removed to a large extent during HTC, almost exclusively exists as highly mobile monovalent ion in biomass. Between 60-90 % of Mg occurs as ionic salts comprising magnesium-nitrate, -phosphate and -chloride. The rest is mostly organically associated e.g. as the central atom of the chlorophyll

molecule. For Ca only 20-60 % is present in water soluble form. The majority of the remaining Ca is present as amorphous or crystalline compounds like e.g. calcium-oxalate, that are insoluble in water, explaining the lower removal of calcium from biomass by HTC. Similarly, Si in plants comprising of mostly amorphous, insoluble silica is hardly removed during HTC [236]. P is present as both ionic phosphates as well as constituent in protein, lipids and nucleic acids [235, 237]. Phosphates are known to form mostly insoluble compounds with metals, with ammonium and alkali-phosphates being the exception to this. Thus, for most feedstock, P increases in concentration after HTC. S in plants exists both as inorganic salt (sulphates) and organic sulphur. The proportion of inorganic and organic sulphur is dependent on soil composition. Metal sulphates, except calcium sulphate, are generally water soluble and thus are easily removed by HTC. The observed differences in sulphur removal could be a consequence of different proportions of organic and inorganic sulphur in the starting materials.

The fate of individual elements during HTC was also investigated by Smith et al. [52] and Reza et al. [46]. Both report high removal of alkalis and chlorine during HTC and more limited removal for earth alkaline and P. While Smith et al. attribute the differences in removal efficiency during HTC to the different inorganic phases the elements occur in biomass, Reza et al. hypothesize, that the association of inorganics with the lignocellulosic matrix determines the effectiveness of HTC in removing these species. Ultimately, both factors influence the removal of inorganics: The phase in which they occur determines the overall removal efficiency; their association within the lignocellulosic biomass structure determines the development of inorganic concentration with HTC temperature and residence time, which will be discussed in detail in the following section. Consequently, the concentration of K, Cl and Mg that occur mostly as soluble salts is reduced significantly in HTC fuels. In contrast, Ca, Si, P and Al, existing mostly in water insoluble phases, are removed to a lesser degree leading to an increase in concentration of the respective element in the hydrochar ash.

Influence of Process Parameters on Ash Composition

The ash composition of HTC fuels is not only dependent on feedstock, but also on HTC process conditions. In the following the influence of treatment temperature and residence time on the removal efficiency of K, Mg, Ca, Al, P, Si, Cl and S is discussed based on the example of AD digestate. Similar observations are made for the other substrates. Figure 8.8 shows the element specific removal efficiencies as a function of treatment temperature at different residence times.

The highest removal efficiencies are observed for K and Cl. For these elements removal efficiency increases with higher treatment temperatures while residence time seems to have limited impact. Cl removal already exceeds 70 % at the lowest treatment temperature of 150 °C and increases steadily to over 97 % with higher treatment temperatures. For K a more significant influence of temperature on removal efficiency, especially at lower treatment temperatures, is observed: K removal strongly improves from 29-55 % at 150 °C to over 70 % at 180 °C. K removal therefore seems to be more related to structural changes in biomass than Cl. Significant structural changes in HTC are induced starting at temperatures of around 180 °C, where hemi-cellulose degradation starts. Therefore, it is possible that a large part of inorganic containing compounds exist in hemi-cellulose and other macromolecular biomass constituents and is made accessible for dissolution upon their degradation. This is also supported by similar findings by Reza et al. [46] and Smith et al. [132]. Smith et al. reported 60-93 % K removal at 200 °C, which increased to 84-97 % at 250 °C. Once more, the high overall removal of K and Cl is most probably attributed to the fact that they occur largely as soluble ionic species.

The observed removal efficiency of earth alkali metals Mg and Ca is lower. Initially, removal efficiency increases with temperature for both elements. Mg and Ca extraction peaks at a maximum of 57 % and 24 % respectively at HTC temperatures of 210 °C.

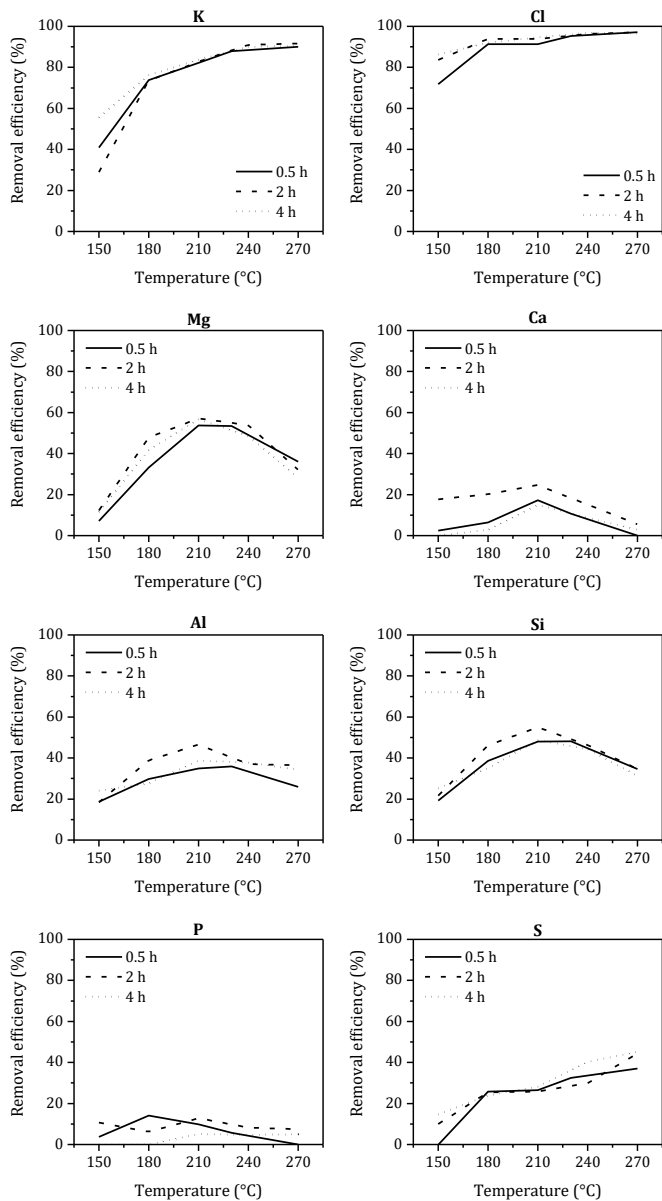


Figure 8.8: HTC removal efficiency of main ash elements K, Cl, Mg, Ca, Al, Si, P and S in treated AD digestate as a function of treatment temperature and residence time.

The highest removal efficiencies approximately correspond to the proportion of ionic phases (up to 60-90 % for Mg, 20-60 % for Ca) in which both elements usually occur in plants [235]. At higher temperatures removal efficiency declines with increasing treatment temperature.

Several explanations are possible for these observations: Reaction severity is known to influence surface functionality of hydrochars and thereby also cation exchange capacity (CEC) [15, 238, 239]. CEC indicates the ability to adsorb metal cations such as Mg^{2+} or Ca^{2+} . At higher temperatures an increase in CEC could lead to the reincorporation of metal cations from the water phase into the hydrochar. Another possibility is that at higher treatment temperatures, metal extraction is hindered due to a built up of an organic layer from hydrolysis-derived products on the hydrochar surface [240]. Finally, Chen et al. [241] have shown that divalent cations such as Mg^{2+} and Ca^{2+} can play a role in polymerisation reactions by acting as a crosslinking agent during secondary char formation. Thus, at higher reaction temperatures and higher re-polymerisation rates they could be reincorporated into the hydrochar. Finally, water characteristics change significantly under hydrothermal conditions. Up to 200 °C, most salts are highly soluble in water. Yet, this solubility is dependent on the dielectric constant of water which is dropping at higher temperatures. In HTG, taking place under super-critical conditions, salt precipitation due to a change in solubility is a known problem for certain salt types [242]. Therefore, salt precipitation at higher temperatures might also play a role in HTC removal efficiencies.

For Al and Si removal a similar peak in efficiency is observed at 210 °C. In other feedstock it seems to be stable at around 20-30 % for Al and 20-40 % for Si with no strong development tendency with neither temperature nor residence time. P removal efficiency is even lower, ranging around 20 %. Further, it is decreasing for most feedstock with increasing treatment temperature. For example, in fallen leaves P removal efficiency is around 30 % at 150 °C and decreases below 5 % at 270 °C. P removal proceeds through both solubilisation of soluble inorganic phosphate salts and by the

decomposition of organic phosphorous containing compounds (i.e. lipids, proteins, etc.). This results in a combination of reactive phosphate anions and organic compounds in HTC process water. The decreasing efficiency in P removal at higher temperature could be due to the presence of Mg^{2+} and Ca^{2+} that are capable of promoting P precipitation as magnesium or calcium phosphate on the hydrochar surface. A decreasing removal efficiency of HTC for Mg, Ca and P, at higher temperatures, has also been observed by Smith et al. [132]. For example, they reported a decrease of removal efficiency from 43 to 18 % upon increase of HTC temperature from 200 to 250 °C for oak wood.

Finally, removal efficiency of S is increasing with increasing HTC temperature. At 150 °C around 10 % of S are removed by a hydrothermal treatment. This proportion increases to roughly 40 % at the highest treatment temperature of 270 °C. For other feedstock, slightly higher removal efficiency of 59 % in fallen leaves and 77 % in spruce bark, but the same behaviour with changes in treatment temperature are observed.

In conclusion, removal efficiencies of inorganic material are element specific and dependent on HTC conditions. HTC temperature has a stronger influence on removal of inorganic biomass constituents than residence time. An increase in removal efficiency with increasing treatment temperature is noted for elements K, Cl and S. Extraction of Mg and Ca is found to be highest at intermediate treatment temperatures around 200 °C. Temperature has a limited impact on Si and Al extraction. For P a decline in removal efficiency was found with increasing treatment temperatures for most feedstock.

Liquid-to-solid ratio

A first indication, the impact of liquid-to-solid (L/S) ratio on the extraction of inorganics is provided. L/S ratio during processing HTC is dependent on feedstock moisture content, i.e. the water content of biomass upon delivery and the use of additional water for biomass mixing or water recycling during the process. Figure 8.9 shows the removal efficiency and relative content of inorganic components in orange peels carbonised at 210 °C for 2 h and L/S ratios of 5, 10 and 20. Removal efficiency increases independent on element

species for higher L/S ratios. Within the selected parameter range a linear relationship between L/S and removal efficiency is observed for all inorganic species. On the whole, ash forming matter is extracted to 35 % at L/S = 5, with this fraction increasing to 61 % at L/S = 20. The element specific removal efficiencies and relative concentrations reflect the finding in the previous section: The highest removal is noted for K and Cl with extraction efficiencies of 67 % and 68 % at the highest solid load. Diluting solid matter increases removal efficiencies to 90.5 % for K and 91 % for Cl. Mg removal is also quite high and between 48-78 %.

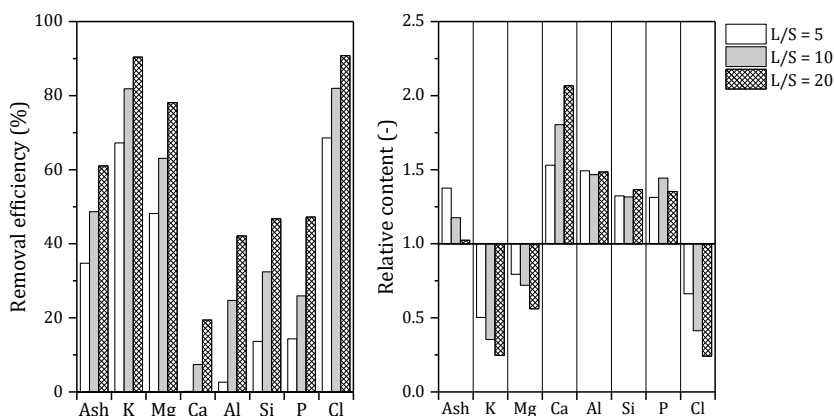


Figure 8.9: Removal efficiency (left) and relative content of inorganic components (right) for liquid-to-solid-ratio 5, 10 and 20 in orange peels HTC treated at 210°C for 2 h.

Lower removal efficiencies are observed for Ca, Al, Si and P. However they show a stronger sensitivity towards L/S ratio compared to well soluble inorganic elements like K, Mg and Cl. For example, P removal efficiency increases from 14 % to 47 % for lower solid concentration, a relative increase of over 200 %, while for e.g. K the relative increase in removal efficiency is only 34 %. The relative element concentrations after HTC are similar to the finding in the previous sections: After HTC, a fuel with altered

ash composition results. Hydrochar ash contains lower alkali, Mg and Cl content, while the proportion of Ca, Al, Si and P in the ash is increased.

Several factors could lead to the lower removal efficiencies of inorganic materials at higher solid concentrations during HTC: The extraction of inorganics might be hindered due to a built up of an organic layer from hydrolysis derived products on the hydrochar surface [240]. Higher solid load also leads to a higher concentration of organic matter and thus to faster built up of such organic structures. Additionally, at high solid concentration the slurry is almost paste-like and the low removal efficiencies could also be due to poor mixing and poor particle dispersion in water. Further, the high solid load also leads to higher concentration of solubilised inorganics making precipitation reactions, i.e. of calcium cations and phosphate anions, more likely. To date, no comprehensive study on the impact of L/S ratio on the fate of inorganic elements during HTC exists, however Singhal et al. [126] studied the impact of L/S ratio in the range of 15-50 on inorganic removal during biomass washing. They reported higher removal of Cl, Ca, P, S and N with increasing L/S ratio. On the other hand, increasing the L/S beyond 10 did not significantly improve K removal any further.

The analysis of saturation effects and phase equilibria of individual components is beyond the scope of this work. The results presented indicate a strong impact on L/S ratio on inorganic composition of HTC fuels. Thus, future work should investigate the effect of L/S ratio on ash composition in more detail: In commercial applications the trade-off between mass yield and ash removal should be considered, i.e. in process design. Further, the impact of process water recycling on ash properties requires more attention.

Impact of CO₂ Additive

Acid addition has proven to be effective in demineralising biomass and accelerating reaction rates in HTC [130]. However, handling of these catalyst is a challenge and can lead to the corrosion of equipment especially at higher temperatures. CO₂ addition could provide an easy to use, inexpensive alternative to conventional acid catalyst.

Figure 8.10 shows mass yield, LHV and ash content of different substrates treated at 210 °C for 2 h with Argon (Ar) and carbon dioxide (CO₂) as pressurising agent.

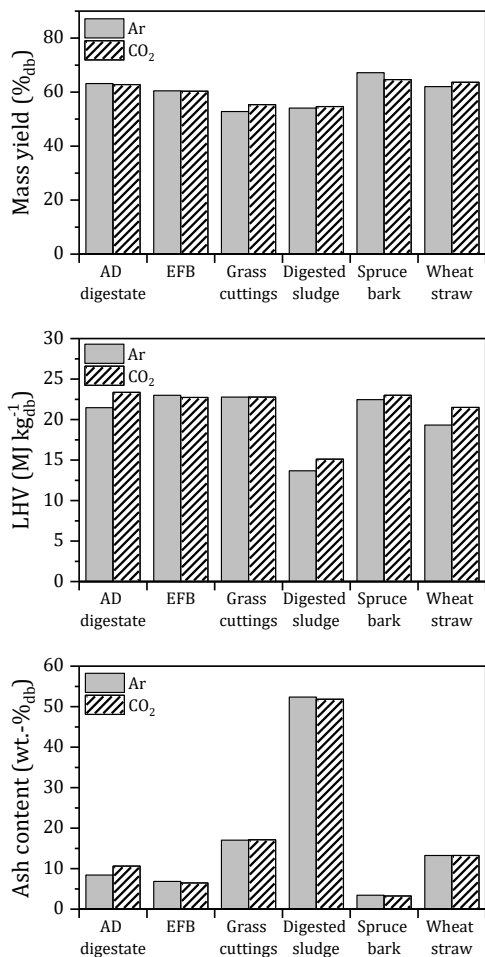


Figure 8.10: Mass yield, HHV and ash content of substrates HTC treated at 210 °C for 2 h with Argon (Ar) and carbon dioxide (CO₂) as pressurising agent.

No significant impact of CO₂ addition on mass yield, HHV and ash content could be observed for the investigated process conditions. This contradicts the findings of Bach et al. [243] who reported lower mass yields, decreased HHV and decreased ash content for hydrochar produced in CO₂. They hypothesized that upon CO₂ addition pH in the reaction medium would decrease, hence accelerating acid-catalysed reactions during HTC. This would lead to enhanced biomass degradation and in consequence to lower mass yields, while also promoting ash removal from the biomass matrix. Indeed such an effect has been shown by Hunter et al. [244] for two reactions in organic synthesis. Using Henry's law for approximation, a pH between 3 and 4 is expected under the investigated HTC conditions. This is in range with findings by Peng et al. [245] who have calculated pH values between 2.97-4.11 of CO₂-saturated water at temperatures between 40 to 150°C, at pressures up to 150 bar. This is only slightly more acidic than the pH of HTC process water after reaction that ranges between 3.6 and 5.2 in the presented work (see Section 9.2).

Consequently, Bach's findings could not be confirmed by the presented work. In the investigated parameter range ($T = 180\text{-}240\text{ }^{\circ}\text{C}$, $t = 2\text{ h}$) no impact of CO₂ addition on fuel characteristics was found. The residence time in Bach's experiments was 30 min. Hence, it is possible that CO₂ addition has a more pronounced effect at shorter residence times and lower temperatures. However, in this work also no effect was observed at lower temperature of 180 °C. Thus, to clarify whether CO₂ addition has any significant effect on the mass yield, LHV and ash properties of hydrochar, more experiments at a broader range process conditions, with a higher number of repetition are needed.

Impact of HTC on Ash Melting Behaviour

In traditional ash melting analysis, the temperatures at which the various stages of ash softening and melting takes place are assessed and described by four characteristic temperatures: shrinkage starting temperature (SST), deformation temperature (DT), hemi-spherical temperature (HT) and flow temperature (FT). It is a widely accepted method to predict the likelihood of

deposition of ash particles on heat exchange surfaces. Slagging and fouling can lead to reduced thermal efficiency, corrosion and difficulties associated with the removal of ash from the power boilers.

Table 8.1 shows the ash melting temperatures of raw biomass and hydrochar ash samples treated at 210 °C and 270 °C for 2 h. The complete dataset for all temperatures and treatment times is provided in Appendix C.

Table 8.1: Ash melting temperatures of substrate and hydrochar ash treated for a residence time of 2 h.

Biomass type	Condition	SST (°C)	DT (°C)	HT (°C)	FT (°C)
AD digestate	raw	863	1040	1147	1164
	HTC 210°C	963	1119	1300	1320
	HTC 270°C	781	1208	1256	1291
EFB	raw	837	954	1035	1230
	HTC 210°C	915	1177	1344	1383
	HTC 270°C	940	1205	1365	1385
Fallen leaves	raw	1189	1470	1464	1477
	HTC 210°C	1037	1441	1524	1519
	HTC 270°C	1070	1410	1509	>1500
Grass cuttings	raw	946	1083	1171	1214
	HTC 210°C	964	1203	1231	1296
	HTC 270°C	781	1206	1233	1282
Digested sludge	raw	772	1169	1218	1232
	HTC 210°C	663	1198	1269	1282
	HTC 270°C	741	1142	1227	1248
Spruce bark	raw	1304	1409	1453	1457
	HTC 210°C	1074	1341	>1550	>1550
	HTC 270°C	1313	1478	1502	1519
Wheat straw	raw	722	1236	1398	1432
	HTC 210°C	852	1086	>1550	>1550
	HTC 270°C	932	1118	>1550	>1550

Depending on feedstock, significant differences in ash melting temperatures are observed: Biomass ashes from feedstock rich in K and P such as sewage sludge, AD digestate and EFB exhibit the lowest initial deformation

temperatures of 772, 863 and 837 °C. Spruce bark, being rich in Ca and shows a higher SST temperature of 1304 °C.

The effect of HTC on the ash melting seems to be quite variable: Figure 8.11 illustrates ash fusion temperatures of different feedstock in raw condition and HTC treated at 210 °C and 270 °C for 2 h.

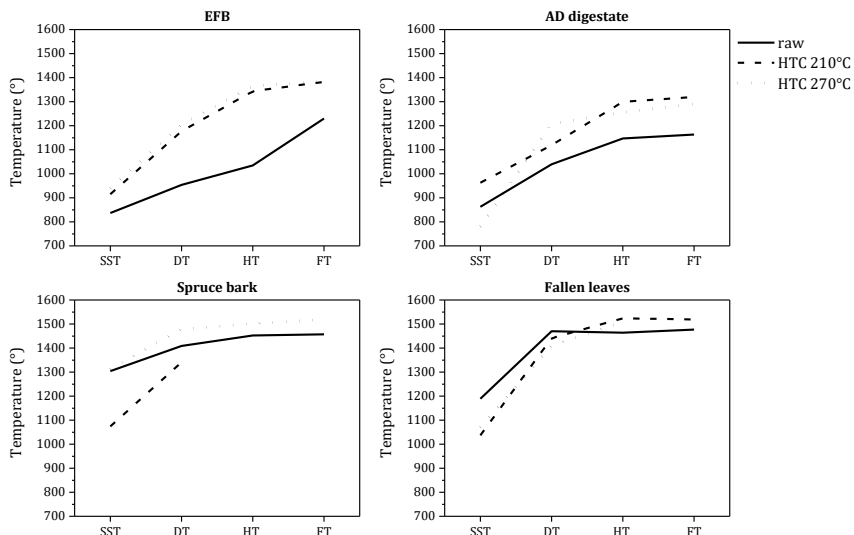


Figure 8.11: Characteristic ash fusion temperatures of untreated and HTC treated EFB, AD digestate, spruce bark and fallen leaves.

For some biomass types like EFB the effect of HTC seems to be highly beneficial increasing the SST of the sample treated at 270°C by over 100°C. Similarly, improvements in ash fusion are observed for HTC treated grass cuttings, wheat straw and AD digestate. A higher treatment temperature however, does not necessarily further lead to significant improvement concerning ash melting temperatures. On the contrary, for spruce bark, fallen leaves and sewage sludge, SST is lowered after pre-treatment by HTC. For these feedstock, HTC yields little to no improvements concerning the other characteristic ash melting temperatures.

Despite high complexity of ash melting behaviour, a number of inorganic biomass constituents have been shown to play an important role: While Mg

and Ca generally increase ash melting temperatures, alkali metals are known to form low-temperature melting alkali silicates in the presence of Si. High P contents and high concentrations of chlorine are also linked to low ash melting temperatures. HTC fundamentally changes the inorganic composition of treated biomass samples, thereby affecting ash melting temperatures. Improvements in ash melting after a pre-treatment are likely a consequence of the removal of elements lowering the ash melting temperature such as alkali metals. Additionally, elements beneficial for high ash melting temperatures, such as Ca, increase in concentration in the hydrochar ash. Therefore, in substrates with low ash melting temperatures due to high alkali content, HTC has a positive effect on SST. Smith et al. [52] have drawn similar conclusions concerning ash-melting temperatures after HTC.

In this study, significant improvements concerning ash fusion characteristics are found in alkali feedstock such as EFB, AD digestate, grass cuttings and wheat straw. Hence, the increase in ash fusion temperatures for these substrates indicate a lowered risk for slagging and fouling during the combustion of HTC fuels. In contrast, a small impact of HTC on ash melting characteristics of substrates rich in Ca and P, like fallen leaves, spruce bark and digested sludge is observed.

8.3 Fuel Quality Assessment

As discussed in the previous section, HTC changes both the organic and the inorganic structure and composition of biomass. It can be expected, that this strongly influences the combustion behaviour of HTC fuels. Fuel indices provide a quick pre-evaluation of the improvements of fuel quality by HTC with respect to combustion-related challenges. Fuel indices are derived from standard fuel analysis and provide predictions on e.g. corrosion risk. Although the accuracy of prediction solely based on fuel indices is limited, they allow for a preliminary assessment of a large number of fuel samples without time-consuming and expensive pilot-scale testing. In the following the implications that the changes in fuel composition after HTC have on combustion-related problems such as corrosion, ash melting, nitrogen oxide

emissions, and particulate matter emissions are discussed using fuel indices that have been proven suitable for biomass fuels. The quality of HTC fuels in terms of fuel indices is compared to wood pellets currently used by power plant operators as reference. Partial results of the presented chapter have already been published in [246].

Corrosion Tendency

One challenge in biomass firing is high temperature corrosion of superheaters due to the formation of alkali chloride, its condensation and subsequent reaction of the superheater material with chlorine. Although the underlying mechanism is quite complex, the molar $2 S/Cl$ has proven to be a useful indicator for corrosion risks to be expected from the combustion of a specific fuel. Only minor corrosion risks have to be expected for a molar $2 S/Cl$ ratio of > 4 . Figure 8.12 (a) shows the evolution of molar $2 S/Cl$ ratio and fuel Cl content for untreated and HTC fuels treated at different temperatures at a residence time of 2 h.

Overall, the values of the molar $2 S/Cl$ ratio are increased with increasing treatment temperature for AD digestate, EFB and fallen leaves. HTC treated fallen leaves even surpass the threshold value of 4 for low corrosion risk. Molar $2 S/Cl$ ratio does not significantly change in hydrochar from grass cuttings, spruce bark and wheat straw. Molar $2 S/Cl$ ratio is decreased in hydrochars from digested sludge. For olive pomace no evaluation is possible due to the Cl concentration being below the detection limit. With the exception of fallen leaves, HTC does not elevate the molar $2 S/Cl$ ratio above the critical value of 4. Compared to wood pellets molar $2 S/Cl$ ratio of HTC fuels is considerably lower, indicating higher corrosion risk.

The changes observed in molar $2 S/Cl$ ratio are a consequence of different concentrations of S and Cl in the hydrochars. As discussed in Section 8.2, HTC removes both S and Cl from the biomass matrix. While Cl occurs almost exclusively in a highly soluble ionic form, S is present both as inorganic and organic species in biomass. Consequently, for substrates where molar $2 S/Cl$ ratio can be improved, Cl removal is more efficient than S removal. Consequently, in feedstock with high Cl removal, like e.g. EFB or AD

digestate, an increase in 2 S/Cl ratio is observed. On the other hand molar 2 S/Cl ratio remains approximately constant in substrates where both Cl and S undergo similar reduction as in grass cuttings, spruce bark and wheat straw.

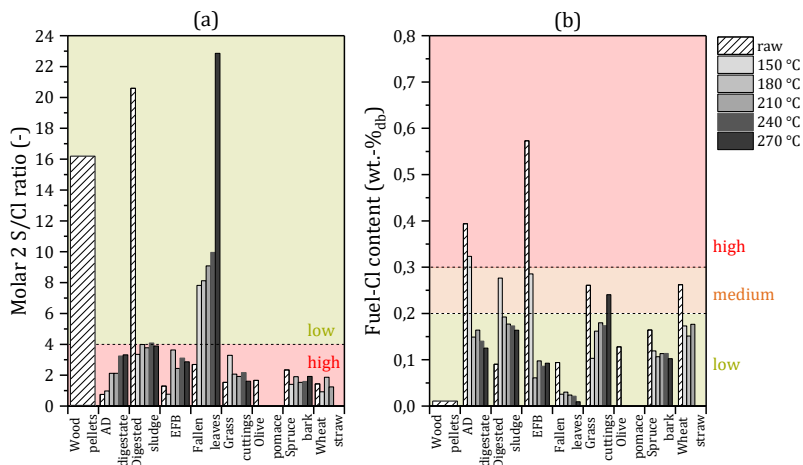


Figure 8.12: Molar 2 S/Cl ratio (a) and fuel Cl content (b) of raw substrates and hydrochars treated at different temperatures for 2 h. Corrosion risk is indicated with coloring (low=green, medium=orange, high= red). The values of wood pellets serve as a reference.

However, the molar 2 S/Cl ratio might not be able to completely assess the performance of HTC in decreasing corrosion risk, since it does not take into account the absolute concentration of both components in the fuel. HTC strongly changes the concentration of S and Cl in the fuels: In 20 of the 145 HTC fuel samples investigated in this set, Cl content is below the detection limit of 0.01 wt% of our device. Therefore, considering the fuel Cl content as an indicator for corrosion risk might be more reliable in evaluating the impact of HTC on corrosion risk. The impact of HTC on fuel Cl concentration is shown in Figure 8.12 (b). Following the classification of Tortosia Masiá et al. [150], a high corrosion risk has to be expected when combusting AD digestate and EFB. An intermediate corrosion risk is predicted for grass cuttings and wheat straw.

Cl content generally decreases after a pre-treatment by HTC. For AD digestate, EFB, fallen leaves, spruce bark and wheat straw Cl concentration in the fuels decrease consistently with increasing treatment temperature. HTC treating these substrates decreases the Cl concentration to a safe concentration concerning corrosion risk. In digested sludge initially Cl concentration increases, but subsequently decreases again with higher treatment temperatures. A safe Cl concentration is reached for all fuels treated at temperatures of 180 °C and above. For grass cuttings Cl content initially strongly decreases but then increases again. For grass cutting treated at 270 C a medium corrosion risk is predicted, but is still lower than for the raw substrate. Cl content after HTC is still higher than for wood pellets, that have a Cl content of 0.01 wt.-%.

Although the impact of HTC on molar S/Cl ratio is ambiguous, it can be expected to have a positive impact on the risk of high temperature corrosion when evaluating the Cl content of the fuels. HTC decreases Cl concentrations in the treated fuels, while also increasing their heating value. This leads to a drastic decrease of Cl input to the combustion process limiting the likelihood of high temperature corrosion.

Risk for Nitrogen Oxide Emissions

Nitrogen oxide (NO_x) emissions are a possible pollutant resulting from the combustion of biomass. The fuel-N content is a common indicator for NO_x emission risk since NO_x formation is known to originate mainly from the oxidation of fuel-N. Figure 8.13 shows the specific fuel-N per unit energy and the fuel-N on weight basis for untreated and HTC treated substrates at different temperatures. According to the threshold value established [143, 146, 149], (see Table 4.3) high NO_x emissions have to be expected for AD digestate, digested sludge and grass cuttings that exhibit the highest concentration of nitrogen.

Figure 8.13 (b) shows a clear dependency of fuel-N on HTC treatment temperature and feedstock type. Compared to wood, the investigated residual biomass exhibits much higher fuel-N content. For most substrates, fuel-N initially decreases at low HTC treatment temperatures and gradually

increases at higher treatment temperatures. For example, in AD digestate fuel-N content decreases by 15 % in hydrochar treated at 150 °C but increases by 72 % in hydrochar treated at 270 °C. Similar behaviour is seen in EFB, grass cuttings, wheat straw and olive pomace. Fuel-N is increased in all samples from spruce bark and fallen leaves. Again, fuel-N further increases with higher treatment temperatures. A different behaviour of fuel-N is noted for HTC fuels originating from digested sludge: fuel-N decreases after HTC and with increasing reaction severity decreases further. This implies fuel-N in this substrate occurs in different structural phases than in lignocellulosic biomass.

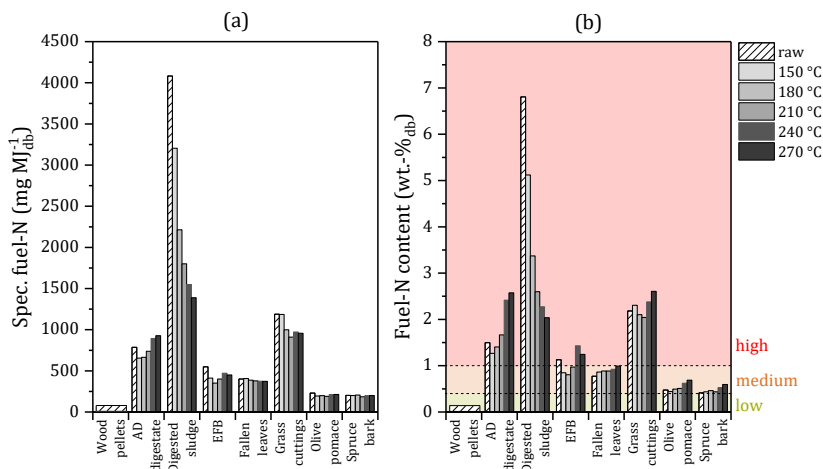


Figure 8.13: Specific fuel-N content per unit energy (a) and fuel-N with indicated ranges of NO_x emission risk (b) of biomass samples HTC treated at different temperatures at a residence time of 2 h and wood pellets as reference. Emission risk propensity is indicated with coloring (low=green, medium=orange, high= red).

The changes in nitrogen concentration in HTC fuels are a consequence of different processes during HTC: On the one hand, nitrogen is released to the process water by solubilisation of N-containing species in the process water. The initial decline in fuel-N at low temperatures can be explained by the removal of nitrogen in the form of water-soluble ammonium and nitrite salts. Also, hydrolysis leads to dissolution of nitrogen in the process water,

causing even higher removal for higher reaction temperatures. On the other hand, higher treatment temperatures also lead to hydrolysis of other organic biomass constituent, lowering mass yield after reaction. Thus, the apparent rise of N content in the solid residue at higher treatment temperatures is a consequence of losses of other organic material.

According to the relationship between fuel-N content and NO_x emission established by Sommersacher et al. [143], the effect of HTC on NO_x emissions is dependent on treatment temperature: At mild conditions, a positive effect and at higher temperatures a negative effect on NO_x emissions is expected during combustion of the hydrochar due to the changes in fuel-N content induced by HTC.

Another approach to assess the NO_x emission risk is to consider the specific nitrogen content per unit energy content. Figure 8.13 (a) depicts the development of specific fuel-N per unit energy in mg MJ⁻¹ as function of treatment temperature for all feedstock treated for 2 h. Compared to the starting material, the specific nitrogen content per energy unit is decreased by roughly 10-30 % at a treatment temperature of 150 °C. Upon further increase of the treatment temperature, the nitrogen contents per energy unit slightly increases with increasing temperature, diminishing the initial reduction to only 10% on average. In the case of HTC treated AD digestate for treatment temperatures above 210 °C, the value of specific fuel-N per energy unit is exceeding the value obtained for the starting material. Again, digested sludge marks the exception for which the fuel-N content per energy unit decreases further with increasing treatment temperature. The same observations on temperature dependence of specific nitrogen content per energy unit can be made analysing the samples that have been treated at 0.5 h and 4 h. Hence, according to this indicator, HTC could have a positive effect on NO_x emission risk. On the other hand, also the volatile matter of the fuels is reduced by HTC. This likely shifts the N partitioning between volatiles and char towards a higher fraction of N in the char, which in general reduces the ability to reduce NO_x formation from volatiles in-situ [247].

The fuel analysis points towards a higher NO_x emission risk for HTC treated fuels, however further experimental validation in combustion tests is required for a final conclusion. Overall, higher NO_x emission risk than for wood has to be expected for all HTC fuels.

Particulate Matter (PM) Emissions

The two main sources of PM in biomass combustion are particles from incomplete combustion such as soot, condensable organic matter and char, as well as particles from ash forming matter in the fuel [137, 138]. The latter PM formation can be traced back to the release of volatile inorganics that are released from the fuel to the gas phase during combustion and start to nucleate or condense [248]. Thus, in biomass fuels the concentration of K, Na, Zn and Pb that often constitute the majority of volatile inorganics is used as an indicator for aerosol emissions.

Figure 8.14 shows the likelihood of PM emissions based on the combined concentration of K, Na, Zn and Pb in the raw feedstock, as well as the feedstock treated at different temperatures and residence time. Based on this index low PM emissions are expected for values < 1000 mg kg⁻¹, medium PM emissions for values between 1000-10.000 mg kg⁻¹ and high emissions for values > 10.000 mg kg⁻¹.

For all investigated fuels, a decline in the sum of K, Na, Zn and Pb is observed after HTC treatment compared to the raw fuel. This means according to this index, PM emissions for HTC fuels are lowered compared to the raw materials. For AD digestate, EFB, olive pomace and wheat straw the PM emission risk can be lowered from a high to a medium risk after HTC at temperatures above 210 °C. The strongest reduction in PM emission risk is seen in olive pomace and EFB. These two substrates both exhibit high content of potassium in their ash. The improvement is a consequence of removal of K by dissolution of potassium salts in the process water, see Section 8.2.

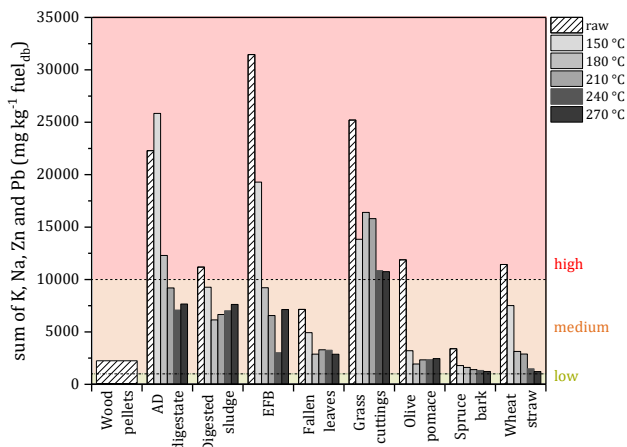


Figure 8.14: Sum of the concentration of K, Na, Zn and Pb in mg per kg fuel as indicator for fine particle emission tendency for raw and HTC treated feedstock, wood pellets shown as reference. Emission risk propensity is indicated with coloring (low=green, medium=orange, high=red).

Thus, the strongest relative reduction in concentration is achieved at 180 °C where significant biomass degradation sets in and facilitates the removal of inorganic species. The concentrations of sodium and zinc only contribute to the sum of the element concentrations to a minor part: their concentrations typically lie below 1.000 mg kg⁻¹ fuel for the investigated feedstock.

For higher treatment temperatures, the improvements concerning PM emission risk stagnate: due to increasing removal of organic matter from the biomass, the ash content of the hydrochar is increasing, which diminishes the positive effect of K removal. At temperatures above 240 °C a concentration of aerosol forming elements below 10.000 mg kg⁻¹ is achieved for all fuels except grass cuttings, lowering the amount of PM emissions that are expected for HTC fuels compared to their untreated counterparts. In comparison, wood pellets contain 2100 mg kg⁻¹ of aerosol forming elements. Thus, regarding PM emissions some HTC fuels reach the same quality as wood pellets.

Slagging and Fouling Risk

Deposit formation is another common challenge in biomass combustion that is associated with operational disturbances and damage of plant components. They are formed from the inorganic matter in fuels and are differentiated depending on their occurrence and nature: Slagging refers to the formation of molten deposits in the areas where heat is mostly transferred by radiation (i.e. furnace). Fouling refers to solid deposits that occur in the area of convective heat transfer surfaces.

Figure 8.15 shows the molar (Si+K+P) to (Mg+Ca) ratio of substrates and HTC fuels which is an indicator for slagging propensity.

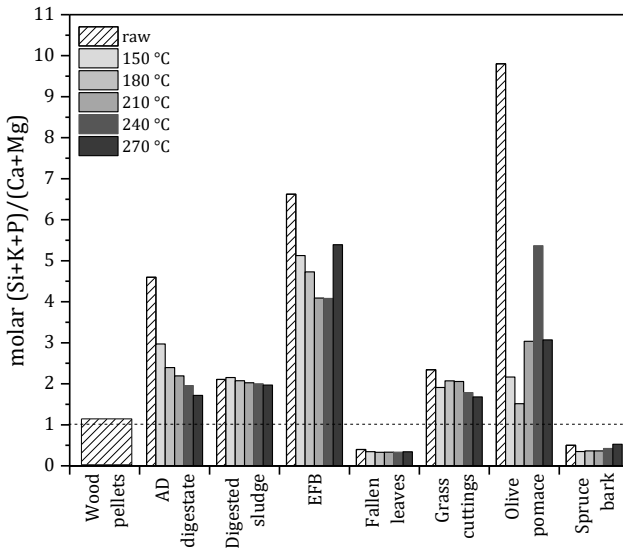


Figure 8.15: Molar (Si+K+P) to (Ca+Mg) ratio of raw biomass including wood pellets as reference and HTC fuels treated at different temperatures at a residence time of 2 h. Below a value of 1 a minor slagging risk is expected.

The index correlates linearly with the ash sintering temperature. Mg and Ca are known to increase ash melting temperatures, while Si, K and P generally reduce ash melting temperatures. A value below 1 indicates a high ash

sintering temperature above 1100 °C. Consequently, a lower value of the ratio indicates reduced slagging risk [146, 147, 155]. As Figure 8.15 shows, HTC decreases the molar $(\text{Si}+\text{K}+\text{P})/(\text{Ca}+\text{Mg})$ ratio for all feedstock, thus reducing slagging risk during the combustion of HTC fuels. A stronger reduction is seen in K-rich feedstock like AD digestate, EFB and olive pomace. Only small changes are observed for Ca-rich feedstock like fallen leaves and spruce bark. For some substrates an increase in molar $(\text{Si}+\text{K}+\text{P})/(\text{Ca}+\text{Mg})$ ratio is seen at higher HTC temperatures. Compared to wood, lower slagging risk is expected for fallen leaves and spruce bark.

Despite the positive impact of the pre-treatment on molar $(\text{Si}+\text{K}+\text{P})/(\text{Ca}+\text{Mg})$ ratio, the majority of HTC fuels are still likely to cause slagging issues. Only spruce bark and fallen leaves, being rich in Ca that increases ash melting temperatures reached a ratio below 1, where slagging risk decreases. As discussed in section 9.2 HTC alters the ash composition of biomass ashes significantly. However, while some ash constituents like K, that lower the ash melting temperatures are removed, other constituents, like P, that decrease ash melting temperatures accumulate. Thus impact of HTC on ash melting and consequently, slagging propensity is again dependent on the nature of inorganic constituents of the starting material and the extent to which they are removed during HTC.

Fouling propensity can be evaluated using the same indicator as for PM emission risk and using the fouling index as introduced in section 4.2. HTC significantly decreases K concentration in the fuels and therefore removes one of the main responsible components of fine particle formation. Therefore, considering this indicator a positive impact of HTC on fouling behaviour is expected. Figure 8.16 shows the calculated fouling indices for raw biomass fuels and HTC fuels. The fouling index is based on the elemental ash oxide concentration determined by XRF analysis. Threshold values for the fouling risk are introduced in Table 4.3.

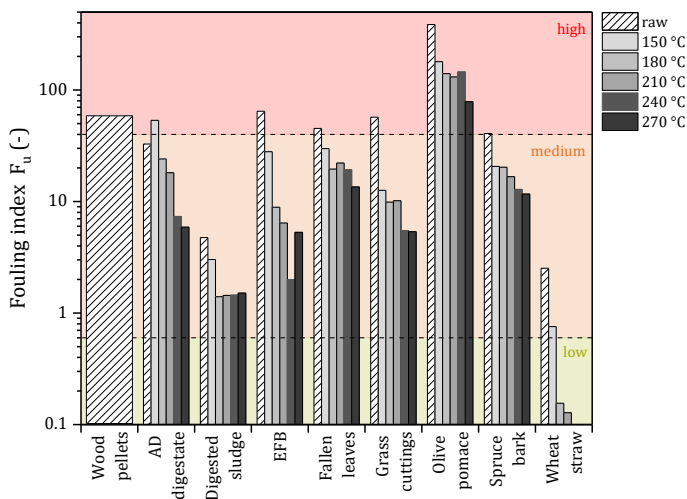


Figure 8.16: Fouling index calculated for raw biomass and HTC fuels treated at different temperatures at a residence time of 2 h. The risk of slagging is indicated with coloring (low=green, medium=orange, high=red).

According to the index, high fouling risk is expected for untreated biofuels from EFB, fallen leaves, grass cuttings and olive pomace. The calculated fouling index for HTC fuels is lower than for the untreated biofuels and decreases with increasing treatment temperature. Yet, for the majority of substrates a moderate fouling risks remains after HTC. Only for wheat straw the low risk range of fouling index is reached. Once again the improvements in fouling index are mostly due to the substantial removal of alkali from the substrates by HTC. The fouling index for wood is fairly high and all HTC fuels except HTC fuels from olive pomace show lower fouling risk according to the fouling index.

In brief, the impact of HTC on slagging propensity is feedstock dependent. A positive impact is expected for alkali rich feedstock, due to the substantial increase in ash fusion temperatures observed for these feedstock. Further, HTC decreases fouling risk due to the removal of fuel alkali, the main contributor to deposit formation.

8.4 Reactivity of HTC Chars

The knowledge of the thermal behaviour of a fuel is essential for the implementation of a new fuel in existing combustion plants. Intrinsic char reactivity is one important factor affecting char burnout and, thus, efficiency of fuel consumption in a power plant. An in depth characterisation of intrinsic kinetic behaviour of HTC fuels is beyond the scope of this work, however a comparison of relative intrinsic reactivity between starting materials and HTC fuels is carried out.

Impact of HTC process conditions on char reactivity

Figure 8.17 (a) shows the impact of residence time and treatment temperature on the relative intrinsic reactivity of HTC chars from EFB in 5 % O₂ atmosphere. The raw data is provided in Appendix C.

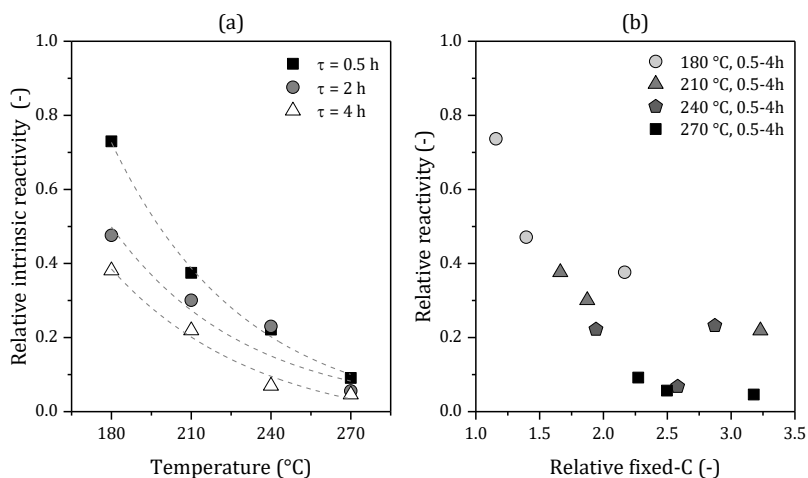


Figure 8.17: (a) Relative intrinsic reaction rate in 5 % O₂ atmosphere conversion of the pyrolysed hydrochar samples versus carbonisation temperatures at residence times of 0.5 h, 2 h and 4 h at 425 °C compared to the pyrolysed raw biomass under the same conditions. (b) Relative C-fix content versus relative intrinsic reactivities for reaction temperatures from 180-270 °C and residence times from 0.5 h-4 h

HTC chars exhibit a lower intrinsic reactivity than the raw material. It can be observed that with increasing temperature and residence time intrinsic

reactivity of the HTC chars declines. At the mildest HTC conditions of 180 °C and 0.5 h the intrinsic reactivity is reduced by 27 %. Intrinsic reactivity HTC chars treated for 4 h at the same temperature is reduced by 62 %. The lowest intrinsic reactivity is observed for HTC chars originating from severe HTC treatment at 270 °C. At these conditions, the intrinsic reactivity is decreased by 90 % at 0.5 h and 95 % at 4 h. It seems at lower temperatures the impact of residence time on char deactivation is more pronounced than at higher temperatures.

As introduced in Section 3.2, with increasing temperature and residence time the coalification of biomass advances during HTC. Thus, an increasing amount of fixed-C can be found in HTC chars with increasing reaction severity. As Figure 8.17 (b) shows, there is a strong correlation between fixed-C in the HTC fuels and the observed intrinsic reactivity. A decrease in reactivity of HTC treated fuels was also reported in other studies [249–253]. Ulbrich et al. [253] reported similar findings for the dependence of reaction rates of HTC chars from brewer's spent grains in CO₂ atmosphere. They attributed the decrease in reactivity to the formation of fixed-C and the accompanying reduction in surface groups that act as active sites for the gasification reaction. In another study Stirling et al. [252] compared the reactivity of HTC treated wood and olive pomace with bituminous coal and torrefied biomass wood. They could show that the decrease in reactivity was rather associated with the removal of catalytically active alkali and earth alkali metals during HTC than to the loss of volatiles.

To determine if fixed-C content or alkali content are the determining factor in reducing char reactivity a comparison between different biomass feedstock with varying ash content and composition is presented in Figure 8.18. After HTC, intrinsic reactivity of the chars is decreased for all investigated substrates. Intrinsic reactivity decreases with increasing fixed-C content and increases with increasing fuel alkali content. Values are scattered more strongly for the correlation between fixed-C and intrinsic reactivity.

Strong differences of reactivity between different HTC fuels are observed. The strongest reduction in reactivity are observed for wheat straw (95 %) and EFB (94 %) that also show the strongest relative reduction in fuel alkali content of 90 % and 78 % respectively. Significantly different intrinsic reactivity was measured for samples treated with a similar fixed-C content of approximately 30 wt.-% such as AD digestate, fallen leaves and wheat straw. However, the same applies for samples with comparable alkali content (i.e. AD digestate and EFB). It seems that for both measured quantities only a weak correlation with intrinsic reactivity can be established. Consequently, more research is needed, to investigate the driving mechanism for a reduction in intrinsic reactivity of the chars.

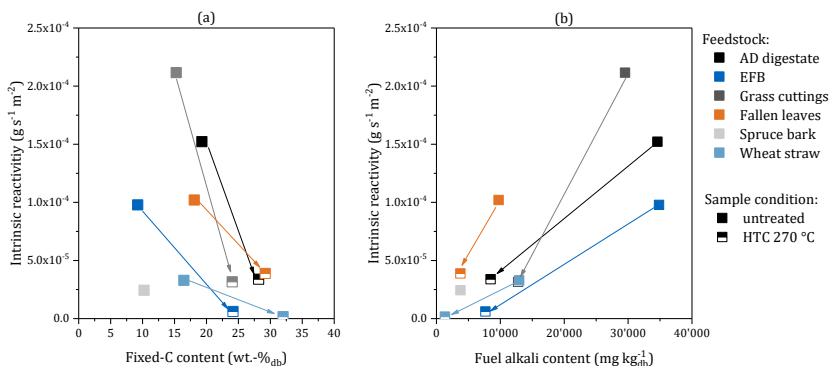


Figure 8.18: Intrinsic reactivity measured for substrate and HTC chars as a function of fixed-C (a) and fuel alkali content (b). HTC samples were treated at 270 °C for 2 h.

In summary, chars from HTC fuels show significantly reduced intrinsic reactivity compared to chars from the untreated counterparts. Char reactivity decreases with treatment temperature and residence time. The reduction in reactivity could be associated with the increased amount of fixed-C formed during HTC. On the other hand, with increasing reaction severity, also the concentration of catalytically active inorganics in HTC chars decreases which could be another explanation for the decrease in reactivity. An initial assessment of five different feedstock points towards a stronger influence of fuel alkalis, but further research is needed to confirm

this observation. It is important to note that the starting feedstock type of a HTC fuel is the governing factor for the determination of its fuel characteristics. Therefore, when comparing HTC fuels with other fuels the substrate type should always be considered in the assessment.

Chapter summary: HTC was found to have a profound effect on fuel properties relevant for combustion. HTC fuels show significantly higher calorific value mostly on account of a higher carbon content. Higher reaction severity leads to a higher degree of biomass coalification and hence higher calorific value. In addition, it was demonstrated that HTC also significantly changes ash characteristics: Overall, the fate of inorganics is defined by feedstock type and phases occurring in the substrate. The ash content after HTC is higher for substrates rich in Ca, P and Si, while lower ash contents after HTC are observed for high K feedstock. Ash content tends to increase for higher treatment temperatures due to rising loss of organic material. Ash composition changes strongly after HTC. Both treatment temperature and nature of the inorganic species play a significant role. Residence time does not strongly impact ash composition. K, Cl and to some extent also S and Mg are effectively removed by HTC. With increasing temperature and biomass degradation, the removal efficiency for these species grows. Poor removal was observed for Ca, Al, Si and P. Some inorganic species like P are initially removed at low treatment temperatures but are reincorporated to hydrochar or precipitated at higher treatment temperatures. Removal efficiencies are also dependent on the L/S ratio during reaction: Lower solid concentrations lead to higher removal efficiencies for all inorganic species. An analysis of fuel indices shows that HTC had a positive impact on expected PM emissions, corrosion and deposit formation during combustion of HTC fuels. The improvements are based on the strong removal of K and Cl during HTC. Adverse effects have to be expected for the influence of HTC on NO_x emissions on the account of higher fuel-N and lower volatile content after the treatment. Finally, reactivity of HTC chars was found to decrease with increasing severity of HTC treatment compared to the substrate due to the removal of catalytically active inorganic constituent and the formation of fixed-C during HTC.

9 Characterisation and Utilisation Options for HTC By-products

HTC can convert any wet biogenic feedstock without the need to include an energy intensive drying step. This is, on the one hand, the strength and distinguishing feature of the technology. On the other hand, this also causes the biggest weakness of the technology: the process produces considerable amounts of contaminated process water during the conversion that needs treatment. Thus, the following chapter provides insights to the amount of process water generated, its characterisation and possible utilisation and treatment options.

9.1 Amount of Process Water Generated

Water represents the biggest mass flow in a hydrothermal conversion of biomass. The exact amount of process water generated depends on the following main influencing factors:

- Feedstock moisture content
- Use of additional water for biomass mixing / pumping
- Extent of biomass conversion

A higher feedstock moisture content and additional water use to create a biomass mixture that can be properly mixed and pumped, increase the amount of process water generated. In addition, a higher degree of conversion of biomass also increases the amount of process water generated due to a higher amount of water generated by biomass dehydration during HTC. More on this topic see section 10.1.

Table 9.1 provides an overview of the amount of process water generated by HTC according to the developed process model (more details follow in Chapter 10.1) and literature values. HTC of EFB with a moisture content of 65 % produces 2.29 m³ process water per ton of product fuel. At 80 % moisture, this value increases to 4.39 m³ t⁻¹. These results are well within

the expected range of 1.89-2.42 m³ t⁻¹ according to reported values in the literature for comparable feedstock moisture content [62, 64, 169, 171].

Table 9.1: Amount of process water generated by HTC according to own calculations and literature values.

Amount process water (m ³ t ⁻¹ product)	Input material	Feedstock moisture (wt.-%)	Process conditions	Ref.
2.29	EFB	65	180 °C, 2 h	-
4.39	EFB	80	180 °C, 2 h	-
1.89	Grape marc	65	220 °C, 1 h	[64]
2.42	EFB	65	220 °C, 4 h	[62]
2.29	N/A	60	N/A	[171]
2.30	Green waste	64	200 °C, 3 h	[169]
4.81	Miscanthus	70	230 °C, 5 min	[63]

To reduce waste water generation, recycled process water should be used for biomass mashing. As discussed in more detail in the following Chapter 10.1, this also offers the advantage that process water- and steam-recycling lowers the thermal energy demand of HTC. However, the possibility to recycle process water is limited for input materials that already possess high water content. In this case, the amount of water that can be recycled to the feed stream decreases, if the solid concentration in the reactor is to be kept constant. Thus, to avoid a strong dilution of biomass in water and associated higher energy costs, a higher proportion of water needs to be sent to treatment.

9.2 Characterisation of HTC Process Water

Table 9.2 shows process water analysis data from five different feedstock treated at temperatures from 150-270 °C for a duration of 4 h. The process conditions investigated, therefore, cover mild and severe HTC conditions. The analysis includes basic analysis of pH and electrical conductivity (EC) as well as a characterisation of organic matter and nutrient concentration. Additional process water characterisation on pH and EC for other feedstock is provided in Appendix E.

Table 9.2: Water analysis data of effluent obtained from hydrothermal carbonisation of various feedstock at different temperatures for a reaction time of 4 h.

Biomass type	Temp. (°C)	pH	EC (mS cm ⁻¹)	TOC (g l ⁻¹)	BOD ₅ (g l ⁻¹)	COD (g l ⁻¹)	P _{tot} (mg l ⁻¹)	TN (mg l ⁻¹)	NO ₃ -N (mg l ⁻¹)	NO ₂ -N (mg l ⁻¹)	NH ₄ -N (mg l ⁻¹)
EFB	150	4.54	4.83	9.1	11.8	22.8	73.0	394	79	0.48	34.40
	180	4.02	4.84	9.3	15.0	24.6	64.4	452	122	0.30	0.88
	210	4.14	4.22	9.8	15.4	24.9	19.0	398	119	0.30	1.36
	240	4.12	4.08	11.4	16.2	28.9	11.8	398	91	0.30	1.72
	270	4.12	5.07	11.4	19.8	29.2	10.8	320	94	0.96	4.22
Grass cuttings	150	4.35	5.82	14.3	22.6	37.5	53.4	780	184	1.10	1.56
	180	4.45	6.17	13.7	20.2	31.7	12.0	1022	136	0.90	1.26
	210	4.62	6.20	14.6	19.4	34.6	6.3	1010	141	0.98	1.34
	240	4.96	6.27	13.0	19.8	32.5	4.6	1006	113	0.70	2.06
	270	5.23	5.76	12.4	17.4	31.2	4.2	786	103	0.44	4.76
Horse manure	150	4.67	3.78	9.6	12.6	24.4	278.0	596	99	0.76	105.00
	180	4.10	4.24	8.8	12.6	21.9	236.0	598	131	1.04	85.60
	210	4.26	4.50	9.4	12.6	23.2	196.0	534	119	1.12	83.20
	240	4.10	4.13	10.1	13.0	25.9	173.4	434	117	1.12	50.40
	270	4.36	3.60	9.4	12.6	25.5	191.0	460	100	0.72	113.00
Fallen leaves	150	4.91	2.72	7.7	12.6	19.5	17.0	173	71	0.86	25.6
	180	4.95	3.73	6.6	9.0	15.4	5.2	268	87	1.00	4.20
	210	4.55	3.43	8.1	12.2	19.9	1.8	226	90	0.94	2.40
	240	4.44	3.78	8.5	14.2	22.5	1.0	256	71	0.58	1.92
	270	4.75	3.22	8.8	13.8	22.5	1.0	268	66	0.30	4.02
Olive pomace	180	3.56	2.57	10.9	18.2	25.8	57.6	152	163	0.30	0.56
	210	3.80	2.53	8.9	14.6	22.0	48.0	134	120	0.30	0.70
	240	3.77	2.25	9.9	16.0	25.6	30.8	107	88	0.30	1.06
	270	3.65	2.29	9.8	16.6	26.8	22.8	119	81	0.30	1.62

pH Value

The pH values of process water samples presented in Table 9.2 are acidic and in the range of 3.6-5.2. For most feedstock a slight decrease of pH is observed for HTC temperatures above 150 °C. The obtained pH values are fairly similar and only minor differences between different feedstock can be observed. Temperature also does not have a strong effect on process water pH. Slightly different observations are made for effluent originating from HTC of grass cuttings: a slight increase in pH with treatment temperature is observed. Biomass degradation during HTC leads to the formation of organic acids like acetic acid, formic acid and levulinic acid, which leads to the acidic pH in HTC process water [109, 114–116]. The slight decrease in pH at temperatures above 150 °C is probably a consequence of more rigorous biomass degradation above this temperature. Grass cuttings contains a considerable amount of nitrogen-containing compounds (fuel-N = 2.2 wt.-%) which form buffering compounds upon degradation during HTC. This leads to an increase of pH value. Higher pH values are also observed for other nitrogen-rich feedstock like e.g. digested sludge (pH = 6.2-9.0 , fuel-N = 6.8 wt.-%), and spirulina (pH = 4.8, fuel-N = 5.2 wt.-%).

Electrical Conductivity

The electrical conductivity (EC) of the process water samples reported in Table 9.2 shows a higher variability and is in the range of 2.2-6.9 mS cm⁻¹. The highest EC is obtained for process water from grass cuttings. HTC temperature does not have strong impact on the measured EC. Grass cuttings and fallen leaves show a maximum of EC at intermediate temperatures of 210 °C and 240 °C. EC of process water from olive pomace slightly decreases with increasing treatment temperature while no clear trend is observed for horse manure and EFB. Feedstock type seems to be the major influencing factor for EC. Since EC is a measure of the salt concentration in the liquid sample investigated, it is also a measure of the amount of inorganics removed by HTC. The total amount of inorganics that are removed from a given substrate is dependent on the substrate ash

content and the proportion of soluble inorganics in the ash. In approximation of this criteria, Figure 9.1 shows the measured EC of process water samples from the feedstock discussed in Chapter 7 as a function of the substrate fuel alkali content.

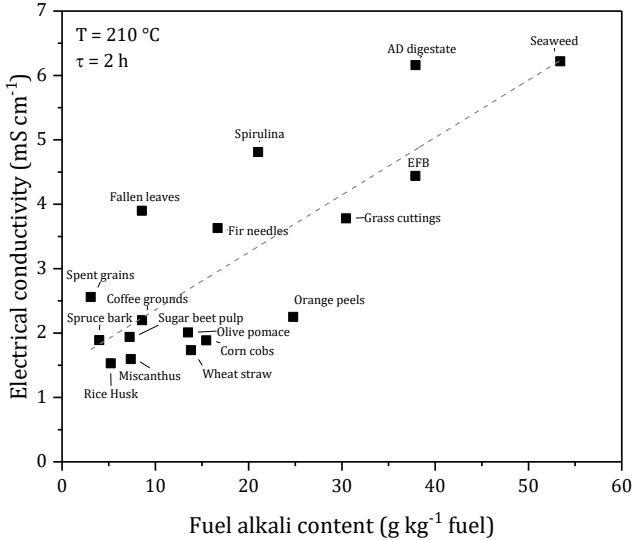


Figure 9.1: EC of process water from various substrates treated at 210 °C for 2 h as a function of the alkali content in the starting material.

For the majority of investigated substrates EC lies in the range of 1.5-3 mS cm⁻¹. Higher EC values are measured for alkali rich, high ash feedstock like seaweed, AD digestate, EFB, grass cuttings and spirulina. Generally, the salt concentration in HTC effluent is in the expected range of industrial waste water (EC ~ 5 mS cm⁻¹) and lower than EC of 70-120 mS cm⁻¹ typical for municipal waste water [254, 255].

Organic matter

Table 9.2 shows the measured concentrations for total organic carbon (TOC), biological oxygen demand after 5 days (BOD₅) and chemical oxygen demand (COD) in process water from HTC treatment of biomass. TOC values

are in the range of 6.5 -14.6 g l⁻¹. This indicates a heavy pollution of process water with organic material originating from biomass degradation processes during HTC. For EFB with increasing HTC temperature an increase in TOC is observed. For the other feedstock, no clear development of TOC with temperature is noted. Again differences in TOC are governed by feedstock type with fallen leaves exhibiting lower TOC values of up to approximately 9.0 g l⁻¹ in comparison to effluent from grass cuttings, olive pomace and EFB where TOC reaches values above 9.0 g l⁻¹. For BOD₅ and COD similar observations can be made: COD values lie in a more narrow range of 15.4-34.6 g l⁻¹. COD of HTC effluents seems to be determined by feedstock type rather than treatment temperature. BOD₅ values follow the same trends and are in the range of 9.0-19.4 g l⁻¹. For comparison typical COD and BOD₅ values for municipal waste water are 0.25-0.8 g l⁻¹ and 0.1-0.35 g l⁻¹ respectively [256]. This means that process water from HTC is heavily contaminated with organic matter. The organic load is comparable with animal manures that are in the range of 20-30 g l⁻¹ for pig slurry and 10-20 g l⁻¹ for cattle manure, respectively [257]. Compared to the COD values the BOD₅ values are relatively high. Figure 9.2 (a) shows the BOD₅/COD ratio for HTC process water from different feedstock treated at temperatures ranging from 150-270 °C. If the BOD₅/COD ratio is ≥ 0.5, the waste water is considered to be easily treatable by biological means [256]. The ratio varies between 0.52-0.71. This means a good biodegradability of the organic substances can be expected.

A way to reduce the organic load in HTC process water, while at the same time accessing some of the chemical energy it contains is anaerobic digestion (AD). An indicator often used to estimate the bio-methane production potential (BMP) is the C/N ratio. A value of 20-35 provides optimal conditions for AD [258, 259]. A lower ratio indicates a protein rich substrate, with high pH causing methanogenic inhibition [260]. A higher ratio points towards a quick depletion of nitrogen, which also lowers biogas production. Typical values for C:N are e.g. 25:1 for grass silage and 13:1 for cattle manure [257]. Figure 9.2 (b) shows the C/N ratio of the obtained process water from HTC of different substrates.

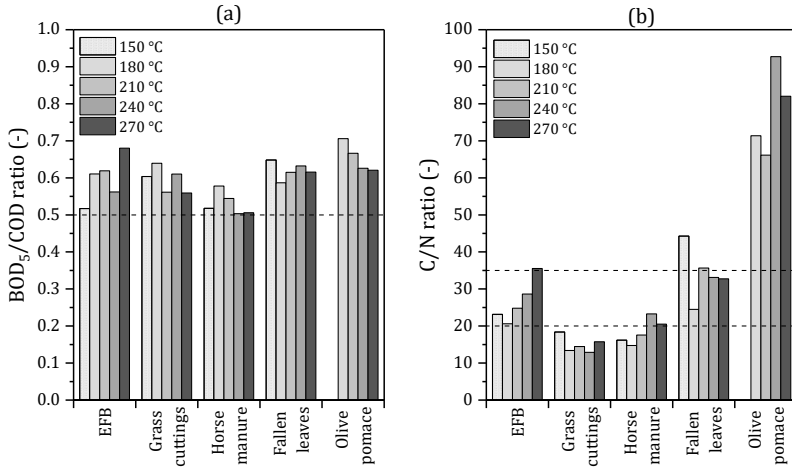


Figure 9.2: BOD₅/COD ratio (a) and C/N ratio (b) of process water obtained after HTC of different biomass types at temperatures of 150-270 °C for 4 h.

Applying the optimum C/N criteria, an efficient AD conversion of effluent from EFB and fallen leaves can be expected. The C/N ratio in effluent from HTC of olive pomace is above the optimum range, while process water from grass cuttings and horse manure contain too much nitrogen and therefore possess a C/N ratio below the optimum range. However, C/N ratio can only serve as a preliminary indicator of BMP potential, the derived trends need to be verified by further experimental investigation.

Nutrient concentration

Table 9.2 shows the concentration of nitrogen nutrients (NO₃-N, NH₄-N, NO₂-N) and total nitrogen (TN) as well as phosphorous (P_{tot}) determined in process water samples from HTC of the five investigated feedstock. Compared to the concentrations of organic matter their concentrations are significantly lower.

The most abundant nitrogen nutrient is NO₃-N with a concentration of 71-103 mg l⁻¹. No strong dependence of NO₃-N concentration on feedstock type is observed. With increasing HTC treatment temperature the concentration of NO₃-N decreases slightly for all substrates.

Ammonia-N ($\text{NH}_4\text{-N}$) was found in high concentrations of 50-113 mg l^{-1} in process water from HTC of horse manure, as typical for manures and faeces. For the other feedstock smaller $\text{NH}_4\text{-N}$ concentrations of 0.6-4.8 mg l^{-1} were measured. With increasing HTC temperature $\text{NH}_4\text{-N}$ concentration decreases rapidly. For example in process water from EFB and fallen leaves 34.4 mg l^{-1} and 25.6 mg l^{-1} was measured in effluent from HTC at 150 °C. In effluent obtained from HTC conducted at 180 °C and higher the concentration of $\text{NH}_4\text{-N}$ rapidly decreases to below 5 mg l^{-1} for all feedstock except horse manure. This might indicate the precipitation of ammonia salts under hydrothermal conditions at temperatures above 150 °C.

Nitrite ($\text{NO}_2\text{-N}$) was detected in low concentrations of 0.30-1.12 mg l^{-1} . Fluctuations in $\text{NO}_2\text{-N}$ concentrations are observed with treatment temperature, but no coherent trend is observed.

Overall, values obtained for TN in effluent are higher than measured $\text{NO}_3\text{-N}$, $\text{NO}_2\text{-N}$ and $\text{NH}_4\text{-N}$ concentrations indicating the presence of more organic nitrogen species. In HTC effluent TN concentrations of 107-1022 mg l^{-1} are obtained. TN concentration is also feedstock dependent: The highest TN concentrations were measured in process water from grass cuttings, which is also the feedstock that has the highest fuel-N content of the investigated feedstock as presented in Table 7.1. During HTC nitrogen is released to the process water. The increase in TN at washing conditions can be explained by the dissolution of water soluble ammonium and nitrite salts and some nitrogen containing compounds to the washing water. At higher temperatures hydrolysis of nitrogen containing compounds leads to a further increase of TN in the effluent.

Finally, P_{tot} values measured seem to be both temperature and feedstock dependent. Highest P_{tot} values are detected in process water from grass cuttings (up to 238 mg l^{-1}), the lowest in effluent from fallen leaves (up to 18 mg l^{-1}). For all feedstock a decline in P_{tot} in effluent is observed with increasing treatment temperature. For example at 150 °C 53.4 mg ml^{-1} of phosphorous is detected in process water from grass cuttings. This value drastically decreases to 4.2 mg ml^{-1} at HTC conditions of 270 °C. This finding

also supports the observations made for phosphorous concentration in the HTC fuels as discussed in Chapter 8.2 which, after an initial decline at low HTC temperatures, increases again for higher treatment temperatures at HTC conditions. This suggests that at higher treatment temperature phosphorous is precipitated and reincorporated to the hydrochar.

9.3 Valorisation and Treatment Options for Process Water

As the findings in the previous sections demonstrate, process water from HTC contains various nutrient and is heavily contaminated with organics. Consequently, a cost efficient and environmentally friendly treatment for process water from HTC needs to be developed and is the key for its commercial success. Different approaches are discussed. An overview of possible treatment options is provided in Figure 9.3.

Biological		Chemical / Physical	Mechanical / Physical
Waste water treatment plant Classic multi-stage wastewater treatment	Anaerobic digestion Microbiological conversion of COD to biogas	Wet oxidation Degradation of refractory COD to biodegradable compounds	Filtration Separation of COD into biodegradable and refractory fractions by molecular size

Figure 9.3: Overview on possible treatment and valorisation options for HTC process water.

Waste water treatment: Sending HTC process water to a regular waste water treatment plant (WWTP) is the easiest solution. However, this way the chemical energy contained in HTC process water is lost and the opportunity to gain higher thermal efficiency by its utilisation missed. Further, according to environmental standards the maximum allowed COD value in waste water is limited to e.g. 200 mg l⁻¹ in Germany [261]. This value is exceeded many times in HTC process water with a COD of 15,400-34,600 mg l⁻¹. Additionally, process water from HTC contains non-biodegradable (refractory) compounds that cannot be treated in a conventional WWTP. Consequently, excessive dilution and/or pre-treatment is needed prior to waste water discharge.

Anaerobic digestion: AD offers the possibility to valorise the chemical energy contained in the process water by its conversion to biogas. AD is able to eliminate between 50-75 % of COD [61, 262]. Biogas production related to COD is about 0.5 L g^{-1} COD removed, corresponding to a methane production of roughly 0.35 L g^{-1} of COD removed [263]. For instance, for a 70% conversion of COD to methane, AD of process water could produce enough methane to cover 11 % of the thermal energy need of the process. This calculation is based on the base case design from Chapter 10.1, where 2.36 m^3 of effluent are produced and a thermal energy consumption of 1.5 MWh per ton of HTC fuel is needed. This way, the thermal efficiency of the process could be improved from 61 % to 63 %. Yet, AD of process water also faces several challenges: COD load of the process water is too high for a direct conversion, thus dilution is needed prior to AD. Second, phenols and other intermediates formed during biomass degradation can act as inhibitors during AD [264]. Further, the remaining COD content is mostly refractory, i.e. non-biodegradable and needs to be removed otherwise, for example by adsorption with activated carbon [69]. And in addition, COD after AD is still above the legal limits for discharge, and consequently, needs to be diluted further.

Filtration: Filtration techniques aim to separate the refractory from the biodegradable COD by differences in molecular sizes. Applied technologies are membrane filtration, nano-filtration and reverse osmosis. The refractory compounds are retained and send back to the HTC reactor to increase solid and energy yield. Alternatively, they can be thermally utilised by combustion. The biodegradable permeate is send to AD for energetic valorisation or to biological waste water treatment. In some cases a membrane or nano-filtration is combined with reverse osmosis in a multi stage process: Organics are separated in the first filtration step, while reverse osmosis aims to retain a fraction of the salts present in the effluent, preventing the refeeding of inorganics to the HTC reactor [265, 266].

Wet oxidation: Wet oxidation (WO) is another established method for the treatment of waste water. During WO pollutants contained in waste water

are oxidized using pure oxygen or air as oxidizing agent at temperatures around 100-320 °C and pressures of 5-200 bar. The process is exothermic and self-sustaining above a COD load of 20 g l⁻¹ [267]. COD elimination of 50-70 % can be reached with this technology [267, 268]. Synergy effects between HTC and WO result from the similar operating conditions used. With this technique the biodegradability of process water from HTC is improved since refractory compounds are degraded. Yet, similarly to AD COD load after WO is still above legal limits and therefore dilution of the process water is needed.

All of the above treatment options are characterised by some short-comings. On the one hand, the COD reduction for some technologies is not sufficient for discharging effluent to WWTPs and refractory COD is not degraded upon treatment, while for others the chemical energy contained in the process water is not valorised. Thus, a combination of different treatment methods is needed for an efficient and economical process water disposal. One possible combination would be using filtration as a pre-treatment to separate refractory COD and valorising the remaining COD by AD. Another option would be WO as process water pre-treatment prior to AD.

Chapter summary: To conclude, HTC produces a large amount of contaminated process water that needs treatment. Based on process modelling (see section 10.1) the volume of process water generated per t of HTC fuel is estimated to be in the range of 2.3-4.4 m³. Characterisation of HTC process water showed that its characteristics are strongly feedstock dependent. HTC effluent is acidic and its EC is dependent on the substrate ash content and composition. The organic load of HTC effluent determined by COD was found to be very high and in the range of 15-35 g l⁻¹. Nutrients were found in much lower concentrations. To date several methods for the treatment of process water from HTC exists. However, a combination of different techniques has to be used to overcome the challenges in the treatment of process water from HTC that arise from the exceptionally high organic contamination and the presence of refractory, non-biodegradable compounds.

10 Techno-economic Evaluation of HTC

This chapter discusses the technical and economic performance of HTC as a technology for fuel upgrading. Initially, the thermal and electrical energy demand of a HTC plant is assessed in a process simulation. In the base design, the modelled HTC plant processes 40.000 t a^{-1} EFB with a moisture content of 70 wt.-%. The impact of feedstock moisture and process temperature on specific energy consumption and thermal process efficiency is discussed. Subsequently, the total cost of production for HTC fuels are calculated in a techno-economic analysis for two different plant locations.

10.1 Results of Process Simulation

The design of the modelled plant is introduced in detail in section 6.5.1. In short, HTC conversion in the modelled plant comprises heating of the biomass slurry, HTC conversion, cooling of the HTC slurry, liquid solid separation in a filter press and finally drying of the HTC fuels. Heat recovery is implemented through steam and process water recycling.

Energy Consumption

Table 10.1 shows the electric and thermal power requirements of the proposed plant layout for different process temperatures and reaction times. The electrical power requirements are considered for the main power consumers, i.e. pumps and filter press, while the electrical energy need of the mixer is neglected since its contribution is below 5 % of the total electricity consumption [64]. External thermal power is required for heating up biomass slurry to reaction temperature and for drying of the hydrochar.

As seen in Table 10.1, the thermal power requirement is two orders of magnitude larger than the electrical power requirement. With increasing reaction temperature, both the electrical and thermal demand increase. The electrically operated components in the model are slurry pumps 1 to 3 and the membrane filter press. As the reaction temperature increases, so do the operational pressures, leading to increased electricity consumptions of the

pumps. The electrical demand of the membrane filter press correlates with the mass flow rate, which is lower at higher temperatures. This is, on the one hand, consequence of a lower mass yield after reaction at higher temperatures. On the other hand, in the given design, the amount of steam removed from the slurry in the third stage is higher at higher temperatures lowering the mass flow to the membrane filter press.

Table 10.1: Electric and thermal power requirements at different HTC process conditions for a plant processing 40 kt a⁻¹ (2.7 t h⁻¹) EFB at 70 % moisture.

Temperature (°C)	Time (h)	Electrical power (kW)			Thermal power (kW)		
		Pump	Press	Total	Heater	Dryer	Total
180	0.5	6.9	11.0	17.9	1426	1234	2660
	2	7.1	11.2	18.3	1445	1143	2588
	4	7.4	11.4	18.8	1468	1194	2663
210	0.5	10.5	11.0	21.5	1611	1076	2686
	2	11.0	11.2	22.1	1638	973	2611
	4	11.4	11.4	22.8	1671	1020	2691
240	0.5	18.1	10.0	28.2	1915	953	2867
	2	19.4	10.3	29.7	1971	695	2666
	4	21.8	10.8	32.6	2069	856	2924
270	0.5	31.5	9.5	41.0	2231	705	2935
	2	32.9	9.7	42.6	2274	667	2941
	4	32.2	9.6	41.8	2254	634	2889

Similar to the increase in the electrical demand of the slurry pumps, the heater also must provide more energy for biomass heating at elevated temperatures leading to higher thermal power demands with increasing HTC temperature. However, at higher reaction temperatures also a higher thermal flux is available for the pre-heating of biomass so the increase in thermal power demand is moderate. In contrast, dryer power consumption decreases due to the lower mass output at higher temperatures, as less filter cake needs to be dried.

Specific Energy Consumption and Process Efficiency

Figure 10.1 (a) shows the specific thermal energy demand at different HTC temperatures in kWh per kg hydrochar produced. The specific thermal energy demand ranges between 1.34-2.63 kWh kg⁻¹ hydrochar produced. It increases significantly with reaction temperature, which is on the one hand a consequence of the higher heat demand for heating up the slurry to reaction temperature. In addition, mass yield at higher HTC temperatures decreases significantly from 68 % at 180 °C to 39 % at 270 °C. This means that per kg of hydrochar, more thermal energy is necessary for production.

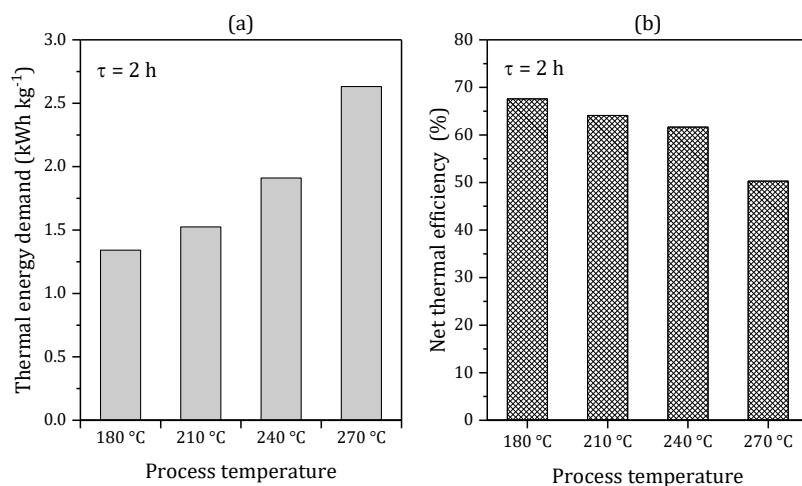


Figure 10.1: (a) Specific auxiliary thermal energy demand per kg hydrochar produced at different reaction temperatures; (b) Net thermal process efficiency of HTC plant at different reaction temperatures.

Figure 10.1 (b) shows the thermal efficiency of the HTC process at different reaction temperatures. The thermal efficiency is a measure of the thermal performance of a process and is provided by the ratio of energy contained in the hydrochar and the chemical energy input from the biomass feed stream plus the auxiliary thermal and electrical energy demand. The thermal efficiency decreases from 68 % at 180 °C to 50 % at 270 °C. One major influencing factor on thermal efficiency is the energy yield of the HTC process. At 180 °C, 67 % of efficiency losses are attributed to the loss of

chemical energy contained in organic matter in the process water. This proportion increases to 92 % at 270 °C, since at higher temperature a higher proportion of the feedstock biomass is liquefied, leading to more losses in chemical energy. Auxiliary energy demand also rises at higher temperatures, since heating of biomass to higher temperatures consumes more thermal power, further decreasing thermal efficiency of HTC at high temperatures.

In the base case design ($T = 210^{\circ}\text{C}$ and $t = 2\text{h}$), the energy yield of HTC was 62 %, which means that 28 % of the energy input from EFB is lost as organic matter dissolved in the process water. For comparison, drying EFB to a moisture content of 10 wt.-% with a rotary dryer requiring typically 3 MJ kg^{-1} water evaporated (see [269]), would consume 36 % of the EFB energy input. Therefore, despite the losses of chemical energy in the process water, the efficiency of HTC in providing a solid fuel is higher than the provision of fuel by drying. Additionally, researchers have proposed that a combination of HTC with anaerobic digestion could help to recover some of the chemical energy contained in the process water. Current research shows process water from HTC yields 0.25-0.30 L methane per g of COD input [81, 270, 271]. With a COD of 25 g l^{-1} reported for EFB at 210°C (see chapter 9.2), in the base case 13 % of the auxiliary thermal energy need could be covered by methane from anaerobic digestion. However, this would only have a small impact on the overall thermal efficiency, which slightly increases from 62.0 % to 63.3 % with this measure.

The impact of feedstock moisture content in the feed stream on specific thermal energy demand is shown in Figure 10.2 (a). The range from 55-95 wt.-% moisture content corresponds to a range of roughly 1-20 expressed as L/S ratio. The obtained specific thermal energy demands range from $0.9\text{-}7.3\text{ kWh kg}^{-1}$ and increases strongly for feedstock with water contents above 80 wt.-%. With increasing feedstock moisture content the proportion of water that needs to be heated up increases, raising the thermal energy demand of the process. At the same time, per unit volume, less hydrochar is produced. Starting from 80 % moisture the specific

thermal energy demand steeply increases. As shown in Figure 10.2 (b) thermal efficiency of the process also decreases with increasing feedstock moisture. For feedstock with 55 wt.-% water the obtained thermal efficiency is 65 % and decreases to 37 % if the feedstock moisture is 95 wt.-%. Consequently, water management in HTC process design is critical. Biomass streams with high water content (> 80 %) should be mechanically dewatered prior to HTC. For an energy efficient process the water content of the feedstock should be as low as possible while still ensuring proper mixing in the reactor and a biomass slurry that can be easily pumped. However, determining the exact optimum moisture content that meets these criteria is beyond the scope of the present study and should be investigated in future work.

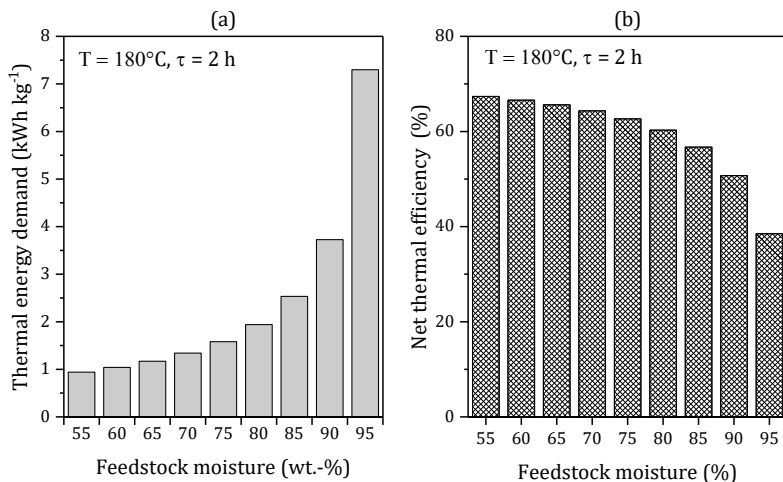


Figure 10.2: (a) Specific thermal energy demand per kg hydrochar as a function of feedstock moisture; (b) Net thermal process efficiency of HTC plant as a function of feedstock moisture.

A comparison of the obtained results from the base case scenario, where EFB is processed at a temperature of 210 °C for 2 h with data reported in the literature and by commercial HTC companies is shown in Table 10.2.

Although there are significant differences in key process parameters like plant capacity, feed moisture content or biomass type, the reported thermal

and electrical energy demands are in the same order of magnitude. For EFB treated at 210 °C for 2 h, the auxiliary thermal energy demand is 1.49 kWh per kg hydrochar produced. This is within the range of other modelling studies by Stemann et al. [62] and Lucian et al. [64] who reported 1.74 kWh kg⁻¹ and 1.17 kWh kg⁻¹ respectively and also close to the value of 1.38 kWh kg⁻¹ that Ingelia reports for its commercial process [171]. The electrical energy demand per kg of hydrochar produced is 0.01 kWh kg⁻¹ and considerably smaller compared to the thermal energy demand. The calculated value in this study is lower than the reference values, since some consumers of electrical energy like a grinder prior to processing or pelletiser at the end of the process scheme were not considered. Overall, the thermal process efficiency HTC is 62 % for EFB treated at 210 °C and 2 h, which is slightly lower than the values of 66-78% for reported for lignocellulosic feedstock in the literature. This is probably a consequence of the conservative assumptions used in the modelling approach, like for instance, the low performance of the dewatering step to 50 wt.-% dry substance.

Table 10.2: HTC process specifications for energy demand calculations, process energy demand and efficiency of own and data from literature.

	Base case	Stemann et al. [62]	Lucian et al. [64]	Ingelia [171]	Terra Nova [163]
Process conditions	210 °C, 2 h	220 °C, 4 h	220 °C, 1 h	200 °C, 4 h	180 C, 2-4 h
Plant capacity (t h ⁻¹)	2.7 t h ⁻¹	5.7 t h ⁻¹	2.5 t h ⁻¹	1.0 t h ⁻¹	1.1 t h ⁻¹
Biomass type	EFB	EFB	Grape marc	N/A	Digested sludge
Feed moisture (wt.-%)	70	85	65	60	77
Thermal energy demand (kWh kg ⁻¹)	1.49	1.74	1.17	1.38	0.93
Electrical energy demand (kWh kg ⁻¹)	0.01	0.42	0.02	N/A	0.22
Thermal efficiency (%)	62	66	78	N/A	56

*N/A = no information available

Using the thermal efficiency, a first indication of the energetic performance of HTC compared to other pre-treatment technologies like torrefaction or steam explosion can be made: For woody feedstock with moisture contents around 50 wt.-% torrefaction and steam-explosion outperform HTC with reported values for thermal efficiency being in the range of 75-95 % for torrefaction and around 86 % for steam-explosion [272-274]. However, for feedstock with higher moisture content of around 70 wt.-%, thermal efficiency of torrefaction decreases to 53-63 % [181]. This decrease is a consequence of higher energy demand for the drying step prior to torrefaction. Additionally, the energy yield of torrefaction for residual biomass streams like roadside grass (energy yield = 61 %) or wheat straw (energy yield = 71 %) is significantly lower compared to torrefaction of wood (energy yield = 93-97 %) [181, 273]. Thus, for biomass with high water content, HTC exceeds the energetic performance of torrefaction, while also providing other significant fuel quality improvements through i.e. the removal of undesirable fuel constituents. Still, to the author's knowledge no comprehensive study comparing the energetic performance of HTC, torrefaction and steam-explosion for residual biomass streams exists. This could be content of future work, further highlighting the strengths and weaknesses of each of the three thermochemical pre-treatment technologies.

Process Mass Balance

Figure 11.2 shows a simplified mass balance of the modelled HTC process with a biomass input of 1000 kg_{db} with data from EFB that is treated at 210 °C for 2 h.

In the presented scheme, EFB enters the process with 65 % moisture. The feed stream is further diluted with recycled water from the filter press and by recycling of steam from the flash tanks. The HTC reactor is operated at a solid concentration of 20 wt.-% which corresponds to a L/S ratio of 4. Mass yield after HTC is 60 % with the main losses being attributed to the dissolution of organic matter (TOC) in the process water. 13 % of the process water is recycled as steam in the flash tanks, 44 % is recirculated

and mixed with the biomass feed stream and 25 % need to be discharged as waste water. In this scenario, the amount of process water produced is $2.29 \text{ m}^3 \text{ t}^{-1}$ of hydrochar produced which corresponds to the data reported by Ingelia for a slightly lower moisture content of 60 % in the biomass feed [171].

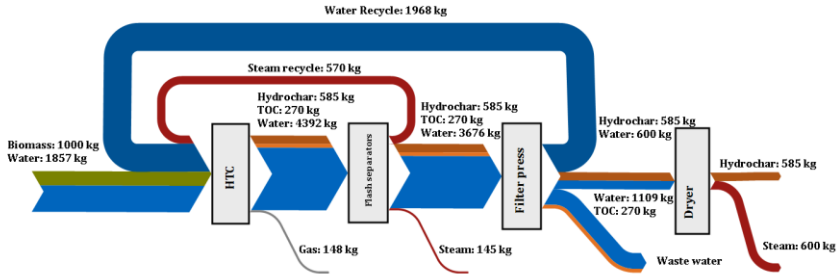


Figure 10.3: Simplified mass balance of the modelled HTC plant operating at $210 \text{ }^\circ\text{C}$, 2 h.

If the solid concentration in the HTC reactor is to be kept constant irrespective of feedstock moisture content, the amount of process waste water increases with feedstock moisture content. The amount of water that can be recycled to the feed stream decreases and a higher proportion of water needs to be sent to treatment. For example, for a feed stream with 80 % moisture the amount of waste water produced increases to $4.33 \text{ m}^3 \text{ t}^{-1}$. This also has an impact on the profitability of the process due to higher associated costs for process water treatment. Overall water management in HTC process design is critical. Future work should therefore consider the impact of process water recycling and management on the technical and economic performance in more detail.

10.2 Economic Evaluation

The process model developed in the previous section was used to provide technical data for the economic study of the total cost of production of HTC fuels and their provision to a European market. Using cost correlations for capital and operational expenses a minimum selling price above which the

production of HTC fuels is profitable is calculated. A case study considering two site locations is carried out. Table 10.3 contains key data, equipment cost as well as total fixed capital costs for both sites. For all other assumptions and framework conditions see section 6.5.

Table 10.3: Key data on both considered plant sites and total cost for on-site equipment.

	HTC plant Germany	HTC plant Malaysia
Key data		
Plant Capacity (t a ⁻¹ , ar)	40,000	80,000
Operating time (h a ⁻¹)	7,000	7,000
Workers per shift	2	3
HTC conditions	180 °C, 2 h	180 °C, 2 h
Feedstock type	Green cut	EFB
Feedstock moisture (%)	65	65
Biomass cost (€ t ⁻¹ , ar)	-25	3
Fuel production (t a ⁻¹ , db)	9,408	25,336
Equipment cost		
Heat exchanger (€)	229,000	372,000
Heater (€)	206,000	335,000
Reactor (€)	1,588,000	2,580,000
Flash tanks (€)	476,000	773,000
Slurry Pumps (€)	422,000	685,000
Filter press (€)	113,000	183,000
Dryer (€)	350,000	568,000
Grinder /Mixer (€)	81,000	131,000
Pelletizer (€)	268,000	435,000
Total fixed capital cost (Mio €)	7.6	12.3

One site is located in Germany and converts 40 kt of landscaping materials per year. The other site is located in Malaysia and converts 80 kt of EFB from palm oil plantations per year. After production the HTC fuel is shipped to Germany by sea. Both plants operate at moderate HTC severity at 180 °C and a residence time of 2 h.

The German plant produces approximately 9.5 kt, the Malaysian plant 25.5 kt of HTC fuel per year. Table 11.3 also contains the bare-module costs for the equipment needed in the plant. The values are calculated using a sizing factor as introduced in section 6.5.2 following Erlach [178] and Towler and Sinnott [177]. Adding costs for other needed infrastructure, start-up and engineering work, the total capital investment is calculated as 7.6 Mio € and 12.3 Mio € for the German and Malaysian plant, respectively.

The plant location has no strong effect on total capital investment since the location factors are fairly similar (1.11 for Germany and 1.12 for Malaysia) [177]. The reported total fixed capital cost is slightly lower than investment values provided by commercial HTC technology providers: C-green states a budget of 5.5 Mio € for their commercial 16 kt plant converting paper mill sludge in Finland [275]. In another commercial project, Ingelia indicates a sum of 15 Mio € of investment for a plant processing 75 kt of municipal waste in Italy [276]. Adding costs for labour, utilities, waste management and shipping, as summarised in Table 10.4, the cost of production per ton of HTC fuel is calculated.

Table 10.4: Annual capital and cash costs of production for HTC fuels in Germany from a local plant and a Malaysian plant including delivery.

Cost category	HTC Plant Germany	HTC plant Malaysia
Annual capital cost (€ a ⁻¹)	833,888	1,344,819
Personnel (€ a ⁻¹)	631,800	166,163
Overhead (€ a ⁻¹)	325,629	227,917
Maintenance (€ a ⁻¹)	149,285	242,514
Insurance (€ a ⁻¹)	52,250	84,880
Water (€ a ⁻¹)	51,600	52,413
Electricity (€ a ⁻¹)	52,676	52,029
Natural gas (€ a ⁻¹)	445,250	953,102
Biomass procurement (€ a ⁻¹)	-1,000,000	240,000
Wastewater treatment (€ a ⁻¹)	350,981	880,583
Shipping (€ a ⁻¹)		910,560
HTC fuel price (€ t⁻¹, db)	201	203
HTC fuel price (€ GJ⁻¹, HHV)	8.8	8.9

In Figure 10.4 the proportion of the different cost categories for HTC fuel production are shown. In the German plant the biggest cost factor is capital depreciation cost (28 %) followed by labour costs (22 %) and utility cost (19 %). The overhead and waste water treatment costs each amount to 12 %; maintenance to 7 % of the total production cost. The gate fee of 25 € t⁻¹ for landscaping material adds a big financial bonus to the production at the German site. For the production of HTC fuels in Malaysia the main cost factors are depreciation cost (25 %), utilities (23 %), shipping costs (17 %) and waste water treatment cost (18 %). Biomass supply contributes 5% to the production cost. Personnel costs are much lower in Asia and only account for 3 % of the production cost.

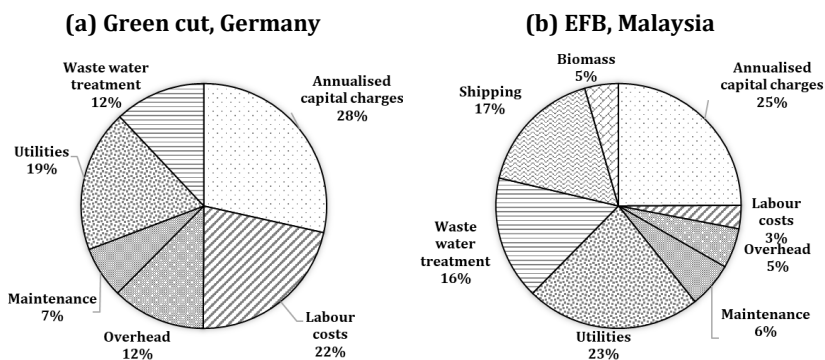


Figure 10.4: Proportionate costs of different cost categories in the cost of production of fuels originating from a HTC plant processing (a) green cut in Germany, (b) EFB in Malaysia.

In Germany, the total cost of production for HTC fuels is 201 € t⁻¹ corresponding to 8.8 € GJ⁻¹ on HHV basis. The production cost of HTC fuels in Malaysia, including delivery to Europe, is 203 € t⁻¹ resp. 8.9 € GJ⁻¹ on HHV basis. If HTC fuels were to be produced for the local market, fuel production cost in Malaysia would reduce to 168 € t⁻¹ resp. 7.3 € GJ⁻¹. In comparable techno-economic studies similar prices in the range of 6.1-9.7 € GJ⁻¹ for HTC fuels are reported [62, 64]. As mentioned above, the production price in Germany relies heavily on the gate-fee provided for the disposal of green cut. Without this gate fee, the total cost of production would rise to 308 € t⁻¹ (resp. 15 € GJ⁻¹).

For comparison, in 2019 fuel prices for commercial wood pellets were in the range of 100-200 € t⁻¹ and 6-13 € GJ⁻¹, respectively [277]. Even lower fuels costs are associated with fossil fuels, such as coal, that was around 79 € t⁻¹ (resp. 2.7 € GJ⁻¹) in 2019 [278]. This means that in the current market situation, the production of HTC fuels is economically not competitive. HTC is also more expensive, when compared to other pre-treatment technologies. For example, Abelha et al. [181] reported a biocoal production cost between 2.9-6.2 € GJ⁻¹ for washed and torrefied roadside grass.

Yet, HTC might still be a viable upgrading route for challenging biomass. Neither torrefaction, nor steam-explosion are suitable for high moisture biomass and do not remove problematic ash components like K or Cl to the same extent as HTC. Therefore, they are not able to access the large energetic potential that these challenging biomass fuels offer. Additionally, the disposal of these feedstock often provides a gate-fee. Considering the framework of the HTC plant in Germany, a fuel price of 3.2 € t⁻¹ (comparable to coal) could be achieved, if a feedstock with a gate fee of 55 € t⁻¹ is converted. Another possibility is to use HTC solely as a waste reduction and treatment technology for sludges from industry or waste water treatment. For example, the treatment cost that occur in the German plant could be fully covered if the feedstock provides a gate-fee of 72 € t⁻¹, assuming that the plant design remains unchanged. Municipal sewage sludge with a current disposal cost of roughly 100-200 € t⁻¹ would satisfy this criteria easily.

Another factor that could lead to the implementation of the HTC technology in the future is that the legal framework for the utilisation of fossil fuels is changing in Europe and other developed countries. Financial penalties for the combustion of fossil fuels add to the cost of their utilisation. Considering the price-spread of roughly 6 € GJ⁻¹ a break-even point for CO₂ pricing can be calculated above which the use of HTC fuels would be economically favourable towards fossil fuels. Hard coal emits 94 kg CO₂ per GJ [279]. Thus, a CO₂ price of 65 € t⁻¹ would render HTC fuels competitive to coal. In 2021, Germany introduced a CO₂ price of 25 € t⁻¹ that will gradually be

increased to 55-65 € t⁻¹ by 2026 [280]. This offers a prospect for the technology to provide price-competitive and environmentally friendly fuels in the future.

Chapter summary: The energetic efficiency of HTC was determined by process modelling of an HTC plant. Overall a thermal efficiency of 62 % was determined for a plant processing 40 kt a⁻¹ of EFB with a moisture of 70 %. Thermal process efficiency is influenced by treatment temperature and feedstock moisture content. It was determined that the majority of losses are attributed to the loss of chemical energy in the process water. Higher treatment temperature was found to lead to lower thermal efficiency due to a higher thermal energy demand for biomass heating and increasing losses of chemical energy by the dissolution of organic material in the process water. It was demonstrated that a higher feedstock moisture leads to a greater thermal mass that needs heating for the same HTC fuel yield, thus decreasing thermal efficiency. For higher feedstock moisture also the amount of contaminated process water that needs treatment is increased. A techno-economic analysis of HTC fuel production from landscaping material and EFB revealed a minimum fuel price of 8.8-15 € GJ⁻¹. Consequently, HTC currently does not offer an economically viable alternative to conventional and other renewable fuels such as wood pellets. HTC fuels are also more costly than fuels from other thermo-chemical pre-treatment such as torrefaction and steam-explosion. Competitive fuel prices could be reached for the conversion feedstock with a gate-fee above 55 € t⁻¹ or by implementing higher CO₂ taxation.

11 Summary and Recommendations

The upgrading of residual biomass by hydrothermal carbonisation for the provision of fuels has been investigated in detail. The selection of suitable feedstock, fuel quality after upgrading, economic competitiveness as well as treatment options for process water, the main side product of HTC, have been assessed. A focus was set on the fate of inorganic elements during HTC, since ash-related problems pose the main challenges in biomass combustion. The main findings are summarised in the following.

11.1 Summary of Findings

The transformation of energy systems towards climate neutrality requires renewable energy sources. Bioenergy is an important building block of renewable energy systems, since they are able to provide energy independent of season and weather conditions. With an increasing demand for biofuels and rising environmental concerns towards the utilisation of wood, new biomass streams need to be explored. Residual biomass waste streams from agriculture, forestry and other sources offer a great potential for energy use. Their use is environmentally friendly, since no additional land use is caused and GHG emissions from biological biomass degradation or on-site incineration is prevented. However, these feedstock often suffer from poor fuel quality. High moisture content, low energy density and high concentrations of inorganic pollutants that cause undesirable reactions in boilers being the most pressing issues preventing their widespread utilisation in power plants. Hydrothermal carbonisation is a new technology that allows upgrading of these residual biomass feedstock to high quality fuels. During HTC, biomass is treated in hot compressed water at temperatures between 150-300 °C to produce a lignite-like solid fuel. For the first time, a holistic assessment of HTC for the provision of solid fuels from residual biomass has been conducted. An initial screening of 19 substrates was conducted to identify suitable feedstock for HTC based on current utilisation options, competing energetic valorisation pathways and performance of HTC in terms of energy densification and yield. Next, the

impact of HTC on fuel characteristic relevant for combustion was investigated in detail in a parameter study. The influence of feedstock type, reaction severity, solid concentration and additives on the inorganic composition of HTC fuels was examined. Subsequently, the energetic and economic performance of HTC for the provision of fuels from landscaping material and EFB, a residue from palm oil production, was assessed by process modelling and techno-economic analysis. Finally, HTC process water, which constitutes the main by-product of HTC, was characterised and subsequent utilisation and valorisation options were discussed.

Selection of Suitable Feedstock for HTC

In principle all biogenic material can be converted by HTC. To decide which substrates would be most suited for HTC conversion four criteria were applied in the selection of feedstock. An initial assessment of fuel quality of the untreated substrates revealed poor fuel quality considering ash-, chlorine- and nitrogen content for all substrates except spruce bark. Feedstock that is currently used as animal feed was deemed unsuited for HTC. The quality of carbonisation was assessed by means of mass- and energy yield as well as energy densification. Energy yield is a preliminary indicator of the efficiency of the hydrothermal conversion of any feedstock. The lignocellulosic composition was found to have a strong effect on mass yield, with lower mass yields being linked to high protein and hemi-cellulose content of the substrates. Similarly, the energy densification of the organic dry matter was also found to correlate with lignocellulosic biomass composition with the lowest energetic compaction being observed for feedstock with high lignin content. A comparison of the efficiency of direct-combustion of the substrates with HTC demonstrated that HTC prior to combustion is energetically favourable for feedstock with a moisture content exceeding 50 wt.-%. The exact threshold moisture is feedstock specific and primarily depends on energy yield of HTC conversion and the initial LHV prior to upgrading. Finally, a conversion by HTC was compared to a conversion by anaerobic digestion (AD), which is a competing technology for the valorisation of wet feedstock. AD of micro algae and grass cuttings was found to perform better than HTC due to the higher proportion

of bio-available carbon in these feedstock. Contrarily, HTC was favoured for the conversion of poorly fermentable fuels with high proportion of lignocellulosic material. Taking into account all of the abovementioned aspects, AD digestate, digested sewage sludge, EFB, fallen leaves, fir needles, horse manure, orange peels, seaweed and spruce bark were identified as well suitable substrates for HTC.

Impact of HTC on Fuel Quality

During HTC, the organic and inorganic composition of the treated biomass feedstock is changed dramatically. A parameter study including eight different feedstock that were treated at temperatures ranging from 150-270 °C for 0.5-4 h was performed. It was demonstrated that HTC increases LHV of the fuels by 13-35 % at a typical treatment temperature of 210 °C. Increasing reaction severity (i.e. higher temperature and longer treatment) further increases LHV by up to 60 %. On the downside, mass yield declines for increasing reaction severity due to partial biomass liquefaction and mass loss to the process water. Energy yield, i.e. the amount of chemical energy recovered in the solid fuel was found to be in the range of 57-94 %. Overall, temperature was determined to be the main factor affecting LHV, mass- and energy yield. Different observations were made for HTC of digested sewage sludge: HTC slightly decreased LHV of this feedstock due to the high ash content of above 30 wt.-%. Ash analysis revealed a strong impact on HTC on ash content and composition. Ash content was found to decrease after HTC for substrates that possess a large proportion of soluble species such as potassium or chlorine in their ash. At higher treatment severity, organic material is removed to the same or to a larger extent than inorganic matter, consequently ash content often was found to increase after severe HTC treatment. Further, the impact of feedstock type, process condition, L/S ratio as well as CO₂ additive on the fate of inorganics was investigated. Overall, HTC proved to be effective in reducing K, Mg, Cl and S in hydrochar ash, while the concentration of Ca, Al and Si increased. P removal was feedstock dependent but in most HTC fuels increased P concentrations were found in the ash. Temperature was discovered to have a strong effect on the removal efficiencies of individual elements: K, Cl, and S extraction from the biomass

matrix increased steadily with temperature, while for Mg and Ca the strongest reduction was observed at intermediate HTC temperatures. Temperature had limited impact on Si and Al extraction. For P, a decline in removal efficiency was found with increasing treatment temperatures for most feedstock. The influence of residence time on the removal of inorganics was small. L/S ratio was determined as another major factor influencing inorganic removal: Lower removal efficiencies were found for higher solid concentrations. An impact of CO₂ addition on inorganic composition of HTC fuels, as postulated in other studies could not be confirmed. Ash melting temperatures of alkali-rich substrates were discovered to increase significantly after HTC, while little effect of HTC on ash fusion characteristics was found for Ca and P rich substrates. Overall, fuel quality assessed by fuel indices suitable for biofuels revealed that HTC fuels reduce corrosion, deposit formation and PM emission risk compared to untreated fuels. The improvements are mainly due to the high removal of K and Cl during HTC. On the downside, higher NO_x emissions have to be expected due to higher fuel-N and lower volatile content. All in all, the biggest improvements concerning fuel quality were observed for alkali- and chlorine-rich feedstock.

Valorisation Options for HTC Process Water

Process water is the largest by-product of HTC. The process model was used to calculate the amount of process water generated per ton of HTC fuel. Feedstock moisture and process water recycling were determined to be the main influencing factors for the amount of process water generated. At 65 % feedstock moisture 2.3 m³ of process water are produced per ton of HTC fuel. This increases to 4.3 m³ t⁻¹ for lower solid concentration at 80 % feedstock moisture. Without process water recycling even higher amounts of process water are generated: 2.6 m³ t⁻¹ at 65% moisture and 5.7 m³ t⁻¹ at 80 % moisture. Experimental investigations showed that HTC process water is highly contaminated with organic matter. COD values between 15.-35 g l⁻¹ were obtained. An energetic valorisation by AD of the chemical energy contained in HTC effluent could contribute around 10 % of the thermal energy demand of the process. Several treatment methods for HTC

process water exist. However, the valorisation and treatment of HTC process water is challenging due to its exceptionally high organic load and the presence of non-biodegradable, refractory compounds. An optimal treatment method or combination of several treatment steps is yet to be identified.

Techno-economic Evaluation of the Technology

A process model of a HTC plant has been developed in Aspen Plus. The thermal efficiency of the process was determined to be 62 % for a plant treating 40 kt a⁻¹ of EFB at a temperature of 210 °C and a moisture content of 70 %. Treatment temperature and solid concentration were found to have major impact on the thermal efficiency of the process. Higher treatment temperature leads to higher energy demand for biomass heating and causes higher losses of chemical energy to the process waster. The latter was determined to be the main source of efficiency losses accounting for 67-92 % of the losses depending on treatment temperature. Higher water content in the feedstock also lead to lower thermal efficiencies. At lower solid concentrations a larger amount of thermal mass needs to be heated for the same output of HTC fuels. Thus, mechanical dewatering should be considered to increase HTC efficiency. The fuel production cost was calculated in a techno-economic analysis of two plant sites: a plant processing landscaping material in Germany and a plant processing EFB in Malaysia were considered. The calculation showed that in both scenarios HTC, with a fuel production cost of 8.8-15 €GJ⁻¹ is currently not a competitive technology for the production of solid fuels. However, economically viable fuel costs of 3.2 €GJ⁻¹ could be achieved treating feedstock that provides considerable gate-fees of 55 €t⁻¹ and more. Alternatively, introducing a CO₂ tax of 65 €t⁻¹ would render HTC fuels competitive to fossil fuels, if renewables are utilised to provide the auxiliary energy demand of HTC.

11.2 Recommendations for Future Work

The presented work includes an in-depth assessment of HTC as a technology for the provision of fuels. A decision tree has been developed which facilitates the selection of suitable feedstock for HTC. Further, the impact of HTC on fuel quality has been discussed in detail. Especially fuel quality of feedstock suffering from high moisture content, high alkali and chlorine content can be greatly improved by HTC. A techno-economic analysis revealed current bottlenecks for the market introduction of HTC fuels: Either feedstock with a considerable gate-fee should be treated or a CO₂ tax needs to be introduced for HTC fuels to become economically competitive. The efficient treatment and management of HTC process water still constitute the biggest challenge on the path to commercialisation of the technology.

Future work therefore should investigate efficient treatment strategies for process water originating from HTC. Developing effective water management strategies during HTC process design are key to an economically and environmentally viable process. At best, an energetic valorisation of the organic matter contained in HTC process water should be implemented. In addition, the findings of this work considering improvements of fuel quality need verification. Although fuel indices provide a first indication on biomass related challenges during combustion, investigations in real systems on pilot- and full-scale are needed for reliable risk assessment. Apart from changes in ash-chemistry, HTC also improves other physio-chemical fuel properties that have not been quantified within the scope of this work. However, evaluating these properties in depth like e.g. dewatering characteristics, storage properties, bulk density and pelletisation of HTC fuels constitutes an important contribution in demonstrating advantages that HTC fuels have over traditional biomass fuels.

12 References

1. Sellers S, Ebi KL, Hess J (2019) Climate Change, Human Health, and Social Stability: Addressing Interlinkages. *Environ Health Perspect* 127:45002. <https://doi.org/10.1289/EHP4534>
2. Hsiang SM, Burke M (2014) Climate, conflict, and social stability: what does the evidence say? *Climatic Change* 123:39–55. <https://doi.org/10.1007/s10584-013-0868-3>
3. Buhaug H, Nordkvelle J, Bernauer T et al. (2014) One effect to rule them all? A comment on climate and conflict. *Climatic Change* 127:391–397. <https://doi.org/10.1007/s10584-014-1266-1>
4. IEA (2019) *World Energy Outlook 2019*, Paris
5. European Commission (2018) *Renewable Energy Progress Report*, Brussels
6. Fajardy M, Mac Dowell N (2017) Can BECCS deliver sustainable and resource efficient negative emissions? *Energy Environ Sci* 10:1389–1426. <https://doi.org/10.1039/C7EE00465F>
7. Banja M, Sikkema R, Jégard M et al. (2019) Biomass for energy in the EU – The support framework. *Energy Policy* 131:215–228. <https://doi.org/10.1016/j.enpol.2019.04.038>
8. European Commission (2020) *EU Biodiversity Strategy for 2030: - Bringing nature back into our lives*, Brussels
9. (2019) *The Role of Bioenergy in the Bioeconomy*. Elsevier
10. Stermann JD, Siegel L, Rooney-Varga JN (2018) Does replacing coal with wood lower CO₂ emissions? Dynamic lifecycle analysis of wood bioenergy. *Environ Res Lett* 13:15007. <https://doi.org/10.1088/1748-9326/aaa512>
11. Unknown (2019) *Global Bioenergy Statistics 2019*
12. Jenkins BM, Baxter LL, Miles TR (1998) Combustion properties of biomass. *Fuel Processing Technology* 54:17–46. [https://doi.org/10.1016/S0378-3820\(97\)00059-3](https://doi.org/10.1016/S0378-3820(97)00059-3)
13. Miles TR, Baxter LL, Bryers RW et al. (1996) Boiler deposits from firing biomass fuels. *Biomass and Bioenergy* 10:125–138. [https://doi.org/10.1016/0961-9534\(95\)00067-4](https://doi.org/10.1016/0961-9534(95)00067-4)

14. Hoekman SK, Broch A, Robbins C (2011) Hydrothermal Carbonization (HTC) of Lignocellulosic Biomass. *Energy Fuels* 25:1802–1810. <https://doi.org/10.1021/ef101745n>
15. Libra JA, Ro KS, Kammann C et al. (2011) Hydrothermal carbonization of biomass residuals: a comparative review of the chemistry, processes and applications of wet and dry pyrolysis. *Biofuels* 2:71–106. <https://doi.org/10.4155/bfs.10.81>
16. Kambo HS, Dutta A (2014) Strength, storage, and combustion characteristics of densified lignocellulosic biomass produced via torrefaction and hydrothermal carbonization. *Applied Energy* 135:182–191. <https://doi.org/10.1016/j.apenergy.2014.08.094>
17. Ulbrich MD (2019) Optimierung der Prozessparameter der Hydrothermalen Karbonisierung für den Einsatz in Vergasungsprozessen. *Energietechnik*. Verlag Dr. Hut, München
18. World Bioenergy Association (2016) Global Biomass Potential towards 2035: WBA Factsheet. https://www.google.com/url?sa=t&rct=j&q=&esrc=s&source=web&cd=&cad=rja&uact=8&ved=2ahUKEwjhg_umqcnyAhVv_7sIHW_vCuQQFnoECAQQAQ&url=http%3A%2F%2Fwww.worldbioenergy.org%2Fuploads%2FFactsheet_Biomass%2520potential.pdf&usg=AOvVaw34pTvDp5WGWxVJubVDVtgK. Accessed 24 Aug 2021
19. Wit M de, Faaij A (2010) European biomass resource potential and costs. *Biomass and Bioenergy* 34:188–202. <https://doi.org/10.1016/j.biombioe.2009.07.011>
20. Berien Elbersen, Igor Startisky, Geerten Hengeveld, Mart-Jan Schelhaas, Han Naeff, Hannes Böttcher (2012) Atlas of EU biomass potentials: Deliverable 3.3: Spatially detailed and quantified overview of EU biomass potential taking into account the main criteria determining biomass availability from different sources
21. Jori Sihvonen SE (2016) How much sustainable biomass does Europe have in 2030?
22. Cristina Calderón (2019) Bioenergy Europe Statistical Report 2019: Report Biomass Supply
23. Ric Hoefnagel, Ingeborg Kluts, Martin Junginger, Lotte Visse (2017) Biomass supply potentials for the EU and biomass demand from the

material sector by 2030: Technical Background Report of the “BioSustain” study: Sustainable and optimal use of biomass for energy in the EU beyond 2020.

https://ec.europa.eu/energy/sites/ener/files/documents/biosustain_annexes_final.pdf. Accessed 24 Aug 2021

24. European Commission’s statistical office (2022) Eurostat: Complete energy balances.
https://ec.europa.eu/eurostat/databrowser/view/nrg_bal_c/. Accessed 13 Jun 2022
25. Cook E (2018) Agriculture, forestry and fishery statistics: 2018 edition, 2018 edition. Agriculture, forestry and fishery statistics, vol 2018. Publications Office of the European Union, Luxembourg
26. Magelli F, Boucher K, Bi HT et al. (2009) An environmental impact assessment of exported wood pellets from Canada to Europe. *Biomass and Bioenergy* 33:434–441.
<https://doi.org/10.1016/j.biombioe.2008.08.016>
27. Vassilev SV, Baxter D, Andersen LK et al. (2010) An overview of the chemical composition of biomass. *Fuel* 89:913–933.
<https://doi.org/10.1016/j.fuel.2009.10.022>
28. Kaltschmitt M, Hartmann H, Hofbauer H (eds) (2016) *Energie aus Biomasse: Grundlagen, Techniken und Verfahren, 3., aktualisierte und erweiterte Auflage*. Springer Vieweg, Berlin, Heidelberg
29. Overend RP, Milne TA, Mudge LK (eds) (1985) *Fundamentals of Thermochemical Biomass Conversion*. Springer Netherlands, Dordrecht
30. Jin F, Coronella CJ, Lynam JG et al. (eds) (2014) Application of hydrothermal reactions to biomass conversion // *Hydrothermal Carbonization of Lignocellulosic Biomass. Green Chemistry and Sustainable Technology*, vol 15. Springer, Heidelberg
31. Meine N, Hilgert J, Kaldstrom M et al. (2012) *Katalytisches Vermahlen: Ein neuer Zugang für Lignocellulose-Bioraffinerien*
32. Scarlat N, Dallemand J-F, Monforti-Ferrario F et al. (2015) The role of biomass and bioenergy in a future bioeconomy: Policies and facts. *Environmental Development* 15:3–34.
<https://doi.org/10.1016/j.envdev.2015.03.006>

33. CHEN H (2016) BIOTECHNOLOGY OF LIGNOCELLULOSE: Theory and practice. Springer, [Place of publication not identified]
34. Vassilev SV, Baxter D, Andersen LK et al. (2012) An overview of the organic and inorganic phase composition of biomass. *Fuel* 94:1–33. <https://doi.org/10.1016/j.fuel.2011.09.030>
35. Bahadur B, Venkat Rajam M, Sahijram L et al. (2015) *Plant Biology and Biotechnology*. Springer India, New Delhi
36. Ranzi E (ed) (2014) Characterization of Ashes from Different Wood Parts of Norway Spruce Tree: IconBM, International Conference on BioMass : 4-7 May 2014, Florence, Italy. *Chemical engineering transactions*, volume 37 (2014). AIDIC Associazione Italiana di Ingegneria Chimica, Milano
37. Benson SA, Holm PL (1985) Comparison of inorganics in three low-rank coals. *Ind Eng Chem Prod Res Dev* 24:145–149. <https://doi.org/10.1021/i300017a027>
38. Miles TR, Miles TR, JR., Baxter LL et al. (1995) Alkali deposits found in biomass power plants: A preliminary investigation of their extent and nature. Volume 1
39. Zevenhoven-Onderwater M (2001) Ash-forming matter in biomass fuels. Dissertation. Abo Akademi University, Åbo
40. Thrän D, Dotzauer M, Lenz V et al. (2015) Flexible bioenergy supply for balancing fluctuating renewables in the heat and power sector—a review of technologies and concepts. *Energ Sustain Soc* 5. <https://doi.org/10.1186/s13705-015-0062-8>
41. Fang Z (ed) (2013) *Pretreatment Techniques for Biofuels and Biorefineries*. Green Energy and Technology. Springer Berlin Heidelberg, Berlin, Heidelberg
42. Kambo HS, Dutta A (2015) A comparative review of biochar and hydrochar in terms of production, physico-chemical properties and applications. *Renewable and Sustainable Energy Reviews* 45:359–378. <https://doi.org/10.1016/j.rser.2015.01.050>
43. Negi S, Jaswal G, Dass K et al. (2020) Torrefaction: a sustainable method for transforming of agri-wastes to high energy density solids (biocoal). *Rev Environ Sci Biotechnol* 19:463–488. <https://doi.org/10.1007/s11157-020-09532-2>

44. Bach Q-V, Skreiberg Ø (2016) Upgrading biomass fuels via wet torrefaction: A review and comparison with dry torrefaction. *Renewable and Sustainable Energy Reviews* 54:665–677
45. Joronen T, Björklund P, Bolhar-Nordenkampf M High Quality Fuel by Steam Explosion
46. Reza MT, Lynam JG, Uddin MH et al. (2013) Hydrothermal carbonization: Fate of inorganics. *Biomass and Bioenergy* 49:86–94. <https://doi.org/10.1016/j.biombioe.2012.12.004>
47. Yan W, Acharjee TC, Coronella CJ et al. (2009) Thermal pretreatment of lignocellulosic biomass. *Environ Prog Sustainable Energy* 28:435–440. <https://doi.org/10.1002/ep.10385>
48. Adapa P, Tabil L, Schoenau G (2011) Grinding performance and physical properties of non-treated and steam exploded barley, canola, oat and wheat straw. *Biomass and Bioenergy* 35:549–561. <https://doi.org/10.1016/j.biombioe.2010.10.004>
49. Acharya B, Dutta A (2013) Characterization of Torrefied Willow for Combustion Application. *J Biobased Mat Bioenergy* 7:667–674. <https://doi.org/10.1166/jbmb.2013.1372>
50. Mišljenović N, Bach Q-V, Tran K-Q et al. (2014) Torrefaction Influence on Pelletability and Pellet Quality of Norwegian Forest Residues. *Energy Fuels* 28:2554–2561. <https://doi.org/10.1021/ef4023674>
51. Reza MT, Lynam JG, Vasquez VR et al. (2012) Pelletization of biochar from hydrothermally carbonized wood. *Environ Prog Sustainable Energy* 31:225–234. <https://doi.org/10.1002/ep.11615>
52. Smith AM, Singh S, Ross AB (2016) Fate of inorganic material during hydrothermal carbonisation of biomass: Influence of feedstock on combustion behaviour of hydrochar. *Fuel* 169:135–145. <https://doi.org/10.1016/j.fuel.2015.12.006>
53. Ballesteros I, Oliva JM, Navarro AA et al. (2000) Effect of Chip Size on Steam Explosion Pretreatment of Softwood. *ABAB* 84-86:97–110. <https://doi.org/10.1385/ABAB:84-86:1-9:97>
54. Brownell HH, Yu EK, Saddler JN (1986) Steam-explosion pretreatment of wood: Effect of chip size, acid, moisture content and pressure drop. *Biotechnol Bioeng* 28:792–801. <https://doi.org/10.1002/bit.260280604>

55. (1991) Steam explosion techniques: Fundamentals and industrial applications ; proceedings, Philadelphia
56. Shevchenko SM, Beatson RP, Saddler JN The Nature of Lignin from Steam Explosion/Enzymatic Hydrolysis of Softwood, pp 867–876
57. Tooyserkani Z, Sokhansanj S, Bi X et al. (2013) Steam treatment of four softwood species and bark to produce torrefied wood. *Applied Energy* 103:514–521.
<https://doi.org/10.1016/j.apenergy.2012.10.016>
58. Cara C, Ruiz E, Ballesteros I et al. (2006) Enhanced enzymatic hydrolysis of olive tree wood by steam explosion and alkaline peroxide delignification. *Process Biochemistry* 41:423–429.
<https://doi.org/10.1016/j.procbio.2005.07.007>
59. Garrote G, Domínguez H, Parajó JC (1999) Hydrothermal processing of lignocellulosic materials. *Holz als Roh- und Werkstoff* 57:191–202.
<https://doi.org/10.1007/s001070050039>
60. Stemann J (2013) Hydrothermale Carbonisierung: Stoffliche und energetische Kreislaufführung. Technische Universität Berlin
61. Blöhse D (2017) Hydrothermale Karbonisierung – Nutzen dieser Konversionstechnik für die optimierte Entsorgung feuchter Massenreststoffe. Universitätsbibliothek Duisburg-Essen, Duisburg, Essen
62. Stemann J, Erlach B, Ziegler F (2013) Hydrothermal Carbonisation of Empty Palm Oil Fruit Bunches: Laboratory Trials, Plant Simulation, Carbon Avoidance, and Economic Feasibility. *Waste Biomass Valor* 4:441–454. <https://doi.org/10.1007/s12649-012-9190-y>
63. Saba A, McGaughy K, Reza M (2019) Techno-Economic Assessment of Co-Hydrothermal Carbonization of a Coal-Miscanthus Blend. *Energies* 12:630. <https://doi.org/10.3390/en12040630>
64. Lucian M, Fiori L (2017) Hydrothermal Carbonization of Waste Biomass: Process Design, Modeling, Energy Efficiency and Cost Analysis. *Energies* 10:211. <https://doi.org/10.3390/en10020211>
65. Da Costa Gomez C (2013) Biogas as an energy option: an overview. In: *The Biogas Handbook*, vol 109. Elsevier, pp 1–16

66. Biosantech TAS, Rutz D, Janssen R et al. (2013) Biomass resources for biogas production. In: *The Biogas Handbook*, vol 22. Elsevier, pp 19–51
67. Jeihanipour A (2011) Waste textiles bioprocessing to ethanol and biogas. Zugl.: Göteborg, Univ., Diss., 2011. *Skrifter från Högskolan i Borås*, vol 32. Chalmers Univ. of Technology, Göteborg
68. Teghammar A (2013) Biogas production from lignocelluloses: Pretreatment, substrate characterization, co-digestion, and economic evaluation. Zugl.: Göteborg, Univ., Diss., 2013. *Skrifter från Högskolan i Borås*, vol 41. Chalmers Univ. of Technology, Göteborg
69. Ramke H.G., Blöhse D, Lehmann H.J., Antonietti M, Fettig J (2010) Machbarkeitsstudie zur Energiegewinnung aus organischen Siedlungsabfällen durch Hydrothermale Carbonisierung: Abschlussbericht
70. Funke A, Ziegler F (2010) Hydrothermal carbonization of biomass: A summary and discussion of chemical mechanisms for process engineering. *Biofuels*, Bioprod Bioref 4:160–177. <https://doi.org/10.1002/bbb.198>
71. Titirici M-M, Thomas A, Antonietti M (2007) Back in the black: hydrothermal carbonization of plant material as an efficient chemical process to treat the CO₂ problem? *New Journal of Chemistry*, 31(6), 787. <https://doi.org/10.1039/B616045J>
72. Mao C, Feng Y, Wang X et al. (2015) Review on research achievements of biogas from anaerobic digestion. *Renewable and Sustainable Energy Reviews* 45:540–555. <https://doi.org/10.1016/j.rser.2015.02.032>
73. Angelonidi E, Smith SR (2015) A comparison of wet and dry anaerobic digestion processes for the treatment of municipal solid waste and food waste. *Water Environ J* 29:549–557. <https://doi.org/10.1111/wej.12130>
74. Thomas M. Kläusli (2013) *Hydrothermal Carbonisation: Energy from Biomass*, Zug, Switzerland
75. Khanal S (2011) *Anaerobic Biotechnology for Bioenergy Production: Principles and Applications*. Wiley, Somerset

76. Viola E, Zimbardi F, Cardinale M et al. (2008) Processing cereal straws by steam explosion in a pilot plant to enhance digestibility in ruminants. *Bioresour Technol* 99:681–689. <https://doi.org/10.1016/j.biortech.2007.02.001>
77. Castro FB de, Paiva TCB, Arcaro I (1995) Substitution of sugar cane with steam-treated eucalyptus (*Eucalyptus grandis*): effects on intake and growth rate of dairy heifers. *Animal Feed Science and Technology* 52:93–100. [https://doi.org/10.1016/0377-8401\(94\)00704-D](https://doi.org/10.1016/0377-8401(94)00704-D)
78. Lucian M, Volpe M, Merzari F et al. (2020) Hydrothermal carbonization coupled with anaerobic digestion for the valorization of the organic fraction of municipal solid waste. *Bioresour Technol* 314:123734. <https://doi.org/10.1016/j.biortech.2020.123734>
79. Erdogan E, Atila B, Mumme J et al. (2015) Characterization of products from hydrothermal carbonization of orange pomace including anaerobic digestibility of process liquor. *Bioresour Technol* 196:35–42. <https://doi.org/10.1016/j.biortech.2015.06.115>
80. Marin-Batista JD, Villamil JA, Rodriguez JJ et al. (2019) Valorization of microalgal biomass by hydrothermal carbonization and anaerobic digestion. *Bioresour Technol* 274:395–402. <https://doi.org/10.1016/j.biortech.2018.11.103>
81. Wirth B, Mumme J (2014) Anaerobic Digestion of Waste Water from Hydrothermal Carbonization of Corn Silage. *Applied Bioenergy* 1. <https://doi.org/10.2478/apbi-2013-0001>
82. Brown AE, Finnerty GL, Camargo-Valero MA et al. (2020) Valorisation of macroalgae via the integration of hydrothermal carbonisation and anaerobic digestion. *Bioresour Technol* 312:123539. <https://doi.org/10.1016/j.biortech.2020.123539>
83. Parmar KR, Ross AB (2019) Integration of Hydrothermal Carbonisation with Anaerobic Digestion; Opportunities for Valorisation of Digestate. *Energies* 12:1586. <https://doi.org/10.3390/en12091586>
84. Pagés-Díaz J, Cerda Alvarado AO, Montalvo S et al. (2020) Anaerobic bio-methane potential of the liquors from hydrothermal carbonization of different lignocellulose biomasses. *Renewable Energy* 157:182–189. <https://doi.org/10.1016/j.renene.2020.05.025>

85. Vogel F (2016) Hydrothermale Verfahren. In: Kaltschmitt M, Hartmann H, Hofbauer H (eds) *Energie aus Biomasse: Grundlagen, Techniken und Verfahren*, 3., aktualisierte und erweiterte Auflage, vol 31. Springer Vieweg, Berlin, Heidelberg, pp 1267–1337
86. Savage PE, Levine RB, Huelsman CM (2010) Chapter 8. Hydrothermal Processing of Biomass. In: Crocker M (ed) *Thermochemical Conversion of Biomass to Liquid Fuels and Chemicals*. Royal Society of Chemistry, Cambridge, pp 192–221
87. Kruse A, Funke A, Titirici M-M (2013) Hydrothermal conversion of biomass to fuels and energetic materials. *Curr Opin Chem Biol* 17:515–521. <https://doi.org/10.1016/j.cbpa.2013.05.004>
88. Akiya N, Savage PE (2002) Roles of water for chemical reactions in high-temperature water. *Chem Rev* 102:2725–2750. <https://doi.org/10.1021/cr000668w>
89. U Grigull (1983) Dielektrizitätskonstante und Ionenprodukt von Wasser und Wasserdampf. *Brennstoff-Wärme-Kraft*
90. Lemmon EW, McLinden MO, Friend DG (2014) Thermophysical properties of fluid systems. <http://webbook.nist.gov>. Accessed 26 Mar 2021
91. Dinjus E, Kruse A, Tröger N (2011) Hydrothermal Carbonization - 1. Influence of Lignin in Lignocelluloses. *Chem Eng Technol* 34:2037–2043. <https://doi.org/10.1002/ceat.201100487>
92. Funke A (2012) Hydrothermale Karbonisierung von Biomasse - Reaktionsmechanismen und Reaktionswärme. Technische Universität Berlin
93. Ruyter HP (1982) Coalification model. *Fuel* 61:1182–1187. [https://doi.org/10.1016/0016-2361\(82\)90017-5](https://doi.org/10.1016/0016-2361(82)90017-5)
94. Van Krevelen (1950) Graphical-statistical method for the study of structure and reaction processes of coal. In:
95. Peterson AA, Vogel F, Lachance RP et al. (2008) Thermochemical biofuel production in hydrothermal media: A review of sub- and supercritical water technologies. *Energy Environ Sci* 1:32. <https://doi.org/10.1039/b810100k>

96. Bobleter O (1994) Hydrothermal degradation of polymers derived from plants. *Progress in Polymer Science* 19:797–841.
[https://doi.org/10.1016/0079-6700\(94\)90033-7](https://doi.org/10.1016/0079-6700(94)90033-7)
97. Smith AM, Ross AB (2019) The Influence of Residence Time during Hydrothermal Carbonisation of Miscanthus on Bio-Coal Combustion Chemistry. *Energies* 12:523. <https://doi.org/10.3390/en12030523>
98. Sevilla M, Fuertes AB (2009) Chemical and structural properties of carbonaceous products obtained by hydrothermal carbonization of saccharides. *Chemistry* 15:4195–4203.
<https://doi.org/10.1002/chem.200802097>
99. Reza MT, Yan W, Uddin MH et al. (2013) Reaction kinetics of hydrothermal carbonization of loblolly pine. *Bioresour Technol* 139:161–169. <https://doi.org/10.1016/j.biortech.2013.04.028>
100. Yan W, Hoekman SK, Broch A et al. (2014) Effect of hydrothermal carbonization reaction parameters on the properties of hydrochar and pellets. *Environ Prog Sustainable Energy* 33:676–680.
<https://doi.org/10.1002/ep.11974>
101. Landais P, Michels R, Elie M (1994) Are time and temperature the only constraints to the simulation of organic matter maturation? *Organic Geochemistry* 22:617–630. [https://doi.org/10.1016/0146-6380\(94\)90128-7](https://doi.org/10.1016/0146-6380(94)90128-7)
102. Engel MH, Macko SA (eds) (1993) *Organic Geochemistry: Principles and Applications*. Topics in Geobiology, vol 11. Springer US, Boston, MA, s.l.
103. Stach E, Murchison G (1982) [Erich] Stach's textbook of coal petrology: By E[rich] Stach [u.a.] Transl. and English rev. by G. Murchison, 3., rev. and enlarged ed. Borntraeger, Berlin, Stuttgart
104. Wright NJR (1980) TIME, TEMPERATURE AND ORGANIC MATURATION-the evolution of rank within a sedimentary pile. *J Petroleum Geol* 2:411–425. <https://doi.org/10.1111/j.1747-5457.1980.tb00969.x>
105. Berge ND, Ro KS, Mao J et al. (2011) Hydrothermal carbonization of municipal waste streams. *Environ Sci Technol* 45:5696–5703.
<https://doi.org/10.1021/es2004528>

106. Berger S (2002) Entwicklung und technische Umsetzung der mechanisch/thermischen Entwässerung zum Einsatz als Vortrocknungsstufe in braunkohlegefeuerten Kraftwerken. Zugl.: Dortmund, Univ., Diss., 2001. Berichte aus der Verfahrenstechnik. Shaker, Aachen
107. Cai J, Chen S (2008) Determination of Drying Kinetics for Biomass by Thermogravimetric Analysis under Nonisothermal Condition. *Drying Technology* 26:1464–1468.
<https://doi.org/10.1080/07373930802412116>
108. Peng C, Zhai Y, Zhu Y et al. (2016) Production of char from sewage sludge employing hydrothermal carbonization: Char properties, combustion behavior and thermal characteristics. *Fuel* 176:110–118.
<https://doi.org/10.1016/j.fuel.2016.02.068>
109. Becker R, Dorgerloh U, Paulke E et al. (2014) Hydrothermal Carbonization of Biomass: Major Organic Components of the Aqueous Phase. *Chem Eng Technol* 37:511–518.
<https://doi.org/10.1002/ceat.201300401>
110. Stemann J, Putschew A, Ziegler F (2013) Hydrothermal carbonization: process water characterization and effects of water recirculation. *Bioresour Technol* 143:139–146.
<https://doi.org/10.1016/j.biortech.2013.05.098>
111. Austermann-Haun U, Meier JF, Wichern M et al. (2013) Management, Aufbereitung und Ressourceneffizienz. Management, Aufbereitung und Ressourceneffizienz, Fulda, Germany
112. Agrokraft & KIT (2010) Hydrothermale Carbonisierung (HTC) – Produktanalyse, technische Evaluierung, landwirtschaftliche Einsatzfelder: Schlussbericht
113. DBFZ Deutsches Biomasseforschungszentrum gemeinnützige GmbH (ed) (2014) Biobasierte hydrothermale Prozesse – Technologien zur stofflichen und energetischen Nutzung
114. Weiner B, Wedwitschka H, Poerschmann J et al. (2016) Utilization of Organosolv Waste Waters as Liquid Phase for Hydrothermal Carbonization of Chaff. *ACS Sustainable Chem Eng* 4:5737–5742.
<https://doi.org/10.1021/acssuschemeng.6b01665>

115. Yue F, Pedersen CM, Yan X et al. (2018) NMR studies of stock process water and reaction pathways in hydrothermal carbonization of furfural residue. *Green Energy & Environment* 3:163–171. <https://doi.org/10.1016/j.gee.2017.08.006>
116. Kambo HS, Minaret J, Dutta A (2018) Process Water from the Hydrothermal Carbonization of Biomass: A Waste or a Valuable Product? *Waste Biomass Valor* 9:1181–1189. <https://doi.org/10.1007/s12649-017-9914-0>
117. Hoekman SK, Broch A, Robbins C et al. (2013) Hydrothermal carbonization (HTC) of selected woody and herbaceous biomass feedstocks. *Biomass Conv Bioref* 3:113–126. <https://doi.org/10.1007/s13399-012-0066-y>
118. Basso D, Weiss-Hortala E, Patuzzi F et al. (2018) In Deep Analysis on the Behavior of Grape Marc Constituents during Hydrothermal Carbonization. *Energies* 11:1379. <https://doi.org/10.3390/en11061379>
119. Bryers RW (1996) Fireside slagging, fouling, and high-temperature corrosion of heat-transfer surface due to impurities in steam-raising fuels. *Progress in Energy and Combustion Science* 22:29–120. [https://doi.org/10.1016/0360-1285\(95\)00012-7](https://doi.org/10.1016/0360-1285(95)00012-7)
120. Ekpo U, Ross AB, Camargo-Valero MA et al. (2016) A comparison of product yields and inorganic content in process streams following thermal hydrolysis and hydrothermal processing of microalgae, manure and digestate. *Bioresour Technol* 200:951–960. <https://doi.org/10.1016/j.biortech.2015.11.018>
121. Turn SQ, Kinoshita CM, Ishimura DM (1997) Removal of inorganic constituents of biomass feedstocks by mechanical dewatering and leaching. *Biomass and Bioenergy* 12:241–252. [https://doi.org/10.1016/S0961-9534\(97\)00005-6](https://doi.org/10.1016/S0961-9534(97)00005-6)
122. Abelha P, Mourão Vilela C, Nanou P et al. (2019) Combustion improvements of upgraded biomass by washing and torrefaction. *Fuel* 253:1018–1033. <https://doi.org/10.1016/j.fuel.2019.05.050>
123. Deng L, Zhang T, Che D (2013) Effect of water washing on fuel properties, pyrolysis and combustion characteristics, and ash fusibility of biomass. *Fuel Processing Technology* 106:712–720. <https://doi.org/10.1016/j.fuproc.2012.10.006>

124. Ma Q, Han L, Huang G (2017) Evaluation of different water-washing treatments effects on wheat straw combustion properties. *Bioresour Technol* 245:1075–1083.
<https://doi.org/10.1016/j.biortech.2017.09.052>
125. Singhal A, Konttinen J, Joronen T (2021) Effect of different washing parameters on the fuel properties and elemental composition of wheat straw in water-washing pre-treatment. Part 1: Effect of washing duration and biomass size. *Fuel* 16:120206.
<https://doi.org/10.1016/j.fuel.2021.120206>
126. Singhal A, Konttinen J, Joronen T (2021) Effect of different washing parameters on the fuel properties and elemental composition of wheat straw in water-washing pre-treatment. Part 2: Effect of washing temperature and solid-to-liquid ratio. *Fuel* 94:120209.
<https://doi.org/10.1016/j.fuel.2021.120209>
127. Wu S, Chen J, Peng D et al. (2019) Effects of Water Leaching on the Ash Sintering Problems of Wheat Straw. *Energies* 12:387.
<https://doi.org/10.3390/en12030387>
128. Bandura AV, Lvov SN (2006) The Ionization Constant of Water over Wide Ranges of Temperature and Density. *Journal of Physical and Chemical Reference Data* 35:15–30.
<https://doi.org/10.1063/1.1928231>
129. Benavente V, Calabuig E, Fullana A (2015) Upgrading of moist agro-industrial wastes by hydrothermal carbonization. *Journal of Analytical and Applied Pyrolysis* 113:89–98.
<https://doi.org/10.1016/j.jaap.2014.11.004>
130. Smith AM, Ekpo U, Ross AB (2020) The Influence of pH on the Combustion Properties of Bio-Coal Following Hydrothermal Treatment of Swine Manure. *Energies* 13:331.
<https://doi.org/10.3390/en13020331>
131. Mäkelä M, Yoshikawa K (2016) Ash behavior during hydrothermal treatment for solid fuel applications. Part 2: Effects of treatment conditions on industrial waste biomass. *Energy Conversion and Management* 121:409–414.
<https://doi.org/10.1016/j.enconman.2016.05.015>

132. Smith AM, Ross AB (2016) Production of bio-coal, bio-methane and fertilizer from seaweed via hydrothermal carbonisation. *Algal Research* 16:1–11. <https://doi.org/10.1016/j.algal.2016.02.026>
133. Baumbach G, Hartmann H, Höfer I et al. (2016) Grundlagen der thermo-chemischen Umwandlung biogener Festbrennstoffe. In: Kaltschmitt M, Hartmann H, Hofbauer H (eds) *Energie aus Biomasse: Grundlagen, Techniken und Verfahren, 3., aktualisierte und erweiterte Auflage, vol 13*. Springer Vieweg, Berlin, Heidelberg, pp 579–814
134. Nielsen HP, Frandsen FJ, Dam-Johansen K (1999) Lab-Scale Investigations of High-Temperature Corrosion Phenomena in Straw-Fired Boilers. *Energy Fuels* 13:1114–1121. <https://doi.org/10.1021/ef990001g>
135. Aho M, Vainikka P, Taipale R et al. (2008) Effective new chemicals to prevent corrosion due to chlorine in power plant superheaters. *Fuel* 87:647–654. <https://doi.org/10.1016/j.fuel.2007.05.033>
136. Salmenoja K (2000) Field and laboratory studies on chlorine-induced superheater corrosion in boilers fired with biofuels. Dissertation, Abo Akademi University
137. Johansson LS, Tullin C, Leckner B et al. (2003) Particle emissions from biomass combustion in small combustors. *Biomass and Bioenergy* 25:435–446. [https://doi.org/10.1016/S0961-9534\(03\)00036-9](https://doi.org/10.1016/S0961-9534(03)00036-9)
138. Williams A, Jones JM, Ma L et al. (2012) Pollutants from the combustion of solid biomass fuels. *Progress in Energy and Combustion Science* 38:113–137. <https://doi.org/10.1016/j.pecs.2011.10.001>
139. Jöller M, Brunner T, Obernberger I (2007) Modeling of aerosol formation during biomass combustion for various furnace and boiler types. *Fuel Processing Technology* 88:1136–1147. <https://doi.org/10.1016/j.fuproc.2007.06.013>
140. Glarborg P (2003) Fuel nitrogen conversion in solid fuel fired systems. *Progress in Energy and Combustion Science* 29:89–113. [https://doi.org/10.1016/S0360-1285\(02\)00031-X](https://doi.org/10.1016/S0360-1285(02)00031-X)

141. Houshfar E, Løvås T, Skreiberg Ø (2012) Experimental Investigation on NO_x Reduction by Primary Measures in Biomass Combustion: Straw, Peat, Sewage Sludge, Forest Residues and Wood Pellets. *Energies* 5:270–290. <https://doi.org/10.3390/en5020270>
142. Houshfar E, Skreiberg Ø, Todorović D et al. (2012) NO_x emission reduction by staged combustion in grate combustion of biomass fuels and fuel mixtures. *Fuel* 98:29–40. <https://doi.org/10.1016/j.fuel.2012.03.044>
143. Sommersacher P, Brunner T, Obernberger I (2011) Fuel Indexes: A Novel Method for the Evaluation of Relevant Combustion Properties of New Biomass Fuels. *Energy Fuels* 26:380–390. <https://doi.org/10.1021/ef201282y>
144. Näzelius I-L, Boström D, Rebbing A et al. (2017) Fuel Indices for Estimation of Slagging of Phosphorus-Poor Biomass in Fixed Bed Combustion. *Energy Fuels* 31:904–915. <https://doi.org/10.1021/acs.energyfuels.6b02563>
145. Blomberg TE Free Alkali-Index for Optimizing the Fuel Mixture in Biomass Co-Firing
146. Zeng T, Weller N, Pollex A et al. (2016) Blended biomass pellets as fuel for small scale combustion appliances: Influence on gaseous and total particulate matter emissions and applicability of fuel indices. *Fuel* 184:689–700. <https://doi.org/10.1016/j.fuel.2016.07.047>
147. Feldmeier S, Wopienka E, Schwarz M et al. (2019) Applicability of Fuel Indexes for Small-Scale Biomass Combustion Technologies, Part 1: Slag Formation. *Energy Fuels* 33:10969–10977. <https://doi.org/10.1021/acs.energyfuels.9b02409>
148. Feldmeier S, Wopienka E, Schwarz M et al. (2019) Applicability of Fuel Indexes for Small-Scale Biomass Combustion Technologies, Part 2: TSP and NO_x Emissions. *Energy Fuels* 33:11724–11730. <https://doi.org/10.1021/acs.energyfuels.9b02589>
149. Obernberger I (2014) Strategy for the Application of Novel Characterization Methods for Biomass Fuels: Case Study of Straw. *Energy Fuels* 28:1041–1052. <https://doi.org/10.1021/ef402249x>

150. Tortosa Masiá AA, Buhre BJP, Gupta RP et al. (2007) Characterising ash of biomass and waste. *Fuel Processing Technology* 88:1071–1081. <https://doi.org/10.1016/j.fuproc.2007.06.011>
151. Nielsen HP, Frandsen FJ, Dam-Johansen K et al. (2000) The implications of chlorine-associated corrosion on the operation of biomass-fired boilers. *Progress in Energy and Combustion Science* 26:283–298. [https://doi.org/10.1016/S0360-1285\(00\)00003-4](https://doi.org/10.1016/S0360-1285(00)00003-4)
152. Zevenhoven M, Yrjas P, Skrifvars B-J et al. (2012) Characterization of Ash-Forming Matter in Various Solid Fuels by Selective Leaching and Its Implications for Fluidized-Bed Combustion. *Energy Fuels* 26:6366–6386. <https://doi.org/10.1021/ef300621j>
153. Pronobis M (2005) Evaluation of the influence of biomass co-combustion on boiler furnace slagging by means of fusibility correlations. *Biomass and Bioenergy* 28:375–383. <https://doi.org/10.1016/j.biombioe.2004.11.003>
154. Spliethoff H (2010) *Power Generation from Solid Fuels*, 1. Aufl. Power Systems. Springer-Verlag, s.l.
155. Teixeira P, Lopes H, Gulyurtlu I et al. (2012) Evaluation of slagging and fouling tendency during biomass co-firing with coal in a fluidized bed. *Biomass and Bioenergy* 39:192–203. <https://doi.org/10.1016/j.biombioe.2012.01.010>
156. Bevan E, Fu J, Zheng Y (2020) Challenges and opportunities of hydrothermal carbonisation in the UK; case study in Chirnside. *RSC Adv* 10:31586–31610. <https://doi.org/10.1039/D0RA04607H>
157. Marc Buttman (2016) Durchbruch für preisgekröntes Ingenieurs-Start Up: Erste kommerzielle TerraNova® Ultra Anlage in China eröffnet
158. Erik Odén (2020) Significant interest in C-Green's environmental technology in oversubscribed new share issue of SEK 55 million
159. Vogel F (2017) Hydrothermal Conversion of Biomass. In: Meyers RA (ed) *Encyclopedia of Sustainability Science and Technology*, vol 17. Springer New York, New York, NY, pp 1–46
160. Remy C, Warneke J, Lesjean B, Chauzy J, Sardet C (2013) HTC-Check: Energiebilanz und Carbon footprint von Referenztechnologien und HTC-Prozess bei der Klärschlamm Entsorgung. HTC-Workshop

- „Hydrothermale Carbonisierung eine energieeffiziente Behandlung von Klärschlämmen und Bioabfällen?, Berlin, Germany
161. Söhnke Neumann (2014) Planung und Vision Klärschlammverwertung ab 2015. LAV Fachtagung, Markanstädt, Germany
 162. Michael Child (2014) Industrial-scale Hydrothermal Carbonisation of Waste Sludge Materials for Fuel Production, Lappeenranta University of Technology
 163. Buttman M (2011) Klimafreundliche Kohle durch Hydrothermale Karbonisierung von Biomasse. Chemie Ingenieur Technik 83:1890–1896. <https://doi.org/10.1002/cite.201100126>
 164. Hernández Latorre (2011) Solid HTC Biofuel from Hydrothermal Carbonisation. 6. Int Bioenergy Congress, Valladolid, Spain
 165. Antaco (UK) Limited What is Hydrothermal Carbonisation (HTC)? <https://www.antaco.co.uk/technology/>. Accessed 07 Dec 2020
 166. Ohman F, Lundquist F, Oden E SYSTEM AND METHOD FOR HEAT TREATMENT OF SLUDGE(WO 2017/003358 A1)
 167. Klaus Serfass (2011) Vorstellung REVATEC - Verfahren: Präsentation im Rahmen der „GrünenWoche“ 2011. Grüne Woche, Berlin, Germany
 168. Erlach B, Wirth B, Tsatsaronis G (2011) Co-Production of Electricity, Heat and Biocoal Pellets from Biomass: A Techno-Economic Comparison with Wood Pelletizing. In: Proceedings of the World Renewable Energy Congress – Sweden, 8–13 May, 2011, Linköping, Sweden. Linköping University Electronic Press, pp 508–515
 169. Stobernack N, Mayer F, Malek C et al. (2020) Evaluation of the energetic and environmental potential of the hydrothermal carbonization of biowaste: Modeling of the entire process chain. *Bioresour Technol* 318:124038. <https://doi.org/10.1016/j.biortech.2020.124038>
 170. Akbari M, Oyedun AO, Kumar A (2019) Comparative energy and techno-economic analyses of two different configurations for hydrothermal carbonization of yard waste. *Bioresource Technology Reports* 7:100210. <https://doi.org/10.1016/j.biteb.2019.100210>
 171. O. Borja (2020) Ingelia Process Scheme. E-Mail Korrespondenz

172. Deutsches Institut für Normung e. V. (1997) Genauigkeit (Richtigkeit und Präzision) von Meßverfahren und Meßergebnissen: Teil 1: Allgemeine Grundlagen und Begriffe(ISO 5725-1)
173. Briesemeister L, Wittmann T, Gaderer M et al. Study of a decentralized entrained-flow gasification plant in combination with biomass from hydrothermal carbonization for chp. In: EUBCE 2014
174. Andreas Möbius (2020) Techno-ökonomische Betrachtung der Hydrothermalen Carbonisierung von Reststoffen. Semesterarbeit, Technical University of Munich
175. Ischia G, Fiori L (2020) Hydrothermal Carbonization of Organic Waste and Biomass: A Review on Process, Reactor, and Plant Modeling. *Waste Biomass Valor* 151:630. <https://doi.org/10.1007/s12649-020-01255-3>
176. Yan W, Hastings JT, Acharjee TC et al. (2010) Mass and Energy Balances of Wet Torrefaction of Lignocellulosic Biomass †. *Energy Fuels* 24:4738–4742. <https://doi.org/10.1021/ef901273n>
177. Towler GP, Sinnott RK (2013) *Chemical engineering design: Principles, practice and economics of plant and process design*, 2nd ed. Butterworth-Heinemann, Amsterdam, London
178. Erlach B (2014) Biomass upgrading technologies for carbon-neutral and carbon-negative electricity generation. Technische Universität Berlin
179. Wiegel M (2011) *Hochwertige Verwertung von Mähgut und Laub im Land Berling*, Berlin
180. Schernthaler GmbH (2020) Schernthaler GmbH: Garten- & Landschaftsbau, Kompostwerk, Mietpark, Kieswerk. <https://www.schernthaler.de/kompostwerk.html>. Accessed 01 Jun 2020
181. Abelha P, Kiel J (2020) Techno-economic assessment of biomass upgrading by washing and torrefaction. *Biomass and Bioenergy* 142:105751. <https://doi.org/10.1016/j.biombioe.2020.105751>
182. Malaysian Palm Oil Board (2020). Accessed 11 Mar 2021
183. Statistics Malaysia (2020) *Statistics yearbook Malaysia 2019*
184. Tatiana WeK, Valentin K, Gustave D et al. (2016) Quantitative assessment of palm oil wastes generated by mills in Southern Benin.

- Afr J Agric Res 11:1787–1796.
<https://doi.org/10.5897/AJAR2013.8124>
185. MIDA - Malaysian Investment Development Authority (2020) Utilities. <https://www.mida.gov.my/home/utilities/posts/>. Accessed 01 Jun 2020
186. Visser L, Hoefnagels R, Junginger M (2020) Wood pellet supply chain costs – A review and cost optimization analysis. *Renewable and Sustainable Energy Reviews* 118:109506.
<https://doi.org/10.1016/j.rser.2019.109506>
187. Hamzah N, Tokimatsu K, Yoshikawa K (2019) Solid Fuel from Oil Palm Biomass Residues and Municipal Solid Waste by Hydrothermal Treatment for Electrical Power Generation in Malaysia: A Review. *Solid Fuel from Oil Palm Biomass Residues and Municipal Solid Waste by Hydrothermal Treatment for Electrical Power Generation in Malaysia: A Review; Sustainability* 11:1060.
<https://doi.org/10.3390/su11041060>
188. Youssef Walha (2020) Availability and Options for the Energetic Utilization of Biomass Residues. Bachelor Thesis, Technical University of Munich
189. Stadtwerke München GmbH (2019) Wasser-Preise.
<https://www.swm.de/geschaefskunden/m-wasser/preise.html>. Accessed 01 Jun 2020
190. GlobalPetrolPrices (2019) Malaysia natural gas prices: September 2019.
https://www.globalpetrolprices.com/Malaysia/natural_gas_prices/. Accessed 01 Jun 2020
191. Arbeitsgruppe Energie-Monitoring (2021) Monitoring Bericht 2020, Bonn
192. Dipl.-Volkswirt Thomas Brandt (2018) Factsheet Malaysia: Allgemeine Energiemarktinformationen. Factsheet Malaysia
193. Tim Hermann VW (2017) Bioabfallkomposte und -gärreste in der Landwirtschaft.
https://www.umweltbundesamt.de/sites/default/files/medien/377/publikationen/170131_uba_pos_bioabfall_bf.pdf. Accessed 03 Oct 2021

194. Frank Scholwin, Johan Grope, Angela Clinkscales (2018) Aktuelle Entwicklung und Perspektiven der Biogasproduktion aus Bioabfall und Gülle.
https://www.umweltbundesamt.de/sites/default/files/medien/1410/publikationen/2019-04-15_texte_41-2019_biogasproduktion.pdf. Accessed 03 Oct 2021
195. Kent NL, Evers AD (1994) Technology of cereals: An introduction for students of food science and agriculture, Fourth edition. Woodhead Publishing Series in Food Science, Technology and Nutrition. Elsevier Science Ltd, Oxford, England
196. Silva JcD, Oliveira Rcd, Neto AdS et al. (2015) Extraction, Addition and Characterization of Hemicelluloses from Corn Cobs to Development of Paper Properties. *Procedia Materials Science* 8:793–801. <https://doi.org/10.1016/j.mspro.2015.04.137>
197. FAO Stat (2019) Crops and livestock products: Crops, Production Quantity, Maize. www.fao.org/faostat/en/
198. Gemeinschaftsveröffentlichung der DWA (Deutsche Vereinigung für Wasserwirtschaft, Abwasser und Abfall e. V. und des Statistischen Bundesamtes Abwasser und Klärschlamm in Deutschland - statistische Betrachtungen. *Korrespondenz Abwasser, Abfall* 2015:46–53
199. Umweltbundesamt (2018) Klärschlamm-entsorgung in der Bundesrepublik Deutschland
200. Sulaiman F, Abdullah N (2011) Optimum conditions for maximising pyrolysis liquids of oil palm empty fruit bunches. *Energy* 36:2352–2359. <https://doi.org/10.1016/j.energy.2010.12.067>
201. Food and Agriculture Organization of the United Nations (2016) Crops and livestock products: Crops, Area harvested, Oil palm fruit. www.fao.org/faostat/en/
202. (2009) *Biotechnology for Agro-Industrial Residues Utilisation: Utilisation of Agro-Residues*, 1st edn. Springer eBook Collection Biomedical and Life Sciences. Springer Netherlands, Dordrecht
203. Springer TL (2012) Biomass yield from an urban landscape. *Biomass and Bioenergy* 37:82–87.
<https://doi.org/10.1016/j.biombioe.2011.12.029>

204. ICU Ingenieurconsulting Umwelt und Bau (2011) Hochwertige Verwertung von Mähgut und Laub im Land Berlin, Berlin
205. Braber K (1995) Anaerobic digestion of municipal solid waste: A modern waste disposal option on the verge of breakthrough. *Biomass and Bioenergy* 9:365–376. [https://doi.org/10.1016/0961-9534\(95\)00103-4](https://doi.org/10.1016/0961-9534(95)00103-4)
206. Wartell BA, Krumins V, Alt J et al. (2012) Methane production from horse manure and stall waste with softwood bedding. *Bioresour Technol* 112:42–50. <https://doi.org/10.1016/j.biortech.2012.02.012>
207. Murphy F, Devlin G, McDonnell K (2013) Miscanthus production and processing in Ireland: An analysis of energy requirements and environmental impacts. *Renewable and Sustainable Energy Reviews* 23:412–420. <https://doi.org/10.1016/j.rser.2013.01.058>
208. Barbanera M, Lascaro E, Stanzione V et al. (2016) Characterization of pellets from mixing olive pomace and olive tree pruning. *Renewable Energy* 88:185–191. <https://doi.org/10.1016/j.renene.2015.11.037>
209. Food and Agriculture Organization of the United Nations (2019) Crops and livestock products: Crops, Production Quantity, Olives. www.fao.org/faostat/en/
210. Hamdi M (1996) Anaerobic digestion of olive mill wastewaters. *Process Biochemistry* 31:105–110. [https://doi.org/10.1016/0032-9592\(95\)00035-6](https://doi.org/10.1016/0032-9592(95)00035-6)
211. Food and Agriculture Organization of the United Nations (2019) Crops and livestock products: Crops, Production Quantity, Oranges. www.fao.org/faostat/en/
212. Merve Deniz Köse and Oguz Bayraktar (2018) Valorization of Citrus Peel Waste. *Natural Volatiles & Essential Oils*:10–18
213. Mariana O-S, Alzate C, Ariel C (2021) Comparative environmental life cycle assessment of orange peel waste in present productive chains. *Journal of Cleaner Production* 322:128814. <https://doi.org/10.1016/j.jclepro.2021.128814>
214. Kapoor M, Panwar D, Kaira GS (2016) Bioprocesses for Enzyme Production Using Agro-Industrial Wastes. In: Gurpreet Dhillon Surinder Kaur (ed) *Agro-Industrial Wastes as Feedstock for Enzyme Production*, vol 37. Elsevier, pp 61–93

215. Glibert P, Burford M (2017) Globally Changing Nutrient Loads and Harmful Algal Blooms: Recent Advances, New Paradigms, and Continuing Challenges. *Oceanog* 30:58–69. <https://doi.org/10.5670/oceanog.2017.110>
216. McNutt J, He Q (2019) Spent coffee grounds: A review on current utilization. *Journal of Industrial and Engineering Chemistry* 71:78–88. <https://doi.org/10.1016/j.jiec.2018.11.054>
217. Leow Y, Yew PYM, Chee PL et al. (2021) Recycling of spent coffee grounds for useful extracts and green composites. *RSC Adv* 11:2682–2692. <https://doi.org/10.1039/D0RA09379C>
218. Wolfgang Preißinger, Anton Obermaier, Katrin Söldner, Olaf Steinhöfel (2008) *Biertreber: Futterwert, Konservierung und erfolgreicher Einsatz beim Wiederkäuer*
219. National Institute of Industrial Research (India) (2006?) *Wheat, rice, corn, oat, barley and sorghum processing handbook (cereal food technology)*. Asia Pacific Business Press, Delhi
220. Nurmatov N, Leon Gomez D, Hensgen F et al. (2016) High-Quality Solid Fuel Production from Leaf Litter of Urban Street Trees. *Sustainability* 8:1249. <https://doi.org/10.3390/su8121249>
221. Lee P, Sims E, Bertham O et al. (2017) *Towards a circular economy - waste management in the EU: Study*. European Parliament, Brussels
222. Panoutsou C, Alexopoulou E (2020) Costs and Profitability of Crops for Bioeconomy in the EU. *Energies* 13:1222. <https://doi.org/10.3390/en13051222>
223. Caputo AC, Scacchia F, Pelagagge PM (2003) Disposal of by-products in olive oil industry: waste-to-energy solutions. *Applied Thermal Engineering* 23:197–214. [https://doi.org/10.1016/S1359-4311\(02\)00173-4](https://doi.org/10.1016/S1359-4311(02)00173-4)
224. Ortiz-Sanchez M, Solarte-Toro JC, Orrego-Alzate CE et al. (2020) Integral use of orange peel waste through the biorefinery concept: an experimental, technical, energy, and economic assessment. *Biomass Conv Bioref* 94:173. <https://doi.org/10.1007/s13399-020-00627-y>
225. Barbero S, Toso D (2010) Systemic design of a productive chain: Reusing coffee waste as an input to agricultural production. *Environ Qual Manage* 19:67–77. <https://doi.org/10.1002/tqem.20254>

226. European Environment Agency (2013) Typical charge (gate fee and landfill tax) for legal landfilling of non-hazardous municipal waste in EU Member States and regions. <https://www.eea.europa.eu/data-and-maps/figures/typical-charge-gate-fee-and>. Accessed 02 Apr 2021
227. Esa Kurkela (2019) Flexible combined production of power, heat and transport fuels from renewable energy sources: Report on the sustainably available feedstock basis. https://www.google.com/url?sa=t&rct=j&q=&esrc=s&source=web&cad=rja&uact=8&ved=2ahUKEwiNi8Dxy9_vAhXb_rsIHXYoAY0QFjADegQIBhAD&url=http%3A%2F%2Fwww.flexchx.eu%2Fpdf%2FD2_3_Report_on_the_sustainably_available_feedstock_basis_Feb2019_110419.pdf&usg=AOvVaw2B0M9TdXrYEDFYfiwOSo0T. Accessed 02 Apr 2021
228. Kovalcik A, Obruca S, Marova I (2018) Valorization of spent coffee grounds: A review. *Food and Bioproducts Processing* 110:104–119. <https://doi.org/10.1016/j.fbp.2018.05.002>
229. Simon Kühner (2013) Biomass based energy intermediates boosting biofuel production: D1.1 Feedstock costs. https://www.google.com/url?sa=t&rct=j&q=&esrc=s&source=web&cad=rja&uact=8&ved=2ahUKEwiNi8Dxy9_vAhXb_rsIHXYoAY0QFjAAegQIAxAD&url=https%3A%2F%2Fwww.bioboost.eu%2Fuploads%2Ffiles%2Fbioboost_d1.1-syncom_feedstock_cost-vers_1.0-final.pdf&usg=AOvVaw0o-GVJJUMukm-yXqbT7wZe. Accessed 02 Apr 2021
230. Constantinos S. Psomopoulos and Nickolas J. Themelis (2014) *A Guidebook for Sustainable Waste Management in Latin America*. https://www.google.com/url?sa=t&rct=j&q=&esrc=s&source=web&cad=rja&uact=8&ved=2ahUKEwi0tTPk9_vAhXzhP0HHaVIC6UQFjAFegQIBRAD&url=https%3A%2F%2Fwww.vivis.de%2Fwp-content%2Fuploads%2FWM4%2F2014_wm_121_136_psomopoulos.pdf&usg=AOvVaw1_AcNRKggJAC71hH4OHwBu. Accessed 02 Apr 2021
231. Warnatz J, Maas U (1993) *Technische Verbrennung: Physikalisch-Chemische Grundlagen, Modellbildung, Schadstoffentstehung*. Springer-Lehrbuch. Springer, Berlin, Heidelberg

232. Dzurenda L, Banski A (2015) Dependence of the boiler flue gas losses on humidity of wood biomass. *Archives of Thermodynamics* 36:77–86. <https://doi.org/10.1515/aoter-2015-0034>
233. Coronella CJ, Lynam JG, Reza MT et al. (2014) Hydrothermal Carbonization of Lignocellulosic Biomass. In: Jin F, Coronella CJ, Lynam JG et al. (eds) *Application of hydrothermal reactions to biomass conversion // Hydrothermal Carbonization of Lignocellulosic Biomass*, vol 15. Springer, Heidelberg, pp 275–311
234. Lynam JG, Reza MT, Yan W et al. (2015) Hydrothermal carbonization of various lignocellulosic biomass. *Biomass Conv Bioref* 5:173–181. <https://doi.org/10.1007/s13399-014-0137-3>
235. (2012) *Marschner's Mineral Nutrition of Higher Plants*. Elsevier
236. Currie HA, Perry CC (2007) Silica in plants: biological, biochemical and chemical studies. *Ann Bot* 100:1383–1389. <https://doi.org/10.1093/aob/mcm247>
237. Salisbury FB, Ross CW (1985) *Plant physiology*, 3. ed. Wadsworth, Belmont, Cal.
238. Röhrdanz M, Rebling T, Ohlert J et al. (2016) Hydrothermal carbonization of biomass from landscape management - Influence of process parameters on soil properties of hydrochars. *J Environ Manage* 173:72–78. <https://doi.org/10.1016/j.jenvman.2016.03.006>
239. Gascó G, Paz-Ferreiro J, Álvarez ML et al. (2018) Biochars and hydrochars prepared by pyrolysis and hydrothermal carbonisation of pig manure. *Waste Manag* 79:395–403. <https://doi.org/10.1016/j.wasman.2018.08.015>
240. Mosteiro-Romero M, Vogel F, Wokaun A (2014) Liquefaction of wood in hot compressed water. *Chemical Engineering Science* 109:111–122. <https://doi.org/10.1016/j.ces.2013.12.038>
241. Chen J, Chen Z, Wang C et al. (2012) Calcium-assisted hydrothermal carbonization of an alginate for the production of carbon microspheres with unique surface nanopores. *Materials Letters* 67:365–368. <https://doi.org/10.1016/j.matlet.2011.10.017>
242. Voisin T, Erriguible A, Ballenghien D et al. (2017) Solubility of inorganic salts in sub- and supercritical hydrothermal environment:

- Application to SCWO processes. *The Journal of Supercritical Fluids* 120:18–31. <https://doi.org/10.1016/j.supflu.2016.09.020>
243. Bach Q-V, Tran K-Q, Skreiberg Ø (2015) Accelerating wet torrefaction rate and ash removal by carbon dioxide addition. *Fuel Processing Technology* 140:297–303. <https://doi.org/10.1016/j.fuproc.2015.09.013>
244. Hunter SE, Savage PE (2003) Acid-Catalyzed Reactions in Carbon Dioxide-Enriched High-Temperature Liquid Water. *Ind Eng Chem Res* 42:290–294. <https://doi.org/10.1021/ie020565z>
245. Peng C, Crawshaw JP, Maitland GC et al. (2013) The pH of CO₂-saturated water at temperatures between 308K and 423K at pressures up to 15MPa. *The Journal of Supercritical Fluids* 82:129–137. <https://doi.org/10.1016/j.supflu.2013.07.001>
246. Hansen LJ, Fendt S, Spliethoff H (2020) Impact of hydrothermal carbonization on combustion properties of residual biomass. *Biomass Conv Bioref* 15:3. <https://doi.org/10.1007/s13399-020-00777-z>
247. Williams A, Jones JM, Ma L et al. (2012) Pollutants from the combustion of solid biomass fuels. *Progress in Energy and Combustion Science* 38:113–137. <https://doi.org/10.1016/j.pecs.2011.10.001>
248. Brunner T, Obernberger I, Brouwers JJH (eds) (2006) *Aerosols and coarse fly ashes in fixed-bed biomass combustion: Formation, characterisation and emissions*, Eindhoven
249. Lin Y, Ma X, Peng X et al. (2015) Effect of hydrothermal carbonization temperature on combustion behavior of hydrochar fuel from paper sludge. *Applied Thermal Engineering* 91:574–582. <https://doi.org/10.1016/j.applthermaleng.2015.08.064>
250. Lin Y, Ma X, Peng X et al. (2016) Combustion, pyrolysis and char CO₂-gasification characteristics of hydrothermal carbonization solid fuel from municipal solid wastes. *Fuel* 181:905–915. <https://doi.org/10.1016/j.fuel.2016.05.031>
251. Peng C, Zhai Y, Zhu Y et al. (2016) Production of char from sewage sludge employing hydrothermal carbonization: Char properties, combustion behavior and thermal characteristics. *Fuel* 176:110–118. <https://doi.org/10.1016/j.fuel.2016.02.068>

252. Stirling RJ, Snape CE, Meredith W (2018) The impact of hydrothermal carbonisation on the char reactivity of biomass. *Fuel Processing Technology* 177:152–158.
<https://doi.org/10.1016/j.fuproc.2018.04.023>
253. Ulbrich M, Preßl D, Fendt S et al. (2017) Impact of HTC reaction conditions on the hydrochar properties and CO₂ gasification properties of spent grains. *Fuel Processing Technology* 167:663–669.
<https://doi.org/10.1016/j.fuproc.2017.08.010>
254. (2007) *Siedlungswasserwirtschaft*. Springer Berlin Heidelberg
255. Henze M, van Loosdrecht MCM, Ekama GA et al. (2008) *Biological Wastewater Treatment: Principles, Modelling and Design*. *Water Intelligence Online* 7:9781780401867-9781780401867.
<https://doi.org/10.2166/9781780401867>
256. Tchobanoglous G (2003) *Wastewater engineering: Treatment and reuse*, 4. ed. McGraw-Hill higher education. McGraw-Hill, Boston, Mass.
257. Jingura RM, Kamusoko R (2017) Methods for determination of biomethane potential of feedstocks: a review. *Biofuel Res J* 4:573–586. <https://doi.org/10.18331/BRJ2017.4.2.3>
258. Kwietniewska E, Tys J (2014) Process characteristics, inhibition factors and methane yields of anaerobic digestion process, with particular focus on microalgal biomass fermentation. *Renewable and Sustainable Energy Reviews* 34:491–500.
<https://doi.org/10.1016/j.rser.2014.03.041>
259. Gerardi MH (2003) *The Microbiology of Anaerobic Digesters*. *Wastewater microbiology series*. John Wiley & Sons, Hoboken, New Jersey
260. Khalid A, Arshad M, Anjum M et al. (2011) The anaerobic digestion of solid organic waste. *Waste Manag* 31:1737–1744.
<https://doi.org/10.1016/j.wasman.2011.03.021>
261. (1991) *Verordnung über Anforderungen an das Einleiten von Abwasser in Gewässer: AbwV*
262. Wirth B, Reza T, Mumme J (2015) Influence of digestion temperature and organic loading rate on the continuous anaerobic treatment of process liquor from hydrothermal carbonization of sewage sludge.

- Bioresour Technol 198:215–222.
<https://doi.org/10.1016/j.biortech.2015.09.022>
263. Angelidaki I, Alves M, Bolzonella D et al. (2009) Defining the biomethane potential (BMP) of solid organic wastes and energy crops: a proposed protocol for batch assays. *Water Science and Technology* 59:927–934. <https://doi.org/10.2166/wst.2009.040>
264. Kühni M, Wanner R, Baier U et al. (2015) Treatment of process water of hydrothermal carbonised sewage sludge before discharging in a waste water treatment plant 156:1004–1011
265. Arne Stark RM Method and apparatus for the treatment of process water from a hydrothermal organic material conversion process(EP2746231A1)
266. Unknown Verfahren zur Behandlung von Prozesswasser aus einem hydrothermalen Karbonisierungsprozess(DE102012002590A1)
267. Riedel G, Koehler R, Poerschmann J et al. (2015) Combination of hydrothermal carbonization and wet oxidation of various biomasses. *Chemical Engineering Journal* 279:715–724.
<https://doi.org/10.1016/j.cej.2015.05.086>
268. Weiner B, Breulmann M, Wedwitschka H et al. (2018) Wet Oxidation of Process Waters from the Hydrothermal Carbonization of Sewage Sludge. *Chemie Ingenieur Technik* 90:872–880.
<https://doi.org/10.1002/cite.201700050>
269. Li H, Chen Q, Zhang X et al. (2012) Evaluation of a biomass drying process using waste heat from process industries: A case study. *Applied Thermal Engineering* 35:71–80.
<https://doi.org/10.1016/j.applthermaleng.2011.10.009>
270. Marin-Batista JD, Villamil JA, Qaramaleki SV et al. (2020) Energy valorization of cow manure by hydrothermal carbonization and anaerobic digestion. *Renewable Energy* 160:623–632.
<https://doi.org/10.1016/j.renene.2020.07.003>
271. Aragón-Briceño CI, Grasham O, Ross AB et al. (2020) Hydrothermal carbonization of sewage digestate at wastewater treatment works: Influence of solid loading on characteristics of hydrochar, process water and plant energetics. *Renewable Energy* 157:959–973.
<https://doi.org/10.1016/j.renene.2020.05.021>

272. Uslu A, Faaij APC, Bergman PCA (2008) Pre-treatment technologies, and their effect on international bioenergy supply chain logistics. Techno-economic evaluation of torrefaction, fast pyrolysis and pelletisation. *Energy* 33:1206–1223.
<https://doi.org/10.1016/j.energy.2008.03.007>
273. Manouchehrinejad M, Mani S (2019) Process simulation of an integrated biomass torrefaction and pelletization (iBTP) plant to produce solid biofuels. *Energy Conversion and Management: X* 1:100008. <https://doi.org/10.1016/j.ecmx.2019.100008>
274. McKechnie J, Saville B, MacLean HL (2016) Steam-treated wood pellets: Environmental and financial implications relative to fossil fuels and conventional pellets for electricity generation. *Applied Energy* 180:637–649.
<https://doi.org/10.1016/j.apenergy.2016.08.024>
275. Margaret Rainey (2019) Q&A OxyPower HTC plant project: Stora Enso, C-Green, and ÖMV have built the first full-scale Hydrothermal Carbonization (HTC) plant for sludge conversion into biocoal at the Heinola fluting mill.
276. Ingelia (2015) Ingelia substitutes its subsidiary in Italy.
<https://ingelia.com/index.php/2015/02/05/ingelia-constituye-sufilial-en-italia/?lang=en>. Accessed 12 Mar 2021
277. Future Metrics (2019) Industrial Wood Pellets Spot Price in US Dollars. Accessed 12 Mar 2021
278. Statistik der Kohlenwirtschaft e.V. (2021) Energiepreise Zeitreihe. www.kohlestatistik.de. Accessed 12 Mar 2021
279. Bundesamt für Wirtschaft und Ausfuhrkontrolle (2019) Merkblatt zu den CO₂ - Faktoren: Energieeffizienz in der Wirtschaft – Zuschuss und Kredit.
https://www.bafa.de/SharedDocs/Downloads/DE/Energie/eew_merkblatt_co2.pdf?__blob=publicationFile&v=2. Accessed 01 Jun 2020
280. Presse- und Informationsamt der Bundesregierung (2020) CO₂-Bepreisung. <https://www.bundesregierung.de/breg-de/themen/klimaschutz/co2-bepreisung-1673008>. Accessed 01 Jun 2020

281. Arranz JI, Miranda MT, Sepúlveda FJ et al. (2018) Analysis of Drying of Brewers' Spent Grain. *Proceedings* 2:1467.
<https://doi.org/10.3390/proceedings2231467>
282. Bernardo G. del Campo (2010) Corn cob dry matter loss in storage as affected by temperature and moisture content, Iowa State University
283. Agee JK, Wright CS, Williamson N et al. (2002) Foliar moisture content of Pacific Northwest vegetation and its relation to wildland fire behavior. *Forest Ecology and Management* 167:57–66.
[https://doi.org/10.1016/S0378-1127\(01\)00690-9](https://doi.org/10.1016/S0378-1127(01)00690-9)
284. Hosseinizand H, Sokhansanj S, Lim CJ (2018) Studying the drying mechanism of microalgae *Chlorella vulgaris* and the optimum drying temperature to preserve quality characteristics. *Drying Technology* 36:1049–1060. <https://doi.org/10.1080/07373937.2017.1369986>
285. Wang J, Cheng W, Liu W et al. (2019) Field study on attached cultivation of *Arthrospira* (*Spirulina*) with carbon dioxide as carbon source. *Bioresour Technol* 283:270–276.
<https://doi.org/10.1016/j.biortech.2019.03.099>
286. Lewandowski I, Heinz A (2003) Delayed harvest of miscanthus— influences on biomass quantity and quality and environmental impacts of energy production. *European Journal of Agronomy* 19:45–63. [https://doi.org/10.1016/S1161-0301\(02\)00018-7](https://doi.org/10.1016/S1161-0301(02)00018-7)
287. Lewandowski I, Clifton-Brown JC, Andersson B et al. (2003) Environment and Harvest Time Affects the Combustion Qualities of *Miscanthus* Genotypes. *Agron J* 95:1274–1280.
<https://doi.org/10.2134/agronj2003.1274>
288. Zema DA, Calabrò PS, Folino A et al. (2018) Valorisation of citrus processing waste: A review. *Waste Manag* 80:252–273.
<https://doi.org/10.1016/j.wasman.2018.09.024>
289. MANSARAY KG, GHALY AE (1997) Physical and Thermochemical Properties of Rice Husk. *Energy Sources* 19:989–1004.
<https://doi.org/10.1080/00908319708908904>
290. El-Said GF, El-Sikaily A (2013) Chemical composition of some seaweed from Mediterranean Sea coast, Egypt. *Environ Monit Assess* 185:6089–6099. <https://doi.org/10.1007/s10661-012-3009-y>

291. Herrmann C, FitzGerald J, O'Shea R et al. (2015) Ensiling of seaweed for a seaweed biofuel industry. *Bioresour Technol* 196:301–313. <https://doi.org/10.1016/j.biortech.2015.07.098>
292. Tuntiwiwattanapun N, Monono E, Wiesenborn D et al. (2017) In-situ transesterification process for biodiesel production using spent coffee grounds from the instant coffee industry. *Industrial Crops and Products* 102:23–31. <https://doi.org/10.1016/j.indcrop.2017.03.019>
293. Routa J, Brännström H, Laitila J (2020) Effects of storage on dry matter, energy content and amount of extractives in Norway spruce bark. *Biomass and Bioenergy* 143:105821. <https://doi.org/10.1016/j.biombioe.2020.105821>
294. Kelly P (1983) Sugar beet pulp — A review. *Animal Feed Science and Technology* 8:1–18. [https://doi.org/10.1016/0377-8401\(83\)90038-X](https://doi.org/10.1016/0377-8401(83)90038-X)
295. Ikram S, Huang L, Zhang H et al. (2017) Composition and Nutrient Value Proposition of Brewers Spent Grain. *J Food Sci* 82:2232–2242. <https://doi.org/10.1111/1750-3841.13794>
296. M. Pointner, P. Kuttner, T. Obrlik Composition of corncobs as a substrate for fermentation of biofuels. In: *Biosystems Engineering 2016, Volume 12*
297. Teater C, Yue Z, MacLellan J et al. (2011) Assessing solid digestate from anaerobic digestion as feedstock for ethanol production. *Bioresour Technol* 102:1856–1862. <https://doi.org/10.1016/j.biortech.2010.09.099>
298. Palamae S, Dechatiwongse P, Choorit W et al. (2017) Cellulose and hemicellulose recovery from oil palm empty fruit bunch (EFB) fibers and production of sugars from the fibers. *Carbohydr Polym* 155:491–497. <https://doi.org/10.1016/j.carbpol.2016.09.004>
299. Cortez J, Demard JM, Bottner P et al. (1996) Decomposition of mediterranean leaf litters: A microcosm experiment investigating relationships between decomposition rates and litter quality. *Soil Biology and Biochemistry* 28:443–452. [https://doi.org/10.1016/0038-0717\(96\)00005-3](https://doi.org/10.1016/0038-0717(96)00005-3)
300. JOHANSSON M-B (1995) The chemical composition of needle and leaf litter from Scots pine, Norway spruce and white birch in

- Scandinavian forests. *Forestry* 68:49–62.
<https://doi.org/10.1093/forestry/68.1.49>
301. R. J. Leemhuis and R. M. de Jong (1997) Biomassa: biochemische samenstelling en conversiemethoden, Petten
302. Zhang J, Loh K-C, Lee J et al. (2017) Three-stage anaerobic co-digestion of food waste and horse manure. *Sci Rep* 7:1269.
<https://doi.org/10.1038/s41598-017-01408-w>
303. Khan Z, Bhadouria P, Bisen PS (2005) Nutritional and therapeutic potential of Spirulina. *Curr Pharm Biotechnol* 6:373–379.
<https://doi.org/10.2174/138920105774370607>
304. Rajendran K, Drielak E, Sudarshan Varma V et al. (2018) Updates on the pretreatment of lignocellulosic feedstocks for bioenergy production—a review. *Biomass Conv Bioref* 8:471–483.
<https://doi.org/10.1007/s13399-017-0269-3>
305. Ouaini R, Estephan N, Chébib H et al. Chemical composition of olive cakes resulting from various mills in Lebanon. *Agrochimica* 2010:321–330
306. Rivas-Cantu RC, Jones KD, Mills PL (2013) A citrus waste-based biorefinery as a source of renewable energy: technical advances and analysis of engineering challenges. *Waste Manag Res* 31:413–420.
<https://doi.org/10.1177/0734242X13479432>
307. Rodrigues D, Freitas AC, Pereira L et al. (2015) Chemical composition of red, brown and green macroalgae from Buarcos bay in Central West Coast of Portugal. *Food Chem* 183:197–207.
<https://doi.org/10.1016/j.foodchem.2015.03.057>
308. Ballesteros LF, Teixeira JA, Mussatto SI (2014) Chemical, Functional, and Structural Properties of Spent Coffee Grounds and Coffee Silverskin. *Food Bioprocess Technol* 7:3493–3503.
<https://doi.org/10.1007/s11947-014-1349-z>
309. Burhenne L, Messmer J, Aicher T et al. (2013) The effect of the biomass components lignin, cellulose and hemicellulose on TGA and fixed bed pyrolysis. *Journal of Analytical and Applied Pyrolysis* 101:177–184. <https://doi.org/10.1016/j.jaap.2013.01.012>

310. Aarabi A, Mizani M, Honarvar M (2017) The use of sugar beet pulp lignin for the production of vanillin. *Int J Biol Macromol* 94:345–354. <https://doi.org/10.1016/j.ijbiomac.2016.10.004>
311. Bougrier C, Dognin D, Laroche C et al. (2018) Use of trace elements addition for anaerobic digestion of brewer's spent grains. *J Environ Manage* 223:101–107. <https://doi.org/10.1016/j.jenvman.2018.06.014>
312. Vítěz T, Koutný T, Šotnar M et al. (2016) On the Spent Coffee Grounds Biogas Production. *Acta Univ Agric Silv Mendelianae Brun* 64:1279–1282. <https://doi.org/10.11118/actaun201664041279>
313. Blandino M, Fabbri C, Soldano M et al. (2016) The use of cobs, a by-product of maize grain, for energy production in anaerobic digestion. *Ital J Agronomy* 11:195. <https://doi.org/10.4081/ija.2016.754>
314. Thygesen O, Sommer SG, Shin SG et al. (2014) Residual biochemical methane potential (BMP) of concentrated digestate from full-scale biogas plants. *Fuel* 132:44–46. <https://doi.org/10.1016/j.fuel.2014.04.062>
315. Dibdiakova J, Vadla K (2012) Basic density and moisture content of coniferous branches and wood in Northern Norway. *EPJ Web of Conferences* 33:2005. <https://doi.org/10.1051/epjconf/20123302005>
316. Pick D, Dieterich M, Heintschel S (2012) Biogas Production Potential from Economically Usable Green Waste. *Sustainability* 4:682–702. <https://doi.org/10.3390/su4040682>
317. Hadin S, Eriksson O (2016) Horse manure as feedstock for anaerobic digestion. *Waste Manag* 56:506–518. <https://doi.org/10.1016/j.wasman.2016.06.023>
318. El-Mashad HM (2015) Biomethane and ethanol production potential of *Spirulina platensis* algae and enzymatically saccharified switchgrass. *Biochemical Engineering Journal* 93:119–127. <https://doi.org/10.1016/j.bej.2014.09.009>
319. Kiesel A, Lewandowski I (2017) Miscanthus as biogas substrate - cutting tolerance and potential for anaerobic digestion. *GCB Bioenergy* 9:153–167. <https://doi.org/10.1111/gcbb.12330>

320. Tekin AR, Dalgıç AC (2000) Biogas production from olive pomace. *Resources, Conservation and Recycling* 30:301–313. [https://doi.org/10.1016/S0921-3449\(00\)00067-7](https://doi.org/10.1016/S0921-3449(00)00067-7)
321. M. S. Kalra, J. S. Panwar Anaerobic Digestion of Rice Crop Residues. *Agricultural Wastes* 1986:263–269
322. Song M, Pham HD, Seon J et al. (2015) Overview of anaerobic digestion process for biofuels production from marine macroalgae: A developmental perspective on brown algae. *Korean J Chem Eng* 32:567–575. <https://doi.org/10.1007/s11814-015-0039-5>
323. Makk ÁN, Rétfalvi T, Hofmann T (2017) Utilization of Oak (*Quercus petraea* (Matt.) Liebl.) Bark for Anaerobic Digested Biogas Production. *Acta Silvatica et Lignaria Hungarica* 13:125–134. <https://doi.org/10.1515/aslh-2017-0009>
324. Koppa A, Pullammanappallil P (2008) Single-stage, batch, leach-bed, thermophilic anaerobic digestion of spent sugar beet pulp. *Bioresour Technol* 99:2831–2839. <https://doi.org/10.1016/j.biortech.2007.06.051>

Appendix

A. Repeatability of HTC Experiments

Table A1: Lower heating value, mass yield, proximate and ultimate analysis on dry basis measured for 3 different repetitions of the HTC experiment treating EFB at 180, 230 and 280 °C for 4 h. The obtained standard deviation (Std. Dev) is in the expected range of an experimental investigation.

Temp. (°C)		Ash (wt.-%)	Volatiles (wt.-%)	Fixed-C (wt.-%)	N (wt.-%)	C (wt.-%)	S (wt.-%)	H (wt.-%)	O (wt.-%)	Cl (wt.-%)	HHV (MJ kg⁻¹)	Y_m (%)
180	Exp. 1	7.93	73.43	18.65	1.06	56.49	0.25	7.01	27.26	0.26	23.44	69.18
	Exp. 2	7.36	71.30	21.34	1.23	55.74	0.15	7.01	28.19	0.20	23.23	70.09
	Exp. 3	7.29	71.10	21.61	0.93	57.59	0.09	6.22	27.89	0.38	23.29	65.97
Average value		7.52	71.94	20.53	1.07	56.60	0.17	6.75	27.78	0.28	23.32	68.42
Std. Dev.		0.35	1.29	1.64	0.15	0.93	0.08	0.46	0.48	0.09	0.11	2.16
230	Exp. 1	8.29	62.43	29.28	1.54	65.55	0.25	7.02	17.35	0.19	27.78	50.99
	Exp. 2	7.71	61.48	30.81	1.72	66.59	0.37	7.00	16.61	0.17	28.65	50.70
	Average value	8.00	61.96	30.05	1.63	66.07	0.31	7.01	16.98	0.18	28.21	50.84
Std. Dev.		0.41	0.67	1.08	0.13	0.73	0.08	0.01	0.52	0.01	0.62	0.21
280	Exp. 1	9.57	55.17	35.26	1.89	71.71	0.27	7.02	9.53	0.05	30.58	38.32
	Exp. 2	9.08	52.46	38.46	1.87	70.50	0.33	7.03	11.19	0.04	30.28	40.26
	Average value	9.33	53.81	36.86	1.88	71.11	0.30	7.03	10.36	0.04	30.43	39.29
Std. Dev.		0.35	1.91	2.26	0.02	0.86	0.04	0.00	1.18	0.01	0.21	1.37

Table A2: Lower heating value, mass yield, proximate and ultimate analysis on dry basis measured for 3 different repetitions of the HTC experiment treating Brewers spent grains at 180, 230 and 280 °C for 4 h. The obtained standard deviation (Std. Dev) is in the expected range of an experimental investigation.

Temp. (°C)		Ash (wt.-%)	Volatiles (wt.-%)	Fixed-C (wt.-%)	N (wt.-%)	C (wt.-%)	S (wt.-%)	H (wt.-%)	O (wt.-%)	Cl (wt.-%)	HHV (MJ kg⁻¹)	Ym (%)
180	Exp. 1	3.10	74.36	22.53	3.89	61.16	0.56	6.99	24.30	0.01	31.25	60.00
	Exp. 2	3.09	72.93	23.97	3.89	62.33	0.44	7.02	23.22	0.02	26.69	61.85
Average value		3.10	73.65	23.25	3.89	61.74	0.50	7.01	23.76	0.02	28.97	60.92
Std. Dev.		0.01	1.01	1.02	0.00	0.83	0.08	0.02	0.76	0.00	3.23	1.31
230	Exp. 1	3.50	62.25	34.25	4.60	70.51	0.53	7.03	13.83	0.01	30.95	47.65
	Exp. 2	3.13	61.30	35.57	4.44	70.24	0.48	7.04	14.68	0.01	30.23	48.39
Average value		3.31	61.78	34.91	4.52	70.37	0.51	7.03	14.26	0.01	30.59	48.02
Std. Dev.		0.26	0.67	0.93	0.12	0.19	0.04	0.00	0.60	0.00	0.51	0.52
280	Exp. 1	3.78	57.79	38.43	4.08	66.46	0.42	7.03	18.23	0.01	32.47	44.84
	Exp. 2	4.12	55.70	40.17	4.53	72.99	0.42	7.02	10.91	0.02	31.58	45.55
Average value		3.95	56.75	39.30	4.30	69.72	0.42	7.03	14.57	0.01	32.03	45.20
Std. Dev.		0.25	1.47	1.23	0.32	4.62	0.00	0.01	5.18	0.00	0.63	0.50

Table A3: Lower heating value, mass yield, proximate and ultimate analysis on dry basis measured for 3 different repetitions of the HTC experiment treating spruce bark at 180, 230 and 280 °C for 4 h. The obtained standard deviation (Std. Dev) is in the expected range of an experimental investigation.

Temp. (°C)		Ash (wt.-%)	Volatiles (wt.-%)	Fixed-C (wt.-%)	N (wt.-%)	C (wt.-%)	S (wt.-%)	H (wt.-%)	O (wt.-%)	Cl (wt.-%)	HHV (MJ kg⁻¹)	Ym (%)
180	Exp. 1	2.64	71.61	25.75	0.48	60.08	0.26	7.01	29.54	0.01	23.35	74.42
	Exp. 2	3.14	71.42	25.44	0.56	58.50	0.21	7.02	30.58	0.02	23.25	72.30
Average value		2.89	71.52	25.60	0.52	59.29	0.23	7.02	30.06	0.02	23.30	73.36
Std. Dev.		0.36	0.13	0.22	0.05	1.11	0.04	0.01	0.73	0.01	0.07	1.50
230	Exp. 1	3.32	60.18	36.50	0.56	68.07	0.19	7.01	20.85	0.01	26.95	61.97
	Exp. 2	3.50	56.49	40.01	0.69	68.37	0.24	7.00	20.21	0.01	27.41	61.17
Average value		3.41	58.34	38.25	0.62	68.22	0.22	7.01	20.53	0.01	27.18	61.57
Std. Dev.		0.13	2.61	2.49	0.09	0.21	0.04	0.01	0.46	0.00	0.32	0.57
280	Exp. 1	2.99	50.38	46.63	0.74	74.35	0.34	7.03	14.55	0.01	30.04	50.00
	Exp. 2	2.95	49.40	47.66	0.82	74.95	0.23	7.00	14.05	0.01	30.58	51.49
Average value		2.97	49.89	47.14	0.78	74.65	0.28	7.02	14.30	0.01	30.31	50.74
Std. Dev.		0.03	0.69	0.72	0.06	0.43	0.08	0.02	0.36	0.00	0.38	1.05

Table A4: Ash composition determined by XRF for three different repetitions of the HTC experiment treating EFB at 180 °C for 4 h. The obtained standard deviation is in the expected range of an experimental investigation.

	Na2O	MgO	Al2O3	SiO2	P2O5	SO3	K2O	CaO	TiO2	Fe2O3
	(wt.-%)	(wt.-%)	(wt.-%)	(wt.-%)	(wt.-%)	(wt.-%)	(wt.-%)	(wt.-%)	(wt.-%)	(wt.-%)
Experiment 1	0.45	4.39	6.34	46.04	5.30	2.09	22.12	8.35	0.23	4.41
Experiment 2	0.69	4.41	6.21	44.47	5.89	1.99	22.99	9.03	0.19	3.87
Experiment 3	1.06	3.55	7.14	46.65	5.54	1.45	20.64	8.10	0.25	5.30
Average value	0.73	4.12	6.56	45.72	5.58	1.84	21.92	8.50	0.22	4.53
Std. Dev.	0.31	0.49	0.50	1.12	0.29	0.34	1.19	0.48	0.03	0.72

B. Feedstock Data

Table B1: Typical moisture contents upon collection of different biomass substrates.

Biomass type	Moisture content (wt.-%)	Ref.
Brewer's spent grains	75-80	[281]
Corn cobs	20-55	[282]
Dewatered sewage sludge	55-70	[178]
AD Digestate	90-95	[188]
Empty fruit bunches	60-65	[188]
Fallen leaves	48-74	[188]
Fir needles	63-76	[283]
Grass cuttings	65-80	[178]
Horse Manure	45-80	[188]
Micro algae	80-90	[284, 285]
Miscanthus	26-45	[286, 287]
Olive pomace	45-72	[208]
Orange peels	73-87	[288]
Rice husk	7-18	[289]
Seaweed	74-89	[290, 291]
Spent coffee grounds	60-75	[292]
Spruce bark	50-65	[293]
Sugar beet pulp	78-85	[294]
Wheat straw	10-20	[178]
Wood		[178]

Table B2: Lignocellulosic composition of investigated biomass feedstock.

Biomass type	Cellulose (wt.-%)	Hemi- cellulose (wt.-%)	Lignin (wt.-%)	Proteins (wt.-%)	Ref.
Spent grains	16-25	20-29	11-25	15-25	[295]
Corn cobs	40-44	31-33	16-18	4-5	[296]
AD Digestate	34	16	21	-	[297]
EFB	28-37	15-36	31-35	-	[298]
Fallen leaves	30	26	24	-	[299]
Fir needles	29	21	32	-	[300]
Grass cuttings	15	5	5	-	[301]
Horse Manure	34	22	17		[302]
Micro algae	-	24	-	62	[303]
Miscanthus	32-37	29-35	24-25	-	[304]
Olive pomace	32-37	20-23	19-24	3-5	[305]
Orange peels	34	10	7	30	[306]
Rice husk	25-35	18-21	26-31	3	[304]
Seaweed	-	5-75	-	5-15	[307]
Coffee grounds	12	28	24	17	[308]
Spruce bark	42	27	26	-	[309]
Sugar beet pulp	5	67	6	46	[310]
Wheat straw	38-48	23-29	17-20	-	[304]
Soft Wood	27-30	35-40	25-30		[304]

Table B3: Literature data on biomethane production potential (BMP) and own experimental HTC data for different feedstock.

Feedstock	AD data	HTC Data			Ref.
	BMP (m ³ CH ₄ t ⁻¹ Input _{db})	HHV (MJ kg ⁻¹)	Mass yield (%)	Energy densification (-)	
Brewer's grains	115.6	21.37	50.6	1.30	[311]
Coffee grounds	298.0	22.79	56.1	1.33	[312]
Corn cobs	146.0	17.50	56.5	1.29	[313]
AD Digestate	106.9	18.86	63.1	1.20	[314]
EFB	55.0	20.58	60.5	1.18	[188]
Fallen leaves	105.5	19.31	61.0	1.22	[188]
Fir needles	5.5	21.30	58.2	1.24	[315]
Grass cuttings	352.1	18.40	52.8	1.22	[316]
Horse manure	171.9	18.35	57.0	1.23	[317]
Micro algae	339.3	21.57	20.3	1.46	[318]
Miscanthus	247.0	19.61	64.7	1.16	[319]
Olive pomace	90.9	21.96	62.1	1.22	[320]
Orange peels	242.9	17.99	44.5	1.46	[188]
Rice husk	47.8	18.26	59.5	1.11	[321]
Seaweed	89.4	15.41	38.3	1.57	[322]
Sewage sludge	29.0	16.70	54.1	0.86	[69]
Spruce bark	59.2	20.57	67.2	1.15	[323]
Sugar beet pulp	139.2	17.99	44.1	1.34	[324]
Wheat straw	89.5	17.55	62.0	1.16	[69]

C. Additional Data on HTC Fuels

Table C1: Relative ash content of different substrates after HTC at temperatures between 150-270 °C and residence times of 0.5 and 4 h.

Temperature (°C)	Residence time (h)	Digestate	Digested Sludge	EFB	Fallen leaves	Grass cuttings	Spruce bark	Wheat straw
150	0.5	0.86	1.07	0.87	0.99	1.59	0.97	0.88
	4	0.89	1.12	0.59	0.97	0.89	1.04	0.88
180	0.5	0.79	1.25	0.84	1.01	0.96	0.93	0.96
	4	0.89	1.54	0.88	1.04	1.07	0.91	1.06
210	0.5	0.75	1.63	0.78	1.04	1.58	0.87	1.14
	4	0.85	1.68	0.77	1.07	1.16	1.00	1.19
240	0.5	0.90	1.69	0.85	1.06	1.73	0.96	1.23
	4	1.16	1.79	0.70	1.16	1.51	1.09	1.45
270	0.5	1.30	1.81	0.96	1.16	1.92	0.97	1.49
	4	1.37	1.88	0.68	1.27	1.62	0.81	1.35

Table C2: Characteristic ash melting temperatures of hydrochar ash obtained from complete combustion of the samples at 550 °C according to DIN 14775.

Biomass	Sample	0.5h				2 h				4 h			
		IDT	DT	HT	FT	IDT	DT	HT	FT	IDT	DT	HT	FT
AD digestate	HTC, 150 °C	947	1124	1143	1152	1007	1156	1164	1176	910	1150	1172	1199
	HTC, 180 °C	1004	1188	1213	1252	957	1130	1259	1286	935	1207	1280	1302
	HTC, 210 °C	944	1187	1282	1311	963	1119	1300	1320	951	1217	1308	1327
	HTC, 240 °C	954	1258	1301	1319	940	1231	1312	1328	918	1199	1293	1319
	HTC, 270 °C	915	1240	1273	1297	781	1208	1256	1291	787	1207	1235	1274
Digested sludge	HTC, 150 °C	637	1182	1253	1275	646	1180	1241	1261	653	1197	1245	1267
	HTC, 180 °C	647	1188	1238	1259	666	1151	1218	1231	679	1142	1225	1240
	HTC, 210 °C	670	1093	1219	1236	663	1169	1218	1232	673	1096	1223	1237
	HTC, 240 °C	676	1104	1225	1242	680	1133	1223	1243	680	1152	1227	1240
	HTC, 270 °C	676	1160	1224	1242	741	1142	1227	1248	791	1162	1230	1246
EFB	HTC, 150 °C	967	1127	1171	1204	818	1057	1155	1253	823	1053	1230	1285
	HTC, 180 °C	857	1063	1254	1326	835	1142	1282	1347	945	1109	1292	1373
	HTC, 210 °C	969	1194	1390	1396	915	1177	1344	1383	949	1191	1358	1381
	HTC, 240 °C	914	1048	1364	1390	948	1235	1349	1430	941	1226	1362	1405
	HTC, 270 °C	960	1243	1393	1465	940	1205	1365	1385	946	1210	1347	1393
Fallen leaves	HTC, 150 °C	1099	1343	1407	1443	1042	1401	1441	1463	ND	ND	ND	ND
	HTC, 180 °C	1054	1408	1458	1477	994	1298	1490	1502	1097	1428	1494	1503
	HTC, 210 °C	1100	1448	1513	1528	1037	1442	1524	1519	ND	ND	ND	ND
	HTC, 240 °C	1017	1493	1488	1498	1044	1442	1522	>1500	1045	1495	1495	1505
	HTC, 270 °C	1060	1278	1524	1526	1070	1410	1509	>1500	1025	1472	1486	1560

Table C3: Characteristic ash melting temperatures of hydrochar ash obtained from complete combustion of the samples at 550 °C according to DIN 14775.

Biomass	Sample	0.5h				2 h				4 h			
		IDT	DT	HT	FT	IDT	DT	HT	FT	IDT	DT	HT	FT
Grass cuttings	HTC, 150 °C	1174	1126	1219	1230	1176	1210	1225	1260	1132	1177	1212	1253
	HTC, 180 °C	1151	1208	1255	1298	1155	1209	1227	1255	1148	1167	1237	1303
	HTC, 210 °C	1122	1223	1232	1288	964	1203	1231	1296	1137	1225	1281	1342
	HTC, 240 °C	1145	1217	1240	1281	1065	1195	1239	1294	1117	1234	1257	1313
	HTC, 270 °C	830	1237	1245	1293	781	1206	1233	1282	786	1217	1228	1267
Spruce bark	HTC, 150 °C	1045	ND	ND	ND	1043	1478	>1550	>1550	1059.5	1532	1525	1534
	HTC, 180 °C	1033	ND	ND	ND	1016	842	>1550	>1550	1070	1478	1480	1506
	HTC, 210 °C	1040	ND	ND	ND	1074	1341	>1550	>1550	1056	ND	ND	ND
	HTC, 240 °C	1040	ND	ND	ND	1360	1241	>1550	>1550	1029.5	ND	ND	ND
	HTC, 270 °C	1080	1397	ND	ND	1313	1478	1502	1519	1094.5	1362.5	1385.5	1457.5
Wheat straw	HTC, 150 °C	754	1485	>1550	>1550	753	1525	>1550	>1550	755	1196	ND	ND
	HTC, 180 °C	748	1500	>1550	>1550	815	301	>1550	>1550	820	317	>1550	>1550
	HTC, 210 °C	834	304	>1550	>1550	852	1086	>1550	>1550	ND	ND	ND	ND
	HTC, 240 °C	882	930	>1550	>1550	919	525	>1550	>1550	ND	ND	ND	ND
	HTC, 270 °C	946	313	>1550	>1550	932	1118	>1550	>1550	ND	ND	ND	ND

Table C4 Substrate and hydrochar properties and reaction data for chars from isothermal measurements in 5 % O₂ atmosphere at 420 °C.

Sample	DFT surface area (m ² g ⁻¹ _{daf})	Γ _{obs} (s ⁻¹)	Γ _{int} (g s ⁻¹ m ⁻²)
EFB, raw	562	4.62·10 ⁻²	9.78·10 ⁻⁵
EFB, 180 °C, 0.5 h	631	7.12·10 ⁻²	7.20·10 ⁻⁵
EFB, 180 °C, 2 h	511	4.47·10 ⁻²	4.61·10 ⁻⁵
EFB, 180 °C, 4 h	628	3.61·10 ⁻²	3.68·10 ⁻⁵
EFB, 210 °C, 0.5 h	485	4.54·10 ⁻²	3.68·10 ⁻⁵
EFB, 210 °C, 2 h	591	2.35·10 ⁻²	2.94·10 ⁻⁵
EFB, 210 °C, 4 h	626	2.31·10 ⁻²	2.14·10 ⁻⁵
EFB, 240 °C, 0.5 h	489	1.79·10 ⁻²	2.17·10 ⁻⁵
EFB, 240 °C, 2 h	565	1.74·10 ⁻²	2.27·10 ⁻⁵
EFB, 240 °C, 4 h	609	1.34·10 ⁻²	6.62·10 ⁻⁶
EFB, 270 °C, 0.5 h	511	1.06·10 ⁻²	8.99·10 ⁻⁶
EFB, 270 °C, 2 h	500	1.28·10 ⁻²	5.54·10 ⁻⁶
EFB, 270 °C, 4 h	470	4.62·10 ⁻²	4.52·10 ⁻⁶

D. Experimental Data for Process Modelling

Table D1: Experimental HTC data from EFB used for Aspen Plus model. All values except moisture content reported on db.

T (°C)	t (h)	Moisture	Ash	Volatiles	Fixed-C	C	H	O	N	S	Cl	LHV	HHV	Mass yield
		(wt.-%)				(wt.-%)						(MJ kg ⁻¹)		%
raw		7.7	9.0	81.0	10.0	50.6	5.9	33.1	1.13	0.34	0.57	19.1	20.6	-
180	0.5	4.4	7.6	80.7	11.7	55.2	5.6	30.7	0.83	0.11	0.16	18.9	20.2	72.0
180	2	4.1	7.0	79.0	14.1	56.5	5.6	30.0	0.81	0.10	0.06	21.6	23.0	66.6
180	4	2.5	7.9	73.4	18.6	56.5	6.7	27.5	1.06	0.25	0.26	21.9	23.4	69.2
210	0.5	4.5	7.0	76.3	16.7	59.5	5.8	26.7	0.89	0.12	0.16	21.7	23.0	62.6
210	2	3.9	6.8	74.4	18.8	59.5	5.6	26.9	0.97	0.11	0.10	23.0	24.3	60.5
210	4	4.2	6.9	60.5	32.6	61.4	5.7	24.9	1.03	0.09	0.24	24.1	25.4	57.1
240	0.5	3.5	7.6	72.9	19.5	62.3	5.9	23.0	1.01	0.13	0.12	24.9	26.2	55.7
240	2	3.4	7.7	63.2	29.1	71.2	6.3	13.2	1.43	0.12	0.09	26.3	27.7	50.9
240	4	3.5	6.3	68.3	25.4	71.5	6.2	14.5	1.45	0.10	0.21	28.7	30.1	41.3
270	0.5	3.3	8.6	68.8	22.6	68.7	6.3	15.0	1.29	0.13	0.04	28.4	29.8	42.0
270	2	3.1	7.7	67.4	24.9	66.6	6.1	18.2	1.24	0.12	0.09	28.9	30.4	37.9
270	4	3.1	7.1	61.1	31.8	73.9	6.6	10.9	1.43	0.10	0.11	30.4	31.9	39.5

E. Additional Process Water Characterisation

Table E1: Measured electrical conductivity (EC) and pH of effluents from HTC of different feedstock treated at 210 °C for 2 h.

Feedstock type	HTC condition	EC (mS cm ⁻¹)	pH (-)
AD digestate	210 °C, 2 h	6.2	4.6
Coffee grounds	210 °C, 2 h	2.2	4.2
Corn cobs	210 °C, 2 h	1.9	3.9
Digested sludge	210 °C, 2 h	7.2	7.2
EFB	210 °C, 2 h	3.9	4.1
Fallen leaves	210 °C, 2 h	3.8	4.6
Fir needles	210 °C, 2 h	3.6	4.0
Grass cuttings	210 °C, 2 h	3.8	4.7
Micro algae	210 °C, 2 h	4.8	5.2
Miscanthus	210 °C, 2 h	1.6	3.9
Olive pomace	210 °C, 2 h	2.0	3.7
Orange peels	210 °C, 2 h	2.3	4.3
Rice Husk	210 °C, 2 h	1.5	3.9
Seaweed	210 °C, 2 h	6.2	4.8
Spent grains	210 °C, 2 h	2.6	4.7
Spruce bark	210 °C, 2 h	1.9	3.7
Sugar beet pulp	210 °C, 2 h	1.9	4.2
Wheat straw	210 °C, 2 h	2.5	3.8